A THESIS SUBMITTED TO THE INSTITUTE OF CELLULAR MEDICINE, UNIVERSITY OF NEWCASTLE UPON TYNE IN FULFILMENT OF THE REQUIREMENTS FOR MD DEGREE

The use of Cell Penetrating Peptides to treat inflammatory responses in uterine cells

Dr Leo Gurney MBBS BMedSci

September 2016

Abstract

A lack of effective therapies continues to impair attempts to prevent preterm birth associated with inflammation. This study aimed to broaden the scope of candidate agents available to address this clinical problem. Using live cell confocal microscopy, Western immunoblotting, cell toxicity assay, and quantitative polymerase chain reaction techniques this study investigated the ability of a novel class of peptide vectors, termed Cell Penetrating Peptides (CPPs), to deliver cargo to human uterine and placental cells. It examined the ability of a CPP-linked peptide cargo: the Nemo Binding Domain (NBD) peptide, to inhibit inflammatory Nuclear Factor Kappa B (NFκB) signalling in uterine cells; comparing this response to a group of small molecule inhibitors of inflammatory pathways.

Three CPP derived vectors were able to deliver fluorescent cargo to uterine myometrial and placental amnion cells within one hour over a concentration range of 1-10μM. Similar uptake kinetics in uterine cells were observed with the use of a fluorescently-tagged CPP conjugated to NBD. The NBD peptide, conjugated to a CPP derived from antennopaedia protein (Pen-NBD), was able to inhibit cytokine-stimulated cyclooxygenase-2 (COX2) protein induction at four hours; an effect that was not seen with other CPP-NBD conjugations, nor with NBD-mutant or unconjugated peptide controls. Data derived from both Western blots and gene arrays indicated that the anti-inflammatory effects of Pen-NBD were comparable to non-peptidic small molecule inhibitors of NFκB. However, Pen-NBD peptide did not prevent the cytokine-induced degradation of Inhibitor of Kappa B Alpha (IκBα) protein; nor did it inhibit the cytokine-induced expression of NFκB pathway genes, thus the precise targeting of NBD peptide within uterine cells remains uncertain and may be distinct to the canonical NFκB pathway.

This research demonstrates the proof of concept that CPPs can enter human utero-placental cells and can deliver bioactive cargo to exert an anti-inflammatory effect. It provides a framework by which future research can examine CPP mediated delivery of a broad variety of potential cargo into uterine cells and thus offers a novel approach for the development of treatments aimed at preventing preterm birth.

Acknowledgements

Without the help of many people this thesis would not have come to light and I owe them all a large debt of gratitude. Firstly Julie Taggart and Michele Sweeney, both of whom have shown extremes of patience when showing me the ropes in the laboratory and teaching me techniques for which I was previously a complete novice such as Western blotting and confocal microscopy. Throughout my time in the lab I have only hoped to emulate the high level of skill that was demonstrated to me by Julie and Michele in those early days.

Thanks go to all the women who have selflessly donated myometrial biopsies or placentas during the course of this study, demonstrating a willingness to aid the research effort despite the impending distractions that come with any new baby. I also wish to thank the research midwife team for helping co-ordinate and consent patients, and the clinical team at the Royal Victoria Infirmary maternity department for the myometrial samples received.

I would like to thank Professor Arwyn Jones and his team at the Welsh School of Pharmacy in Cardiff for the expert help and guidance given to me during numerous trips to their laboratory and Skype meetings, without them my understanding of the Cell Penetrating Peptide field would have remained in its infancy. Special thanks also to Cardiff PhD student Noura Eissa for our many discussions regarding the NBD peptide and for permitting me to use a data figure from her work in the General Discussion of this thesis.

Both my supervisors deserve great thanks for guiding me through this experience and helping me over the finish line. Firstly; appreciation goes to Professor Robson for giving me the opportunity to enter postgraduate research, and supporting me throughout the funding application process, and then through the course of data generating and thesis writing. Secondly gratitude goes to Professor Taggart because without the careful supervision, scrutiny of data, encouragement, fresh ideas and friendship displayed by him throughout the process, this thesis would not have come to fruition.

Finally, I'd like to thank my very tolerant wife and two (not so tolerant) small children whose love and smiles have helped me through the more testing times of the last three years.

Table of contents

Abstract 1
Acknowledgements 2
Table of contents 3
List of Figures 8
List of Tables 11
List of Abbreviations 12
Chapter One 16
1.1 Preterm birth – the clinical problem 17
1.2 Human parturition 19
1.3 Aetiology of preterm birth 20
1.4 The role of infection and inflammation in preterm birth 21
1.4.1 Infection and preterm birth 21
1.4.2 Inflammation in preterm and term birth 22
1.5 Molecular pathways associated with inflammatory preterm birth 23
1.5.1 P38 MAP Kinase pathway and preterm birth 24
1.5.2 AP1 pathway and preterm birth 24
1.5.3 The Nuclear Factor Kappa B pathway 25
1.5.3.1 The NFκB protein family 25
1.5.3.2 The IκB proteins 26
1.5.3.3 The Inhibitor of κB Kinase (IKK) complex 26
1.5.3.4 The canonical activation pathway 26
1.6 The role of NFκB in preterm birth 29
1.6.1 NFκB and uterine cells 29
1.6.2 NFκB and placental cells 30
1.6.3 NFκB antagonism with pro-quiescent pathways 30
1.6.4 NFκB and animal preterm birth 31
1.7 Drugs in clinical use for the acute prevention of preterm birth 32
1.8 Novel agents for the acute prevention of preterm birth 35
1.9 Cell Penetrating Peptides as drug delivery vectors 36
1.9.1 Mechanism of CPP uptake 37
1.9.2 Therapeutic potential of CPP-cargo conjugations 37
1.9.3 Cell Penetrating Peptide inhibitors of NFκB 38

1.9.4 The Nemo Binding Domain (NBD) peptide as a tool for NFκB inhibition 38
1.10 Small molecule, non-peptide inhibitors of NFκB 40
1.11 Study Hypothesis and Aims 42
Chapter Two 43
2.1 Materials 44
2.2 Subjects and samples 44
2.3 Cell culture 45
2.3.1 Cell culture consumables and reagents 45
2.3.2 Preparation of myometrial cells 45
2.3.3 Preparation of amnion mesenchymal cells 46
2.3.4 Frozen cells 46
2.3.5 Cell maintenance 46
2.3.6 Cell splitting and transfer 46
2.3.7 Freezing cells 47
2.4 Cell Penetrating Peptides 47
2.4.1 Peptide labelling 47
2.4.2 Peptides used in confocal experimentation 49
2.4.3 Peptides used in cell stimulation experiments 51
2.5 Live cell confocal microscopy 52
2.5.1 Dyes and emission / excitation wavelength spectra used in confocal experimentation 52
2.5.2 Preparation of cells for microscopy 52
2.5.3 Labelling of endoplasmic reticulum or mitochondria 52
2.5.4 Labelling of endosomes / lysosomes 52
2.5.5 Cell Imaging 53
2.6 Picture analyses 54
2.6.1 Use of Cell Profiler 54
2.6.2 Use of Image J 55
2.7 Cell stimulation protocol 57
2.7.1 Materials used in cell stimulation experiments 57
2.7.2 Cell stimulation experiment protocol for protein extraction 57
2.7.3 Cell stimulation experiment protocol for RNA extraction 58
2.8 Cell Toxicity Assay 58
2.9 Measurement of protein expression 59
2.9.1 Western blotting reagents 59

2.9.2 Antibodies used 59
2.9.3 Protein assay 59
2.9.4 Preparation of SDS polyacrylamide gels 60
2.9.5 SDS-Polyacrylamide gel electrophoresis 61
2.9.6 Protein transfer onto polyvinylidine difluoride membrane 61
2.9.7 Blocking steps and primary antibody incubation 61
2.9.8 Secondary antibody incubation 62
2.9.9 Development of films 62
2.9.10 Assessment of protein loading 62
2.9.11 Scanning and quantification of blots 62
2.10 Measurement of mRNA expression 63
2.10.1 Materials used for mRNA expression experimentation 63
2.10.2 Isolation of total RNA 63
2.10.3 RNA quantification 63
2.10.4 Synthesis of cDNA 63
2.10.5 Protocol for loading and running qPCR array plates 64
2.10.6 Selection of genes of interest and arrangement of gene array plate 65
2.10.7 Analysis of RNA expression changes 67
2.11 Statistical analysis 68
2.11.1 Cellular uptake studies 68
2.11.2 Biological effectiveness studies 68
2.11.3 Gene array data 68
Chapter Three 69
3.1 Introduction 70
3.2 Demonstrating the intracellular uptake and distribution of CPPs in human myometrial cells 73
3.2.1 Comparison of CPP cellular delivery of fluorescent cargo with control peptide GS_4(GC) 73
3.2.2 Mobility of peptide fluorescence within uterine cells 75
3.2.3 Assessment of peptide distribution within uterine cells 77
3.3 Detailed assessment of uptake of Pen CPP in myometrial cells 78
3.3.1 Pattern of uptake displayed by fluorophore conjugated Pen CPP 78
3.3.2. Quantitative analysis of 10µM rhodamine-Pen uptake 80
3.3.3 Uptake of fluorophore-CPP across a concentration range 83
3.4 Uptake of rhodamine-conjugated TAT peptide in myometrial cells 86
3.5 Uptake of rhodamine-conjugated R8 peptide in myometrial cells 88

3.6 Comparison of intracellular fluorescence of rhodamine-conjugated Pen, TAT and R8 88
3.7 CPP entry into amnion mesenchymal cells 90
3.8 Examination of CPP-NBD peptide myometrial cell uptake 91
3.8.1 The intracellular uptake of rhodamine conjugated Pen-NBD 91
3.8.2 The uptake of rhodamine conjugated TAT-NBD and R8-NBD 92
3.8.3 Cell uptake of rhodamine-Pen-NBD mutant 95
3.8.4 Cell application of rhodamine-NBD 95
3.9 Discussion 96
Chapter Four 100
4.1 Introduction 101
4.2 Assessing the time frame and agonist concentration for IL1β and TNFα stimulated COX2 expression in myometrial cells 103
4.2.1 Optimising the time frame of COX2 protein induction 103
4.2.2 Optimising the agonist concentration range for COX2 protein induction 104
4.3 Examination of cell toxicity effects 106
4.4 The effect of Pen-NBD on cytokine stimulated COX2 protein expression 107
4.4.1 Pen-NBD inhibition of IL1β stimulated responses 107
4.4.2 Pen-NBD inhibition of TNFα stimulated responses 109
4.5 The effect of peptide and vehicle controls on cytokine stimulated COX2 expression 111
4.5.1 Effect of Pen-NBD mutant peptide on COX2 induction 111
4.5.2 Unconjugated Pen and NBD effect on cellular COX2 responses to IL1β 115
4.5.3 DMSO vehicle effects 116
4.6. The efficacy of NBD conjugated to different CPP vectors 117
4.6.1 Determination of half maximal concentration 117
4.6.2 Comparison of three CPP vectors conjugated to NBD 118
4.7 Assessing the time frame and agonist concentration for IL1β and TNFα stimulated IκBα in myometrial cells 120
4.7.1 Optimising the time frame for cytokine stimulated IκBα expression 120
4.7.2 Optimising the agonist concentration range for IκBα protein degradation 122
4.8 Clarifying the identity of IκBα protein band on Western blot 124
4.9 Effect of Pen-NBD on IL1β dependent degradation of IκBα in myometrial cells 126
4.10 Effect of Pen-NBD on TNFα dependent degradation of IκBα in myometrial cells 128
4.11 Effect of different CPP vector NBD conjugations on IL1β induced IκBα degradation 131
4.12 IκBα cytokine degradation in response to peptide controls 133

4.13 Comparison of the effects of Pen-NBD against a panel of non-peptidic putative NFκB inhibitors 134
4.13.1 Comparison of non-peptide and Pen-NBD effect on cytokine stimulated COX2 induction 134
4.13.2 Comparison of non-peptide and Pen-NBD effect on IL1β stimulated IκBα degradation 137
4.14 Discussion 139
Chapter Five 142
5.1 Introduction 143
5.2 Changes in myometrial cell gene expression following cytokine exposure 144
5.3 Effects of CPP-linked and small molecule inhibitors on cytokine induced gene expression changes in human uterine cells 148
5.3.1 Anti- inflammatory effects of Pen-NBD, or Sc514 148
5.3.2 Effects of Pen-NBD, or Sc514 on panel of labour associated genes 150
5.3.3 Effects of Pen-NBD, or Sc514 on NFκB pathway genes 152
5.3.4 Effects of Pen-NBD, or Sc514 on genes involved in prostaglandin regulation 153
5.3.5 Effects of Pen-NBD, or Sc514 on cytokine-stimulated changes in novel target genes 154
5.4 Discussion 155
Chapter Six 158
6.1 The choice of CPP and the potential for CPP-cargo interaction 159
6.2 NBD peptide targeting in human myometrial cells 162
6.3 Myometrial cell gene expression changes in response to inflammatory stimuli 168
6.4 Translation of a CPP-cargo approach to clinical scenarios of preterm birth 169
Appendix 172
Funding awards 172
Oral presentations 172
Poster presentations 172
Other awards / prizes 172
References 173

List of Figures

Chapter 1 **Page**

1.1 Percentage of preterm births occurring at the Newcastle upon Tyne Foundation Hospitals Trust 18
1.2 Schematic representation of the canonical NFκB pathway 28
1.3 Mechanism of action of existing tocolytic therapies 34
1.4 The Nemo Binding Domain (NBD) peptide 39

Chapter 2

2.1 High performance liquid chromatography and mass spectrometry tracings of Alexa488 conjugated TAT peptide 48
2.2 Example pipeline demonstrating Cell Profiler image analysis process 55
2.3 Cell fluorescence analysis via Image J software 56

Chapter 3

3.1 Confocal image z-series of live myometrial cells demonstrating capture of fluorescent uptake throughout the cell 72
3.2 Comparison of rhodamine-CPP cellular uptake with a non-cell permeable control peptide 74
3.3 Demonstration of peptide mobility within a myometrial cell 76
3.4 Demonstration of peptide distribution throughout myometrial cells 77
3.5 Pattern of 10μM rhodamine-Pen CPP uptake over 120 minutes 79
3.6 Quantitative analysis of rhodamine-Pen 10μM uptake in myometrial cells 82
3.7 Cellular uptake of concentration range of rhodamine-Pen compared to control peptide 84
3.8 Quantitative analysis of rhodamine-Pen uptake via image J 85
3.9 Cellular uptake of rhodamine-TAT peptide 87
3.10 Cellular uptake of rhodamine-R8 peptide 89
3.11 Representative confocal images demonstrating CPP entry to amnion mesenchymal cells 90
3.12 Cellular uptake of concentration range of rhodamine-Pen-NBD 92
3.13 Quantitative analysis of rhodamine-Pen-NBD uptake via image J 93
3.14 Comparison of rhodamine conjugated CPP-NBD uptake 94
3.15 Application of rhodamine conjugated Pen-NBD (mutant) and NBD peptides to myometrial cells 95

Chapter 4

4.1 Time frame of COX2 protein cytokine response in myometrial cells 103
4.2 COX2 protein response across a cytokine agonist concentration range 105

4.3 Myometrial cell viability in presence of cytokine agonist or peptide 106
4.4 Effect of Pen-NBD on IL1β-induced COX2 protein expression 108
4.5 Effect of Pen-NBD on TNFα-induced COX2 protein expression 110
4.6 Effect of Pen-NBD mutant peptide on IL1β-stimulated COX2 protein expression 112
4.7 Effect of Pen-NBD mutant peptide on TNFα-stimulated COX2 protein expression 113
4.8 Effect of unconjugated Pen CPP or NBD peptide on IL1β-stimulated COX2 protein expression 114
4.9 Vehicle (DMSO) effects on cytokine-stimulated COX2 protein expression 115
4.10 Concentration response curve for Pen-NBD 117
4.11 Comparison of effect of different CPP-NBD conjugations on IL1β-induced COX2 protein expression 118
4.12 The time frame of IκBα protein phosphorylation, degradation and re-synthesis in myometrial cells 120
4.13 IκBα protein responses to varying concentrations of cytokine agonist 122
4.14 Identification of the IκBα protein band using full length (FL) and C-terminal (C21) anti-IκBα antibodies 124
4.15 Effect of Pen-NBD on IL1β stimulated IκBα protein degradation 125
4.16 Quantification of effect of Pen-NBD on IL1β-stimulated IκBα protein degradation 126
4.17 Effect of Pen-NBD on TNFα-stimulated IκBα protein degradation 128
4.18 Variability of IκBα protein responses to TNFα 129
4.19 Effect of different CPP-NBD conjugations on IL1β simulated IκBα protein responses 131
4.20 Effect of peptide and vehicle controls on IL1β stimulated IκBα protein responses 132
4.21 Effect of non-peptide inhibitors on IL1β-stimulated COX2 protein expression 134
4.22 Comparison of effect of non-peptide inhibitors and Pen-NBD on IL1β-stimulated COX2 protein signal 134
4.23 Effect of non-peptide inhibitors on IL1β-stimulated IκBα protein responses: comparison with Pen-NBD 137

Chapter Five

5.1 Clustergram demonstrating the hierarchical clustering of myometrial cell gene expression in response to IL1β cytokine stimulation 144
5.2 Volcano plot demonstrating gene expression changes in myometrial cells following IL1β exposure 146
5.3 Anti-inflammatory effects of Pen-NBD or Sc514 on IL1β stimulated pro-inflammatory in myometrial cells 148
5.4 Effects of Pen-NBD or Sc514 on cytokine induced expression changes of labour associated genes 150
5.5 Effects of Pen-NBD or Sc514 on cytokine induced expression changes of NFκB pathway genes 151

5.6 Effects of Pen-NBD or Sc514 on cytokine induced expression changes of genes involved in prostaglandin regulation 152
5.7 Effects of Pen-NBD or Sc514 on cytokine induced expression changes of STAT1 and TRIB1 genes 153

Chapter Six

6.1 IκBα protein responses to TNFα in HeLa cells 163
6.2 Schematic diagram displaying potential Pen-NBD sites of action in myometrial cells 166

List of Tables

Chapter Two **Page**

2.1 Demographic characteristics of the study population 44
2.2 The nomenclature, structure and excitation / emission wavelengths of fluorophore conjugated peptides used for live cell confocal microscopy experimentation 50
2.3 The nomenclature and structure of peptides used for cell stimulation experimentation 51
2.4 Recipe for preparing 2x 10% SDS poly-acrylamide gels as used in this study 60
2.5 Genes used in RT2 profiler PCR array plates 66

Chapter Six

6.1 The structure and properties of peptides used in experimentation 161

List of Abbreviations

AC: Adenylyl cyclase

ANOVA: Analysis of variance

AntP: Cell Penetrating Peptide derivative of Antennopaedia protein

AP1: Activator protein 1

APS: Ammonium persulfate

ATP: Adenosine-5'-triphosphate

AU: Arbitrary units

BMK1: Big mitogen activated kinase 1

BSA: Bovine serum albumin

$CaCl_2$: Calcium chloride

cAMP: Cyclic adenosine monophosphate

CBP: Cyclic adenosine monophosphate response element binding protein

cDNA: Complementary deoxyribose nucleic acid

cGMP: Cyclic guanosine monophosphate

COX2: Cyclo-oxygenase 2

CPP: Cell penetrating peptide

CRH: Corticotrophin-releasing hormone

CRH R: Corticotrophin- releasing hormone receptor

CSAIDS: Cytokine suppressant anti-inflammatory drugs

Ct: Cycle threshold

CTCF: Corrected total cell fluorescenc

CXCL: Chemokine (C-X-C motif) ligand

DMSO: Dimethyl sulphoxide

DNA: Deoxyribonucleic acid

ECL: Enhanced chemiluminescent

EDTA: Ethylene-diamine-tetra-acetic acid

ERK: Extracellular signal-related kinase

FACS: Fluorescence-activated cell sorting

FCS: Fetal calf serum

FIRS: Fetal inflammatory response syndrome

FLS: Fibroblast-like synovial cells

g: grams

GBS: Group B Streptococcus

GOI: Gene of interest

HAT: Histone acetyl transferase

HCL: Hydrogen chloride

HDAC: Histone deacetylase

HeLa: Henrietta Lacks cell

HGDC: Human genomic DNA control

HIV: Human immunodeficiency virus

IC_{50}: Half maximal inhibitory concentration

IκBα: Inhibitor of κB alpha

IKK: Inhibitor of κB kinase

IL1β: Interleukin 1β

IL: Interleukin

iNKT: Invarient natural killer T-cell

IP3: Inositol 1,4,5-triphophosphate

JNK: c-Jun N-terminal kinase

KCl: Potassium chloride

KDa: Kilo Dalton

LPS: Lipopolysaccharide

M: Molar

m: Metres

MAPK: Mitogen activated protein kinase

$MgSO_4$: Magnesium sulphate

MLCK: Myosin light chain kinase

MMP: Matrix metalloproteinase

mRNA: Messenger ribonucleic acid

Mut: Mutant

MW: Molecular weight

NAC: N-acetylcysteine

NaCl: Sodium chloride

NBD: Nemo binding domain

NEMO: NFκB essential modulator

NFkB: Nuclear factor κB

NHP: Non-human primate

NLS: Nuclear localisation sequence

OXTR: Oxytocin receptor

P: Cell passage

PAGE: Polyacrylamide gel electrophoresis

PBS: Phosphate buffered saline

PCR: Polymerase chain reaction

Pen: CPP derivative of Antennopaedia protein

Pen-NBD Mut: Pen CPP with mutant NBD peptide conjugation

Pen-NBD WT: Pen CPP with wild type NBD peptide conjugation

PGE2: Prostaglandin E2

PGF2a: Prostaglandin F2α

PIP3: Phosphatidylinositol 3,4,5 trisphosphate

PLC: Phospholipase C

PPC: Positive PCR control

PPROM: Preterm pre-labour rupture of membranes

PR: Progesterone receptor

PRR: Pattern recognition receptor

PVDF: Polyvinylidene difluoride

qPCR: Quantitative PCR

R8: Poly-arginine CPP (number of arginines – 8)

R8 NBD: Polyarginine CPP with wild type NBD peptide conjugation

RASF: Rheumatoid arthritis synovial fluid cells

RHD: Rel-homology domain

RPM: Revolutions per minute

RTC: Reverse transcription control

RT-qPCR: Quantitative reverse transcription PCR

SAPK: Stress activated protein kinases

SD: Standard deviation

SDS: Sodium-dodecyl sulphate

siRNA: Short interfering RNA

SP-A: Surfactant protein A

TAD: Transactivation domain

TAT: Trans-activator of transcription protein / CPP derived from TAT protein

TAT NBD: TAT CPP with wild type NBD peptide conjugation

TBS-T: Tris-buffered saline with Tween

TEMED: Tetramethyethylenediamine

TIFF: Tagged image file format

TLR: Toll like receptor

TNFα: Tumour necrosis factor alpha

TNFR: Tumour necrosis factor alpha receptor

WHO: World health organisation

Chapter One

General Introduction

1.1 Preterm birth – the clinical problem

Preterm birth is defined by the World Health Organisation (WHO) as birth before 37 weeks completed gestation. It is the main cause of neonatal death in developed countries and presents an enormous global problem. Worldwide it is estimated that fifteen million babies are born preterm each year, a figure which constitutes 11% of all livebirths (Blencowe et al., 2013).

Although there are uncertainties regarding the collection of accurate data in many countries, the incidence of preterm birth appears to be increasing in both the developing world and in parts of the developed world (Blencowe et al., 2013). The reasons behind this differ between countries: in the developing world the increased risk of maternal infection such as HIV and malaria is a contributory factor, and in the developed world a lack of evident reduction in the preterm birth rate is related to a number of complex factors including an increase in multiple pregnancy and an increased rate of caregiver-initiated delivery secondary to clinical concerns regarding fetal or maternal health (Morisaki et al., 2014).

According to the most recent figures released by the Office of National Statistics the preterm birth rate in the UK in 2012 was 7.3% of all livebirths (Office of National Statistics, (2014)). Comparative data taken from a database search (E3, Euroking) at the Newcastle upon Tyne Foundation Hospitals Trust for 2012 and 2013 reveals a marginally higher rate of preterm births than the UK figure with the majority of these births occurring between 33-<37 weeks (Figure 1.1).

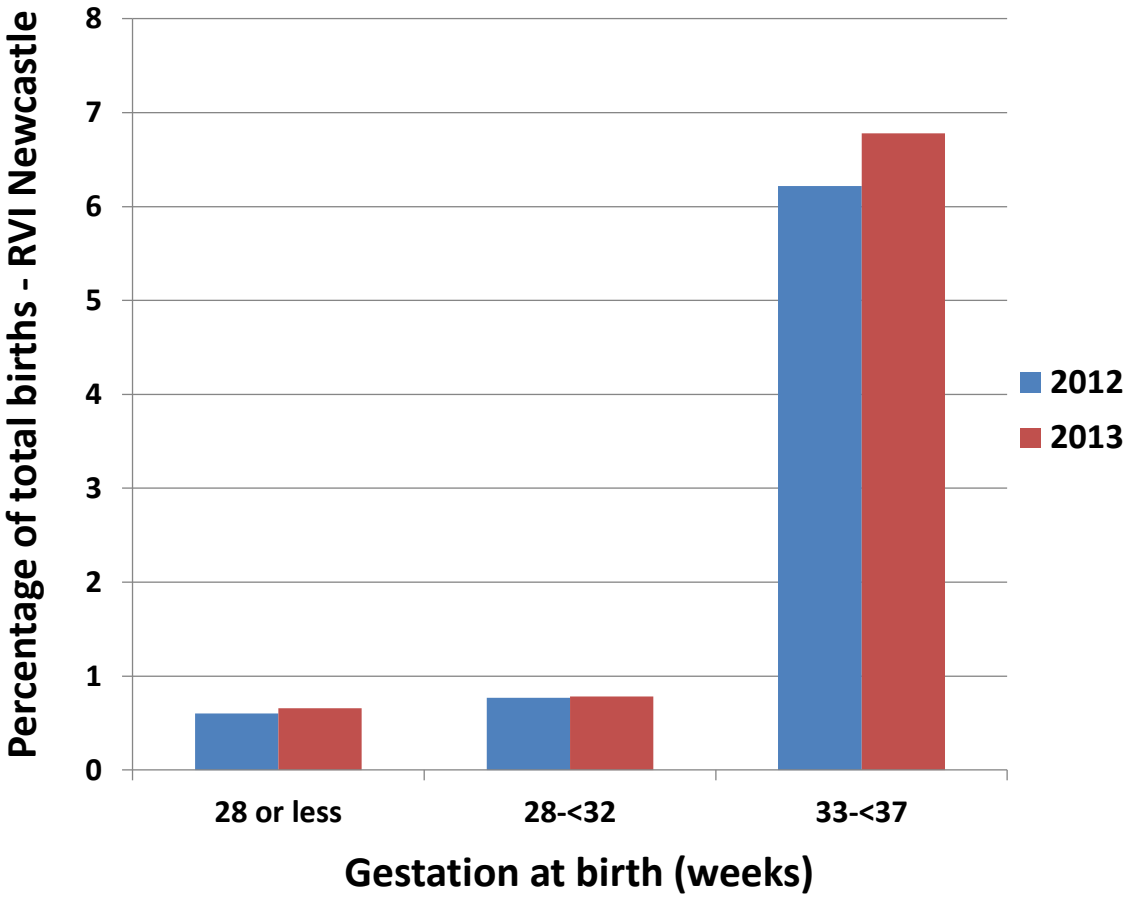

Figure 1.1 Percentage of preterm births occurring at the Newcastle upon Tyne Foundation Hospitals Trust in 2012 (Total births =7156) and 2013 (Total births =7271).

Bar chart illustrating the distribution of preterm births over two years in three categories of gestation as defined by the WHO: extremely preterm (<28 weeks), very preterm (28-<32 weeks) and moderate to late preterm (33-<37 weeks). The overall rate of preterm birth for these years was 7.9% in 2012 and 8.1% in 2013 (Howey et al., 2012).

Being born too soon can confer significant clinical deficits throughout life, leading to neuro-developmental disorders such as cerebral palsy, learning impairment and visual disorders (Rogers and Velten, 2011); problems which are more likely to occur with greater severity at earlier gestations of birth (Costeloe et al., 2012). Preterm birth may also affect long-term physical health with a higher risk of cardiovascular disease, and lays a huge emotional and economic burden on affected families (Hodek et al., 2011).

Despite this being a common and potentially devastating condition, clinical efforts to prevent its occurrence have not been uniformly successful. The reasons behind this historic disappointment are complex and multifactorial, but in part lie in a failure to fully understand the mechanisms that lead to normal human birth. The following section briefly describes an overview of the mechanisms of human birth (referred to as parturition) as currently understood, before going on to examine the pathological processes leading to preterm birth.

1.2 Human parturition

Successful human parturition broadly requires three processes to occur: the uterus must switch from a non-contractile phenotype to achieve regular expulsive contractions, the fetal membranes must be degraded sufficiently to allow their potential rupture and the cervix must ripen and dilate to allow the passage of the fetus (Smith, 2007). These processes occur in a number of phases from uterine quiescence through to involution of the uterus following delivery of the fetus and placenta (Challis et al., 2000). Over the course of these phases, and secondary to alterations in both local (paracrine) and systemic (endocrine) maternal physiology, a number of molecular modifications occur within the uterus and fetal membranes that promote readiness for both labour and birth, the key processes of which are outlined below.

During pregnancy the uterus remains relaxed to accommodate the growing fetus; this requires high levels of pro-quiescent mediators in the paracrine environment including progesterone, prostacyclin, nitric oxide, relaxin and parathyroid hormone, that have a relaxant effect on uterine smooth muscle and act via G-protein coupled receptors linked to adenylyl cyclase (Europe-Finner et al., 1994). Prior to labour the uterus upregulates a series of genes encoding ‘contraction associated proteins’ including the inducible prostaglandin

synthase enzyme cyclooxygenase-2 (COX2), the major myometrial gap junction protein connexin-43 as well as the oxytocin receptor (Garfield et al., 1977, Fuchs et al., 1982, Slater et al., 1999). This allows the transformation of the uterus from a state of reduced contractile excitability to a state of preparedness so that it can respond to increases in both prostaglandins and oxytocin: endogenous stimuli that promote the regular sustained contractions characteristic of labour (Mitchell et al., 1995, Fuchs et al., 1991).

Remodelling of the extracellular matrix of the cervix also takes place to allow for dilatation, a development mediated through the action of collagenases, matrix metalloproteinases (MMPs), and cytokines IL6 and IL8 (Osmers et al., 1995, Sennstrom et al., 2000). Parallel to this, the fetal membranes become activated, increasing the production of prostaglandins and weakening to allow their potential rupture during labour. Such processes occur via upregulation of COX2 and MMP type 9 (Athayde et al., 1998).

1.3 Aetiology of preterm birth

Preterm birth is a syndrome and best understood as the final endpoint of a number of possible pathological events (Romero et al., 2006b). It can be initiated by an array of disease processes including: uterine over-distension, utero-placental haemorrhage or ischaemia, maternal stress, cervical insufficiency, and inflammation with or without clinically apparent infection (McLean et al., 1995, Romero et al., 2006a, Terzidou et al., 2005, Elovitz et al., 2001, Guzman et al., 1998). Inflammation associated preterm birth is estimated to account for 50% of preterm births occurring at less than 28 weeks gestation (Behrman RE, 2007), babies born at these gestations are the most severely affected by complications of prematurity; and the molecular pathways involved offer potential for amelioration by therapeutic intervention (Ng et al., 2015). It is worthwhile, therefore, to consider the evidence supporting the contribution of inflammation to preterm birth and the intracellular molecular pathways that are involved in this process, in particular the Nuclear Factor Kappa B (NFκB) pathway.

1.4 The role of infection and inflammation in preterm birth

1.4.1 Infection and preterm birth

A causal link between infection and preterm birth in animals is well established: in pregnant mammals such as rats, mice and sheep, local injection of microbes or microbial products including lipopolysaccharide (LPS) will promote early delivery (Pirianov et al., 2009, Schlafer et al., 1994, Beloosesky et al., 2006). A non-human primate (NHP) model of chronic uterine catheterisation from 118 days pregnancy gestation onwards (the equivalent of 28 weeks human gestation) has been developed that allows for serial measurements of amniotic fluid substrates (Adams Waldorf et al., 2011). Inoculation of the amniotic fluid in this primate model with Group B Streptococcus (GBS) led to a rise in concentration of the amniotic fluid cytokines IL1β, TNFα and IL6, with concomitant increases in levels of prostaglandins PGE2 and PGF2α. Increased uterine activity was subsequently observed and GBS inoculated pregnant animals had a mean interval between inoculation and delivery of 2 days, compared to 30 days for non-inoculated controls (Gravett et al., 1994).

Interestingly this model also demonstrated that preterm birth could occur following intra-amniotic infusion of IL1β or TNFα alone (Sadowsky et al., 2006). This suggests that, in the absence of an infectious stimulus, upregulation of pro-inflammatory pathways within the utero-placental environment have the potential to promote early delivery.

Evidence for infectious association with human preterm delivery derives from a number of sources: infection within the uterine cavity as demonstrated by either clinical or histopathological chorioamnionitis is strongly associated with preterm birth (Guzick and Winn, 1985, Hillier et al., 1993), and alterations in the microbial environment of the upper vagina, defined as bacterial vaginosis, have been shown to be associated with increased risk of preterm delivery (Hillier et al., 1995). Recent research using longitudinal sampling of the vaginal microbial environment in pregnant women has identified a greater diversity of upper vaginal bacteria and subsequently low numbers of lactobaccillus species bacteria in the vagina amongst women who deliver preterm, a finding that may offer the opportunity for preterm predictive testing using the vaginal microbiome (DiGiulio et al., 2015). Extra genital infections including malaria, pyelonephritis and periodontal disease have also been

shown to increase preterm birth risk, although the mechanisms underpinning this are unclear (Menendez et al., 2000, Cunningham et al., 1973, Rosa et al., 2012).

Microbial invasion of the amniotic cavity as identified by amniotic fluid aspiration and culture is associated with spontaneous preterm birth, an association that strengthens when techniques are employed to detect microbial DNA alongside standard culture (Romero et al., 1988, Hitti et al., 1997). Women for whom preterm Caesarean section is indicated during spontaneous preterm labour are also significantly more likely to have positive bacterial amniotic cultures than non-labouring preterm controls requiring Caesarean section (Cassell et al., 1993). In the absence of cultured infection, elevated concentrations of amniotic fluid IL6, MMP9, TNFα and IL1β detected in the second trimester of pregnancy confer an increased subsequent risk of preterm birth (Wenstrom et al., 1998, Di Ferdinando et al., 2010, Thomakos et al., 2010, Romero et al., 1992).

The microorganisms identified commonly in the amniotic cavity are genital mycoplasma species and *Ureaplasma urealyticum* (Romero et al., 1989). These are commensal bacteria that normally reside in the upper vagina. Therefore, in humans the most likely passage of infection is via organisms ascending from this site to the uterine cavity and crossing the fetal membranes to invade the amniotic fluid (Goldenberg et al., 2000).

1.4.2 Inflammation in preterm and term birth

There is growing evidence to associate spontaneous labour whether term or preterm with an immune cell infiltration of uterine and placental tissues and local tissue production of pro-inflammatory mediators such as cytokines, chemokines, matrix metalloproteinases and prostaglandins (Romero et al., 2007).

The specific immune cell response has yet to be fully delineated and appears to differ depending on the type of gestational tissue examined; however, the majority of evidence points to involvement of the innate immune system. Macrophage and neutrophil numbers in fetal membranes, myometrium and cervix are increased in tissue derived from labouring compared to non-labouring patients (Thomson et al., 1999, Gomez-Lopez et al., 2009, Osman et al., 2003b). Such invasion leads to increases in local cytokine and chemokine production (Osman et al., 2003a, Hamilton et al., 2013); furthermore, invasion of the decidua by these cell types occurs in animal models of preterm birth and precedes the onset

of labour (Hamilton et al., 2012). Interestingly, it has recently been demonstrated that pregnant mice depleted of neutrophils can still undergo LPS-induced preterm birth, indicating that complex local immune interactions are involved, and that the system is not reliant on just one immune cell type (Rinaldi et al., 2014).

The part that the adaptive immune system plays in the regulation of term and preterm labour remains uncertain but current research has suggested that phenotypically unique T regulatory (CD25 bright, FoxP3+) cells and invariant natural killer (iNKT) cells may have future key roles to play in this process (Rinaldi et al., 2015, Gomez-Lopez et al., 2014).

However, the exact extent to which inflammation contributes to both term and preterm labour is yet to be fully defined. A very large study involving over 600 myometrial and decidual biopsies taken from consecutive Caesarean section operations reported increases in the number of inflammatory lesions in tissues from full-term patients who had undergone labour prior to Caesarean (Keski-Nisula et al., 2003). The authors also observed that such changes were more likely following prolonged or advanced labour, or with increasing duration of time from membrane rupture. However, the maximum proportion of tissues with inflammatory changes in any circumstance was 29%, indicating that more than 70% of myometrial or decidual tissue in this study showed no marked inflammatory change despite ongoing progressive labour or membrane rupture. This indicates that inflammatory change due to labour can be focal, and may not be present at all in some cases; underlining the likelihood of multiple causative modalities of both preterm and term labour.

1.5 Molecular pathways associated with inflammatory preterm birth

Within the paradigm of infection / inflammation associated preterm birth, the inflammatory milieu provoked within the uterine environment subsequent to bacterial challenge or non-infectious influx of immunological cells is likely to upregulate a panoply of pro-inflammatory pathways in uterine and placental cells. Although existing data supports the contribution of intracellular activation of signalling pathways involving p38 MAP kinase (p38 MAPK) and Activator Protein 1 (AP1), a greater body of evidence implicates the transcription factor Nuclear Factor κB (NFκB) as playing a central role in the pathophysiology of this syndrome.

1.5.1 P38 MAP Kinase pathway and preterm birth

The mitogen activated protein (MAP) kinases are members of discrete intracellular signalling cascades consisting of four families: the extracellular signal related kinases (ERKs), c-jun N terminal or stress activated protein kinases (JNK/SAPK), ERK / big MAP kinase 1 (BMK 1) and p38 MAP kinase. P38 is a 38 kDa protein that is phosphorylated on tyrosine residues in response to extracellular stimuli such as the cytokines IL1β, TNFα and LPS and plays a role in the cellular regulation of differentiation, programmed cell death (apoptosis) and cell organelle degradation (autophagy) (Zarubin and Han, 2005).

Evidence suggesting a role for p38 MAPK in preterm birth arises largely from in vitro findings: in myometrial cells IL1β application has been shown to activate p38 MAPK leading to an induction of COX2 protein. Further application of a specific MAPK inhibitor (SB203580) can reverse these changes (Bartlett et al., 1999). In both fetal membrane tissues and choriodecidual cell cultures, application of LPS has been shown to lead to activation of all MAP kinase families including p38 (Shoji et al., 2007, Lappas et al., 2007).

1.5.2 AP1 pathway and preterm birth

The AP1 transcription factor is a key regulator of cellular immune responses. It is composed of homodimeric and heterodimeric complexes consisting of members of the Jun, Fos, activating transcription factor and musculoaponeurotic fibrosarcoma protein families (Schonthaler et al., 2011). The prototypic AP1 heterodimer is c-Jun / c-Fos with its activation involving the phosphorylation of c-Jun via the c-Jun N-terminal kinase (JNK) pathway (Davies and Tournier, 2012)

The involvement of AP1 activation in the pathophysiology of preterm birth can be deduced from in vitro studies suggesting that in both fetal amnion and myometrial cells stretch can induce the expression of key labouring genes including COX2 and the gene coding for the oxytocin receptor: OXTR, via activation of AP1 (Mohan et al., 2007, Sooranna et al., 2004). This association has been strengthened by research demonstrating that the injection of an AP1-selective LPS serotype (E. coli; serotype 0111) was capable of inducing preterm labour in a pregnant mouse model (MacIntyre et al., 2014).

1.5.3 The Nuclear Factor Kappa B pathway

The transcription factor Nuclear Factor Kappa B (NFκB) is present in nearly all mammalian cells and plays a ubiquitous role in inflammatory and infectious responses. Genes regulated by NFκB are manifold but broadly include those responsible for control of innate and adaptive immune responses, cell adhesion and proliferation, apoptosis and cellular stress responses (Perkins, 2007).

1.5.3.1 The NFκB protein family

NFκB proteins are a family of five structurally related transcription factors named p65 (Rel A), RelB, c-Rel, p50 (NFκB-1) and p52 (NFκB-2). These proteins share a conserved N-terminal region termed the Rel homology domain (RHD) that contains 3 types of motif: a motif for binding specific DNA sequences (the κB elements) in the promoter regions of specific target genes, a motif for dimerisation and a motif for nuclear localisation (NLS) (Hayden and Ghosh, 2004). Proteins p65, Rel B and c-Rel also contain C-terminal transactivation domains (TADs) that confer the ability to initiate gene transcription.

In contrast to the other family members, NFκB-1 and NFκB-2 are synthesised as precursors (p100 and p105) which are proteolytically processed to their active forms p50 and p52 respectively. These p100 and p105 precursors also contain ankyrin repeat domains similar to the IκB proteins (see below) and, therefore, once cleaved can act as their own inhibitory partners (Hayden and Ghosh, 2004).

All NFκB proteins exist in the form of either heterodimers or homodimers of different subtype combinations which have both gene promotion and repressor actions that function by binding to discrete DNA sequences within gene promoters and enhancers. As p50 and p52 do not contain TADs, homogenous dimers of these factors act as transcriptional repressors (Hayden and Ghosh, 2012). However, when combined with a member containing a transactional domain such as p65 or RelB, they function to promote gene expression.

The heterodimer most commonly described in the reproductive literature is p65/p50 which is known to activate the expression of pro-inflammatory genes (Cookson and Chapman, 2010). The presence of numerous dimeric combinations within the NFκB family that have gene repressive capability allows for multiple levels of control and enables this system to integrate numerous stimuli in order to direct the most appropriate cellular response (Hoesel

and Schmid, 2013). Allied to this, the p65 subunit undergoes post translational modification including phosphorylation and acetylation which may alter NFκB function in a context specific manner allowing for a further level of control (Chen et al., 2001).

1.5.3.2 The IκB proteins

In resting and non-diseased cells NFκB dimers are retained in the cytoplasm in an inactive form through association with the Inhibitor of κB (IκB) proteins. This family of proteins are characterised by multiple ankyrin repeat domains that mask the nuclear localisation sequence (NLS) of NFκB contained in the RHD and thus sequester inactive NFκB dimers within the cytoplasm of cells. There are numerous IκB proteins now described: IκBα, IκBβ, IκBε, IκBζ, BCL3 and IκBns and the NFκB precursors P100 and p105, although the prototypic and best described protein is IκBα (Hayden and Ghosh, 2012). Activation of the canonical NFκB pathway leads to the phosphorylation of serine residues 32 and 36 on IκBα. This targets the inhibitory protein for poly-ubiquitination by E3 ligases and eventual degradation by the 26s proteasome (Chen et al., 1995). Such degradation leads to unmasking of the NLS of NFκB dimers and subsequent shuttling to the nucleus where gene expression or repression can occur (Whiteside and Israel, 1997).

1.5.3.3 The Inhibitor of κB Kinase (IKK) complex

The IKK complex is made up of three subunits, the catalytic protein IKKα which is predominantly active in the non-canonical pathway of activation, IKKβ which phosphorylates IκBα in the canonical activation pathway, and the regulatory subunit NFκB Essential Modulator (NEMO or IKKγ). The active subunits interact with NEMO via a 6 amino acid sequence (LDWSWL) termed the Nemo Binding Domain (NBD) (May et al., 2002).

1.5.3.4 The canonical activation pathway

There are two distinct pathways of NFκB activation: the canonical or classical pathway, and the non-canonical pathway. The non-canonical pathway is integral to lymphoid organogenesis but not standard inflammatory responses. Atypical forms of NFκB induction have also been described whereby cellular stresses such as hypoxia or UV light can phosphorylate IκBα independent of IKK complex action (Perkins, 2007).

The canonical pathway is triggered by cell exposure to bacterial LPS or pro-inflammatory cytokines such as IL-1β, TNFα or IL6. These ligands interact with specific receptors on the

cell surface including the Toll-like receptor 4 (TLR4), IL1β receptor, or TNFα receptor (TNFR) which in turn activate the IKK complex via the phosphorylation of IKKβ. Following this step, the IKK complex phosphorylates IkBα, which is degraded as described above. The degradation of IkBα unmasks the nuclear localisation sequence of the p50/p65 heterodimer allowing it to translocate to the nucleus of the cell and bind to target gene promoters to regulate the expression of genes including those that transcribe IL1β, TNFα, CXCL8, MMP 8, MMP 9 and COX2, thus leading to increased production of prostaglandins in utero-placental cells. Once internal to the nucleus p65/p50 recruits transcriptional co-regulators such as CREB Binding Protein p300 (CBP p300), histone deacytylases (HDACs) and histone acetyl transferases (HATs) which add further levels of transcriptional control (Hayden and Ghosh, 2012). During the activation process p65 itself can undergo further post-translational modification such as phosphorylation and acetylation, thus altering its specificity of gene transcription or repression (Campbell and Perkins, 2004). Due to the presence of κB binding sites on the IκBα gene promoter, activation of NFκB leads to the synthesis of new IκBα which can dissociate NFκB from DNA complexes and is shuttled out of the nucleus in an inactive complex (Scott et al., 1993). This pathway is displayed schematically in Figure 1.2.

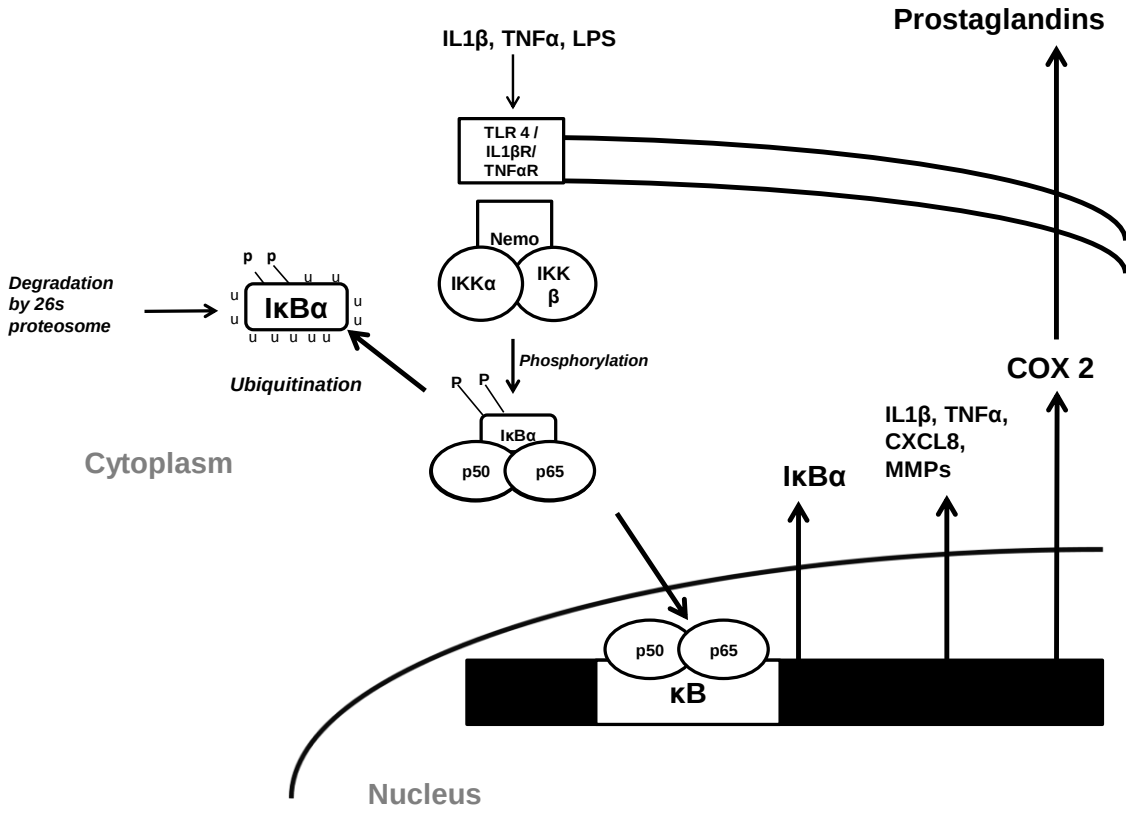

Figure 1.2: **Schematic representation of the canonical NFκB pathway**

Full description of the events leading to pathway activation are found in the main body of text (section 1.5.3.4)

1.6 The role of NFκB in preterm birth

The evidence that serves to underline the contribution made by NFκB activation in the pathogenesis of preterm birth is largely derived from in vitro studies on human primary cells of uterine and placental origin, with additional insights from animal models.

1.6.1 NFκB and uterine cells

The myometrium is the middle layer of the uterine wall, consisting mainly of uterine smooth muscle or myometrial cells, but also of supporting stromal and vascular tissue. During pregnancy it remains in a quiescent state to allow for fetal maturation but at term must be activated to allow for a series of powerful and co-ordinated contractions that expel the fetus during labour (Challis et al., 2000). Alteration of myometrial cell function has been the main target of the majority of treatments aimed at the prevention of preterm birth.

All the major components of the NFκB pathway have been identified within myometrial cells and tissues. The three components of the IKK family (IKKα, IKKβ and NEMO), the NFκB proteins Rel A, c-Rel, p105, p100 and p50 plus the inhibitory protein IκBα have been detected in human upper and lower myometrium (Chapman et al., 2004).

A link between NFκB activation, COX-2 expression and prostaglandin synthesis has been demonstrated in human myometrial cells in vitro (Belt et al., 1999). In this study, cells were exposed to the cytokine IL1β: within 15 minutes of stimulation 90% of IkBα was degraded, a concomitant increase in DNA binding of NFκB was observed alongside increases in COX2 mRNA and COX2 protein; this was followed by increases in prostaglandin production. With the addition of a synthetic peptide inhibiting the degradation and ubiquitination of IkBα these changes were inhibited, indicating an NFκB specific effect.

The activation of NFκB has been shown to promote the production of pro-inflammatory cytokines such as IL6 and IL8 (Soloff et al., 2004), matrix metalloproteinases (Choi et al., 2007), and to up-regulate the expression of genes associated with labour including the oxytocin receptor and connexin-43 within myometrial cells (Terzidou et al., 2006, Lye et al., 1993).

1.6.2 NFκB and placental cells

The fetal membranes, or chorioamniotic membranes, are made of two placental-derived layers: the amnion and chorion which surround and protect the developing fetus. The fetal surface of the amnion consists of an epithelial cell layer with an underlying mixed fibroblastic layer containing amnion mesenchymal cells. The chorion is comprised of cytotrophoblast cells and by late pregnancy is heavily invested in the decidua: the highly vascularised transformed endometrium which represents the innermost layer of the uterus during pregnancy. The role of placental-derived cells within the fetal membranes are broad and encompass barrier, paracrine signalling and immunologically protective roles during pregnancy (Myatt and Sun, 2010)

The key molecular components of the NFkB pathway have been identified in primary amnion cell cultures and fetal membrane tissue explants (Elliott et al., 2001, Lappas et al., 2002). IL1β addition to amnion mesenchymal cells activates the main components of the NFκB canonical pathway including the phosphorylation of IKK subunits, IκBα and p65. This leads to subsequent up regulation of COX2 mRNA and protein and increased production of prostaglandins and such changes can be reversed with the application of compounds capable of NFκB inhibition (Yan et al., 2002b, Ackerman et al., 2008). Amnion tissue explants when exposed to LPS demonstrated increased NFκB binding to DNA. Subsequently, increased production of cytokines IL6 and IL8 and matrix metalloproteinases was observed in these explants. These changes were reversed by the addition of the putative NFκB inhibitors N-acetylcysteine or sulphasalazine (Lappas et al., 2003, De Silva et al., 2010).

1.6.3 NFκB antagonism with pro-quiescent pathways

Studies have examined the interaction of NFκB with other pathways thought to promote myometrial quiescence and subsequent activation during labour as further evidence of the role of this transcription factor in promoting labour.

For lower order mammals such as mice and rats, labour and parturition are preceded by a decrease in circulating progesterone levels, thus highlighting the central role of progesterone in promoting myometrial quiescence (Csapo and Wiest, 1969). This phenomenon most likely does not occur in humans, although it remains a source of much debate (Smith et al., 2009). Many researchers have suggested that the myometrium may

become less sensitive to the effects of progesterone: a phenomenon referred to as 'functional progesterone withdrawal' (Mitchell and Wong, 1993). Mutual repression of NFκB and the progesterone receptor (PR) has been demonstrated using luciferase reporter activity in transfected amnion cells (Allport et al., 2001). Pre-treatment with progesterone reduced NFκB binding to COX2 promoter sites and subsequent COX2 mRNA expression in IL1β treated myometrial cell lines, whilst co-incubation with the anti-progestogen RU486 effectively blocked this progesterone-mediated inhibition (Hardy et al., 2006).

The G protein Gαs mediates myometrial quiescence through its action via the cyclic AMP pathway and subsequent increased activation of protein kinase A. Gαs protein expression is increased in the myometrium during gestation and is subsequently reduced during labour (Europe-Finner et al., 1993). In TNFα and LPS-treated primary myometrial cell cultures reductions in luciferase GαS reporter activity and reductions in GαS gene expression have been seen to correspond with increases in NFkB luciferase reporter activity. Thus, TNFα and LPS may repress the expression of the Gαs gene, an effect potentially mediated through the Rel-A NFkB subunit (Chapman et al., 2005)

Another level of uterine regulation during fetal maturation is placental corticotropin-releasing hormone (CRH) and its receptors CRH R1/2, which are thought to repress myometrial contractility via cAMP and nitric oxide synthase up-regulation (Grammatopoulos, 2007). In IL1β-stimulated myometrial cell cultures, CRH R1 gene expression was increased subsequent to IκBα degradation and p65 nuclear translocation, effects that were attenuated with the use of an IKK kinase inhibitor (Markovic et al., 2007).

The studies discussed above suggest that canonical activation of NFκB can be suppressed by pathways that promote myometrial quiescence during pregnancy and that activation of this transcription factor with the onset of term or preterm labour could override the inhibitory effect of such pro-quiescent pathways.

1.6.4 NFκB and animal preterm birth

In an elegant study which details the events that lead to mouse parturition, Condon et al. demonstrated that secretion of surfactant protein A (SP-A) from the maturing fetal mouse lung into amniotic fluid led to a macrophage invasion of the myometrium and increased IL1β secretion prior to delivery (Condon et al., 2004). Amniotic fluid macrophages isolated from

this mouse model expressed increased IL1β and p65 when exposed to SP-A, and injection of SP-A into amniotic sacs of pregnant mice caused preterm birth when compared to sham injection; similar injection of an inhibitor of NFκB nuclear localisation (SN50) produced a significant delay in the onset of labour when compared with an SN50 mutant control. Thus, the findings from this paper implicate the activation of NFκB as being central to murine labour.

Preterm birth may be precipitated in TLR4 normal mice by amniotic injection of heat killed bacteria. Toll Like Receptor 4 (TLR4) mutant pregnant mouse models have been developed that are resistant to this effect (Wang and Hirsch, 2003). This highlights the importance of signalling pathways downstream of TLR4, including the NFκB pathway, in effecting preterm birth in this model.

1.7 Drugs in clinical use for the acute prevention of preterm birth

Agents aimed at the acute prevention of preterm birth are a class of drugs referred to as tocolytics. Figure 1.3 details tocolytics that have been historically used in clinical practice and their respective mechanisms of action. Worldwide the therapies most commonly used for this purpose are β-agonists, calcium channel blockers, oxytocin receptor antagonists and COX inhibitors (Olson et al., 2008).

A Cochrane review of data from 20 clinical trials concluded that β agonists can delay birth for women in preterm labour by up to 7 days; however, they offer no benefit in terms of improving neonatal outcome or reducing neonatal deaths and are associated with significant maternal side effects including tachycardia, flushing, chest pain and maternal pulmonary oedema (Neilson et al., 2014).

Trials comparing the calcium channel blocker nifedipine to β-agonist tocolytic therapy have shown nifedipine to reduce the number of women giving birth within 7 days with reduced frequency of neonatal problems such as respiratory distress. Nifedipine also has a better side effect profile than β-agonists (King et al., 2003). This has led to the off license use of nifedipine within the UK as a first line tocolytic. This usage is not unproblematic however as calcium channel blockers have no specificity for the uterus and exhibit equal ability to relax vascular smooth muscle which has led to case reports of profound maternal hypotension with ensuing fetal death (van Veen et al., 2005).

Compared to placebo or β-agonist therapy a specific blocker of the oxytocin receptor (atosiban) has failed to show reduction in preterm birth incidence or improvements in neonatal outcome (Papatsonis et al., 2005). A trial comparing atosiban with nifedipine suggested similar ability to delay onset of preterm birth at 48 hours, but numbers were too small to be definitive, and this comparison is currently being addressed in a much larger multicentre study (Salim et al., 2012, van Vliet et al., 2014). Use of atosiban continues to be widespread in the UK as it is licensed for tocolysis use, has a minimal side effect profile and a potentially more specific mechanism of action than other currently available tocolytic therapies.

An alternative tocolytic strategy is non-selective inhibition of COX enzymes. Initial trial outcome data comparing the COX antagonist Indomethacin with placebo or other tocolytic showed promise with a reduction in births before 37 weeks and a reduction in maternal side effects compared to other agents (King et al., 2005). However the numbers involved in these trials were too small to be conclusive and use of these agents is associated with deleterious effects on the foetus including premature closure of the ductus arteriosus, renal and cerebral vasoconstriction and impaired renal development (Loudon et al., 2003).

Despite greater than 3000 clinical trials over 60 years, none of the tocolytic agents listed have led to significant improvements in neonatal outcome without an unacceptably high frequency of unwanted sequelae (Haas et al., 2012, Varner and Esplin, 2005). UK national guidelines, therefore, limit current usage to scenarios requiring patient transfer to another hospital unit or to 'buy time' to allow for effective administration of corticosteroids (Bennett P, 2011).

A partial explanation for this situation is the historic poor design of clinical trials with lack of placebo control, small numbers involved, variable inclusion criteria and use of increase in pregnancy length as the primary outcome measure, as opposed to a more clinically meaningful composite measure of neonatal wellbeing (Olson et al., 2008). However, the paucity of agents available is also a clear barrier to progress. Relatively few substances have been tested for their ability to dampen pathways of inflammation in a preterm birth scenario. This makes a novel approach to drug selection and an emphasis on pathway specificity a prime research consideration.

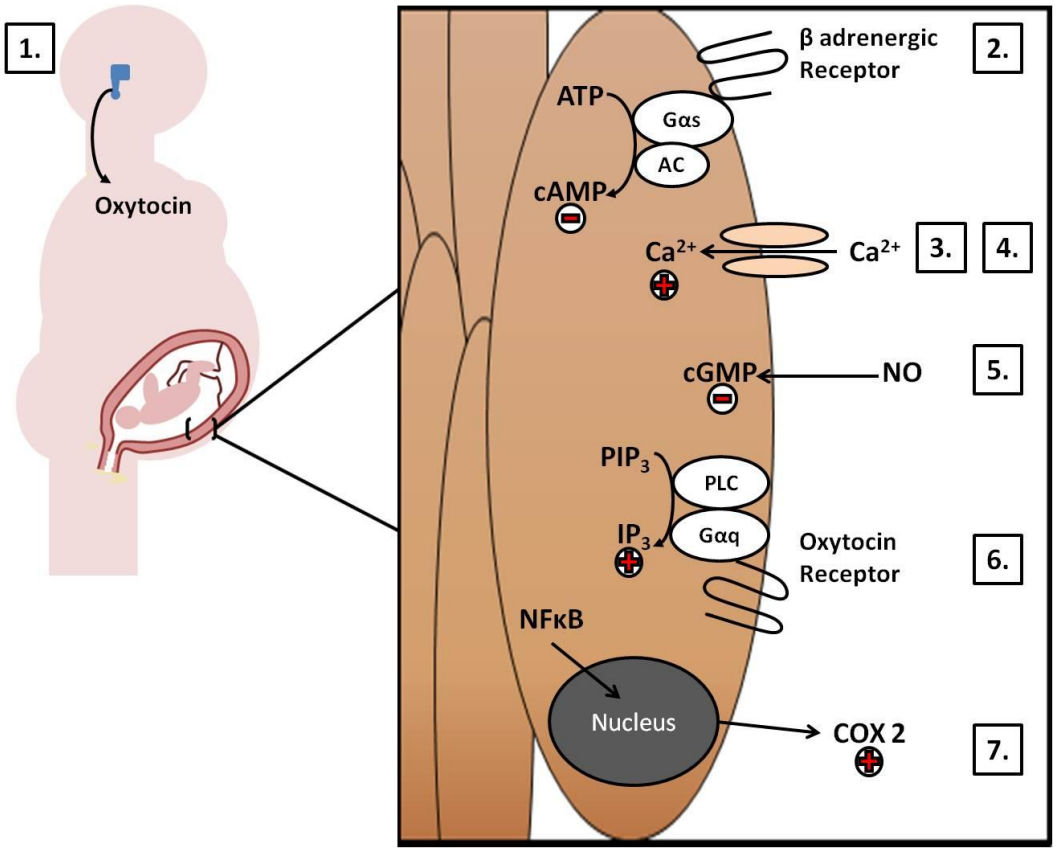

Figure 1.3: Mechanism of action of existing tocolytic therapies.

Pictorial representation of systemic (1) or local (2-7) action of tocolytics. Inset indicates uterine smooth muscle cell.

1. *Ethanol*: thought to diminish hypothalamic secretion of oxytocin when given intravenously.
2. *β–adrenergic agonists*: including isoxuprine, ritodrine, salbutamol, terbutaline and hexaprenaline. They exert action via Gαs-linked β receptors on the surface of myometrial cells. Ligand binding to receptor activates the enzyme adenylyl cyclase (AC) which converts adenosine triphosphate (ATP) into the secondary messenger cyclic adenosine monophosphate (cAMP) (Webb, 2003).
3. *Calcium Channel antagonists*: agents such as nifedipine or nicardipine block the intracellular entry of calcium via cell membrane channels.
4. *Magnesium Sulphate ($MgSO_4$)*: The putative mechanism of action for $MgSO_4$ involves antagonising the intracellular entry of calcium via cell membrane channels.
5. *Nitric Oxide Donors*: The nitric oxide donors glyceryl trinitrate and nitroglycerine increase levels of cyclic guanylate monophosphate (cGMP) within myometrial cells which in turn inhibit MLCK leading to smooth muscle relaxation (Norman and Cameron, 1996).
6. *Oxytocin receptor antagonists*: such as atosiban block oxytocin binding with its Gαq-protein linked receptor on the myometrial cell surface. This prevents activated phospholipase C (PLC) from producing the secondary messenger inositol 1,4,5 triphosphate (IP3) from an inactive precursor (PIP3). IP3 causes intracellular release of calcium from the sarcoplasmic reticulum leading to muscle contraction (Webb, 2003).
7. *Cyclooxygenase (COX) Inhibitors*: COX proteins are rate limiting enzymes in the production of prostaglandins from arachidonic acid. COX1 is a non-inducible housekeeping protein whereas COX2 is a highly inducible protein whose expression in gestational tissues is promoted by activation of NFκB (Belt et al., 1999, Yan et al., 2002).

1.8 Novel agents for the acute prevention of preterm birth

A comprehensive network meta-analysis comparing tocolytic therapies concluded that prostaglandin inhibitors and calcium channel antagonists were the most likely agents to produce delay in labour and that, of these two approaches, prostaglandin inhibitors were the least likely to produce side effects (Haas et al., 2012). Therefore, it is unsurprising that the majority of novel pharmaceutical approaches to acute preterm birth prevention have looked to either directly inhibit prostaglandin production, or to do so indirectly via the inhibitory targeting of either COX2 or pro-inflammatory pathways in uterine and placental cells.

A route to tocolysis is offered by blockade of the Prostaglandin F2α receptor. THG113, an inhibitor specifically targeting this receptor, has been used successfully in sheep models to treat preterm birth initiated by progesterone blockade (Hirst et al., 2005). Due to limited placental transfer THG 113 has the potential to avoid the adverse effects associated with fetal prostaglandin blockade and does not interfere with fetal prostaglandin E2 production (Olson, 2005). However, this agent has yet to get beyond a preclinical stage of testing.

The tocolytic potential of selective COX2 inhibitors has been tested with initial in vitro studies showing promising results (Doret et al., 2002). Unfortunately, the only human trial administering rofecoxib, a specific COX2 inhibitor, to mothers at risk of preterm birth did not achieve delay in birth compared to the placebo controlled group and demonstrated high rates of reversible fetal renal insult in the treatment arm (Groom et al., 2005).

Inhibition of inflammatory pathway signalling has been demonstrated in vitro in utero-placental cells via a number of agents including Pattern Recognition Receptor (PRR) antagonists such as anti-TLR 4 antibodies; p38 MAP Kinase blockers and a range of NFκB inhibitors (Adams Waldorf et al., 2008, Keelan et al., 2009, Lappas et al., 2007). These agents putatively offer targeting of specific molecular components of inflammatory pathways.

Recent research in the preterm birth sphere has examined the effects of a class of drugs referred to as the Cytokine Suppressant Anti-Inflammatory Drugs (CSAIDS). Such agents operate via a broad range of molecular mechanisms and include: inhibitors of IKKβ (TCPA1), TAK 1 (OxZnl), NFκB (N-acetyl cysteine), p38 MAP Kinase (SB239063) and inhibitors of the IKK complex (CPP-conjugated NBD peptide – see below) (Ng et al., 2015). Varying anti-

inflammatory effects have been reported for CSAID compounds used in a pregnant sheep model for both in vivo and ex vivo preparations; however these studies were disadvantaged by a failure to test any one agent across a full dose range, indicating that optimal inhibition effects may not have been elicited (Ireland et al., 2015, Stinson et al., 2014).

Although many of the approaches described above show promise in inhibiting inflammatory responses; they are yet to translate into a clinical setting. Such methods are also reliant on the success of individual therapeutic agents leading to a 'back to the drawing board' approach should these agents fail at any stage of pre-clinical testing. A different therapeutic development strategy, allowing for a broad range of intracellular inhibitory targets, may offer greater success.

1.9 Cell Penetrating Peptides as drug delivery vectors

A major barrier to the development of new pharmaceuticals is presented by the cell membrane: to overcome this obstacle and therapeutically alter intracellular molecular pathways requires the use of vector techniques to deliver biologically effective cargo internal to a cell. Cell Penetrating Peptides (CPPs) offer an attractive solution to this drug delivery puzzle: they have been shown to deliver cargo efficiently at low doses and with low toxicity to a diverse range of cell types (Heitz et al., 2009).

CPPs can be characterised as short peptides, usually less than 30 amino acids length, that have the ability to cross cell membranes without the need for recognition by cell surface receptors (Bechara and Sagan, 2013). The majority of CPPs have a net positive charge at physiological pH and are usually water soluble and hydrophobic, although some variation exists between different CPP classes (Madani et al., 2011).

Most importantly CPPs have the ability to deliver intracellularly an ever growing variety of cargo including proteins, siRNA, liposomes, fluorophores and nanoparticles across cell membranes and also facilitate intracellular endosomal escape of these payloads (Jones and Sayers, 2012, Endoh and Ohtsuki, 2009). Thus CPPs are often referred to in the literature as 'Trojan peptides' (Derossi et al., 1998) and there exists a large field of research evaluating their potential as drug delivery vectors.

Amongst the large number of naturally occurring and synthetic CPPs now described in the literature; the CPPs included in this study are derived from three well characterised peptide vectors. Firstly, a CPP derived from the homeodomain of the antennopaedia protein of the fruit fly Drosophila, $Pen_{(43-56)}$ (Derossi et al., 1994, Christiaens et al., 2004, Fischer et al., 2000), secondly a CPP derived from the transcription transactivating protein of HIV, $TAT_{(47-57)}$ (Vives et al., 1997, Wadia and Dowdy, 2005); and finally a CPP based on synthetically derived poly-arginine residues: R8 (Futaki, 2002, Nakase et al., 2004).

1.9.1 Mechanism of CPP uptake

There are two major mechanisms of CPP cellular uptake described in the literature: energy independent or non-endocytic pathways and endocytic pathways (Madani et al., 2011b). The method of uptake is dependent on a number of factors including the CPP used, the cell type and the experimental or physiological conditions. The same CPP can display different modes of uptake depending on the circumstances described above (Hallbrink et al., 2004).

Non-endocytic uptake or 'translocation' initially involves interaction of the positively charged CPP with negatively charged components of membrane such as heparan sulfate as well as the phospholipid bilayer (Herce and Garcia, 2007). Following this, a membranous pore is formed allowing the CPP and cargo to enter the cytosol (Matsuzaki et al., 1996). Alternatively, CPPs can take advantage of different endocytic forms of cellular entry including phagocytosis, pinocytosis or clathrin-dependent and independent endocytosis (Cleal et al., 2013).

1.9.2 Therapeutic potential of CPP-cargo conjugations

The potential offered by CPPs conjugated to cargo in the clinical setting was demonstrated with the discovery that murine intra-peritoneal injection of β-galactosidase protein (120KDa), linked to a CPP derived from TAT protein, resulted in β-galactosidase uptake in all tissues including the brain (Schwarze et al., 1999). A number of studies in diverse clinical fields have confirmed the potential of CPP-cargo conjugates as therapeutic agents: TAT mediated delivery of a peptide derived from the tumour suppressor protein p53 led to regression of tumour load in a mouse model of peritoneal cancer (Snyder et al., 2004), TAT-Bclxl conjugates have been shown to decrease neuronal damage in mouse models of stroke (Cao et al., 2002) and CPP linked inhibitors of protein kinase Cδ prevented reperfusion injury

in rat ex vivo models of ischaemic hearts (Inagaki et al., 2003). Indeed, the TAT-protein kinase Cδ inhibitor (KAI-9803) has progressed to phase two clinical trial where it was administered into coronary arteries as an adjunct to percutaneous coronary intervention in patients suffering from myocardial infarction (Johnson et al., 2011).

1.9.3 Cell Penetrating Peptide inhibitors of NFκB

Amongst the diverse array of cargoes that can be conjugated to CPPs and delivered intracellularly are molecules with the capability to block NFκB dependent signalling (Orange and May, 2008). Those described in the literature include either peptide or protein cargo directed towards a variety of targets including the IKK complex, the nuclear localisation sequence of p50, p65 phosphorylation sites or the inhibitory protein IκBα (Lin et al., 1995, Takada et al., 2004, Fujihara et al., 2005, May et al., 2000).

Such CPP-cargo conjugates have shown success both in vitro and in vivo at inhibiting NFκB mediated inflammatory responses, including large animal models (Ankermann et al., 2005), and they offer the possibility of translation into the clinical sphere for scenarios whereby discrete inhibition of NFκB signalling is desirable (Orange and May, 2008).

1.9.4 The Nemo Binding Domain (NBD) peptide as a tool for NFκB inhibition

The NBD peptide is an 11 amino acid residue peptide which was designed to prevent IKK activation via the canonical NFκB pathway. It achieves this by spanning the six amino acid (LDWSWL) segment Nemo Binding Domain of the IKK complex and, therefore, disrupting the interaction between the two active IKKα and IKKβ subunits and the regulatory subunit NEMO (May et al., 2000). Linked to a CPP derived from antennopaedia protein, the NBD peptide was able to dose-dependently inhibit TNFα-stimulated NFκB signalling in HeLa cells, a phenomenon that did not occur with the application of a mutant NBD peptide containing two amino acid substitutions (May et al., 2000). Both wild type and mutant forms of this peptide are displayed in Figure 1.4.

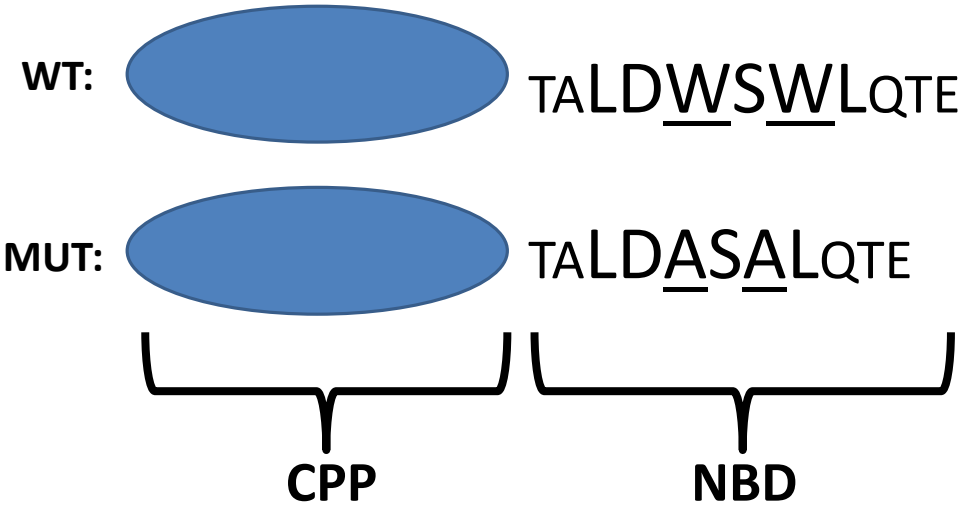

Figure 1.4: The Nemo Binding Domain (NBD) Peptide

Pictorial illustration of the primary amino acid structure of the NBD wild type (WT) and mutant (MUT) peptide conjugated to CPP. Larger text indicates the amino acid structure of the Nemo Binding Domain. The substituted tryptophan (W) to alanine (A) amino acid residues are underlined.

The NBD peptide, conjugated to CPP vectors, has been shown to down-regulate unwanted NFκB responses and thus improve physiological endpoints of inflammation in a number of in vitro and in vivo models (McCorkell and May, 2015). It potentially offers the possibility of preserving basal activity of NFκB whilst impairing cytokine stimulated responses: an approach that may avoid toxic side effects associated with complete NFκB blockade (May et al., 2000). As a result the NBD peptide is currently on the verge of being tested in phase 1 clinical trials for diverse conditions including Muscular Dystrophy and Parkinson's Disease (Reay et al., 2011, Roy et al., 2015).

Therefore, given the promise this of peptide cargo in many pre-clinical research settings and the significant contribution that NFκB plays in the pathogenesis of preterm birth, NBD peptide was selected in this study as the optimal cargo both to test CPP-conjugate delivery and the ability of CPPs to deliver cargo that can be biologically effective in uterine cells.

1.10 Small molecule, non-peptide inhibitors of NFκB

To allow for comparison between the biological effectiveness of CPP-conjugated inhibition of inflammatory signalling and non-CPP linked methods of inhibition, a series of non-peptidic small molecule inhibitors with NFκB inhibitory activity were also used in this study.

Small molecule inhibitors at all levels of the NFκB pathway have been reported including those blocking the phosphorylation of IkBα via IKK complex inhibition or preventing proteasome degradation of this molecule; inhibitors that prevent NFκB localisation to the nucleus or block post translational modifications of p65 (Gupta et al., 2010). The advantages of using small molecule drug inhibition include wide oral bioavailability and a well-established approach that can provide discrete inhibition of specific pathways; however, high concentrations may be required to pass intracellularly thus increasing the potential for toxicity, and such agents are often targets for swift removal via drug efflux proteins (Mandery et al., 2012). Some of the most promising non-peptide small molecule inhibitors of NFκB are outlined below.

Sc514 is a thiophene carboxamide capable of inhibiting IKKβ by reversibly competing with its ATP binding site. In cell free assay, it has a high degree of selectivity for IKKβ above other IKK isoforms or serine-threonine or tyrosine kinases (Kishore et al., 2003), and, therefore, putatively offers discrete inhibition of the NFκB pathway via a mechanism similar to the NBD peptide. It has demonstrated ability to reduce LPS-stimulated TNFα secretion in placentally-derived human primary cells (De Silva et al., 2010).

N-acetylcysteine (NAC) is an antioxidant that increases intracellular glutathione concentrations to act as an endogenous reducing agent. There is evidence that NAC may also mediate effects on NFκB by suppression of the action of the IKK complex on IκBα (Oka et al., 2000). The use of NAC clinically is well established in the acute setting of treatment for paracetamol overdose (Ferner et al., 2011). NAC has been shown to abrogate LPS-stimulated prostaglandin production by fetal membranes in vitro, to attenuate LPS provoked IL6 production in the amniotic fluid of pregnant rats and has been suggested to reduce the recurrence of preterm birth in women with bacterial vaginosis in clinical trial (Lappas et al., 2003, Beloosesky et al., 2006, Shahin et al., 2009). However, its effects on myometrial cells have yet to be examined.

Curcumin is the active ingredient of the spice turmeric and is a naturally occurring polyphenol derived from the Curcuma longa plant with the potential for treatment of various diseases acting via NFκB inhibition (Aggarwal et al., 2007). Application of this natural product led to inhibition of NFkB dependent inflammatory signalling in uterine decidual cells (Devi et al., 2015), and prevented inflammatory cytokine signalling in human fetal membrane explants and uterine myometrial cells (Lim et al., 2013).

Mg132 is a proteasome inhibitor with the capability to prevent NFκB signalling via blocking the proteasome-dependent degradation of phosphorylated IκBα. It has been shown to prevent the IL1β stimulated activation of NFκB in both human myometrial cells and amnion cells (Belt et al., 1999, Mohan et al., 2007).

1.11 Study Hypothesis and Aims

It is hypothesised that CPPs will be able to deliver cargo internal to human uterine and placental cells. Moreover, CPPs linked to biologically effective cargo will dampen NFκB related intracellular signalling within uterine cells by comparison to a series of small molecule inhibitors.

In testing these hypotheses the aims are:

(i) To define the efficacy (time- and dose-dependency) of CPPs to deliver fluorescent cargo to primary human myometrial and amnion cells.

(ii) To determine the ability of fluorescent CPPs conjugated to the NBD peptide to enter human myometrial cells.

(iii) To determine the ability of CPP-NBD peptide conjugates to inhibit inflammatory signalling in human myometrial cells.

(iv) To examine the effectiveness of CPP-NBD peptide conjugates in dampening NFκB related signalling compared to a series of small molecule inhibitors of NFκB in human myometrial cells.

Chapter Two

Materials and Methods

2.1 Materials

For ease of reference the materials and supplier used, including catalogue number, have been included within the relevant section of text. All suppliers are UK-based unless otherwise specified.

2.2 Subjects and samples

Ethical approval was obtained from Newcastle and North Tyneside Research Ethics Committee (10/H0906/71) to perform research on samples collected as part of the Newcastle Utero-placental Tissue Bank. Human myometrial tissue and placentas were obtained following written informed consent from non-labouring women with uncomplicated, singleton pregnancies undergoing elective Caesarean section at term (≥37 weeks gestation).

Myometrial muscle strip biopsies approximately 1cm x 1cm in size were taken from the upper portion of the lower segment uterine incision according to longstanding protocol at Newcastle upon Tyne Hospitals NHS Foundation Trust. Biopsies were excluded from women with underlying medical or obstetric disease, women on any current medication, those with a body mass index out with 20-35 kg/m^2, or who gave birth to a baby with weight below the 10^{th} percentile or above the 90^{th} percentile. Fifty five separate patient samples were included in the study of which forty six were myometrial biopsies and nine placentas. Demographic data of patients included is reported in Table 2.1.

Characteristic	Mean	Range
Gestation (weeks)	39	37- 41
Age (years)	32	21-46
Gravidity	3	1-6
Parity	1	0-3
Booking BMI (kg/m^2)	25	20-33
Birthweight (g)	3422	2710-4135
Birth weight centile (%)	49	10.3-86

Table 2.1 Demographic characteristics of the study population (n=55)

2.3 Cell culture

The majority of experiments used primary myometrial cells prepared from fresh biopsy samples collected as described above. On occasions where such biopsies were not available, previously frozen myometrial cells were defrosted and grown in T75 flasks in readiness for experimentation. Amnion mesenchymal cells were prepared from fresh placental tissue.

2.3.1 Cell culture consumables and reagents

T25 and T75 cell culture flasks (C6481, C7231), were sourced from Sigma Aldrich. 6, 12 and 96 well plates (657160, 665180, 655180) plus 70µm cell strainers (542070) were sourced from Greiner. Fetal calf serum (FCS) (F9665), penicillin / streptomycin (10,000U /10mg) (P0781), 0.5g porcine trypsin / 0.2g EDTA (T3924), Hanks buffered saline solution (H6648), phosphate buffered saline (PBS) (P4417) and heparin sodium salt (H3149), collagenases 1a (C9891) and XI (C7657) and bovine serum albumin (BSA) (A6003) and dimethyl sulfoxide (DMSO) (D2650) were sourced from Sigma Aldrich. GlutaMAX media (61965) and phenol red free Dulbecco modified eagle medium (DMEM) (21063) were sourced from Life Technologies. Mr Frosty freezing container (5100-0001) and 1ml cryovials (5000-1012) were sourced from Thermo- Scientific. Unless otherwise specified the cell media used for all culture and experimentation is GlutaMAX containing 10% FCS and 1% penicillin / streptomycin.

Tissue collection buffer was made up in our laboratory according to the following recipe: NaCl 154mM; KCl 5.4mM; $MgSO_4/7H_2O$ 1.2mM; 3(N-morpholino) propanesulfonic acid 10mM; glucose 5.5mM; $CaCl_2/2H_2O$ 1.6mM; pH7.4.

2.3.2 Preparation of myometrial cells

Lower uterine segment human myometrial biopsies were immediately transferred from the operating theatre to the laboratory in tissue collection buffer. Samples were micro-dissected under a light microscope to isolate myometrial tissue from any remaining decidua. In a microbiological safety cabinet, tissue was cut into small fragments before adding 10mls warmed Hanks balanced salt solution containing 10mg each of collagenase 1A and XI plus 20mg BSA. This tissue digestion mix was placed in an orbital shaker at 110rpm for approximately 40 minutes at 37°C. Checking the digestion mix visually allowed for confirmation that cells had dissociated sufficiently when small tissue fragments appeared

ragged but not fully degraded. At this point, the sample was filtered through a 70µm cell strainer into 10ml media and centrifuged at 1000 rpm for 5 minutes. The supernatant was discarded and cell pellet re-suspended in cell culture media in a T25 cell culture flask (Karolczak-Bayatti et al., 2011).

2.3.3 Preparation of amnion mesenchymal cells

Placentas were transferred immediately from delivery suite to the laboratory. Reflected amnion was separated from choriodecidual tissue by blunt dissection and washed repeatedly in phosphate buffered saline. In a microbiology safety cabinet, amnion tissue was then cut into 2x2cm squares and transferred into a sterile tube containing 20 ml of PBS with 1 mg/ml of collagenase A and then incubated at 37°C with in an orbital shaker for 2 h. After digestion, collagenase was neutralised with a further 20mls of media and the remaining cell suspension filtered through a 70µm cell strainer. The cell suspension was centrifuged at 1000rpm for 5 minutes, the supernatant was discarded and the cell pellet re-suspended in cell culture media in a T25 cell culture flask (Yan et al., 2002b).

2.3.4 Frozen cells

Frozen primary myometrial cells were defrosted from liquid nitrogen into warmed 10ml cell culture media and centrifuged at 1000 rpm for 5mins. The DMSO containing medium was discarded and cell pellets were dispersed in fresh media.

2.3.5 Cell maintenance

All final cell pellets were re-suspended in fresh media containing 10% FCS, 50µg/ml of penicillin and 50µg/ml of streptomycin. This cell suspension was then transferred into a T25 or T75 cell culture flask dependent on the size of the cell pellet and cultured at 37°C, 5% CO2/95% air with fresh media replacement every 2-3 days until 80-90% confluent (Karolczak-Bayatti et al., 2011, Casey and MacDonald, 1996).

2.3.6 Cell splitting and transfer

Once confluent, cells were washed with PBS before the addition of trypsin/EDTA solution (1ml for T25, 3mls for T75). Once cells were fully lifted off the flask surface, cell media was added at a ratio of two parts media: one part trypsin / EDTA to neutralise the trypsin effect. This cell suspension was transferred to a sterile tube for centrifugation at 1000 rpm for 5mins. The trypsin/EDTA containing supernatant was discarded and the cell pellet was re-

suspended in a varying volume of cell culture media, aiming for cell seeding at 30% density in final well destination. For example: if splitting cells from a T75 flask into three further T75's, 9mls cell culture volume was used for re-suspension and 3mls cell suspension added to each flask along with 7mls of further media.

2.3.7 Freezing cells

Cells frozen for storage underwent splitting as described above and were re-suspended in 1ml of FCS containing 10% DMSO before transfer to a 1ml cryovial that was placed in a specialised freezing container (Mr Frosty) overnight in a -80°C freezer before further transfer of the cryovial into liquid nitrogen the following day.

2.4 Cell Penetrating Peptides

CPPs were custom synthesised commercially and purchased from either EZ Biolabs (USA) or Abingdon Health Laboratory services.

2.4.1 Peptide labelling

CPPs were labelled with two types of fluorophore cargo. Alexa 488 peptide labelling was performed at the laboratory of our collaborator (Professor Jones, Cardiff University) according to previously reported methods (Al-Taei et al., 2006). In these cases, labelling occurred at the N-terminus with alexa 488 C_5 maleimide (Invitrogen, A-10254). Labelled samples were then purified by high performance liquid chromatography and characterised by mass spectrometry with example traces given in Figure 2.1. Alexa 488 was used in these circumstances due to relative ease of labelling. CPPs that were custom synthesised via EZ peptides were rhodamine labelled at the N-terminus by the supplier. 5(6)-Carboxytetramethylrhodamine was used in these cases due to ease of availability for the supplier.

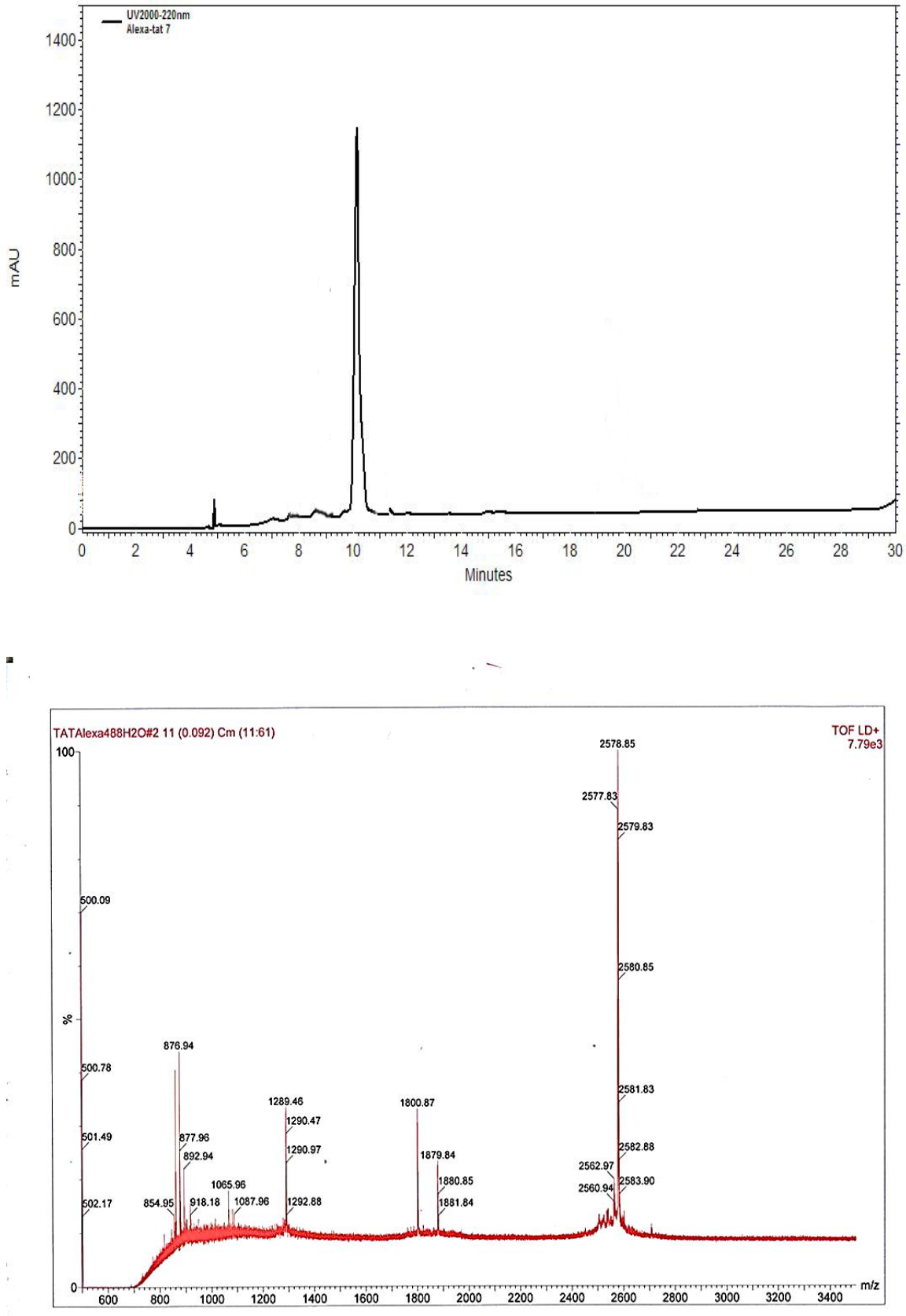

Figure 2.1 High performance liquid chromatography (upper panel) and mass spectrometry (lower panel) tracings of alexa 488 conjugated TAT peptide as labelled and produced by our collaborative group (Professor Jones, Cardiff University)

2.4.2 Peptides used in confocal experimentation

The amino acid structure and excitation / emission spectra of fluorescently labelled peptides used in cellular uptake experimentation and analysed by confocal microscopy are shown in Table 2.2. CPP vector uptake experiments were undertaken using CPPs derived from the proteins antennopedia (Pen: residues 43-56), HIV transcription transactivating domain (TAT: residues 47-57) or synthetic polymers of multiple arginine residues (R8) conjugated to either the fluorophores alexa 488 or rhodamine (peptide conjugates 1-8 as displayed in Table 2.2). Fluorescently labelled peptides with CPP vector conjugated to biological cargo were used in subsequent experimentation (peptide conjugates 9-13 as displayed in Table 2.2) to determine the effects of peptide cargo on cellular uptake.

Peptide No.	Peptide Name	Structure	Excitation	Emission
1	**Alexa 488 labelled Pen**	**Alexa 488 - RQIKIWFQNRRMKWKK**	**488nm**	**525nm**
2	**Alexa 488 labelled TAT**	**Alexa 488 - YGRKKRRQRRR**	**488nm**	**525nm**
3	**Alexa 488 labelled R8**	**Alexa 488 - RRRRRRRR**	**488nm**	**525nm**
4	**Alexa 488 labelled GS_4(GC)**	**Alexa 488 - GSGSGSGSGC**	**488nm**	**525nm**
5	**Rhodamine labelled Pen**	**Rhodamine - RQIKIWFQNRRMKW**	**488nm**	**525nm**
6	**Rhodamine Labelled TAT**	**Rhodamine - YGRKKRRQRRR**	**561nm**	**617nm**
7	**Rhodamine labelled R8**	**Rhodamine - RRRRRRRR**	**561nm**	**617nm**
8	**Rhodamine labelled GS_4(GC)**	**Rhodamine - GSGSGSGSGC**	**561nm**	**617nm**
9	**Rhodamine labelled Pen - Nemo Binding Domain (Wild type)**	**Rhodamine-RQIKIWFQNRRMKW-Aca- TALDWSWLQTE**	**561nm**	**617nm**
10	**Rhodamine labelled Pen - Nemo Binding Domain (Mutant)**	**Rhodamine-RQIKIWFQNRRMKW-Aca-TALDASALQTE**	**561nm**	**617nm**
11	**Rhodamine labelled Nemo Binding Domain**	**Rhodamine - TALDWSWLQTE**	**561nm**	**617nm**
12	**Rhodamine labelled TAT Nemo Binding Domain**	**Rhodamine - YGRKKRRQRRR-Aca-TALDWSWLQTE**	**561nm**	**617nm**
13	**Rhodamine labelled R8 Nemo Binding Domain**	**Rhodamine-RRRRRRRR-Aca-TALDWSWLQTE**	**561nm**	**617nm**

Table 2.2 The nomenclature, structure and excitation / emission wavelengths of fluorophore conjugated peptides used for live cell confocal microscopy experimentation

2.4.3 Peptides used in cell stimulation experiments

The amino acid structure, batch number and supplier of peptides used in cell stimulation experimentation are shown in Table 2.3. Different CPP vectors conjugated to Nemo Binding Domain (NBD) peptide were used to test the ability of NBD cargo to dampen inflammatory responses in uterine cells. Either unconjugated CPP (Pen), NBD peptide alone or a CPP conjugated NBD mutant peptide (Pen-NBD Mut) were used as comparative controls.

Peptide Name	Structure
Pen	**RQIKIWFQNRRMKW**
Nemo Binding Domain	**TALDWSWLQTE**
Pen Nemo Binding Domain Wild Type (Pen-NBD WT)	**Ac-RQIKIWFQNRRMKW-Aca-TALDWSWLQTE-NH2**
Pen Nemo Binding Domain Mutant (Pen-NBD Mut)	**Ac-RQIKIWFQNRRMKW-Aca-TALDASALOTE-NH2**
TAT Nemo Binding Domain Wild Type (TAT-NBD)	**Ac-YGRKKRRQRRR-Aca-TALDWSWLQTE-NH2**
R8 Nemo Binding Domain Wild Type (R8-NBD)	**Ac-RRRRRRRR-Aca-TALDWSWLQTE-NH2**

Table 2.3 The nomenclature and structure of peptides used for cell stimulation experimentation

2.5 Live cell confocal microscopy

To determine the cellular uptake of fluorescent moieties conjugated to CPPs and thus characterise the ability of CPP to deliver cargo internally to myometrial cells, live cell spinning disk confocal microscopy was used (Andor Revolution XD coupled to an Olympus IX-81 inverted microscope; Andor Belfast UK; http://www.andor.com/microscopy-systems/revolution). This technique enabled identification of real time changes in fluorescence across cell populations and also allowed the use of fine optical image slices within the z plane to determine fluorescent cargo uptake across whole cells.

2.5.1 Dyes and emission / excitation wavelength spectra used in confocal experimentation

Hoechst nuclear dye (33342 - excitation 345nm/emission 525nm), ER-tracker (E34250 - excitation 587nm/emission 615nm), Mito-tracker (M22425 - excitation 587nm/ emission 615nm) and Dextran Alexa Fluor 488 (D22910 - excitation 495nm/ emission 519nm) were all sourced from Life Technologies.

2.5.2 Preparation of cells for microscopy

Low passage (P≤4) myometrial or amnion mesenchymal cells were used. Following cell culture and splitting, cells were transferred into 4- or 8-well microscope µ-Slides (Ibidi, Thistle Scientific, IB-80441, IB-80821) and grown up to 80%-90% confluency. Cells were washed in PBS and changed to serum reduced media (0.1% FCS) for 18 to 24 hours to minimise cell cycle related artefact and avoid inhibitory effects caused by serum proteins (Khammanit et al., 2008). Cells were then loaded with 1µM Hoechst nuclear dye for 1 hour and washed with PBS before the microscope µ-slides were transferred to the confocal microscope in readiness for CPP addition and imaging.

2.5.3 Labelling of endoplasmic reticulum or mitochondria

For experiments whereby further labelling of endoplasmic reticulum or mitochondria was desired, ER Tracker dye or Mitotracker dye both at 1µM concentration were added along with Hoescht nuclear dye for 1 hour followed by PBS washout as described.

2.5.4 Labelling of endosomes / lysosomes

In order to assess the co-localisation of CPP with intracellular transportation pathways, dextran conjugated to alexa 488 fluorophore was used. As a large molecule, dextran is taken

up into endosomal / lysosomal pathways within the cell, with the conjugated fluorophore allowing this pathway to be tracked via confocal imaging (Kuipers et al., 2004).

Two approaches were taken to achieve this: firstly, to label endosomes, cells were incubated with 100μg/ml dextran alexa 488 in media for 1 hour before washing with PBS followed by the addition of CPP-rhodamine conjugates. Secondly, to label the lysosomal pathways cells were incubated with 200μg/ml dextran alexa 488 in media for 2 hours, washed with PBS and then left overnight in complete media before the addition of CPP-rhodamine conjugates.

2.5.5 Cell Imaging

During the time course of experimentation cells were maintained on microscope slide wells in serum deprived media within a temperature-controlled chamber (maintained at 37°C, 5%CO_2, Prior Scientific Ltd., Cambridge, UK) on the stage of the inverted microscope.

Initial images were collected to assess baseline cellular auto-fluorescence prior to addition of CPP. Varying concentrations of fluorophore-CPP / fluorophore-CPP-Cargo / fluorophore-cargo combinations (see Table 2.2) were ready made up in serum deprived cell media and added to the cells. Images were then captured at 15, 60 and 120 minutes following application. For the imaging period cells were placed in phenol red free media to reduce background glare. To make a thorough assessment of fluorescent uptake throughout whole cells, all images were captured as a series of slices in the Z plane (range 3-10 slices per area selected, each slice 0.54μm apart) using the 40x objective. Images were captured using separate channels for epifluorescence (Hoechst), fluorophore (rhodamine / alexa-488) and bright-field; all images were digitally recorded with IQ2 software (Andor, Belfast, UK).

2.6 Picture analyses

At each data point 3-5 sets of Z-series images were collected and stored as TIFF files. Each Z-series contained an average of 5 slices (range 3-10). Images were stacked and organised into separate channels according to staining (i.e. Hoechst staining channel to identify cell nucleus, flourophore staining channel to identify peptide uptake), the organised TIFF files were then either fed into Cell Profiler software or further analysed in Image J. Data was collected prior to addition of fluorophore-CPP combination (T0) and 15, 60 and 120 minutes following addition of fluorophore-CPP. To correct for varying levels of cellular auto-fluorescence, the mean average background fluorescence of cells at T0 was calculated and has been subtracted from the data at all subsequent time points.

2.6.1 Use of Cell Profiler

Cell Profiler (http://www.cellprofiler.org/) is free open-source software that allows automated quantitative measurement of thousands of images (Carpenter et al., 2006). Standard cell analysis processes are referred to as pipelines within Cell Profiler. These pipelines take steps to threshold images to remove background noise, identify cells via nuclear staining and subsequently identify cytoplasmic areas of staining in order to measure the intensity of staining within these regions. Such a pipeline was modified for the images in this study to reproducibly recognise areas of staining close to the nucleus of each cell within every z-slice; this pipeline was then run for all image series providing a quantitative result of the intensity of uptake for cells within each Z-slice image. After discarding cells from the edge of the image (for whom whole cell staining could not be measured) staining from all cells within a given image (range 3-27) was measured across all z slices (range 3-10). Three to five image stacks were analysed per time point and this process was repeated across 3 biologically separate experiments. A further explanation of this process is detailed in Figure 2.2.

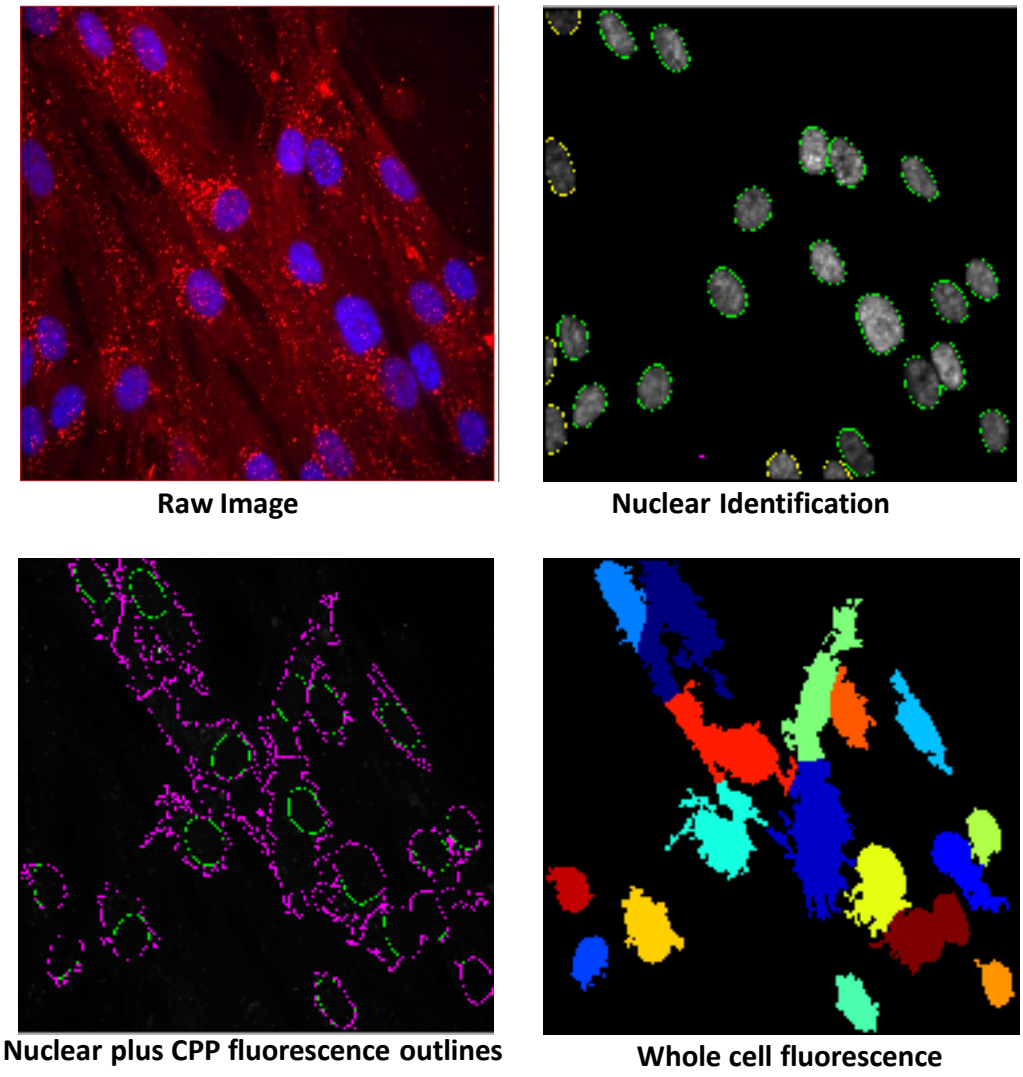

Figure 2.2 Example pipeline demonstrating Cell Profiler image analysis process

The raw data (top left image) is fed into the analysis pipeline as a composite consisting of two images: a nuclear staining channel (blue) and rhodamine CPP fluorescence channel (red). The software identifies cellular location via the nuclear channel (top right image), disregarding any cells on the edge of the picture (outlined yellow). The pipeline superimposes nuclear outlines onto the rhodamine-CPP fluorescence channel (bottom left image) and identifies areas of intense fluorescence located near to nuclei (purple outlines). The software recognises these areas as separate cells and labels them with a different colour for each cell (bottom right image). It then measures the pixel intensity from the fluorescence-CPP channel for nuclear areas, whole cell areas or cytoplasmic areas (whole cell minus nuclear area) for every cell to produce an integrated density (the sum of all pixel intensity values within a given area) or mean intensity (the sum of pixel values divided by area size) value per cell. The software can perform these functions for a series of Z-slice images thus generating whole cell fluorescence data for every cell in a given image series.

2.6.2 Use of Image J

Image J *(http://imagej.nih.gov/ij/)* is a widely used open source image analysis software program. Areas of peptide uptake internal to the cell membrane were selected and the integrated density (the sum of pixel intensity within a given area) was recorded from the Rhodamine channel alongside a background fluorescence measurement external to the cell (demonstrated in Figure 2.3). A value of Corrected Total Cell Fluorescence (CTCF) was arrived at using the following formula: Integrated density – (Area of selected measurement / mean background fluorescence) (Burgess et al., 2010). For each image 3 cells were selected and analysed at 3 z slices (0.54µM thick). Three to five image stacks were analysed per time point and this process was repeated across 3 biologically separate experiments.

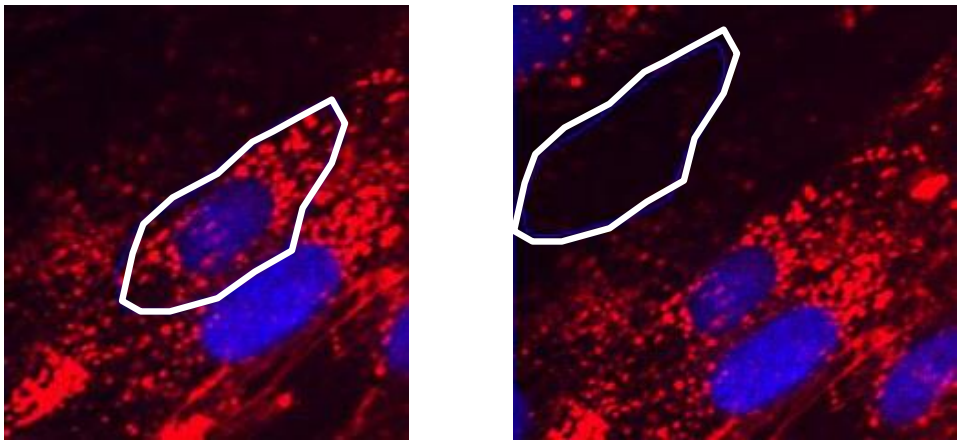

Figure 2.3 Cell fluorescence analyses via Image J software

Areas of peptide intensity were selected (left hand image) and measured with a spline cursor (white line) alongside areas of background fluorescence (right hand image). Fluorescence data from the Rhodamine-CPP (Red) channel was measured within this cursor to produce a value of integrated density (sum of pixel intensities within a given area). Corrected Total Cell Fluorescence was then calculated using the following formula: Integrated density – (Area of selected measurement / mean background fluorescence).

2.7 Cell stimulation protocol

In order to characterise the biological efficacy of CPP-conjugated peptide inhibitors or small molecule inhibitor treatments, in vitro time course experiments were performed to examine the responses of myometrial cells to cytokine stimulation. Initial experiments aimed to define the time course of expression of the highly inducible protein enzyme COX2 and the degradation of the NFκB inhibitory protein IκBα in response to the cytokine agonists IL1β or TNFα. Subsequently, these protein responses were compared to experimental situations whereby cells were pre-incubated with either a CPP-linked peptide inhibitor or a small molecule inhibitor prior to cytokine addition.

The optimal length of CPP pre-incubation was determined via the CPP uptake studies detailed in Chapter Three and the duration of pre-incubation for small molecule inhibitors were determined from study of the literature. Initial experiments defining the time frame of changes in COX2 and IκBα protein expression in response to cytokine agonist and defining the optimal cytokine concentration are detailed in Chapter Four.

2.7.1 Materials used in cell stimulation experiments

IL1β (200-01B) and TNFα (300-01A) were sourced from Peprotech. Sc514 (3318) was purchased from Tocris Bioscience. Curcumin (C7727), N-acetyl-L-cysteine (A7250) and Mg132 (C2211) were from Sigma Aldrich.

Sucrose cell lysis buffer (62.5mM Tris-HCl pH6.8, 2% SDS, 10% saccharose) was made up in our laboratory, 20µl/ml protease inhibitor (P1860) and 5µl/ml phosphatase inhibitor (P2745) were both sourced from Sigma Aldrich and added to the cell lysis buffer prior to experimentation.

2.7.2 Cell stimulation experiment protocol for protein extraction

Myometrial cells (≤ P4) were split equally from a T75 flask between 12 well plates and grown up to 80-90% confluency. At this point normal cell media was replaced with serum deprived (0.1% FCS) media. After 18 to 24 hours the media was discarded from each well and 500µl of fresh media (0.1% FCS) with differing concentrations of inhibitors or vehicle controls were added to the appropriate wells. After 1 hour pre-incubation the cytokine stimulants IL1β or TNFα were added to all wells excepting T0 controls. Eventual agonist doses were arrived at via experimentation across a dose range as detailed in Chapter Four.

At times of 0/15/60/120/240 minutes from cytokine stimulation, cells were washed with PBS before being lysed using sucrose cell lysis buffer. Cell lysates were collected and stored at -80°C.

2.7.3 Cell stimulation experiment protocol for RNA extraction

Myometrial cells (≤ P4) were split equally from a T75 flask between 6 well plates and grown to 80-90% confluency at which point media was changed to serum deprived (0.1% FCS) media. After 18 to 24 hours the media was discarded from each well and 500µl of fresh media (0.1% FCS) alone, or media (0.1% FCS) containing 100µM Pen-NBD or 50µM Sc514 was added one hour prior to addition of 10ng/ml IL1β or equivalent volume DMSO vehicle. After four hours, cells were washed with PBS before RNA was extracted using the RNEasy Mini Kit according to manufacturers' protocol:

https://www.qiagen.com/gb/resources/resourcedetail?id=14e7cf6e-521a-4cf7-8cbc-bf9f6fa33e24&lang=en

2.8 Cell Toxicity Assay

Cell Titre Blue is an assay based on the ability of living cells to reduce the redox dye rezazurin to a fluorescent end product rezarufin and thus enables an assessment of the metabolic capacity of cell populations (Gloeckner et al., 2001). Cell Titre Blue reagent was sourced from Promega (G8080).

Myometrial cells (<P4) were split, cells were counted and a volume equivalent to 5000 cells per well was added to each well of a 96 well plate (Brant and Caruso, 2005). 24 hours later, standard media was changed to media containing unconjugated Pen or NBD peptide, conjugated Pen-NBD or vehicle alone. Cytokines IL1β (10ng/ml) or TNFα (1nM) were added to the vehicle only wells after 1 hour. After 4 hours 20µL Cell Titre Blue was added to each well; this was left for 2 hours before reading the plate on a Tecan Fluorometer at 560nm excitation / 600nm emission. Wells containing media alone were subtracted from final data values as background fluorescence and cells in media containing no peptide or cytokine were used as controls.

2.9 Measurement of protein expression

Cell lysate samples generated from cell stimulation experiments were sonicated and underwent Lowry assay to determine overall protein concentration before addition of Laemmli buffer. Proteins within the lysate samples were then separated by electrophoresis on a sodium dodecyl sulphate poly-acrylamide gel (SDS-PAGE).

Following electrophoretic transfer to a polyvinyllidine difluoride (PVDF) membrane, Western blotting was used to determine the responses of the inflammatory protein enzyme COX2 and the NFκB specific inhibitory protein IκBα.

2.9.1 Western blotting reagents

For Western blotting gels: 30% acrylamide /Bis-acrylamide (A3699), sodium dodecyl sulphate (L4390), ammonium persulphate (A3678) and tetramethylethylenediamine (T9281) were sourced from Sigma Aldrich. Stained protein marker was sourced from Fermentas (11832124) and the chemiluminescent reagent used was ECL Prime Western blotting reagent (12316992) (Fisher Scientific).

The following reagents were made up in our laboratory: 10x running buffer (30.3g tris base, 144g glycine, 800ml water, 100ml 10% SDS, pH adjusted to 8.3, diluted 1:10 with water for experimentation), 10x Transfer Buffer (30.3g Tris base, 144g glycine, 900ml water, pH adjusted to 8.3, diluted 1:10 with water for experimentation), napthol blue black reagent (0.1% napthol blue black, 10% methanol, 2% acetic acid), Laemmli buffer (tris pH6.8 250nM; SDS 4% w/v; Glycerol 10% v/v; β-mercaptoethanol; bromophenol blue).

2.9.2 Antibodies used

Anti - COX2 was sourced from Cayman laboratories (CAY160112), Anti – IκBα (Full length, sc-847) and Anti – IκBα (C-21, sc- 371) were sourced from Santa Cruz. Horse radish peroxidase conjugated goat anti-rabbit (P0448) and goat anti-mouse (P0447) antibodies were sourced from DAKO.

2.9.3 Protein assay

Protein concentration in cell lysate samples was measured using the Bio Rad DC kit (500-0111). On a transparent 96 well plate a standard curve of 80, 60, 40, 20, 10 and 4µg/ml was set up using bovine serum albumin against unknown samples diluted in water (3µl/20µl) and

measured in triplicate. Plate optical density was measured at 750nm using colorimetric plate reader. Following protein assay, samples were diluted in an equal volume of 2x Laemmli buffer.

2.9.4 Preparation of SDS polyacrylamide gels

For ideal separation of proteins, electrophoresis gels were made up in two parts: a stacking gel which was applied on top of a separating gel. Gels were made up to 1.5mm thickness in clamped glass plates according to the recipe detailed in Table 2.4.

1.5mm 15 well plastic gel combs (BioRad) were inserted to the stacking gel prior to gel setting, these combs were removed before protein loading. Gels were made up to a final percentage of 10% acrylamide as this concentration gave optimum protein separation at the molecular weights of the proteins under investigation: COX2 (MW: 72 kDa) and IκBα (MW: 42 kDa).

Material	**Volume used**	
	Stacking (Top gel)	*Separating (Bottom gel)*
Water	6.6ml	7.9ml
30% Acrylamide	1.66ml	6.7ml
Tris 1.5M	-	5ml
Tris 1.0M	2.5ml	-
SDS	100µl	200µl
APS	50µl	200µl
TEMED	18µl	18µl

Table 2.4 Recipe for preparing 2x 10% SDS poly-acrylamide gels as used in this study

2.9.5 SDS-Polyacrylamide gel electrophoresis

Following protein assay, samples were heated to 95°C for 5 minutes to denature the protein structure. 10% SDS-polyacrylamide gels were placed in an electrophoresis tank (Bio Rad Mini Protean system) filled with running buffer, and samples in Laemmli buffer were loaded at 10µg/lane. Once loading was complete vertical electrophoresis was performed at constant current of 0.03A/gel for the stacking portion of gel. The current was increased to 0.04A/gel upon proteins reaching the separating portion of gel. Once stained, protein markers had run to the bottom of the gel this indicated that running was complete.

2.9.6 Protein transfer onto polyvinylidine difluoride membrane

Stacking gel was discarded and separating gels were immediately transferred into cooled transfer buffer. Filter paper and sponges were doused in cooled transfer buffer and PVDF membranes were activated by placing in 100% methanol for 30 seconds. A transfer cassette was then prepared in the following order:

Sponge > filter paper > gel > PVDF membrane > filter paper > sponge

These cassettes were placed in an electrophoresis tank (Bio Rad Mini Protean system) filled with cooled transfer buffer. To ensure that the proteins transferred in the right direction onto the membrane, the gel was on the cathode (red electrode) side relative to the membrane; and the membrane was on the anode (black electrode) side relative to the gel. The tank was connected to a power pack and run at 90 Volts for 90 minutes.

2.9.7 Blocking steps and primary antibody incubation

Successful protein transfer onto PVDF membranes could be visualised by complete transfer of the coloured protein marker onto the PVDF membrane. Blocking of non-specific antibody attachment sites was carried out by washing membranes with 5% non-fat dry milk in Tris-buffered saline with 0.1% Tween-20 (TBS-T) for 1 hour.

Membranes were then incubated overnight at 4°C with primary anti-COX-2 antibody or anti-IκB-α antibody, in 1% non-fat dry milk in 20ml TBS-T. This was followed by three washing steps with TBS-T.

COX2 antibody was tested across a number of different concentrations using both BSA and 1% milk in TBS-T as antibody diluents. The optimal concentration of this antibody was 1:500 for human myometrial cells and this was used throughout all subsequent experimentation.

Initial optimisation using an antibody directed towards the C-terminal end of IκBα (C21, sc-371) suggested that a concentration of 1:500 was optimal. However further optimisation steps were required to delineate the identity of multiple bands seen with subsequent use of this antibody. This process is outlined in Chapter Four.

2.9.8 Secondary antibody incubation

Polyclonal horseradish peroxidise conjugated goat anti-mouse immunoglobulin (diluted 1:3000 in 1% non-fat dry milk) was used in conjunction with COX2 antibody and a polyclonal horseradish peroxidise conjugated goat anti-rabbit immunoglobulin (diluted 1:5000 in 1% non-fat dry milk) was used for IκBα antibody. This was followed by three washing steps with TBS-T.

2.9.9 Development of films

Following the above steps enhanced chemiluminescent (ECL) reagent was applied to PVDF membranes for five minutes. Membranes were then dried, placed in development cassette and developed manually onto photographic film in a dark room.

2.9.10 Assessment of protein loading

Following development, equal loading of proteins was assessed by staining of the PVDF membrane with napthol blue black reagent for a minimum of 30 minutes to detect actin protein (44kDa).

2.9.11 Scanning and quantification of blots

Developed films were densitometrically scanned using UMAX PowerLook III and quantification performed with Bio Image Intelligent Quantifier 2 software.

2.10 Measurement of mRNA expression

Following extraction of RNA, gene expression was assessed via the measurement of mRNA transcripts across a panel of selected genes using reverse transcription quantitative polymerase chain reaction (RT-qPCR) arrays.

2.10.1 Materials used for mRNA expression experimentation

RNA extraction and synthesis of complementary DNA was performed using RNeasy mini kit (74101) and RT2 first strand kit (330404). Quantitative polymerase chain reaction (qPCR) array was performed with bespoke RT2 profiler PCR array plates and SYBR green master mix. These were all sourced from Qiagen.

2.10.2 Isolation of total RNA

The RNeasy Mini Kit (Qiagen) was used to extract total RNA from cells prepared as described in section 2.6.2. All work was carried out in a ribonuclease free environment with ribonuclease free equipment.

2.10.3 RNA quantification

Measurement of the RNA content in each sample was undertaken using the nanodrop spectrophotometer (ND-1000, Labtech). This spectrophotometer measures sample absorbance at 260nm and 280nm. An initial blank reading was taken using 2µL RNA free water, followed by sample assessment. RNA content was measured in ng/µl, suitable RNA purity was considered to be a 260/280 ratio of greater than 2.1. All RNA results included in this study met that standard.

2.10.4 Synthesis of cDNA

0.5µg of total RNA from each sample was added to the genomic DNA elimination mix from RT2 first strand kit; reverse transcription was then carried out according the manufacturers' instructions, via the RT2 array handbook: https://www.qiagen.com/gb/resources/resourcedetail?id=6161ebc1-f60f-4487-8c9e-9ce0c5bc3070&lang=en

2.10.5 Protocol for loading and running qPCR array plates

cDNA as synthesised from 0.5µg of total RNA from each original sample was added to SYBR Green Master Mix. 25µL of this final mix was then added to each well of a 96 well array plate, with each well containing a different primer for a gene of interest or control. The array plates were created bespoke by Qiagen and the genes selected for examination are described in the next section. The plate was sealed with optical film, centrifuged at 1000rpm for 1 minute before inserting the plate into the PCR cycler (Step One Plus, Applied Biosciences) using the following protocol:

Step	**Number of Cycles**	**Temperature (°C)**	**Duration**
1	1	95	10 minutes
2	40	95	15 seconds
		60	1 minute

Fluorogenic data was collected via the FAM channel and the cycle threshold (Ct) values were calculated by applying a threshold limit that represented the exponential phase of amplification. To ensure comparability of gene expression between different array plates the same threshold limit was applied to all experiments (Ct 0.116). This was calculated as a mean threshold value from the first 6 arrays that were run and corresponded to the exponential phase of the amplification curve for all subsequent experiments.

To check for specificity of gene product amplification: for each experiment a 'step and hold' melt curve analysis was carried out according to the following protocol:

Step	Temperature (°C)	Duration	Incremental Temperature Increase (°C)
1	95	15 seconds	
2	60	1 minutes	
3	95	15 seconds	0.3

2.10.6 Selection of genes of interest and arrangement of gene array plate

The results detailed in Chapter Five detail expression changes in uterine cells for a series of genes involved in labour, inflammatory processes and NFκB specific signalling within a 96 well plate array in response to cytokine stimulation, and the effects of CPP linked and non-peptide inhibitors on the cytokine induced response.

With the aim of reducing the effect of biological variation on final results it was necessary to assess 2 conditions across the same plate (e.g. untreated vs IL1β treated); and it was recommended by the manufacturer to have 3 housekeeping controls, one reverse transcription control (RTC), one positive PCR control (PPC) and one human genomic DNA control (HGDC) for each set of genes of interest (GOI). Thus, primers for 42 genes of interest (in duplicate) could be selected for use on one array plate.

The approach taken to gene selection was multifactorial. A number of genes encoding for proteins associated with the physiological events of uterine contraction, cervical dilation and membrane rupture that occur during human labour, termed contraction associated genes, were selected (Challis et al., 2000); also, for comparison, a collection of genes encoding for G-proteins involved in maintaining uterine quiescence were included (Webster et al., 2013). A number of pro inflammatory genes, genes encoding for proteins in the NFκB and AP1 pathways (Hayden and Ghosh, 2004, Davies and Tournier, 2012), and genes involved in the production of prostaglandins (Gibb, 1998) were chosen to aid understanding of the potential mechanism of action of inhibitors used in this study.

To examine potentially new targets associated with human labour, a colleague (P. Palmowski) assisted in the examination of uterine RNAseq data generated in our laboratory and compared this to previously published data (Chan et al., 2014). This enabled the inclusion of novel target genes within the array whose expression may be linked to the regulation of labour. The genes of interest and controls used on the array plates are listed in Table 2.5.

Contraction associated genes
OXTR [1]/ MMP 9[1] / MMP19[1] / TIMP1[1] / GJA1 / GJB2
Inflammatory genes
IL1A / IL1B / TNFA / IL6[2] / IL8 / ICAM1[1] / SOCS3[1] /IL1R1 / IL1R2 / IL4R[1] / CXCL2[2] / CXCL1[1] / CXCL6[1] / CCL2[1]
NFκB pathway genes
NFKB1 / NFKB2[2] / RELA / NFKBIA[2] /NFKBIZ[1]
AP1 pathway genes
FOSB[1] / JUN[2]
Prostaglandin production genes
PTGER3 [2] / PLA2G2A[2] / PTGES[2] / PTGS2[2]
G protein receptor genes
GPR37[2] / GPR34 / RGS10
Novel target genes
S100A9[1] / S100A8[1] /STAT1[2] / FOXO1[2] / ZEB1[2]/ LILRA5[2] / SPINK5[1] / TRIB1[1]
Housekeeping genes and controls
GAPDH / ACTB / B2M / RTC (reverse transcription control) / PPC (Positive PCR control) / HGDC (Human Genomic DNA control)

Table 2.5 Gene used in RT2 profiler PCR array plates

[1]Denotes genes whose uterine expression is altered by labour in our laboratory RNA seq dataset.

[2]Denotes genes whose uterine expression is altered by labour in published literature (Chan et al., 2014).

2.10.7 Analysis of RNA expression changes

Mean Ct values for each gene on the RT2 array plate were exported on an Excel file to the following data analysis website supported by Qiagen:

http://pcrdataanalysis.sabiosciences.com/pcr/arrayanalysis.php

Quality control was performed on each array plate in the following manner:

1. PCR Array Reproducibility:
If the Average PPC C_t is 20±2 and no two arrays have Average PPC C_t are > 2 away from one another then the sample and group were accepted.

2. Reverse Transcription Control (RTC):
Delta C_t (AVG RTC Ct - AVG PPC Ct) < 5 was acceptable.

3. Genomic DNA Contamination (GDC):
A C_t (GDC) > 35 was acceptable.

All array plates used met the above quality control measures therefore none were discarded from analysis.

Genes of interest (GOI) were normalised to the mean average Ct of the three selected housekeeping genes (β2 Macroglobulin, GAPDH, ACTB), to produce a mean average ΔCt value.

Initial experiments compared fold changes between untreated (control group) and IL1β treated samples (treated group) by calculating 2^ΔΔCt values. Fold changes between the groups for each gene of interest were then arrived at by the following calculation:

2^ΔΔCt (Treated Group) /2^ΔΔCt (Control Group)

Fold regulation changes were produced for downregulated genes (i.e. genes with a fold change of <1) with the following calculation:

1/Fold Change

Subsequent experiments sought to compare IL1β treated samples with samples pre-incubated with a small molecule inhibitor or a CPP-linked peptide inhibitor prior to IL1β treatment.

2.11 Statistical analysis

SPSS 22 (IBM) and Prism 6.0 (GraphPad) software were used to perform statistical analysis. Statistical significance was assumed at $p<0.05$. For all conditions each separate n is a myometrial or placental sample taken from a different patient.

2.11.1 Cellular uptake studies

Statistical analysis was performed on Corrected Total Cell Fluorescence values. One-way ANOVA with Bonferroni Post Hoc corrections was performed to compare between different peptides at the same time point. Unpaired T-testing was used to compare changes in fluorophore-conjugated CPP uptake across time points.

2.11.2 Biological effectiveness studies

Statistical analysis was performed on optical densitometry values. One-way ANOVA with Bonferroni Post Hoc corrections was performed to compare difference between groups.

2.11.3 Gene array data

P values were calculated based on a Student's t-test of the replicate 2^ΔΔCt values for each gene in the control and treatment groups.

Chapter Three

The cellular uptake and distribution of Cell Penetrating Peptides in human uterine and placental cells

3.1 Introduction

CPP uptake into cells is dependent on many factors including: the CPP itself, the cell type, the cargo attached to the CPP, the method of cargo attachment (whether covalent or electrostatic); the concentration of CPP used and the density of cells (Hallbrink et al., 2004, Madani et al., 2011). The majority of CPP studies are performed on standard immortalised cell lines such as HeLa (Jones et al., 2005), with relatively few studies available that have reported CPP uptake in primary cells (Manceur and Audet, 2009). This emphasises the requirement to characterise CPP uptake in detail in any new experimental situation, such as the utilisation of human uterine and placental cell types to which CPPs have not been previously applied.

The most common method to evaluate uptake is by coupling a CPP to a fluorescent moiety and measuring the fluorescence of treated cells. Such an approach has the advantages of studying both the location and amount (i.e. fluorescence intensity) of the fluorophore-conjugated CPP within the cell (Madani et al., 2011). Many early studies examining CPP uptake on fixed cells were subject to artefact effects due to cell fixation which overestimated uptake (Richard et al., 2003). Therefore, it is widely accepted that the best currently available method for evaluating CPP uptake is confocal microscopic imaging of live cells (Madani et al., 2011). Such an approach allows the recording of real time changes of fluorescent uptake within cells and the analysis of fine image slices within the z-plane to allow assessment of fluorescent signal through different cell layers (see Figure 3.1).

There are now hundreds of CPP sequences described; but only a few have been extensively studied (Jones and Sayers, 2012). Of these CPPs; vectors derived from the antennopedia protein of drosophila (AntP / Penetratin /Pen) (Derossi et al., 1994, Christiaens et al., 2004, Fischer et al., 2000, Khaja, 2010), the transcription-transactivating protein of HIV1 (TAT) (Vives et al., 1997, Wadia and Dowdy, 2005), or synthetically-derived multiple arginine residues (usually R7-10) (Futaki, 2002, Nakase et al., 2004) are amongst the most widely used peptides for cellular uptake studies and for the transportation of biological cargo across cell membranes. For these reasons the initial part of this chapter determines the uptake of three peptide vectors derived from those sources: Pen, TAT and R8, by measuring their ability to deliver fluorescent cargo into human uterine and placental cells.

CPP vectors may display different uptake characteristics according to the cargo attached (Jones et al., 2005). Therefore, this chapter also examines the delivery of fluorophores by CPP vector conjugated to a potentially biologically effective peptide cargo: the Nemo Binding Domain (NBD) peptide, an 11 amino acid polymer directed at preventing inflammatory ligand induced NFκB activation (see introductory chapter, section 1.9.4) (May et al., 2000).

The specific aims of these studies were:

- To assess the time-dependent and dose-dependent cellular uptake of fluorescent cargo attached to three CPPs: Pen, TAT and R8 in comparison to a non-CPP control peptide $GS_4(GC)$ in primary human myometrial cells.
- To assess the entry of the same three CPPs in primary human amnion cells.
- To assess the myometrial cell uptake of a series of fluorophore conjugated CPPs with NBD peptide cargo attached.

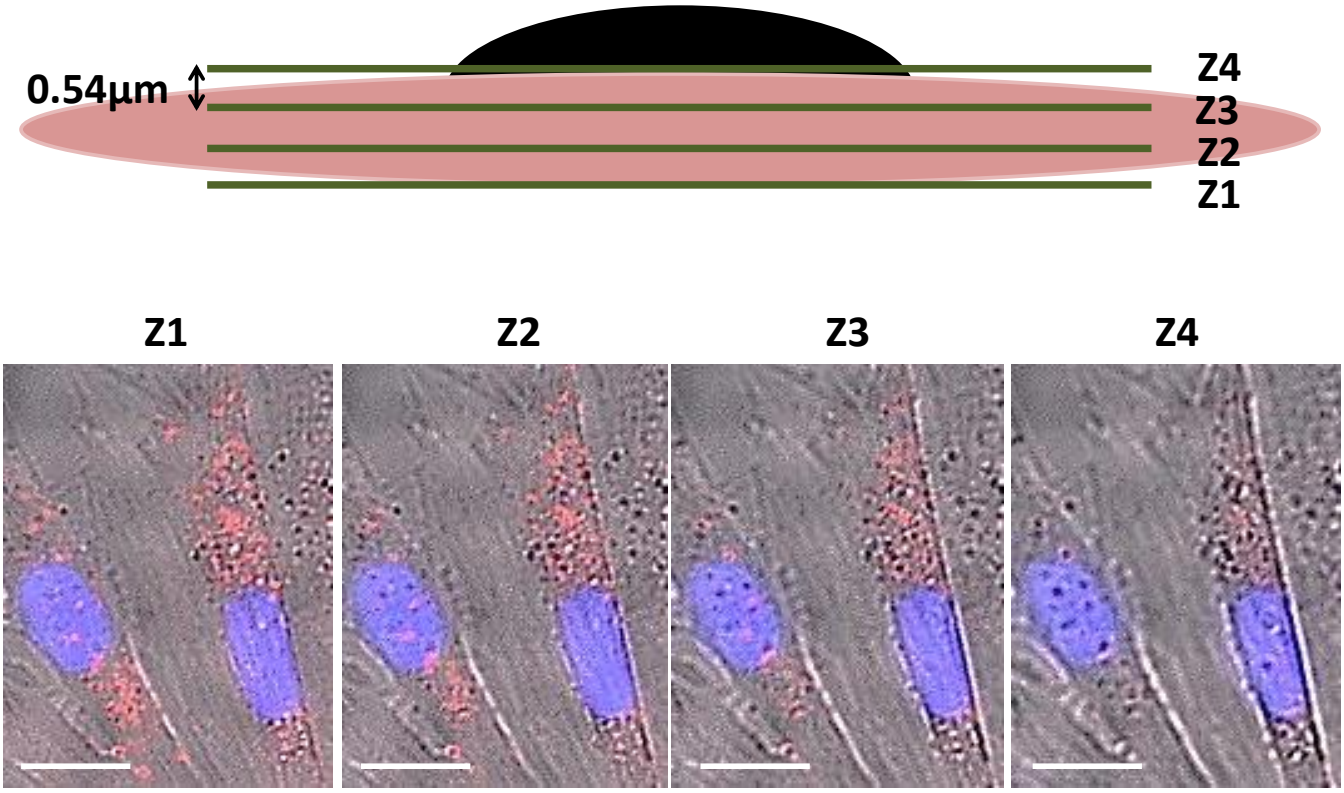

Figure 3.1: Confocal image Z-series of live myometrial cells demonstrating capture of fluorescent uptake throughout the cell.

Upper panel: cartoon of myometrial cell used to indicate Z-plane slices (Z1-Z4) which are 0.54µm thick at 40x magnification.

Lower panel: Confocal microscope images of live myometrial cells one hour following application of 3µM Pen CPP conjugated to rhodamine fluorophore (red). Four consecutive z plane slices (Z1-Z4) 0.54µm apart, are displayed at 40x magnification. Bright field and fluorescent images are overlaid here to demonstrate cell shape, outline and intracellular localisation of fluorophore. Nuclei are stained blue (Hoechst). Red punctate signal indicating fluorophore uptake can be seen internal to the cell membrane at all z-plane images. Scale bars 20µm.

3.2 Demonstrating the intracellular uptake and distribution of CPPs in human myometrial cells

3.2.1 Comparison of CPP cellular delivery of fluorescent cargo with control peptide GS_4(GC)

To provide evidence that CPP intracellular fluorophore delivery was not simply occurring across a concentration gradient, the cellular entry of a control peptide conjugated to a fluorescent moiety (rhodamine) was compared to CPP-fluorescence conjugates at the same concentration over an identical time frame. GS_4(GC) is a 10 amino acid residue peptide with a neutral overall charge; it is used as a flexible bridging group between CPPs and prospective cargo but has no innate cell penetrating activity (Sayers et al., 2014) and, therefore, acts as a suitable control to assess CPP-dependent delivery of cargo.

Figure 3.2 indicates the results of initial experimentation comparing CPP and control peptide delivery of the fluorophore rhodamine. The upper panel displays a scatter graph demonstrating the results of semi-quantitative analysis performed via Image J software on confocal microscope Z-slice image stacks. It compares the fluorescently tagged CPPs Pen, TAT or R8 with the fluorescently tagged control peptide GS_4(GC) at 1µM concentration 60 minutes after peptide application to myometrial cells. The lower panel displays representative confocal images taken from the analysed stacks. The results show that each of the three CPPs achieved intracellular delivery of rhodamine within one hour at 1µM concentration.

Using one-way ANOVA with Bonferroni post hoc testing to compare differences between CTCF values of rhodamine-conjugated GS_4(GC) and all three rhodamine-conjugated CPPs at 1µM after 60 minutes application revealed differences for Pen ($p=0.02$) , TAT ($p=0.002$) and R8 ($p=0.0001$).

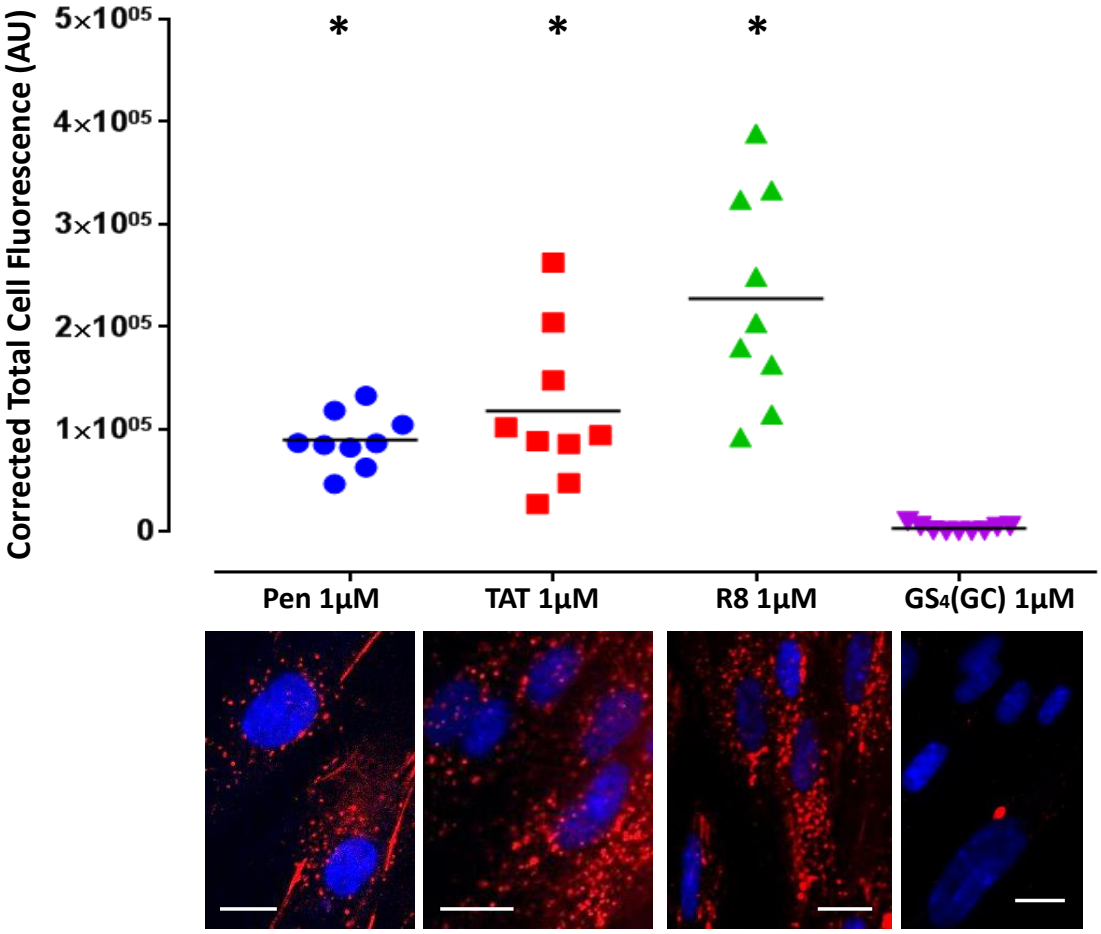

Figure 3.2 Comparison of rhodamine-CPP cellular uptake with a non-cell permeable control peptide

Upper Panel: Scatter plot displaying results of semi-quantitative analysis as performed via Image J of rhodamine conjugated CPPs Pen, TAT, R8 and GS4(GC) control at 1µM concentration 60 minutes after application to myometrial cells. Each data point represents the mean average Corrected Total Cell Fluorescence (Arbitrary Units) of 3 cells through 3 z-slice images in an image series. 3 image sequences were collected per experiment and 3 independent experiments performed. Black lines represent mean of data points.

*= significant difference compared with GS_4(GC); one-way ANOVA with Bonferroni post hoc testing.

Lower Panel: Confocal microscope images illustrating rhodamine conjugated CPP uptake (red) vs control peptide also conjugated to rhodamine (red). Images taken from corresponding data set as presented in upper panel. Nuclei stained blue with Hoechst nuclear dye. Scale bars 20µm.

3.2.2 Mobility of peptide fluorescence within uterine cells

Two pieces of evidence demonstrated that the fluorophore was being delivered intracellularly. Firstly, consecutive image Z-slices indicated that fluorescent signal could be observed internal to the cell membrane in all slices, this has been previously displayed in Figure 3.1; secondly, a portion of fluorescent signal was evidently mobile within the cell for hours after application of CPP-fluorophore conjugates.

As an example used to demonstrate this phenomenon, Figure 3.3 shows still images taken from a time lapse experiment. In the figure, live myometrial cells were co-incubated with incubated with Hoechst nuclear dye and Mito-Tracker dye (to label Mitochondria) to enable a fuller view of the internal components of the cell prior to addition of 10µM rhodamine-Pen. After two hours, cells were imaged to create a time lapse film with images captured every 20 seconds over a total time course of 5 minutes. The larger left hand image in Figure 3.3 shows a representative cell from this experiment. The right hand images demonstrate an enlarged portion of the main image at each minute of the time lapse to demonstrate a mobile fluorescent spot (red punctum) internal to labelled mitochondria. Similar mobility of fluorophore cargo within the cell was also observed with conjugation to TAT (Figure 3.9), R8 (Figure 3.10) and Pen-NBD (Figure 3.12) peptides.

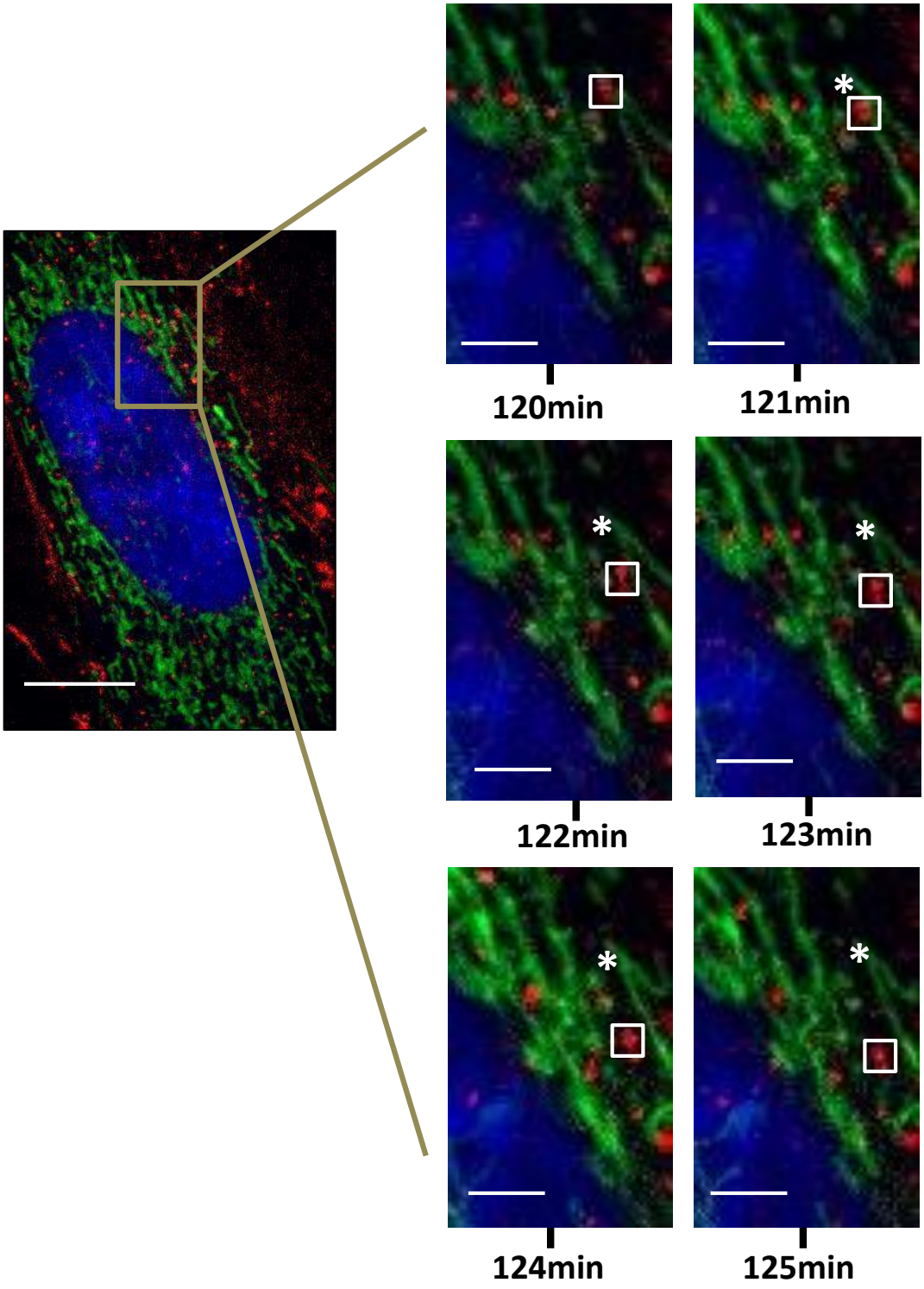

Figure 3.3 Demonstration of peptide mobility within a myometrial cell.

Larger picture: confocal microscope image of myometrial cell with nuclei labelled blue (Hoescht 1µM) and mitochondria labelled green (Mito Tracker 1µM) 120 minutes following addition of 10µM rhodamine-Pen (red). Scale bar 20µm.

Smaller Image series: cropped images sourced from a time-lapse film of the left hand image demonstrating peptide movement over 5 minutes. White box indicates moving fluorophore (red), white asterisk denotes fluorophore starting position. Scale bars 2.5µm.

3.2.3 Assessment of peptide distribution within uterine cells

To gain a greater understanding of peptide and fluorophore distribution within uterine cells, internal structures including the endoplasmic reticulum, mitochondria, endosomes and lysosomes were labelled for visualisation, prior to addition of rhodamine conjugated Pen CPP. Figure 3.4 panels A and B demonstrate that peptide (red) did not co-localise with endoplasmic reticulum and mitochondria (green).

Figure 3.4 panels C and D demonstrate some areas of co-localisation between rhodamine (red) and endosomes or lysosomes (green) within the cell, represented as yellow signal within the Figure. This indicates that a proportion of fluorophore-CPP was distributed within these structures in myometrial cells.

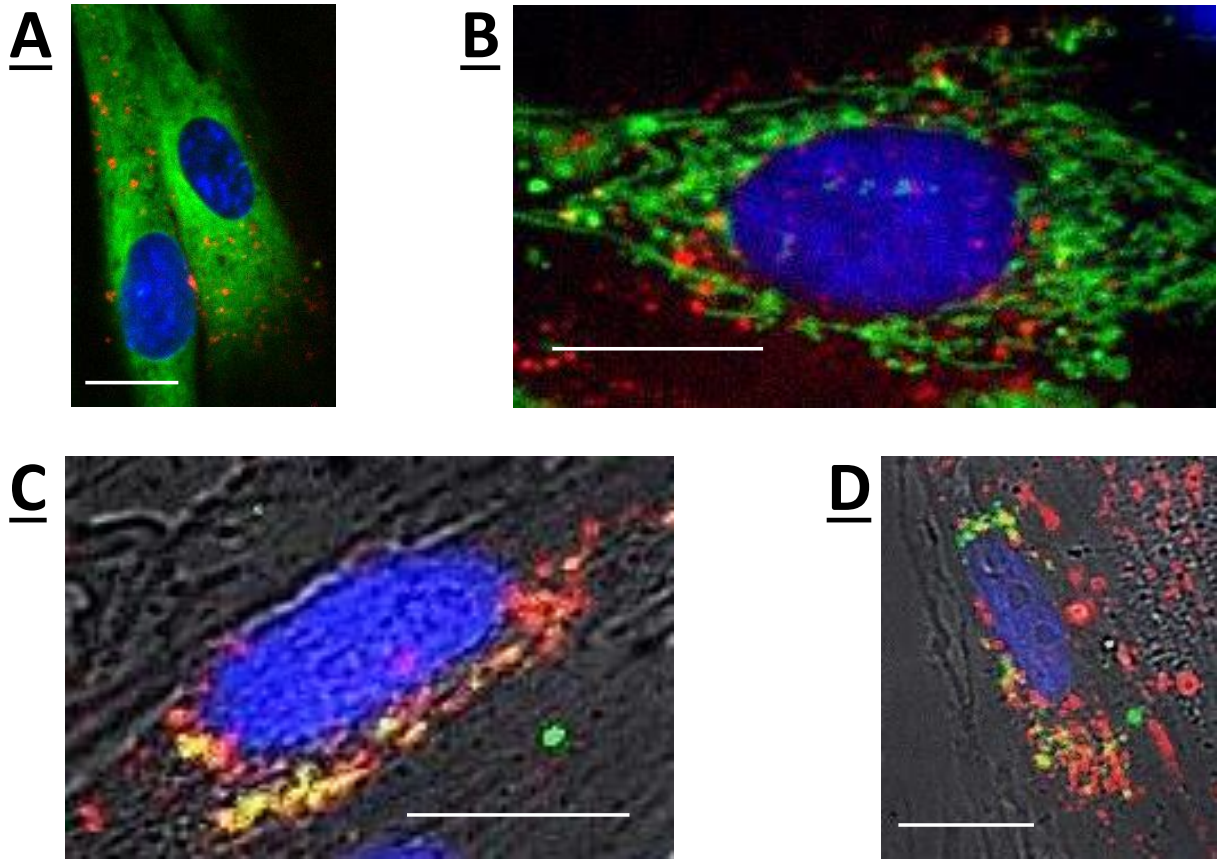

Figure 3.4 Demonstration of peptide distribution throughout myometrial cells

Cells were co-incubated with Hoechst nuclear dye (blue) and dyes to label: **A** endoplasmic reticulum (green), **B** Mitochondria (green), **C** Endosomes (green) or **D** Lysosomes (green), prior to application of Rhodamine-Pen. Cell images captured one hour after Rho-Pen application. Co-localisation of peptide and dye-labelled structures appears yellow. Brightfield channel is included in images **C** and **D** to better illustrate cell shape and outline. Scale bars 20µm. Images are representative of 3 image series (minimum of 5 cells captured per image) taken from 2 independent experiments.

3.3 Detailed assessment of uptake of Pen CPP in myometrial cells

3.3.1 Pattern of uptake displayed by fluorophore conjugated Pen CPP

Figure 3.5 presents live cell confocal images from three experiments (labelled 1-3) whereby cells were exposed to 10μM of rhodamine-Pen over a 120 minute time frame. It demonstrates a pattern of CPP uptake within myometrial cells that was characteristically observed during experimentation. Within 15 minutes fluorescent signal can be seen correspondent to cell membranes (indicated by white arrows), with some punctate fluorescent signal also seen internal to the membrane. At 60 minutes the punctate or vesicular pattern of uptake predominates with some membranous signal still present, by 120 minutes the observed fluorescent signal is predominantly vesicular and intracellular with a polar distribution around cell nuclei, an uptake pattern indicated by white asterisks in the Figure. In one example (Figure 3.5, n=3) this pattern of uptake has occurred within 60 minutes of application.

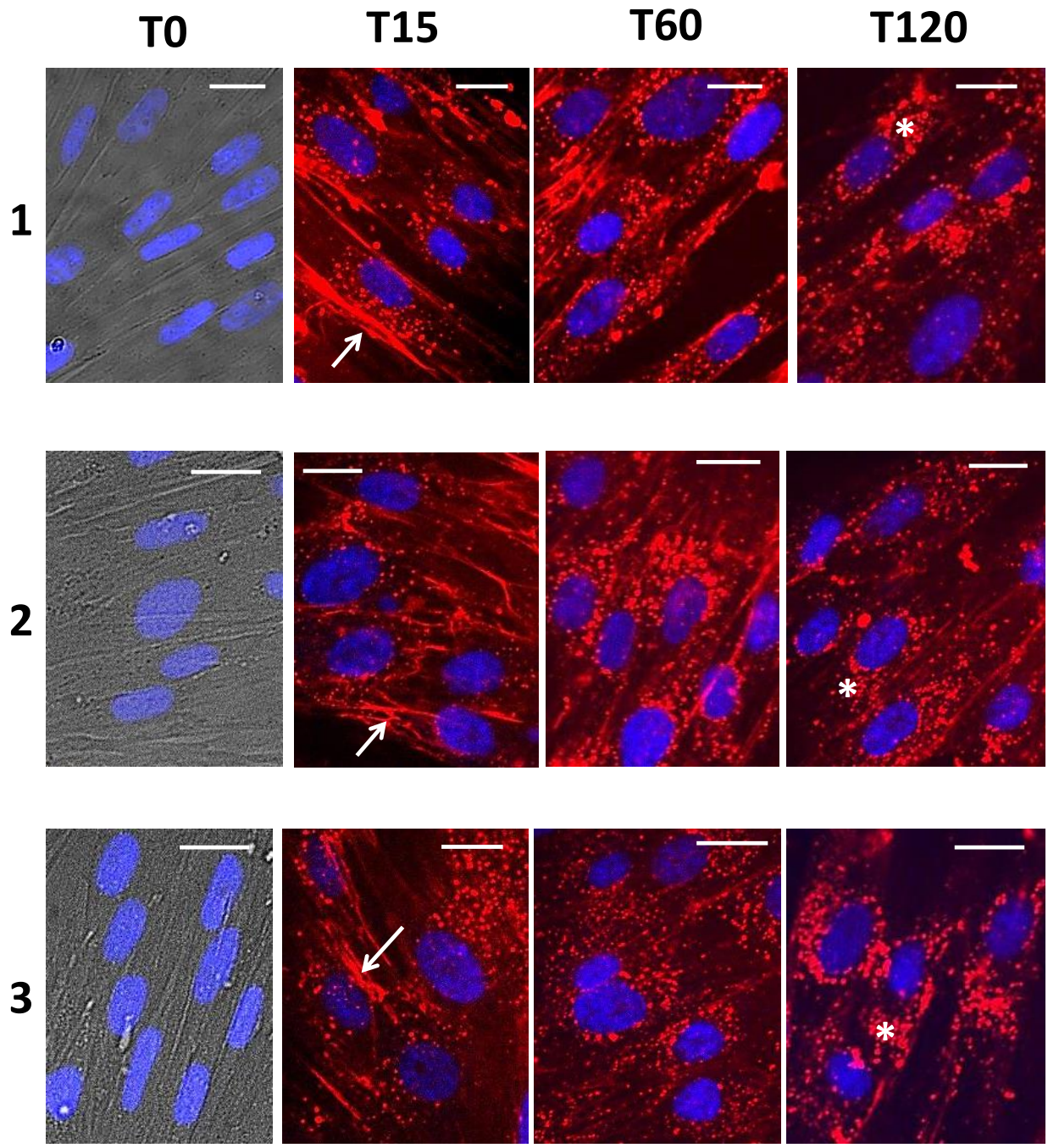

Figure 3.5: Pattern of 10µM rhodamine-Pen CPP uptake over 120 minutes

Each panel series displays representative confocal images from an independent experiment (1-3) demonstrating an 120 minute time frame from prior to CPP application (T0) to times 15, 60 and 120 minutes following application of 10µM rhodamine-Pen (red). White arrows indicate membranous pattern of fluorescent signal, white asterisks indicate vesicular pattern of uptake. Nuclei are stained blue (Hoescht 1µM), T0 pictures include bright field to indicate cell shapes and outlines. Scale bars 20µm.

3.3.2. Quantitative analysis of 10µM rhodamine-Pen uptake

Initial analysis of fluorescent uptake within cells was undertaken using Cell Profiler software which allows high throughput analysis of every cell imaged throughout every z slice as described in Chapter Two (section 2.6) of this thesis.

Figure 3.6 demonstrates the quantitative analysis of myometrial cells exposed to 10µM rhodamine-Pen over a 120 minute timeframe as performed using both Cell Profiler and Image J software. The data here is presented as a line graph showing changes in mean intracellular fluorescence values over time. In this case all data points collected are also displayed in scatter form to allow a better comparison of the two forms of analysis.

As shown in Figure 3.6A, data generated via Cell Profiler revealed a substantial increase in whole cell fluorescent uptake at 15 minutes, the mean data is similar at 60 minutes but increases further at 120 minutes. Using students T-test to compare differences in measured fluorescence data between time points revealed differences between the 60 and 120 minute time points ($p=0.002$) but not between 15 and 60 minutes ($p=0.93$) . Mean cell fluorescence for all time points measured was significantly greater than at T0.

Comparison of the results elicited using Cell Profiler analysis with the visual examination of cells (as seen with the pictorial data presented in Figure 3.5) led to the impression that there was a discrepancy, with the quantitative data overestimating intracellular uptake at the 15 minute time point. Detailed analysis of the software quantifying process revealed that, in many cases, the software pipeline was unable to distinguish between membranous fluorescent signal and intracellular vesicular signal in close proximity to the plasmalemma. The membranous signal is likely to represent electrostatic interaction between CPPs and cell membrane proteoglycans prior to cellular entry and, therefore, does not constitute intracellular uptake (Console et al., 2003). For this reason an alternative approach to analysis of confocal images was undertaken using Image J software. This allowed user selection of intracellular areas of uptake such that membranous areas of signal intensity were not included in the analysis. Data produced via the image J analysis is demonstrated in Figure 3.6B. It demonstrates an initial increase in mean fluorescence 15 minutes after rho-Pen application, with a further increase at 60 minutes and minimal change thereafter. Students T-test comparison of the measured fluorescence data generated via Image J

indicated differences between 15 and 60 minutes time points (p=0.006) but not 60 and 120 minutes (p=0.40). This better reflected the changes observed microscopically: intracellular uptake largely occurred within 60 minutes of application and less additional uptake was seen thereafter (Figure 3.5). Therefore, Image J was the method selected to analyse all subsequent experiments.

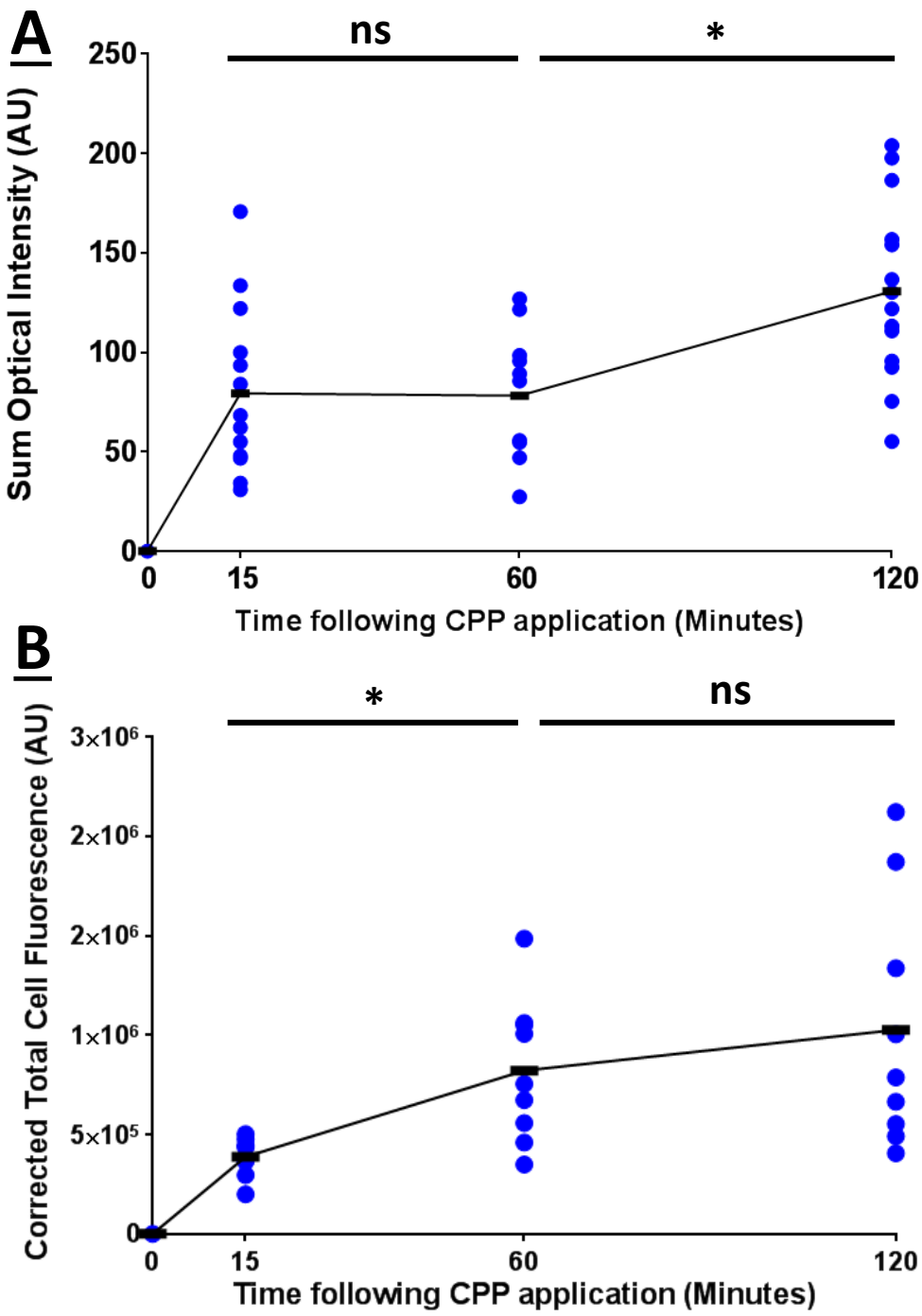

Figure 3.6 Quantitative analysis of rhodamine-Pen 10µM uptake in myometrial cells

A Scatter plot displaying Cell Profiler software analysis of confocal images. Each blue data point represents mean fluorescent intensity of all cells within a given z-series image stack with 3-5 image stacks analysed per experiment and 3 experiments per timepoint. Black line represents mean average of all data points.

B Scatter plot displaying Image J software analysis of confocal images. Each blue data point represents mean fluorescent intensity of 3 cells within a given z-series image stack with 3 image stacks analysed per experiment and 3 experiments per timepoint. Black line represents mean average of all data points.

*indicates significance between fluorescence data at indicated timepoints as compared using Student's t-test.

3.3.3 Uptake of fluorophore-CPP across a concentration range

Figure 3.7 demonstrates myometrial cells following application of 1μM, 3μM and 10μM rhodamine-Pen, as compared to identical doses of control peptide GS_4(GC) over a 120 minute time frame. The data shown for 10μM can also be seen in Figure 3.5 (panel labelled 3) and is displayed again here for ease of comparison. A similar pattern of uptake was seen across concentrations with membranous signal progressing to a vesicular distribution of fluorescence over the experimental time frame. However with the use of 1μM concentration areas of membranous signal persisted up to 120 minutes.

The image J analysis of fluorescent cellular uptake for the three tested concentrations is displayed in Figure 3.8. The data values shown here for 10μM concentration are identical to those seen in Figure 3.6B and are displayed within this figure for ease of comparison. At all doses tested there were rapid increases of cellular fluorescence from 0-15 minutes, with further increases from 15-60 minutes before slowing of the fluorescent uptake. Statistical analysis using Student's t-test to compare differences in mean CTCF values between time points indicated differences between 15 and 60 minutes at all concentrations tested (1μM $p=0.04$, 3μM $p=0.04$, 10μM $p=0.006$), but no differences between 60 and 120 minutes at any concentration (1μM $p=0.22$, 3μM $p=0.55$, 10μM $p=0.40$).

The right hand panels of Figure 3.8 demonstrate quantitative evaluation of the GS_4 (GC) control peptide 120 minutes following cellular application to display a comparison of uptake with rhodamine conjugated Pen. 1μM concentration of GS_4 (GC) led to no increases in cellular fluorescence and application of 3μM and 10μM produced a small amount of fluorescence within cells after 120 minutes. Student's t-test comparison of the fluorescence intensity of this signal with identical concentrations of rhodamine-Pen at the same time point revealed differences at all concentrations tested (1μM $p=0.0002$, 3μM $p=0.001$, 10μM $p=0.0027$).

This indicates that cellular entry of the fluorophore is markedly enhanced when conjugated to a CPP vector as opposed to a non-cell permeant control.

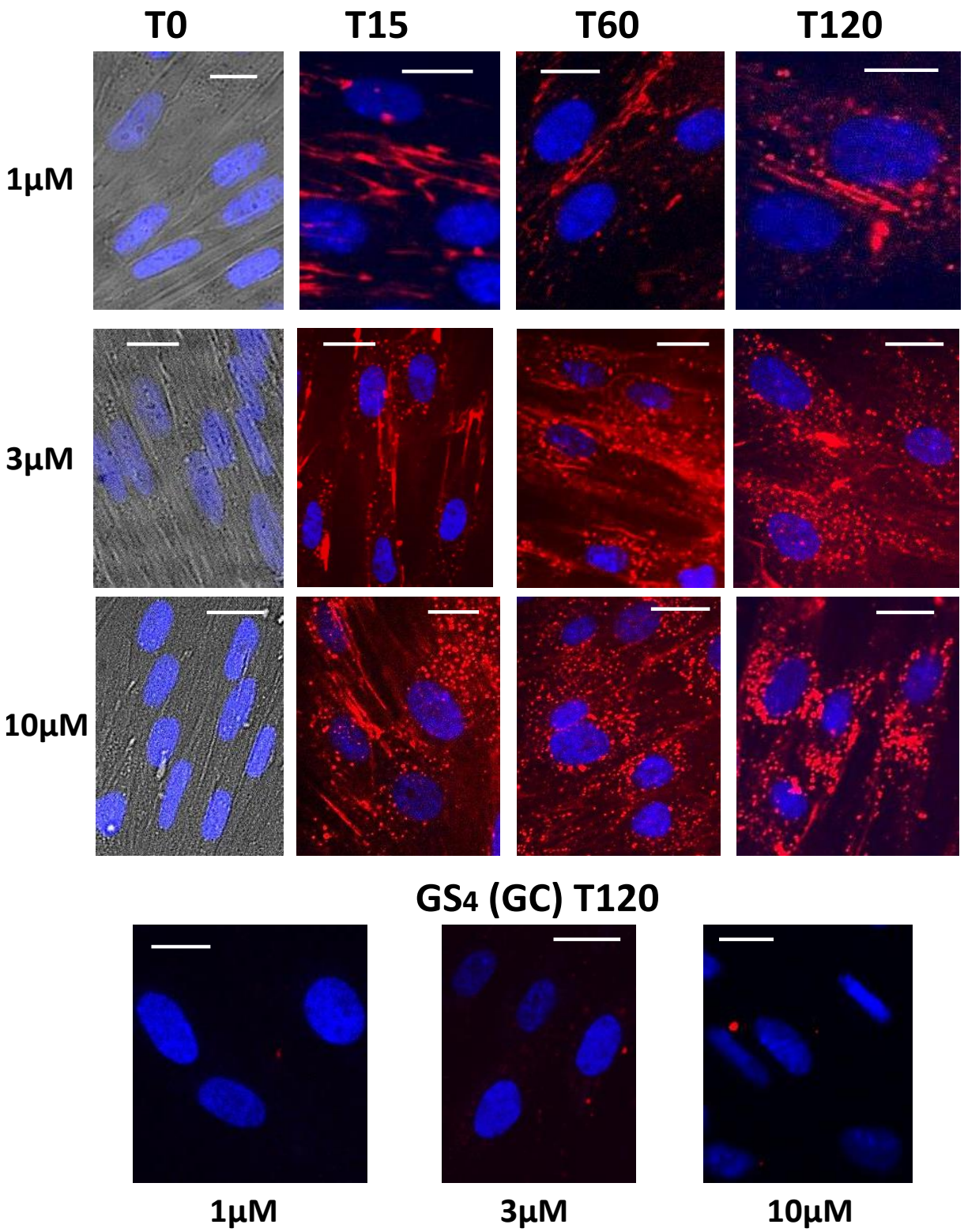

Figure 3.7 Cellular uptake across concentration range of rhodamine-Pen compared to control peptide

Confocal microscope images representing the 120 minute time frame of uptake of 1µM, 3µM and 10µM rhodamine-Pen (red) are displayed. Lowest panels demonstrate representative confocal images of myometrial cells 120 minutes following exposure to indicated concentrations of control peptide rhodamine-GS_4(GC). T0 pictures include bright field to indicate cell shapes and outlines, cell nuclei dyed blue with Hoechst. Scale bars 20µm.

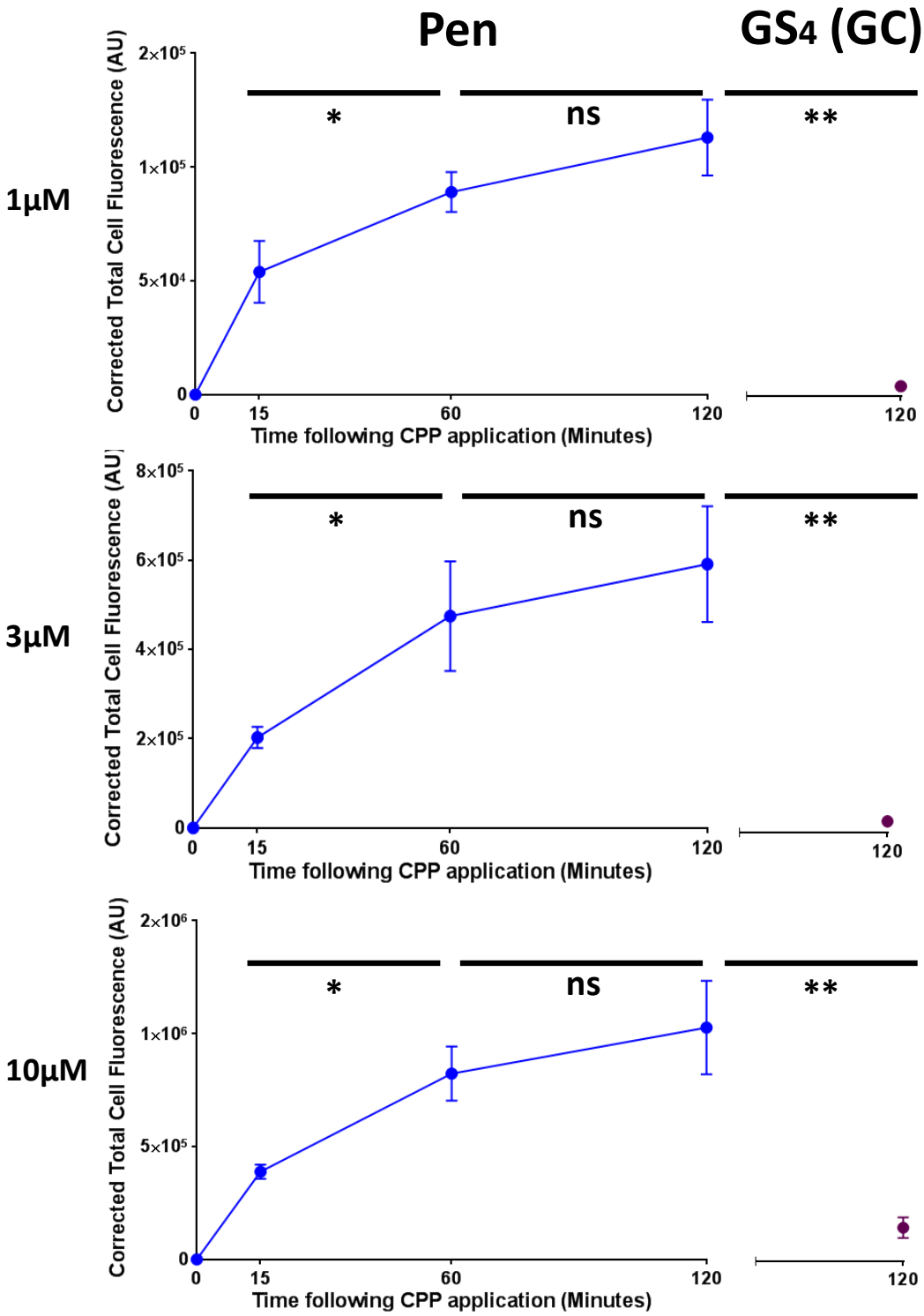

Figure 3.8 Quantitative analysis of rhodamine-Pen uptake via Image J

Line graphs displaying values of 1µM, 3µM and 10µM rhodamine-Pen cellular uptake across a 120 minute timeframe. Adjacent to this, on right hand side, is data representing equivalent concentration of control peptide rhodamine - GS_4(GC) at the 120 minute time point only. Data points represent mean average ± SEM Corrected Total Cell Fluorescence values expressed in arbitrary units.

* indicates significance between 15 and 60 minute time points as compared using Student's t-test.

**indicates significance between rhodamine-Pen and GS_4 (GC) 120 minutes following cellular application as compared using Student's t-test

3.4 Uptake of rhodamine-conjugated TAT peptide in myometrial cells

Once the time and concentration dependence of fluorophore-Pen uptake was established, it was necessary to investigate the cellular uptake of other fluorophore-CPP conjugates.

The upper panel of Figure 3.9 displays representative confocal images of 10µM rhodamine-TAT peptide demonstrating the uptake of this CPP-fluorophore conjugate over 120 minutes. A similar pattern was observed to that described with Pen (Figure 3.2), although some nuclear localisation is also observed with the use of this peptide after 120 minutes.

The lower panel of Figure 3.9 displays the Image-J analysis of rhodamine-TAT at 1µM, 3µM and 10µM over the 120 minute time frame with GS_4(GC) represented at identical concentrations at the 120 minute time point.

Statistical analysis using Student's t-test to compare differences in mean CTCF values between time points indicated a difference between 15 and 60 minutes at 10µM ($p=0.016$), but no differences between these time points when using lower concentrations (1µM $p=0.26$, 3µM $p=0.13$). No differences between 60 and 120 minutes where observed at any concentration (1µM $p=0.89$, 3µM $p=0.55$, 10µM $p=0.13$).

Student's t-test comparison of the fluorescence intensity of the GS_4(GC) signal after 120 minutes with identical concentrations of rhodamine-TAT at the same time point revealed differences at all concentrations tested (1µM $p=0.046$, 3µM $p=<0.0001$, 10µM $p=<0.0001$).

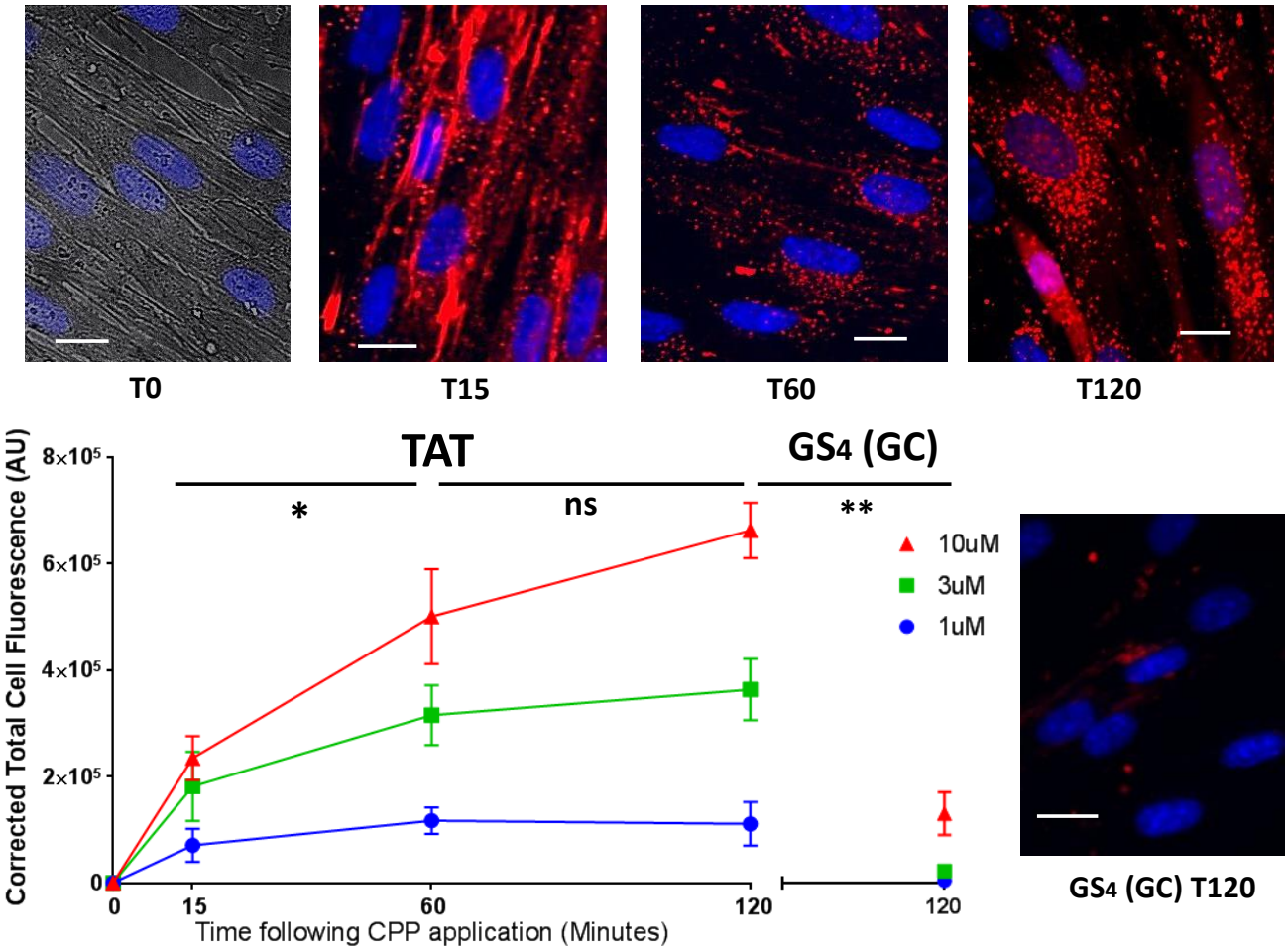

Figure 3.9 Cellular uptake of rhodamine-TAT peptide

Upper Panel: Representative confocal microscopy images of 10µM rhodamine-TAT from pre-application (T0) to 120 minutes following application. Scale bars 20µm.

Lower Panel: Image J analysis of 1µM, 3µM and 10µM rhodamine-TAT across the 120 minute time frame. Data points represent mean average ± SEM Corrected Total Cell Fluorescence values. Adjacent to this, are data values representing equivalent concentrations of rhodamine conjugated control peptide GS_4(GC) at 120 time point only. On right hand is confocal image representative of 10µM rhodamine-GS_4(GC) to illustrate the low level of uptake seen with the control peptide at this concentration.

* indicates significance between 15 and 60 minute time points as compared using Student's t-test.

**indicates significance between rhodamine-TAT and GS_4(GC) 120 minutes following cellular application as compared using Student's t-test

3.5 Uptake of rhodamine-conjugated R8 peptide in myometrial cells

The upper panel of Figure 3.10 displays representative confocal images of 10μM rhodamine-R8 peptide demonstrating the uptake of this CPP-fluorophore conjugate over 120 minutes. . It demonstrates a similar pattern of uptake as with rhodamine-Pen conjugated CPP (Figure 3.2).

The lower panel of Figure 3.9 displays the Image-J analysis of rhodamine-R8 at 1μM, 3μM and 10μM over the 120 minute time frame with GS_4(GC) represented at identical concentrations at the 120 minute time point.

Statistical analysis using Student's t-test to compare differences in mean CTCF values between time points indicated a difference between 15 and 60 minutes at all concentrations tested (1μM p=0.04, 3μM p=0.04, 10μM p=0.006). No differences were observed between 60 and 120 minute time points with the use of 3μM (p=0.50) or 10μM (p=0.42) concentrations of rhodamine-R8; however, for 1μM the difference between 60 and 120 minute time points was statistically significant (p=0.006) indicating that, at this concentration, the peptide may be taken up into cells over a longer time course.

Student's t-test comparison of the fluorescence intensity of the GS_4(GC) signal after 120 minutes with identical concentrations of rhodamine-R8 at the same time point revealed differences at all concentrations tested (1μM p=<0.0001, 3μM p=<0.0001, 10μM p=0.0002).

3.6 Comparison of intracellular fluorescence of rhodamine-conjugated Pen, TAT and R8

Changes in intracellular fluorescence following application of the three rhodamine conjugated CPPs: Pen, TAT and R8, was not compared via direct experimentation across the whole concentration range. However, statistical analysis of the mean CTCF values at the 60 minute time point (as seen in Figures 3.8-3.10) using one way ANOVA with Bonferroni post-hoc testing revealed differences between R8 and Pen at 1μM (p=0.0021) and 10μM (p=0.01) and R8 and TAT at 1μM (p=0.01) and 10μM (p=0.0002), with R8 producing the greatest fluorescence changes.

No differences were seen between Pen and TAT at any concentration tested and no differences were seen between peptides at 3μM concentration.

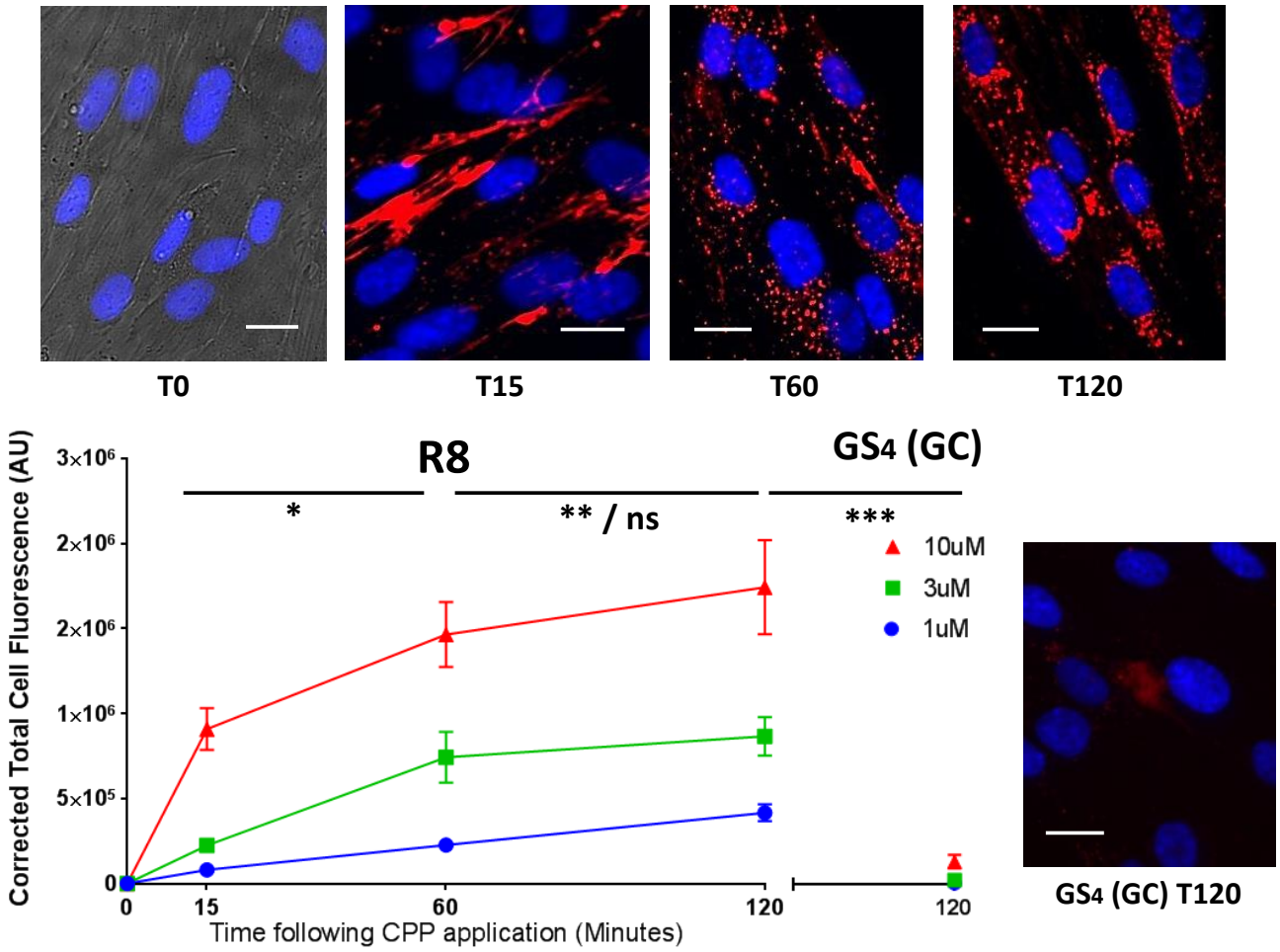

Figure 3.10 Cellular uptake of rhodamine-R8 peptide

Upper Panel: Representative confocal microscopy images of 10µM Rhodamine-R8 from pre-application (T0) to 120 minutes following application. Scale bars 20µm.

Lower Panel: Image J analysis of 1,3 and 10µM Rhodamine-R8 across the 120 minute time frame. Data points represent mean average ± SEM Corrected Total Cell Fluorescence values. Adjacent to this are data values representing equivalent concentrations control peptide GS_4(GC) at 120 time point only. On right hand is confocal image representative of 10µM GS_4(GC) to illustrate the low level of uptake seen with the control peptide at this concentration.

* indicates significance between 15 and 60 minute time points as compared using Student's t-test.

**indicates significance between 60 and 120 minute time points at 1µM concentration only as compared using Student's t-test.

***indicates significance between rhodamine-R8 and GS_4 (GC) 120 minutes following cellular application as compared using Student's t-test.

3.7 CPP entry into amnion mesenchymal cells

It was important to demonstrate whether the CPPs tested in this study could deliver cargo to other human primary cell types including cell types of placental origin. For this purpose, amnion mesenchymal cells derived from fetal amnion membranes were cultured: these are a mixed population of cells including fibroblasts, myofibroblasts and epithelial cells (Soncini et al., 2007).

As demonstrated in Figure 3.11; all three CPPs conjugated to Alexa 488 were able to enter and deliver fluorescent cargo to this cell population at 1µM concentration within an hour, thus indicating the ability of CPPs to enter other gestational cell types at low concentration within a similar timeframe to that seen with myometrial cells.

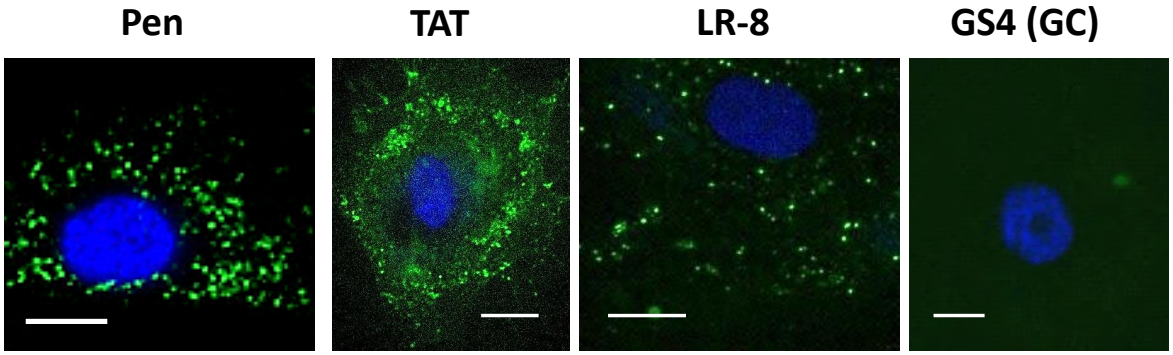

Figure 3.11 Representative confocal images demonstrating CPP entry to amnion mesenchymal cells

Cell nuclei were labelled with Hoescht dye (blue) before application of indicated CPP or control peptide at 1µM and images captured after one hour. CPP and control in these examples are conjugated to Alexa 488 fluorophore (green). Scale bars 20µm.

3.8 Examination of CPP-NBD peptide myometrial cell uptake

Having identified that fluorescently conjugated Pen, TAT and R8 peptides at a concentration range from 1-10µM could enter cells within a one hour time frame, it was necessary to determine if fluorescently labelled CPP vectors would behave similarly with peptide cargo also attached. Testing the uptake of these fluorophore-CPP-NBD conjugates also aimed to provide information on the optimal pre-incubation times for subsequent experimentation.

3.8.1 The intracellular uptake of rhodamine conjugated Pen-NBD

In pictorial data, a similar pattern of myometrial intracellular uptake of rhodamine-Pen-NBD was observed to that seen with rhodamine-Pen. The pattern of fluorescent signal aligned to cell membranes within 15 minutes of application, with fluorescence becoming internalised largely within 60 minutes was seen with the use of 3µM and 10µM; however, the process appeared to take longer at 1µM with internalisation of peptide occurring between 60 and 120 minutes with this concentration. Figure 3.12 demonstrates this uptake over 120 minutes for all three concentrations tested.

Figure 3.13 outlines the quantification of intracellular fluorescence arrived at using Image J software. The graphs display uptake curves with a similar appearance to those seen for rhodamine-Pen (Figure 3.8). Statistical analysis using Student's t-test to compare differences in mean CTCF values between time points indicated a difference between the 15 and 60 minute time point for 1µM concentration ($p=0.0005$), but no differences seen between these time points for the other concentrations tested (3µM $p=0.13$, 10µM $p=0.06$). No differences were seen between the 60 and 120 minute time point for any concentration used. Further analysis of differences across the time course demonstrated differences between the 15 and 120 minute time points for all concentrations (1µM $p=0.001$, 3µM $p=0.02$, 10µM $p=0.001$).

Comparison of the fluorescence intensity of the GS_4(GC) signal after 120 minutes with identical concentrations of rhodamine-Pen-NBD at the same time point revealed differences at all concentrations tested (1µM $p=0.003$, 3µM $p=<0.0001$, 10µM $p=0.0002$).

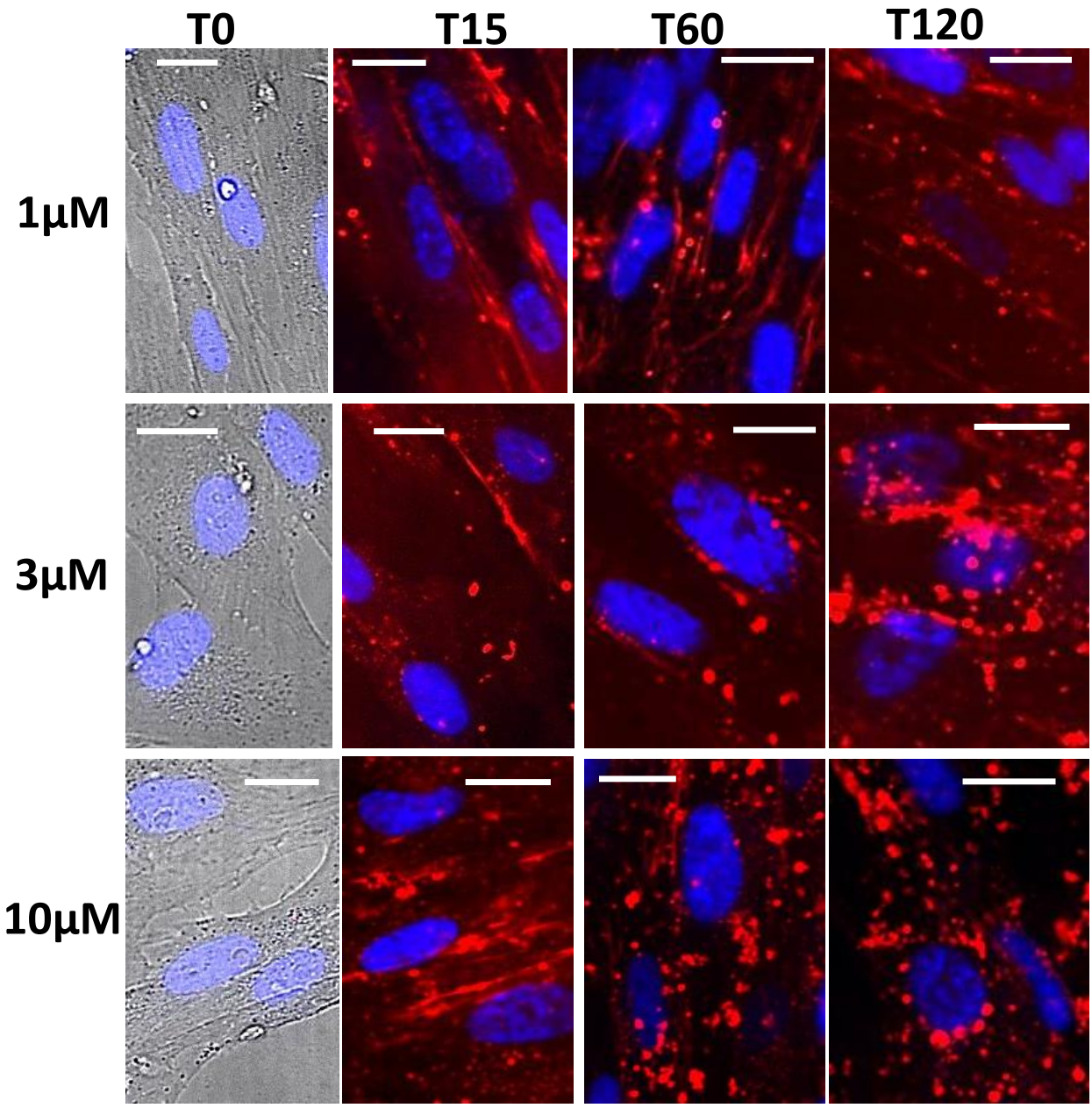

Figure 3.12 Cellular uptake of concentration range of rhodamine-Pen-NBD

Confocal microscope images representing the 120 minute time frame of uptake of 1µM, 3µM and 10µM rhodamine-Pen-NBD (red) are displayed. T0 pictures include bright field to indicate cell shapes and outlines, cell nuclei dyed blue with Hoechst. Scale bars 20µm.

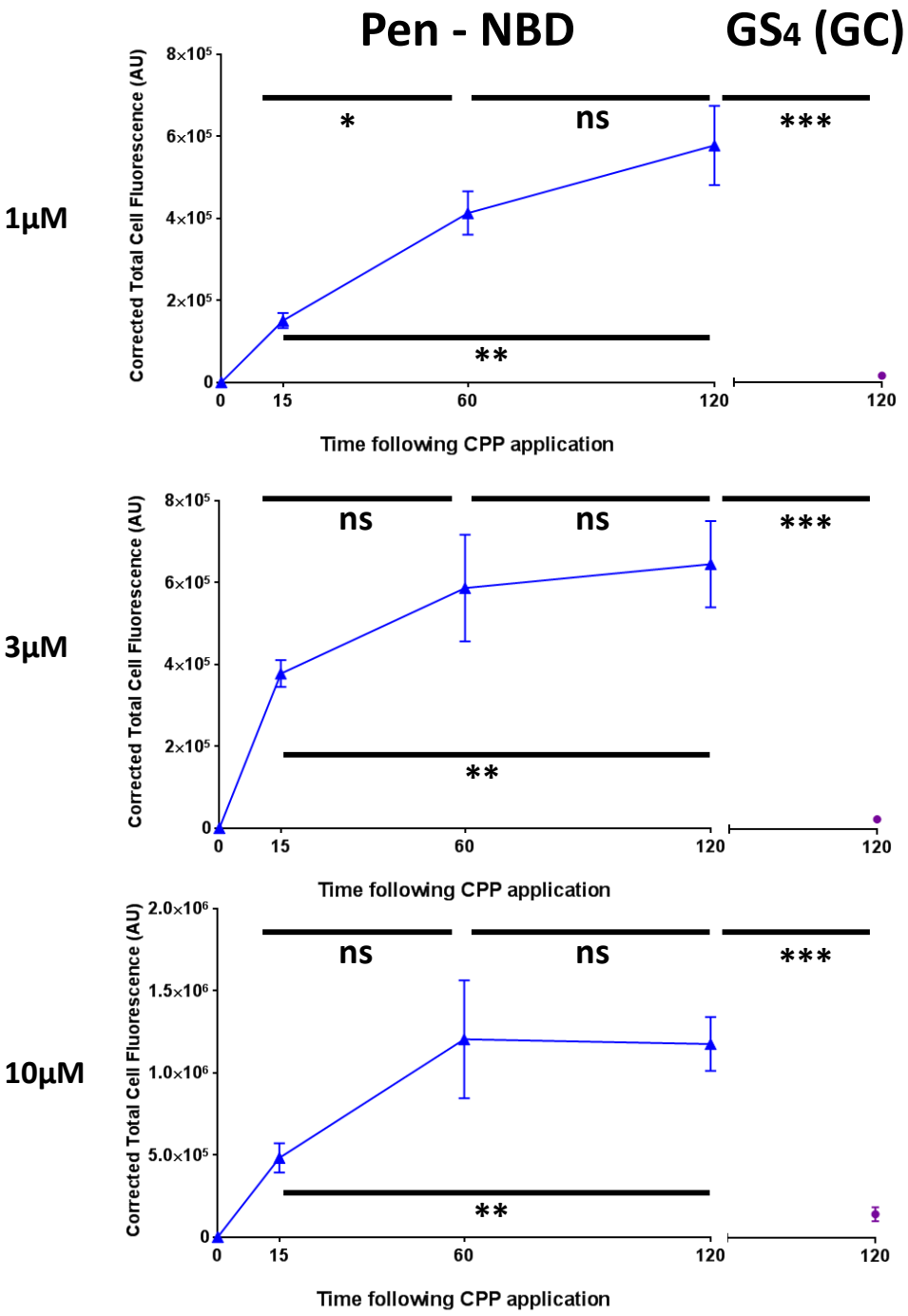

Figure 3.13 Quantitative analysis of rhodamine-Pen-NBD uptake via Image J

Line graphs displaying values of 1µM, 3µM and 10µM rhodamine-Pen-NBD cellular uptake across a 120 minute timeframe. Adjacent to this, on right hand side, is data representing equivalent concentration of control peptide Rhodamine - GS_4(GC) at the 120 minute time point only. Data points represent mean average ± SEM Corrected Total Cell Fluorescence values expressed in arbitrary units.

* indicates significance between 15 and 60 minute time points at 1µM concentration only as compared using Student's t-test.

**indicates significance between 15 and 120 minute time points as compared using Student's t-test.

***indicates significance between rhodamine-Pen-NBD and GS_4 (GC) 120 minutes following cellular application as compared using Student's t-test.

3.8.2 The uptake of rhodamine conjugated TAT-NBD and R8-NBD

It was of interest to interrogate whether NBD conjugated to TAT or R8 could be delivered into cells over a similar time frame as that observed for Pen-NBD.

As demonstrated in figure 3.14: within 60 minutes of cell application of rhodamine-TAT-NBD and rhodamine-R8-NBD a punctate pattern of fluorescence within the cell could be viewed, an effect similar to that seen with the use of TAT and R8 without the NBD cargo (Figures 3.9 and 3.10).

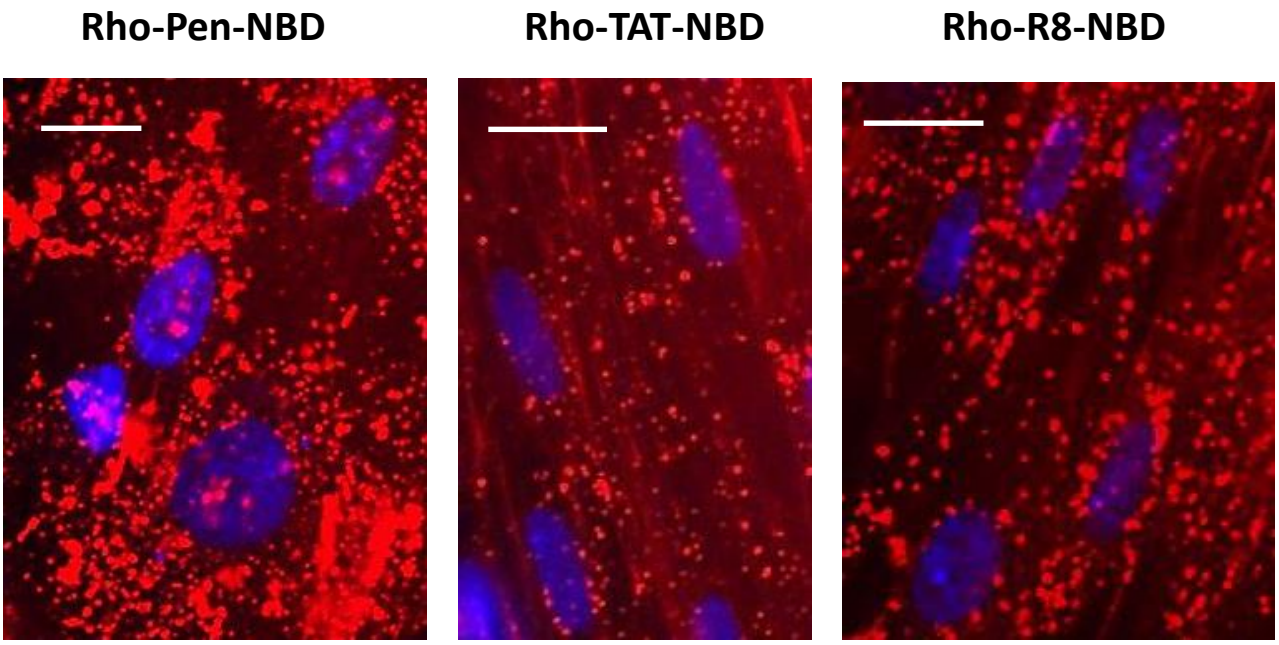

Figure 3.14 Comparison of rhodamine conjugated CPP-NBD uptake

Representative confocal images of myometrial cells 60 minutes following application of 10µM rhodamine conjugated Pen /TAT/R8 with NBD cargo (red). Nuclei stained blue with Hoechst. Scale bars 20µm.

3.8.3 Cell uptake of rhodamine-Pen-NBD mutant

A mutant NBD peptide with both tryptophan amino acid residues substituted for alanine is standardly used in the literature for testing the specificity of biological effects of NBD cargo. Experiments identified that rhodamine-Pen-NBD mutant was internalised to myometrial cells within 120 minutes of application to cells (Figure 3.15A).

3.8.4 Cell application of rhodamine-NBD

To test whether NBD peptide alone had cell penetrating properties, a rhodamine conjugated NBD peptide was applied to myometrial cells. Figure 3.15B indicates that this peptide alone did not show similar cell penetrating ability when compared with CPP conjugations of NBD peptide.

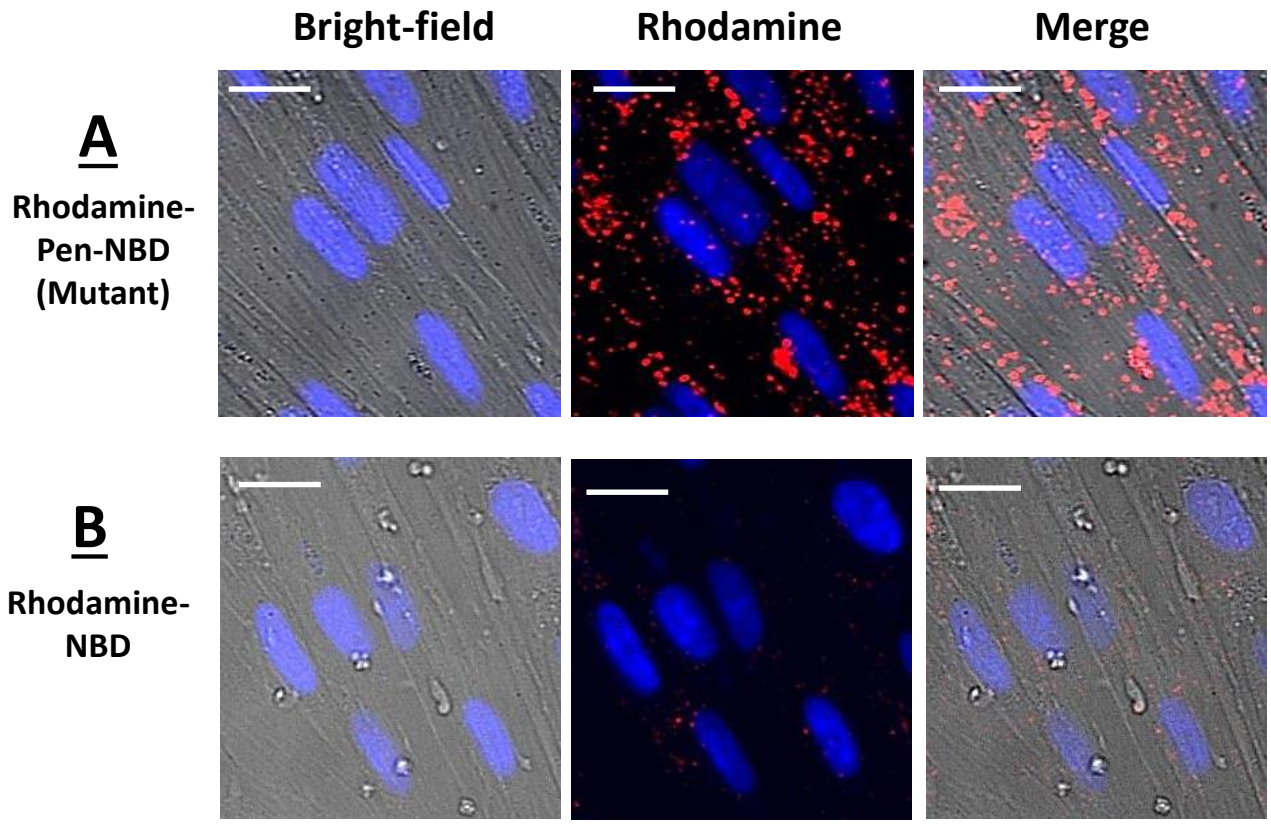

Figure 3.15: Application of rhodamine conjugated Pen-NBD (mutant) and NBD peptides to myometrial cells.

Confocal microscope images of myometrial cells 120 minutes following application of either:

A 10µM rhodamine-Pen-NBD (mutant) or

B 10µM rhodamine-NBD peptide.

Nuclei stained blue with Hoechst, scale bars 20µm.

3.9 Discussion

Cellular uptake and effectiveness of CPPs and CPP-cargo combinations are reliant on many variables including the cell type, cell confluency and the type of cargo or CPP used (Madani et al., 2011b). Human uterine cells constitute the main target for tocolytic treatments aimed at the prevention of preterm birth (Olson et al., 2008). Therefore, it was vital to undertake a thorough stepwise assessment of the effectiveness of CPPs on this cell type. It was also of interest to identify if CPPs could enter cell types derived from human placenta, cells which play a role in the inflammatory response seen in many cases of preterm birth (Mogami et al., 2014).

Firstly, it was imperative to identify that CPPs could enter myometrial cells and deliver cargo. The three CPPs tested (Pen, TAT, R8) delivered fluorescent cargo internally to human primary myometrial cells within one hour of application across a dose range of 1-10µM. All three CPPs were also able to enter primary amnion mesenchymal cells at low concentration within a similar time frame; however, difficulties in propagating this cell type beyond early passages limited the possibility of more detailed assessment of CPP uptake in this cell type.

Once delivered into myometrial cells, CPPs were largely distributed in a vesicular pattern; they remained mobile and achieved a peri-nuclear distribution within 2 hours of application. The fluorescent-CPP conjugations did not predominantly co-localise with the endoplasmic reticulum or mitochondria. However, there was substantial co-localisation with Alexa488-Dextran labelled endosomes and lysosomes within the cell, suggesting that some fluorescently tagged CPP may be distributed within these structures once internalised into uterine cells. This reflects findings from previous studies that have identified endocytosis as a likely route of intracellular uptake for many CPPs (Richard et al., 2005, Jiao et al., 2009). A degree of non-vesicular cytosolic labelling was also observed with the use of higher concentrations (3-10µM) of all three peptides; possibly representing a phenomenon of direct penetration or ‘translocation’ of CPPs across the cell membrane which avoids endocytic pathways via an energy independent mechanism (Madani et al., 2011b). All three CPPs used in this study have been shown previously capable of entering cells via this direct route as an alternative to endocytosis, with poly-arginine demonstrating the highest

likelihood of favouring such an entry route, and Pen most likely to favour endocytic routes of entry (Thorén et al., 2003).

With all CPPs used across all concentrations tested, changes in intracellular fluorescence as measured using Image J software were significantly greater than that observed with the use of a rhodamine-conjugated control peptide with neutral charge (Rhodamine-GS_4GC) at identical concentrations. This indicates that fluorescence delivery is due to the vector properties of the CPPs as opposed to simple diffusion across the cell membrane.

Although limitations of time prevented direct experimental comparison of peptides across the full concentration range and time course, statistical analysis of quantitative data suggested that addition of rhodamine-R8 led to the largest increases in fluorescence within myometrial cells, with the use of rhodamine-TAT and rhodamine-Pen producing a smaller change in cellular fluorescence intensity, mirroring the findings of published data using non-primary cell types (Jones et al., 2005). Such data could indicate that R8 delivers cargo most efficiently of the CPPs tested in myometrial cells. However, previous literature suggests that conjugation of fluorophore cargo to poly-arginine CPPs contributes to the translocation of the CPP across cell membranes (Hirose et al., 2012). The observation that fluorophore interaction with individual CPPs may influence delivery efficacy means direct comparisons of delivery efficacy between CPPs must be interpreted with caution. Furthermore, a study investigating the effect of cargo attachments on CPP uptake efficiency found that the efficacy of poly-arginine delivery was attenuated once peptide cargo was attached (Jones et al., 2005). Such considerations; alongside the fact that many studies examining the effectiveness of the NBD peptide cargo have used CPP conjugations derived from antennopaedia protein (Strickland and Ghosh, 2006), led to the selection of Pen-NBD for more detailed examination in both uptake studies and biological effectiveness experimentation.

Research examining how the cellular uptake of CPPs derived from antennopaedia can be affected by different peptide cargo attachments has found that there can be either attenuation or increase of uptake depending on the cargo tested (Fischer et al., 2002). Thus, it was essential to examine whether attaching the NBD peptide cargo to fluorophore-CPP conjugations would influence the efficiency of intracellular delivery. Rhodamine

conjugated Pen-NBD demonstrated similar patterns of uptake to rhodamine-Pen as observed from both the pictorial and graphical data presented in Figures 3.14 and 3.15. Significant differences in intracellular fluorescence were observed between the 15 and 120 minute time points at all concentrations; however, between 15 and 60 minute time points, the cellular uptake of rho-Pen-NBD only demonstrated statistical significance at 1µM concentration and not for higher concentrations tested. It was also observed that rho-Pen-NBD fluorescent signal correspondent to cell membranes persisted beyond the 15 minute time point in some, but not all of the cells measured. This produced an increased variety of measured responses compared to that seen when using rhodamine-CPPs without NBD cargo attachment. Such observations suggests a degree of attenuation of Pen uptake once NBD cargo is attached due to the persistence of rho-Pen-NBD to reside on or near the cell membrane either prior to, or instead of, cell incorporation.

The uptake kinetics of rho-Pen-NBD in myometrial cells may have been further clarified with the use of Fluorescence-activated cell sorting (FACS) techniques which can allow an assessment of fluorescent intensity from individual cells within a whole population (Manceur et al., 2007). However, FACS may not optimally distinguish between membrane bound fluorescent signal and intracellular fluorescence (Richard et al., 2003). Myometrial cells are adherent and require the use of proteases such as trypsin to aid suspension in cell media (Gargett et al., 2002), thus it is anticipated that such a methodological step could intrinsically alter the barrier properties of cell membranes and influence data regarding CPP uptake. Despite these concerns; FACS data may provide a useful adjunct to confocal microscopy in further work detailing CPP-cargo uptake in human primary cells.

Detailed testing of cellular uptake of NBD peptide conjugated to CPPs other than Pen was not feasible within the temporal constraints of this study, nevertheless the confocal images displayed in Figure 3.16 indicate that the NBD cargo can be delivered into cells within 60 minutes of application when conjugated to TAT and R8 CPPs. Attaching a mutant version of the NBD cargo to Pen CPP did not substantially affect intracellular delivery of cargo to myometrial cells, a result indicating that the subsequent lack of biological effect observed with the use of this mutant peptide control as seen in Chapter Four is not due to failure of this cargo to enter cells. Rhodamine-NBD in the absence of CPP demonstrated similar non

cell permeable properties to rhodamine-GS_4GC, thus underlining the necessity of CPP vector conjugation to achieve efficient cellular entry of cargo.

The NBD peptide has a putative anti-inflammatory mechanism that is of potential benefit in the context of preterm birth; therefore demonstrating the entry of this cargo into uterine cells is the first step towards establishing the biological effectiveness of this peptide, a process which is detailed further in the following chapter.

Chapter Four

The biological effectiveness and specificity of targeting of CPP-linked NBD peptide: a comparison with non-peptide inhibitors

4.1 Introduction

Chapter Three establishes the ability of three CPPs to enter myometrial cells and deliver fluorescent cargo within a one hour time frame at doses of 1μM and above. The data presented in that chapter also supports the notion that potentially bioactive cargo, in the form of the NBD peptide conjugated to CPP, can be transported to sites internal to the myometrial cell membrane. The overall aim of this chapter was, therefore, to test if the CPP-conjugated cargo could exert a biological effect within these cells.

To recap, the cargo tested in this study is the Nemo Binding Domain (NBD) peptide, an 11 amino acid polypeptide directed at preventing the inflammatory ligand-induced activation of the IκB kinase complex (IKK complex) via interference at the site of interaction between the inhibitory NFκB essential modulator (NEMO or IKKγ) subunit and the two active components of IKK (IKKα and IKKβ), and, in doing so, prevent the transcriptional activation of NFκB (May et al., 2000). A broad range of CPP-cargo conjugations are available as putative agents to inhibit inflammatory pathways within cells, and the rationale underpinning the selection of the NBD peptide as a tool in the experimental context of this thesis is dealt with in detail in the introductory chapter of this thesis (section 1.10.4).

COX2 protein was selected to demonstrate both inflammatory changes in uterine cells, and to define the efficacy of CPP-linked and non-peptide inhibitors to block such changes. COX2 is a highly inducible protein enzyme whose increased expression is a key step in the production of prostaglandins from arachidonic acid (Keelan et al., 2003). COX2 protein induction occurs secondary to the upregulation of inflammatory pathways in uterine and placental cells, a change that is associated with preterm birth (Slater et al., 1999, Bartlett et al., 1999b). The human COX2 gene has multiple sites of gene regulation including two NFκB binding sites (Appleby et al., 1994), and increases in COX2 mRNA and protein expression have been seen to synchronously follow degradation of IκBα and translocation of p65 to the nucleus in IL1β stimulated myometrial cells (Soloff et al., 2004). This suggests that, although there may be contribution from other inflammatory pathways, increased expression of COX2 is driven by NFκB activation in these cells.

Cellular cytokine exposure leads to activation of the IKK complex within the canonical NFκB pathway, this complex subsequently phosphorylates the immediate downstream substrate

IκBα, which is then targeted for degradation by the proteasome (Hayden and Ghosh, 2004). Careful examination of IκBα degradation in response to cytokine stimulation was selected as a marker to test the specificity of Pen-NBD effects towards its expected target, the IKK complex, in myometrial cells.

To allow for comparison between the biological effectiveness of CPP-conjugated inhibition of inflammatory signalling and non-CPP linked methods of inhibition, a group of non-peptide small molecule inhibitors with putative NFκB inhibitory activity (Curcumin, Sc514, Mg132 and NAC) were also investigated for their ability to both inhibit cytokine stimulated COX2 protein induction and prevent the degradation of IκBα secondary to IKK complex activation.

The detailed aims for this chapter were:

- To assess the optimal time frame and dose range of the cytokine agonists IL1β and TNFα to induce COX2 protein expression and IκBα protein degradation in human myometrial cells.
- To assess any cell toxicity effects via application of cytokine stimulants or CPP-cargo conjugations to these cells.
- To examine the ability of the NBD cargo conjugated to Pen CPP, derived from the antennopedia protein, to inhibit myometrial cell COX2 protein expression in response to cytokine stimulation.
- To determine the specificity of this effect by examining cytokine induced COX2 protein expression in the presence of a number of peptide and vehicle controls.
- To compare the effectiveness of NBD conjugated to the different CPPs: Pen, TAT and R8.
- To interrogate the discrete targeting of NBD peptide towards the putative IKK complex target by examining the phosphorylation dependent degradation of its immediate downstream substrate IκBα.
- To examine the efficacy of Pen-NBD inhibitory effects against a panel of small molecules putatively capable of NFκB inhibition.

4.2 Assessing the time frame and agonist concentration for IL1β and TNFα stimulated COX2 expression in myometrial cells

It was necessary to establish a time frame of cytokine induced changes in COX2 protein expression in order to both assess normal myometrial cell responses to inflammatory stimuli and the ability of NBD cargo to inhibit this response. Work was subsequently done to define the optimal dose of IL1β and TNFα induction.

4.2.1 Optimising the time frame of COX2 protein induction

Initial doses of cytokine agonists IL1β and TNFα were selected from the literature (Taichman and Hauschka, 1992, Zaragoza et al., 2006). In preliminary experiments, myometrial cells were exposed to 10ng/ml IL1β or 1nM (17ng/ml) TNFα over a 24 hour period and lysed at numerous indicated time points. In Figure 4.1 Western blots representing this time frame are displayed. COX2 protein signal displays little change at 0 and 1 hours; increases at 2 and 4 hours. Although some further increases were also observed over 8 to 24 hours, a time frame with cell lysis points at 0 (prior to cytokine addition), 1, 2 and 4 hours was selected for further experimentation. This was deemed the time frame within which the greatest dynamic changes of the COX2 signal could be elicited, whilst aiming to minimise occurrences whereby the chemiluminescent signal may be saturated.

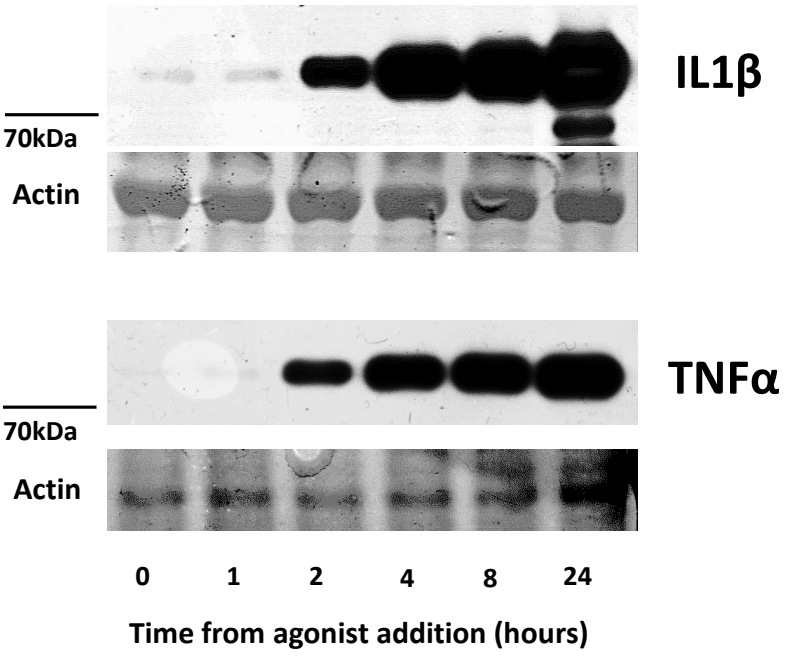

Figure 4.1 Time frame of COX2 protein cytokine response in myometrial cells

Western blots of COX2 protein expression over 24 hours following 10ng/ml IL1β (upper panel) or 1nM TNFα (lower panel) addition to myometrial cells in culture.

PVDF membranes stained with napthol blue black dye are used to demonstrate actin expression as a demonstration of protein loading.

4.2.2 Optimising the agonist concentration range for COX2 protein induction

Following the time frame experiment above, it was necessary to define an optimal agonist concentration to induce increases in myometrial cell COX2 protein expression within 4 hours of application. To assess cytokine dosage concentration ranges of 0.1 to 100 ng/ml IL1β and 0.1 to 10nM TNFα were applied to myometrial cells before cell lysis at 4 hours. Figure 4.2 displays representative Western blots above a bar graph summation of optical densitometry data from 3 experiments demonstrating COX2 protein expression subsequent to IL1β or TNFα application. Responses to IL1β increased up to 1ng/ml then levelled out thereafter; TNFα induced COX2 expression increases up to 1nM; further dose increase of the cytokine beyond this point did not elicit a stronger protein response. Statistical analysis of the differences between groups using one-way ANOVA with Bonferroni post-hoc correction revealed no differences between the concentrations used of either IL1β or TNFα. Figure 4.2 displays a clear pictorial and graphical demonstration of changes in COX2 signal with application and alteration of concentrations of both IL1β and TNFα; therefore, the failure to prove statistical significance is likely due to the low number of replicates used (n=3). Consequently, due to temporal limitations of the study and following examination of the agonist concentration effect on IκBα protein (Figure 4.12), concentrations of 10ng/ml IL1β and 1nM TNFα were selected for further experimentation.

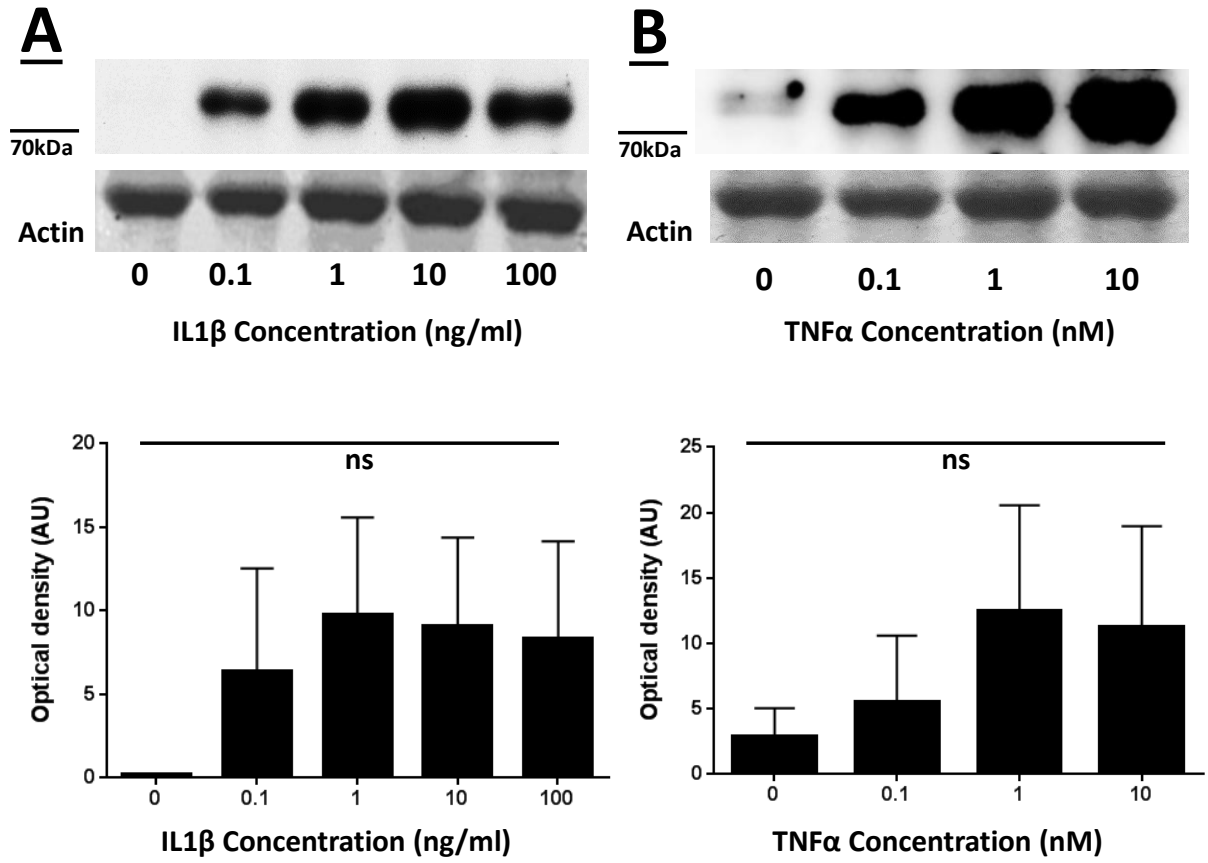

Figure 4.2 COX 2 protein responses across a cytokine agonist concentration range

Upper Panels: representative Western blots demonstrating COX2 protein expression at 4 hours (**A** IL1β, **B** TNFα) in myometrial cells in response to increasing doses of cytokine. Actin expression demonstrated as loading control.

Lower Panels: Bar graphs demonstrating mean (SD) optical densitometry values of COX2 protein expression 4 hours following exposure to indicated concentration of cytokines **A** IL1β or **B** TNFα (n=3).

4.3 Examination of cell toxicity effects

To ensure that the experimental effects under observation were not mediated through peptide or agonist toxicity, a Cell Titre Blue rezazurin reduction assay was undertaken. Figure 4.3A displays the fluorometer values from untreated cells compared to cells treated with 10ng/ml IL1β or 1nM TNFα demonstrating that substantial cell death did not occur with addition of cytokine. Application of neither the unconjugated forms of Pen and NBD peptides at 50µM, nor Pen-NBD at 50µM or 100µM had an effect on cell viability (Figure 4.3B) indicating that subsequent experimental results were not substantially influenced by cell death. The experimental time frame and concentrations displayed here were selected to mirror experiments presented later in this chapter.

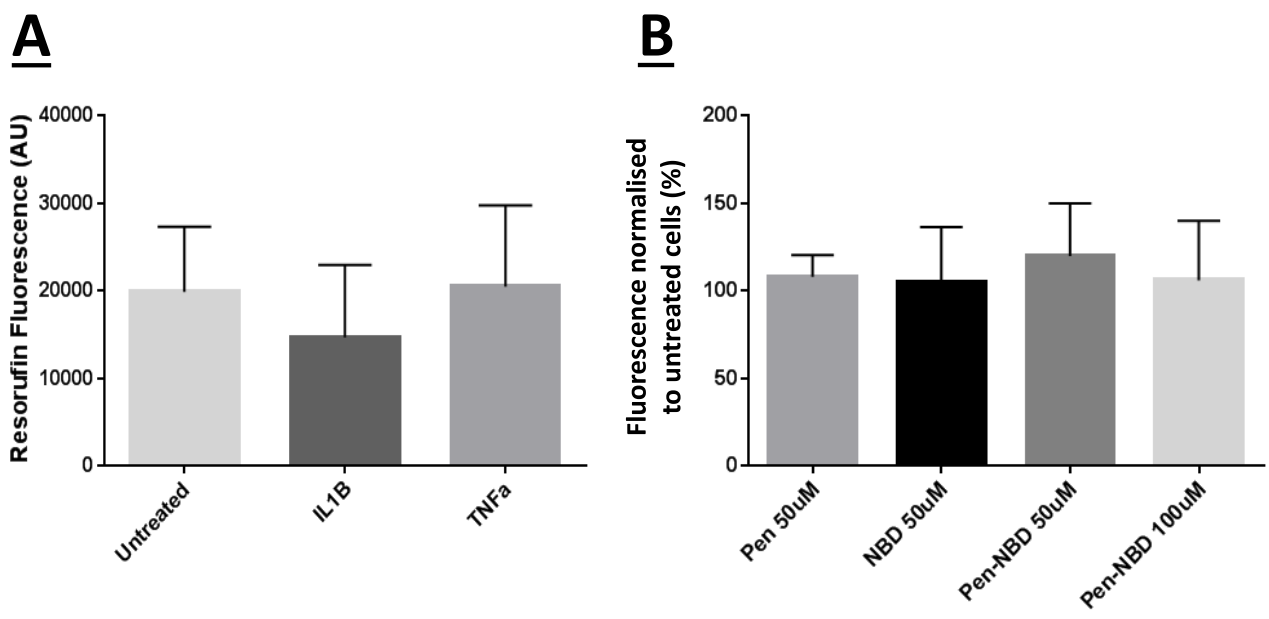

Figure 4.3: Myometrial cell viability in presence of cytokine agonist or peptide

A Comparison of untreated cells with cytokine treated cells after 5 hour incubation period. Bars represent mean average (SD) of fluorometer readings (n=3).

B Comparison of cells treated with indicated peptides at varying concentration over 5 hour incubation period. Bars represent mean fluorometer readings (SD) as a percentage of untreated cells (n=3).

4.4 The effect of Pen-NBD on cytokine stimulated COX2 protein expression

4.4.1 Pen-NBD inhibition of IL1β stimulated responses

The Western blots in Figure 4.4A demonstrate COX2 protein expression in a 4 hour time course following application of IL1β alone (Control) or following pre-incubation with indicated doses of Pen-NBD peptide. The bar chart in Figure 4.4B displays the COX2 protein signal at 4 hours derived from Western blot results of 3 independent experiments. Data here is expressed as a percentage of mean IL1β (Control) optical density values across 3 experiments.

In control experiments a strong IL1β-induced COX2 response was seen at the 4 hour time point, but not reproducibly seen at time points previous to this. Application of 1 and 10μM of Pen-NBD produced a small increase in the COX2 response at 4 hours. Concentrations of 50μM Pen-NBD decreased COX2 protein signal in all three experiments, whilst 100μM of Pen-NBD ablated the protein response to IL1β.

Statistical analysis of the 4 hour time point responses using one-way ANOVA with Bonferroni post-hoc testing revealed differences between the control group and samples pre-incubated with 100μM ($p=0.002$) of Pen-NBD. No differences were seen with the use of 1μM, 10μM or 50μM Pen-NBD or control samples. Analysis using one-way ANOVA at the other time points tested (0,1 and 2 hours) revealed no differences between any groups.

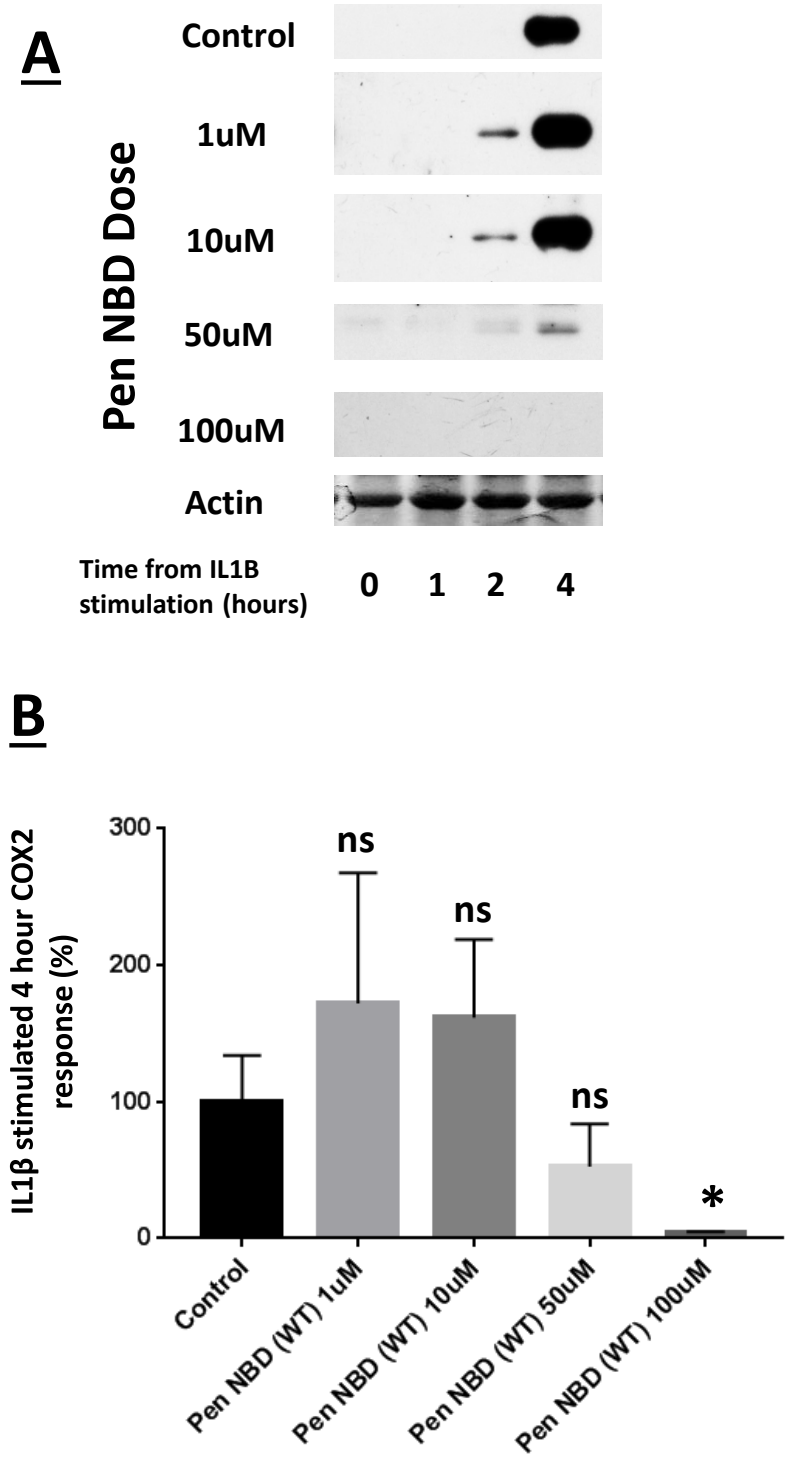

Figure 4.4 Effect of Pen-NBD on IL1β-induced COX2 protein expression

A Representative Western blots indicating COX2 protein expression in myometrial cells over a four hour time frame following IL1B exposure alone (Control) or with 1 hour pre-incubation of increasing concentrations of Pen-NBD.

B*:* Bar graph demonstrating summated mean (SD) optical densitometry values of COX2 protein expression 4 hours following application of IL1β from 3 independent experiments normalised to a percentage of mean Control value.

*indicates significant difference compared with control values. Tested using one-way ANOVA with Bonferroni post-hoc analysis.

4.4.2 Pen-NBD inhibition of TNFα stimulated responses

The Western blots in Figure 4.5A demonstrate COX2 protein expression in a 4 hour time course following application of TNFα alone (Control) or following pre-incubation with indicated doses of Pen-NBD peptide. The bar chart in Figure 4.5B displays the COX2 protein signal at 4 hours derived from Western blot results of 3 independent experiments. Data here is expressed as a percentage of mean TNFα (Control) optical density values across 3 experiments.

In control experiments, a small increase in COX2 protein expression was observed at 1 and 2 hours post cytokine exposure, with a stronger response elicited at the 4 hour time point. It is notable that the COX2 response elicited over the time course with the use of TNFα was more variable than that seen with the use of IL1β.

Application of 1 and 10μM of Pen-NBD produced an increase in the COX2 response at 4 hours. Concentrations of 50μM Pen-NBD did not affect the 4 hour COX2 protein signal, whilst 100μM of Pen-NBD decreased the protein response to IL1β. Statistical analysis of the 4 hour COX2 protein responses from optical densitometry data using one-way ANOVA with Bonferroni's post-hoc testing did not reveal any differences between groups. This may be due to small sample size tested (n=3) and a greater variety of COX2 responses in the TNFα alone group compared with that produced by IL1β. Analysis using one-way ANOVA at the other time points tested (0,1 and 2 hours) revealed no differences between any groups.

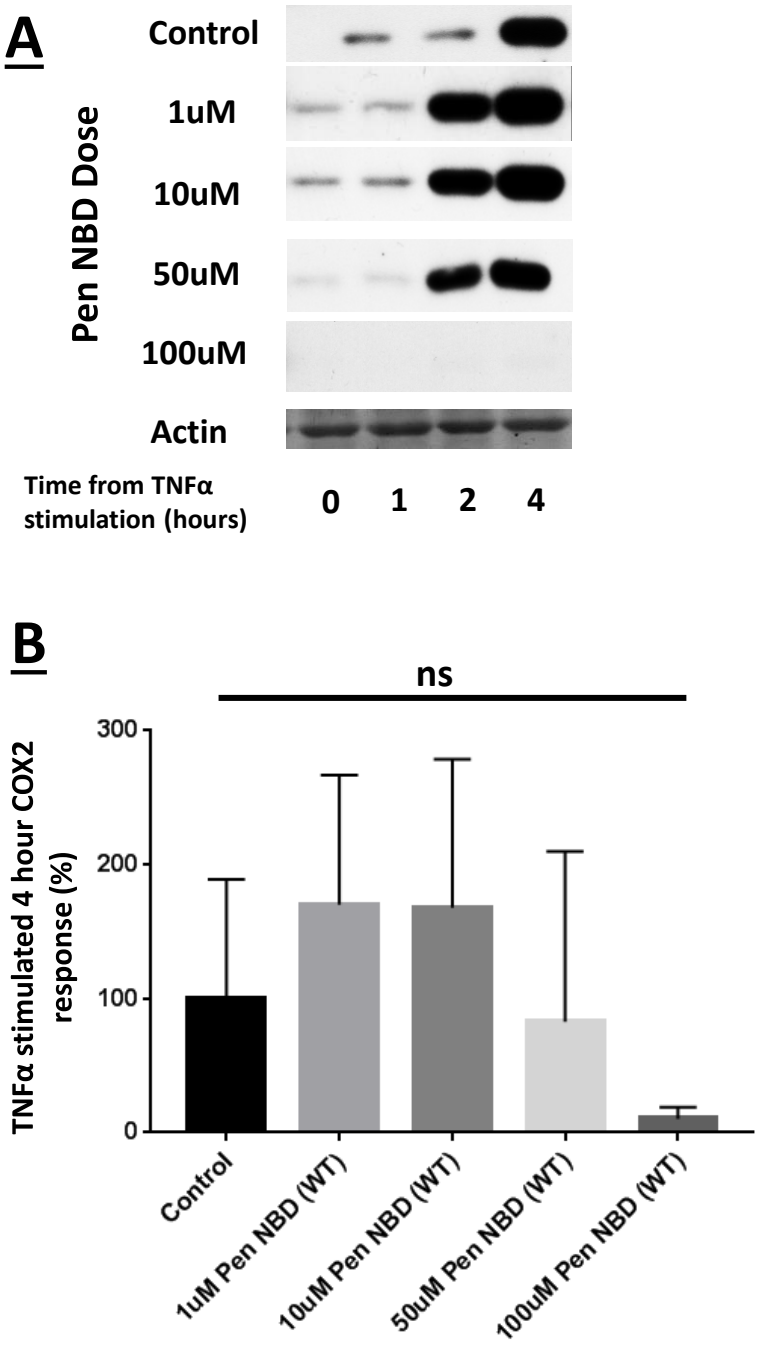

Figure 4.5 Effect of Pen-NBD on TNFα-induced COX2 protein expression

A Representative Western Blots indicating COX2 protein expression in myometrial cells over a four hour time frame following TNFα exposure alone (Control) or with 1 hour pre-incubation of increasing concentrations of Pen-NBD.

B Bar graph summating mean (SD) average optical densitometry values of COX2 protein expression 4 hours following TNFα exposure normalised to a percentage of mean Control (TNFα alone) signal (n=3).

Statistical analysis performed using one-way ANOVA with Bonferroni post-hoc testing.

4.5 The effect of peptide and vehicle controls on cytokine stimulated COX2 expression

As demonstrated above; at higher doses Pen-NBD was capable of inhibiting IL1β-induced COX2 responses in myometrial cells. Effects on TNFα-stimulated responses of the protein remained less clear, although there was an indication that lower doses may increase COX2 protein expression with possible non-significant inhibition occurring at 100μM concentration.

It was necessary to test the specificity of these effects by examining cytokine stimulated COX2 protein expression in the presence of a number of structurally similar peptide and vehicle controls.

4.5.1 Effect of Pen-NBD mutant peptide on COX2 induction

The specificity of CPP-NBD cellular effects has characteristically been examined with the use of an NBD mutant peptide (Strickland and Ghosh, 2006). This is an 11 amino acid peptide with the substitution of two tryptophan residues with alanine to produce the sequence: TALDASALQTE, thus rendering the peptide biologically ineffective (Dai et al., 2004).

Figure 4.6 displays representative Western blots (upper panel) summarising 3 experiments whereby the NBD mutant, conjugated to Pen, was applied at a concentration range of 1-100μM onto cells 1 hour prior to stimulation by IL1β cytokine, with the 100μM concentration presented here for ease of comparison. The Western blot displayed suggests that Pen-NBD mutant may alter the cytokine-induced COX2 protein signal at both 2 and 4 hour time points. The lower panel of Figure 4.6 presents a bar graph summation of optical densitometry data from the same experiments demonstrating the effect of 1-100μM Pen-NBD mutant on COX2 protein signal at four hours. This summated data suggests that doses of 1-50μM Pen-NBD mutant peptide may increase IL1β-induced COX2 protein signalling, an effect similar to that seen in with the use of 1-10μM wild type Pen-NBD in Figure 4.4. Pen-NBD mutant 100μM did not have a reproducible inhibitory effect. Statistical analysis of the 4 hour IL1β-induced COX2 protein responses from optical densitometry data using one-way ANOVA with Bonferroni's post-hoc testing did not reveal differences between any of the concentrations tested or the control group. Further statistical testing using one-way ANOVA at the other time points examined (0,1 and 2 hours) also did not reveal differences between groups. Although the small numbers involved in experimentation (n=3) may have influenced

the likelihood of demonstrating significance, no reproducible inhibitory effects on cytokine-induced COX2 protein expression were observed in these experiments.

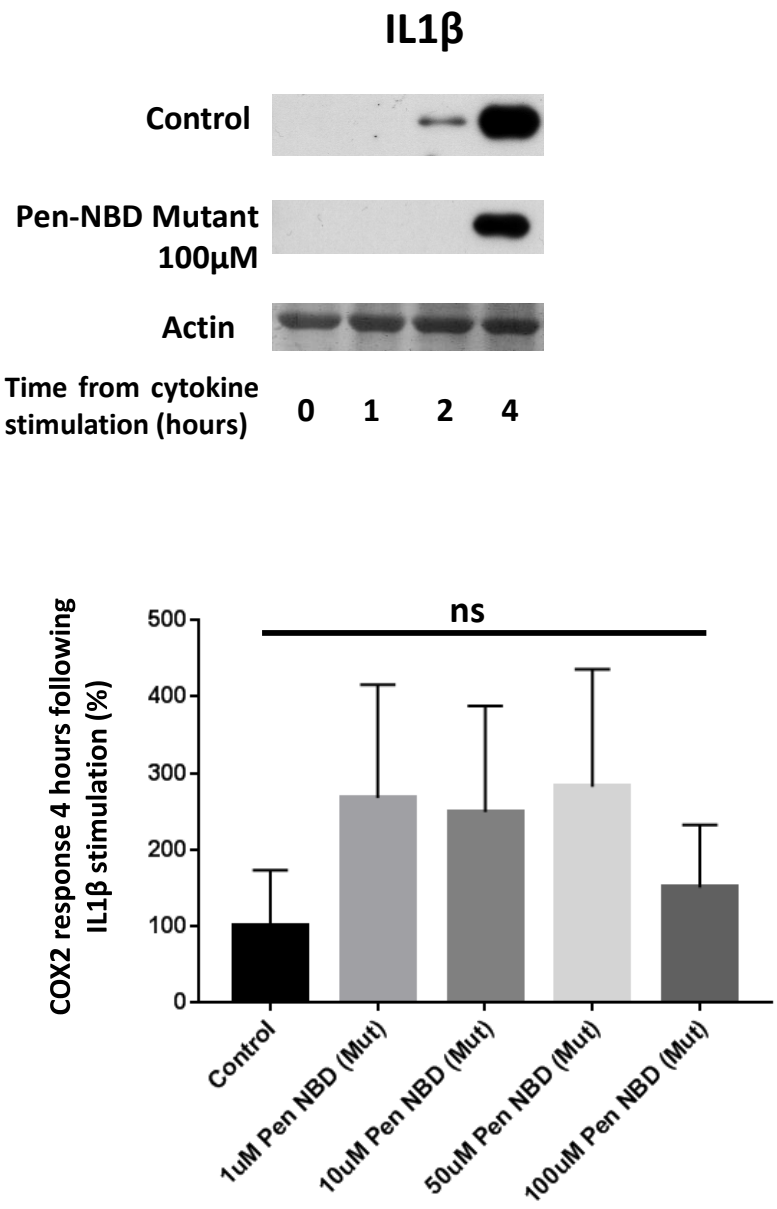

Figure 4.6: Effect of Pen-NBD mutant peptide on IL1β stimulated COX2 protein expression

Upper panel: representative Western Blots of COX2 responses to IL1 β over a 4 hour time frame in the presence and absence (Control) of 100µM mutant peptide.

Lower panel: bar chart of summated optical densitometry readings of 4 hour COX2 signal across a concentration range of 1-100µM (n=3). Data is presented as mean (SD) percentage values of Control signal (IL1β alone).

Statistical analysis performed using one-way ANOVA with Bonferroni post-hoc testing.

Figure 4.7 displays representative Western blots (upper panel) and a bar chart (lower panel) summating 3 experiments whereby Pen-NBD mutant was applied to cells at 1-100µM concentration 1 hour prior to stimulation with TNFα cytokine. Statistical analysis using one-way ANOVA to interrogate the optical densitometry data at each time point (0,1,2 and 4 hours) across the concentration range tested (1-100µM) did not reveal any differences between groups.

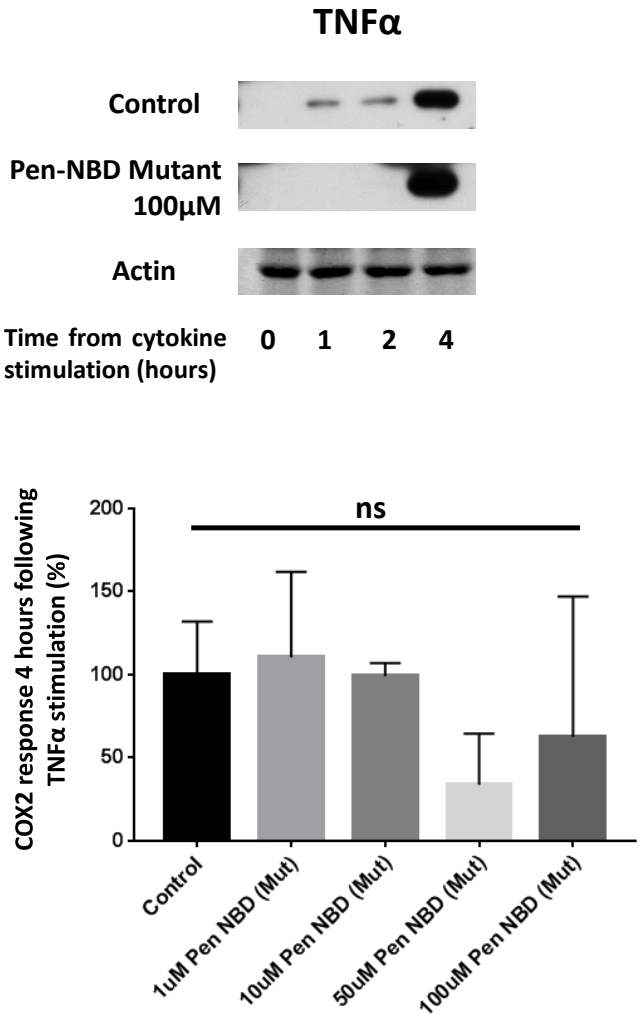

Figure 4.7: Effect of Pen-NBD mutant peptide on TNFα stimulated COX2 protein expression

Upper panel: representative Western blots of COX2 responses to TNFα over a 4 hour time frame in the presence and absence (Control) of 100µM mutant peptide.

Lower panel: bar chart of summated mean (SD) optical densitometry readings of 4 hour COX2 signal across a concentration range of 1-100µM (n=3). Data is presented as mean (SD) percentage values of Control signal (TNFα alone).

Statistical analysis performed using one-way ANOVA with Bonferroni post-hoc testing.

4.5.2 Unconjugated Pen and NBD effect on cellular COX2 responses to IL1β

It remained possible that effects seen on IL1β-induced COX2 expression could be mediated through either the CPP Pen or NBD peptide alone, therefore 50μM of unconjugated Pen or NBD peptide were added to myometrial cells for 1 hour prior to addition of 10ng/ml IL1β. Application of neither peptide influenced cytokine stimulated COX2 expression over 4 hours (Figure 4.8). Statistical analysis using one-way ANOVA to interrogate the optical densitometry data at each time point examined (0,1,2 and 4 hours) did not reveal any differences between groups.

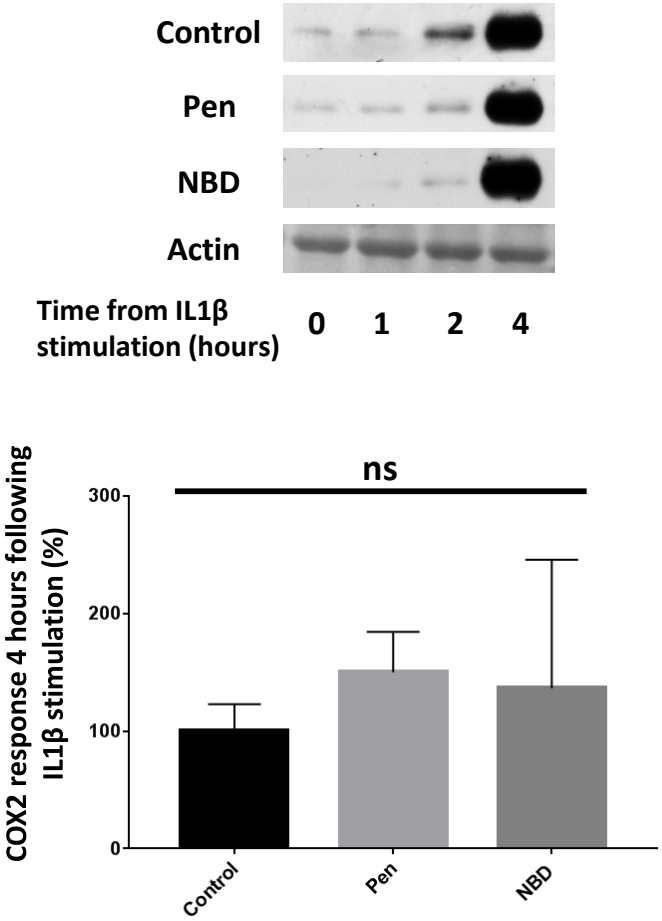

Figure 4.8: Effect of unconjugated Pen CPP or NBD peptide on IL1β stimulated COX2 protein expression

Upper panel: representative Western blots of COX2 responses to IL1β over a 4 hour time frame in the presence and absence (Control) of 50μM of either peptide.

Lower panel: bar chart of mean average (SD) optical densitometry readings of 4 hour COX2 signal across 3 such experiments. Data is presented as mean (SD) average percentage values of Control signal (IL1β alone).

Statistical analysis performed using one-way ANOVA with Bonferroni post-hoc testing.

4.5.3 DMSO vehicle effects

To ensure peptide solubility in the final solutions of cell media required initial creation of a concentrated stock solution in an appropriate solvent. Following the peptide manufacturers' advice, Dimethylsulphoxide (DMSO) was used as a solvent in this study. At high concentrations of DMSO there is the potential for cell toxicity or altered gene and protein expression effects (Pal et al., 2012). These effects vary between different cell types therefore vehicle testing at identical percentages to the final concentration of solvent is always recommended, and it is considered desirable to maintain a final concentration of DMSO at less than 0.1%. In practise it was not possible to dissolve the peptides in anything less than a 20mM stock solution; thus, the final concentration of DMSO applied to cells was 0.25% for 50µM concentration and 0.5% for 100µM concentration.

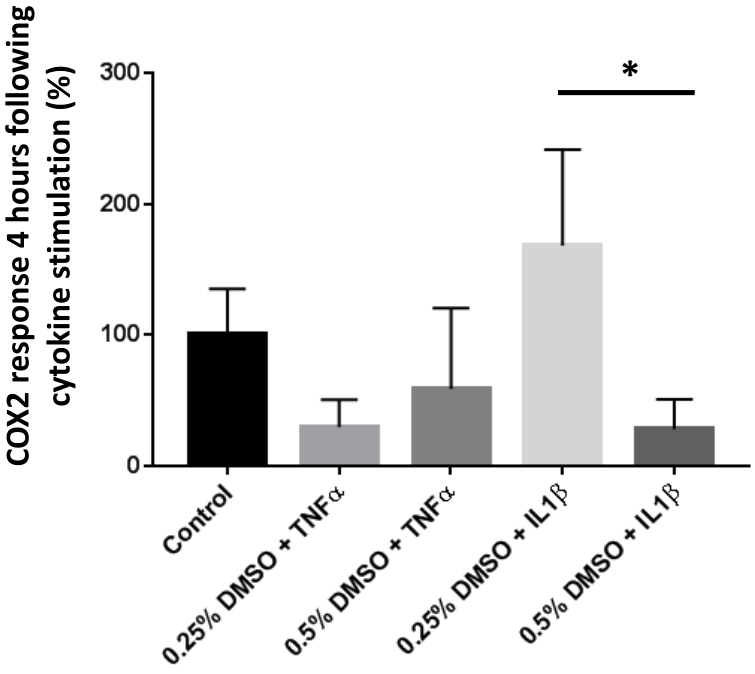

Figure 4.9: Vehicle (DMSO) effects on cytokine-stimulated COX2 protein expression

Bar chart summation of three experiments displaying optical densitometry readings of 4 hour COX2 signal following cytokine exposure alone (Control) or with pre-incubation of indicated concentration of DMSO. Data is presented as mean (SD) average percentage values of Control signal (IL1β alone).

*Indicates significant difference performed using one-way ANOVA with Bonferroni post-hoc testing.

Figure 4.9 displays a bar chart demonstrating the effects on cytokine-induced 4 hour COX2 protein expression in myometrial cells pre-incubated with 0.25% or 0.5% DMSO. In IL1β-induced cells, pre-incubation with 0.25% DMSO increased COX2 protein expression at 4 hours whereas 0.5% concentration reduced protein expression. In TNFα-induced cells, pre-incubation with 0.25% DMSO reduced COX2 protein expression at 4 hours whereas 0.5% concentration increased protein expression. Statistical analysis of the optical densitometry readings of the 4 hour COX2 signal revealed a difference between 0.25% DMSO and 0.5% DMSO treated groups in IL1β-induced cells ($p=0.02$). There were no other differences between groups.

4.6. The efficacy of NBD conjugated to different CPP vectors

To ascertain the most effective CPP delivery vector for NBD, a comparison of COX2 responses to IL1β induction following pre-incubation with R8-NBD or TAT-NBD was undertaken.

4.6.1 Determination of half maximal concentration

Identification of the appropriate dose of R8-NBD or TAT-NBD conjugate was inferred via calculation of the half maximal inhibitory concentration of Pen-NBD required to ablate the IL1β induced COX2 response using the concentration range seen above (Figure 4.4). This is a value often referred to as IC50; however, to produce such a value usually requires reproduction of experimentation no less than six times and given the relatively low numbers involved in this part of the study ($n=4$), half maximal inhibitory concentration was deemed more appropriate terminology. As demonstrated in Figure 4.10 the half maximal inhibitory concentration required for Pen-NBD to inhibit IL1β induced COX2 protein expression at 4 hours was 39.42μM. For simplification: a concentration of 50μM was chosen to compare the differing CPP-NBD vectors.

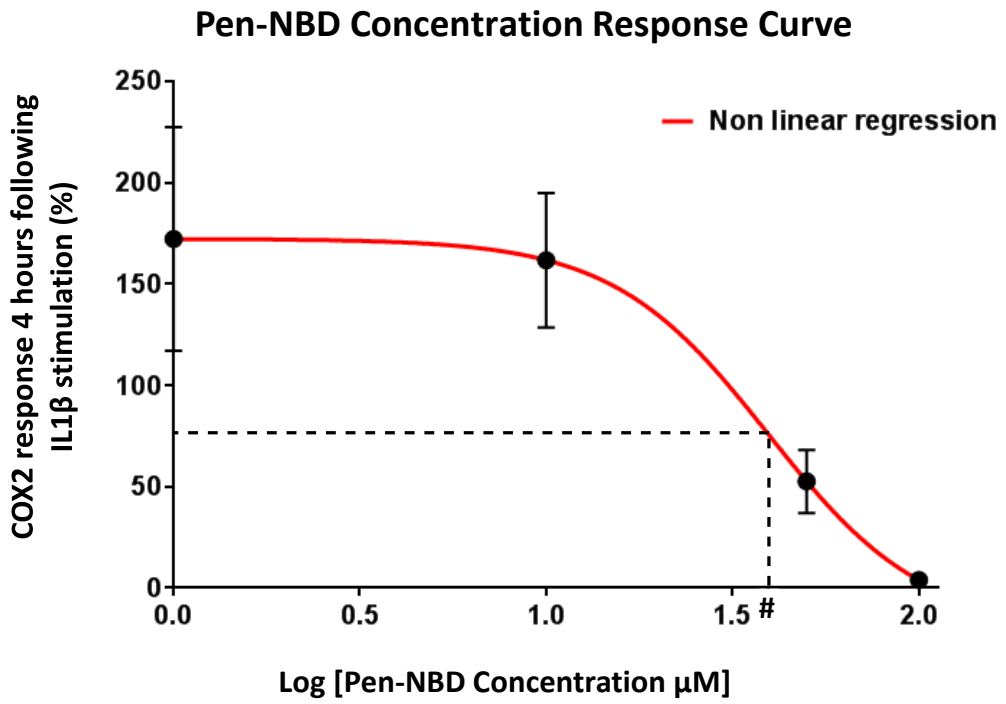

Figure 4.10: Concentration response curve for Pen-NBD

Y axis displays COX2 optical density at 4 hours displayed as a percentage of uninhibited (IL1β alone) response. X axis displays log of concentration values from1 to 100µM. Red line is non-linear regression line of best fit using a variable slope. This was generated using Prism software: hill slope= -2.08, R^2=0.71.

represents half maximal inhibitory concentration corresponding to a dose of 39.42µM

4.6.2 Comparison of three CPP vectors conjugated to NBD

Figure 4.11A displays representative Western Blots comparing Pen-NBD, R8-NBD and TAT-NBD at 50µM against control (IL1β alone) samples over a 4 hour time course of cytokine stimulation. Underneath this is a summary bar graph analysis of three such experiments (Figure 4.11B) of which the summary data displayed for Pen-NBD is replicated from Figure 4.4 and provided here for comparison. Although no statistically significant differences were observed between control and treated groups, the data demonstrates a trend towards an inhibitory effect seen when using Pen-NBD at 50µM, by contrast R8-NBD and TAT-NBD did not diminish IL1β induced COX2 protein response over 4 hours.

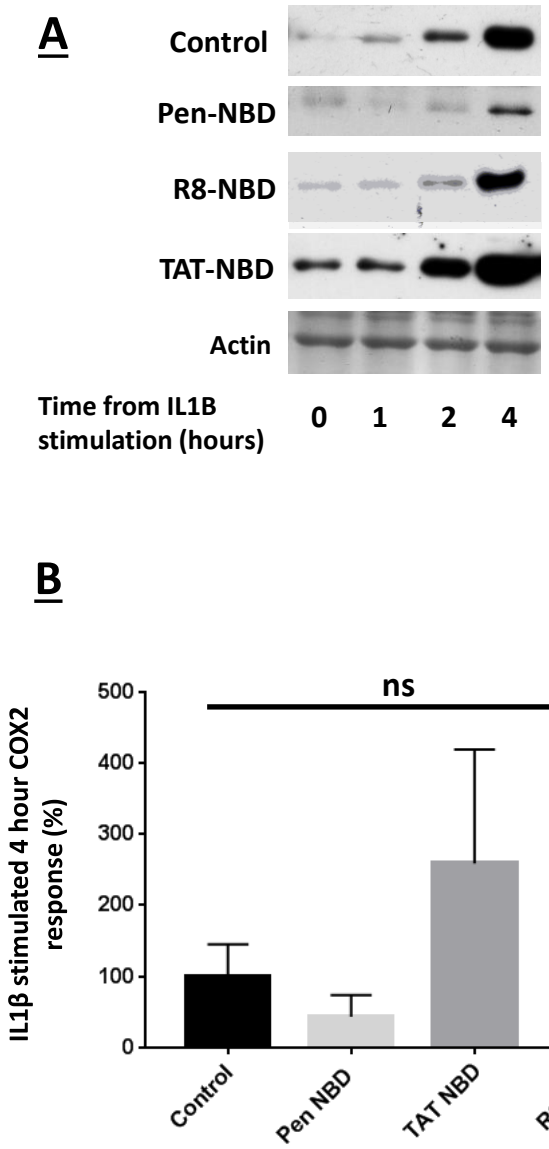

Figure 4.11 Comparison of effect of different CPP-NBD conjugations on IL1β induced COX2 protein expression

A Representative Western Blots indicating COX2 protein expression in myometrial cells over a four hour time frame following IL1β exposure alone (Control) or with 1 hour pre-incubation of different CPP-NBD conjugations at 50μM concentration.

B Bar graph demonstrating mean (SD) optical densitometry values of COX2 protein expression 4 hours following IL1β exposure as percentage of control (n=3).

Statistical analysis performed using one-way ANOVA with Bonferroni post-hoc testing.

4.7 Assessing the time frame and agonist concentration for IL1β and TNFα stimulated IκBα in myometrial cells

As with COX2 protein, it was initially necessary to define an appropriate time frame and cytokine dose regime by which to examine the degradation of this protein.

4.7.1 Optimising the time frame for cytokine stimulated IκBα expression

Protein expression of IκBα subsequent to IL1β or TNFα exposure was examined via Western blotting over a 4 hour time frame with initial cytokine doses selected as described above (section 4.2.1). In Figure 4.12 IκBα degradation commences at 5 minutes following IL1β addition, forms a doublet of both native (lower) and phosphorylated (upper) protein at 10 minutes before full degradation occurs at 15 minutes; an effect that is consistent with other cell types (Chen et al., 1995). De novo NFκB -stimulated production of IκBα can be seen at 120 minutes; however, in subsequent experiments this phenomenon was observed at 60 minutes and therefore a time frame with cell lysis points at 0 (prior to cytokine addition), 15 and 60 minutes was selected for further experimentation.

Addition of TNFα produced a similar pattern of degradation and re-synthesis of IκBα over 4 hours (Figure 4.12 lower panel); although subsequent experimentation displayed greater variability of TNFα induced degradation of IκBα compared to IL1β.

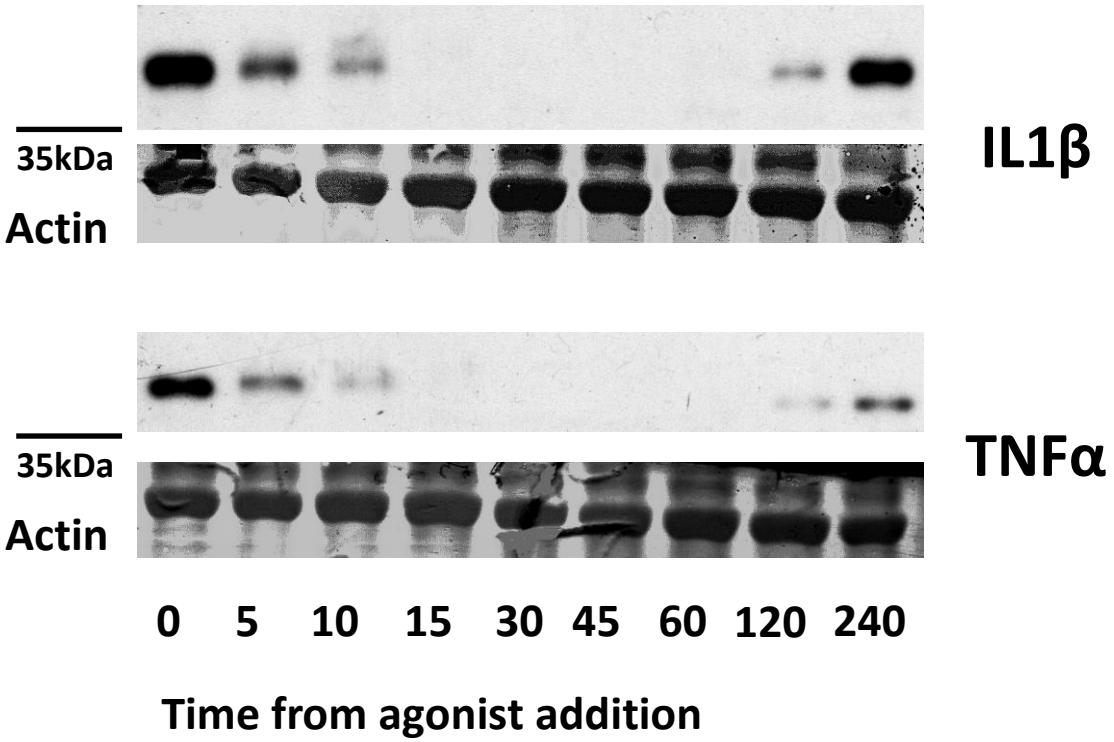

Figure 4.12 The time frame of IκBα protein phosphorylation, degradation and re-synthesis in myometrial cells

Western blots illustrating COX2 protein expression following addition of 10ng/ml IL1β (upper panel) or 1nM TNFα (lower panel) to myometrial cell culture.

4.7.2 Optimising the agonist concentration range for IκBα protein degradation

To ascertain the minimum dose of agonist needed to achieve complete cytokine-induced IκBα degradation, the expression responses of this protein 15 minutes following cytokine addition were examined across a dose range of 0-100ng/ml for IL1β or 0-10nM for TNFα.

As shown in Figure 4.13A: at 1ng/ml IL1β IκBα is partially phosphorylated such that a doublet protein band is observed, consisting of native (lower band) and phosphorylated (upper band) IκBα protein (Chen et al., 1995). With the use of 10ng/ml the lower band can no longer be identified indicating complete degradation of the native protein. A further increase in dose did not appear to increase this effect leading to the conclusion that 10ng/ml IL1β was the optimal dose of IL1β to use for experimentation. Statistical analysis of the optical densitometry data for IL1β using one-way ANOVA and Bonferroni's post-hoc testing revealed differences between 0 ng/ml and 0.1ng/ml compared to all higher concentrations used.

As demonstrated in Figure 4.13B, TNFα cytokine stimulation at 0.1nM partially degraded IκBα; an increase in this effect was observed at 1nM with minimal further effect seen at 10nM, therefore 1nM concentration was used in subsequent experiments. Statistical analysis of the optical densitometry data for TNFα using one-way ANOVA and Bonferroni's post-hoc testing again revealed differences between 0 ng/ml and 0.1ng/ml compared to all higher concentrations used.

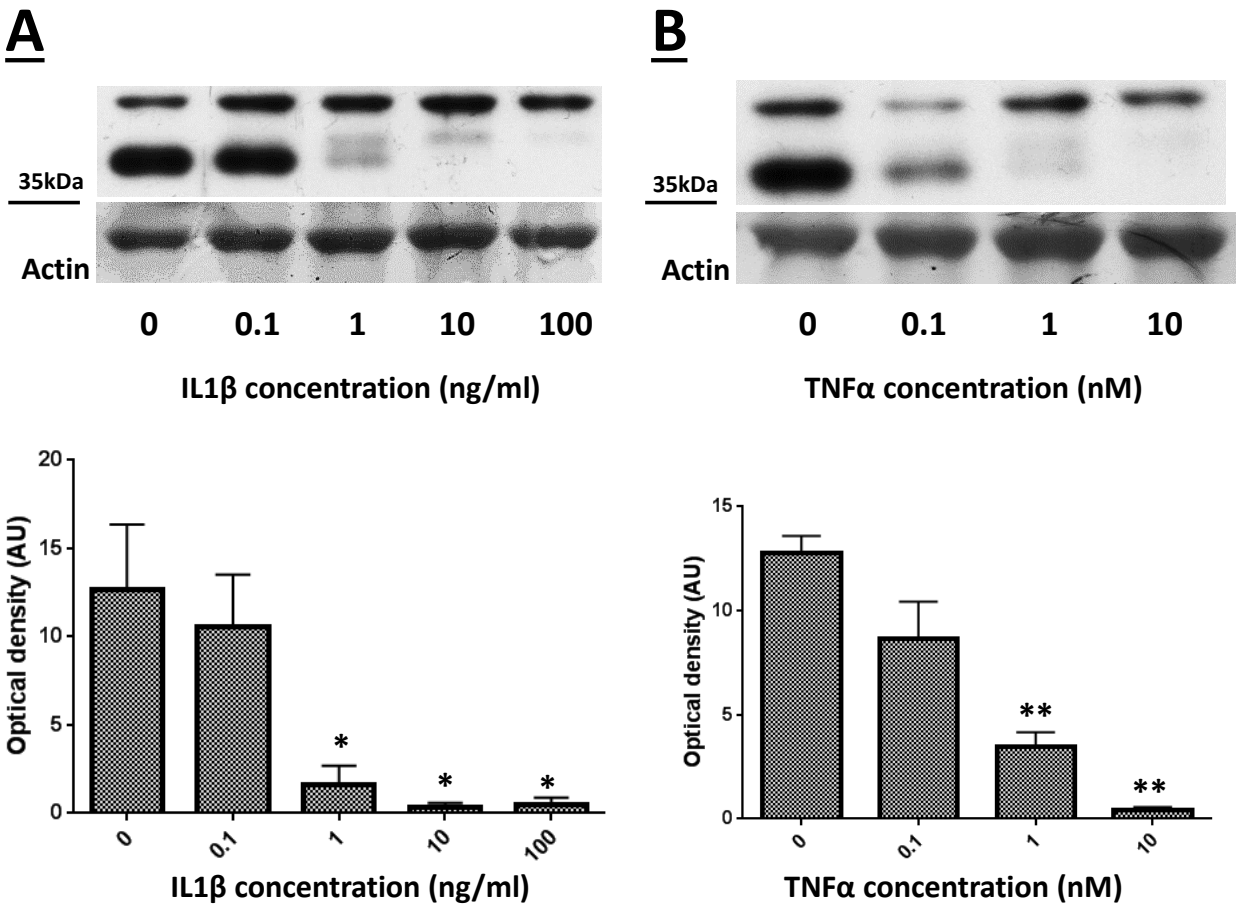

Figure 4.13 IκBα protein responses to varying concentrations of cytokine agonist

Upper Panels: representative western blots demonstrating IκBα protein expression at 15 minutes (**A** IL1β, **B** TNFα) in myometrial cells in response to increasing doses of cytokine. Actin expression demonstrated as loading control.

Lower Panels: Bar graphs demonstrating mean (SD) values of IκBα protein expression 15 minutes following exposure to indicated concentration of cytokine **A** IL1β or **B** TNFα (n=3).

*significant differences compared to 0ng/ml and 0.1ng/ml IL1β.

**significant differences compared to 0nM and 0.1nM TNFα. Statistical analysis performed using one-way ANOVA with Bonferroni post-hoc testing

4.8 Clarifying the identity of IκBα protein band on Western blot

Initial optimisation of IκBα was performed using an antibody directed towards the C-terminal end of the 42kDa IκBα protein (C21, sc-371). This suggested that a primary antibody concentration of 1:500 would produce a single clear band for this protein (Figure 4.12). However, subsequent experimentation using this antibody produced Western blots with multiple bands. To further clarify which band represented IκBα, a second antibody that recognises the full length of the protein (FL, sc-847) was used for comparison.

The proteasome inhibitor Mg132 has previously been shown to prevent the cytokine induced degradation of IκBα in uterine cells (Belt et al., 1999). Therefore, to verify the identity of IκBα protein band, cells were pre-incubated for 1 hour with 50μM of Mg132 or vehicle prior to cytokine stimulation. Identical samples underwent Western blotting using either the full length or C-terminal anti-IκBα antibody. These processes aided identification of the IκBα band as shown in Figure 4.14.

Use of the full length antibody led to the appearance of multiple bands that may represent other IκB subtypes, including IκBε which has close homology to IκBα protein (Mizgerd et al., 2002). The C-21 anti-IκBα antibody recognises an epitope 15-25 amino acids long at the C-terminal end of the protein; and, unlike the full length antibody, it does not recognise other IκB subtypes. When using this antibody, a band was observed immediately superior to IκBα (Figure 4.14B, red arrow). This band did not show substantial alteration either in the presence of cytokine or Mg132 and likely represents basal auto-phosphorylation of IκBα in the C-terminal end of the protein (Lin et al., 1996). For consistent ease of identification, data from further experimentation presented in this thesis was generated using the C-21 Anti-IκBα antibody.

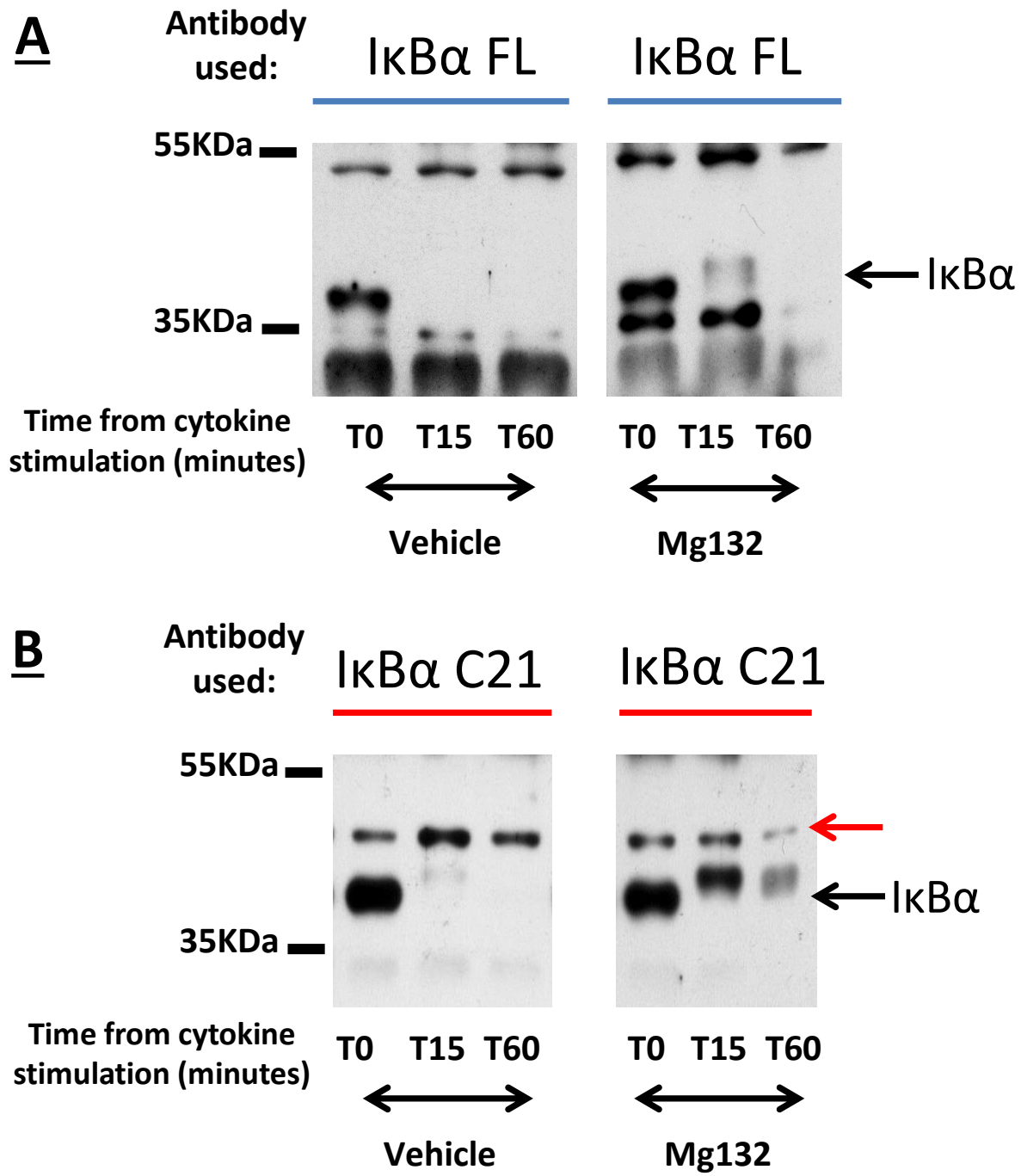

Figure 4.14 Identification of the IκBα protein band using full length (FL) and C-terminal (C21) anti - IκBα antibodies

Western blots demonstrating myometrial cell samples prior to cytokine addition (T0) and then 15 and 60 minutes following application of 10ng/ml IL1β in the presence of 50μM Mg132 or vehicle. Identical samples were then probed with IκBα full length antibody (**A** IκBα FL) or IκBα antibody directed at the C-terminal of the protein (**B** IκBα C21). The IκBα protein band indicated on the figure (black arrow) has been identified by the cytokine induced degradation of this band, and the failure to undergo cytokine stimulated degradation in the presence of Mg132. Red arrow indicates auto-phosphorylated IκBα.

4.9 Effect of Pen-NBD on IL1β dependent degradation of IκBα in myometrial cells

Figure 4.15 displays representative Western blots to demonstrate IκBα protein responses to IL1β cytokine over a 60 minute time frame. Complete degradation of IκBα can be observed within 15 minutes of exposure to IL1β alone (Control). Application of increasing doses of Pen-NBD 1 hour prior to IL1β cell stimulation did not prevent the degradation of IκBα. This was consistent across a dose range of 1-100μM, including concentrations shown to be capable of significantly inhibiting COX2 protein induction (Figure 4.4). Figure 4.16 displays mean optical densitometry values in a bar chart summation demonstrating that the IL1β induced degradation effect on IκBα was consistent. Statistical analysis using one-way ANOVA with Bonferroni's post-hoc testing to compare differences in optical densitometry at the 15 minute and 60 minute time points demonstrated that application of Pen-NBD did not alter this degradation at any concentration used.

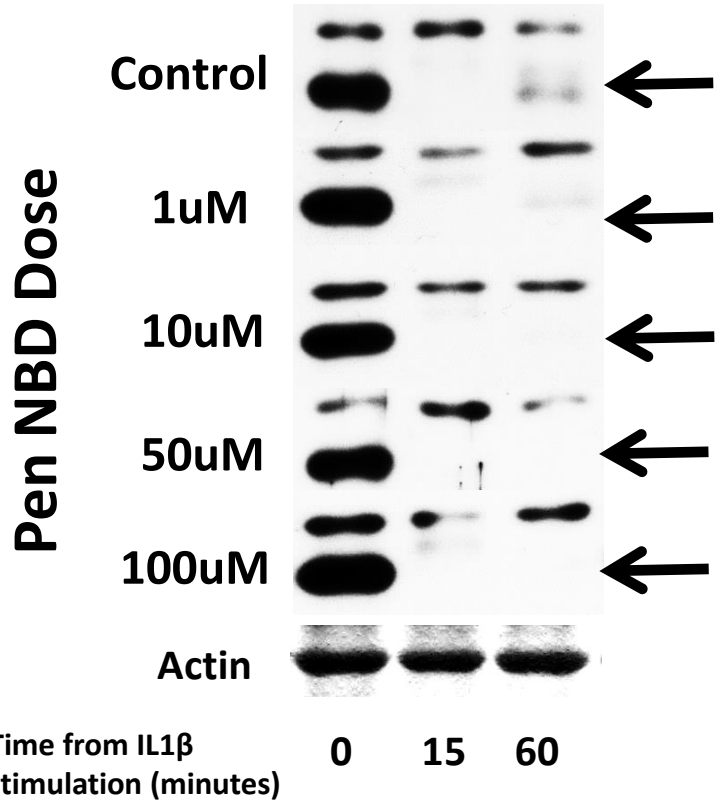

Figure 4.15 Effect of Pen-NBD on IL1β stimulated IκBα protein degradation

Representative Western blots indicating IκBα protein expression (black arrows) in myometrial cells over a 60 minute time frame following IL1B exposure alone (Control) or with addition of increasing concentrations of Pen-NBD 1 hour prior to IL1β application.

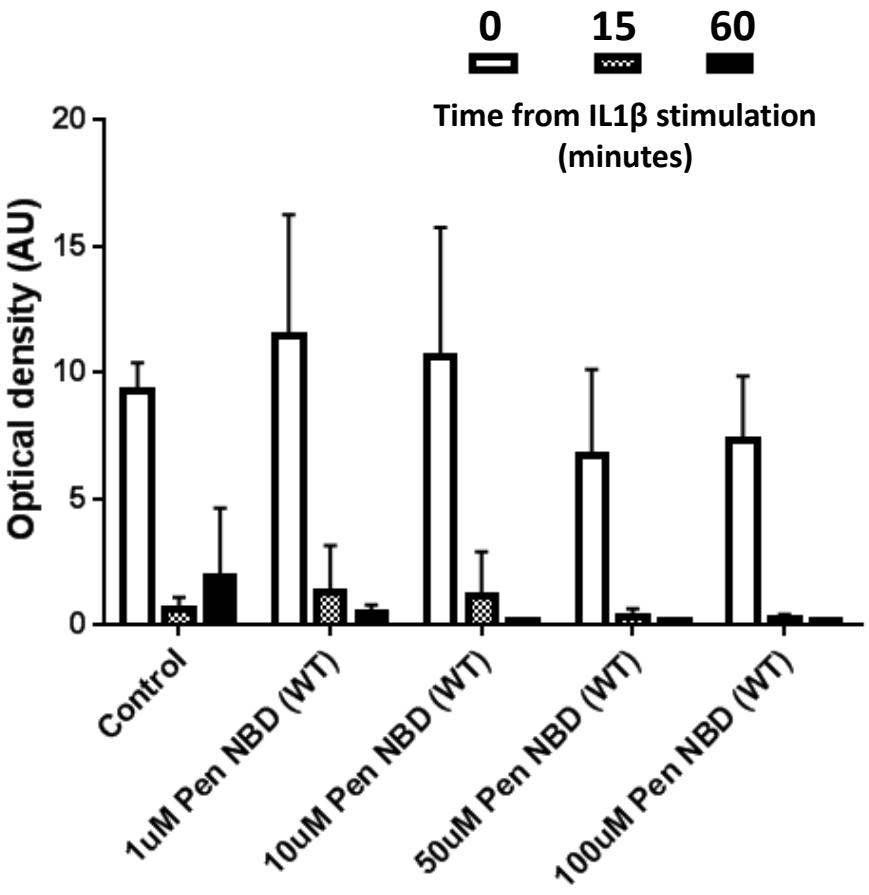

Figure 4.16 Quantification of **e**ffect of Pen-NBD on IL1β stimulated IκBα protein degradation

Bar graph demonstrating mean (SD) average optical density values (AU) of IκBα protein expression in myometrial cells over 60 minutes following IL1B exposure alone (Control) or with addition of increasing concentrations of Pen-NBD one hour prior to IL1β induction (n=3). Times represented are: prior to IL1B exposure (T0) and at 15 and 60 minutes following exposure.

Statistical analysis compared optical densitometry data between the control group and 1-100μM Pen-NBD groups at 0, 15 and 60 minute time points using one-way ANOVA with Bonferroni's post-hoc testing. No significant differences were found.

4.10 Effect of Pen-NBD on TNFα dependent degradation of IκBα in myometrial cells

Figure 4.17 illustrates IκBα protein responses to TNFα induction in the form of representative Western blot (Figure 4.17A) and bar chart summation of optical densitometry data across three experiments (Figure 4.17B). In control experiments partial degradation of IκBα was observed within 15 minutes with limited return of protein signal by 60 minutes. Addition of 1-50μM concentration of Pen-NBD had no evident effect on IκBα degradation, however pre-incubation with 100μM Pen-NBD led to prevention of IκBα degradation at the 15 minute time point in 2 out of 3 experiments. Figure 4.18 displays the Western blots from all three experiments for both control samples (TNFα alone) and samples pre-incubated with Pen-NBD 100μM to illustrate the variety of responses produced.

Statistical analysis using one-way ANOVA with Bonferroni's post-hoc testing to compare differences in optical densitometry at the 15 minute and 60 minutes time point did not demonstrate any differences at any concentration used.

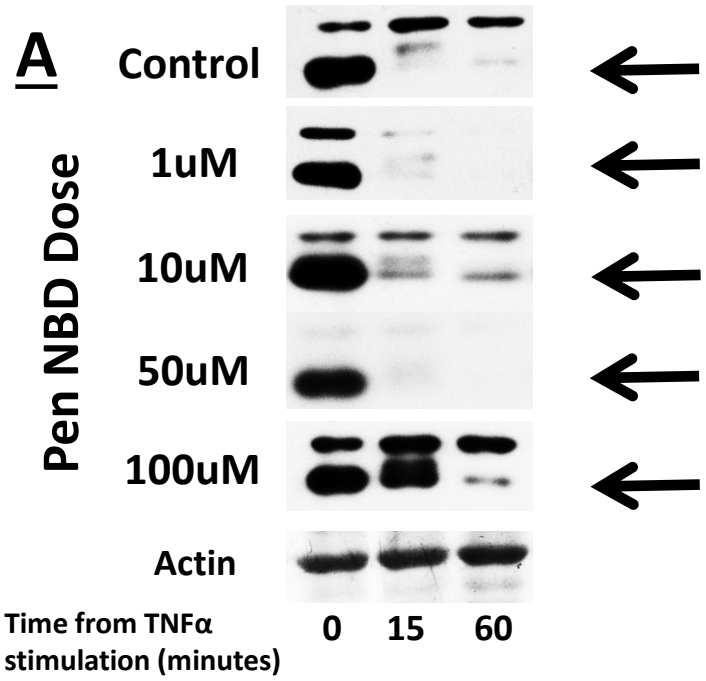

Figure 4.17 Effect of Pen-NBD on TNFα stimulated IκBα protein degradation

A Representative Western blots indicating IκBα protein expression (black arrows) in myometrial cells over a sixty minute time frame following TNFα exposure alone (control) or with addition of increasing concentrations of Pen-NBD 1 hour prior to TNFα induction.

B Bar graph demonstrating mean (SD) optical density values (AU) of IκBα protein expression at all three time points indicated (n=3).

Statistical analysis compared optical densitometry data between the control group and 1-100μM Pen-NBD groups at 0, 15 and 60 minute time points using one-way ANOVA with Bonferroni's post-hoc testing. No significant differences were found.

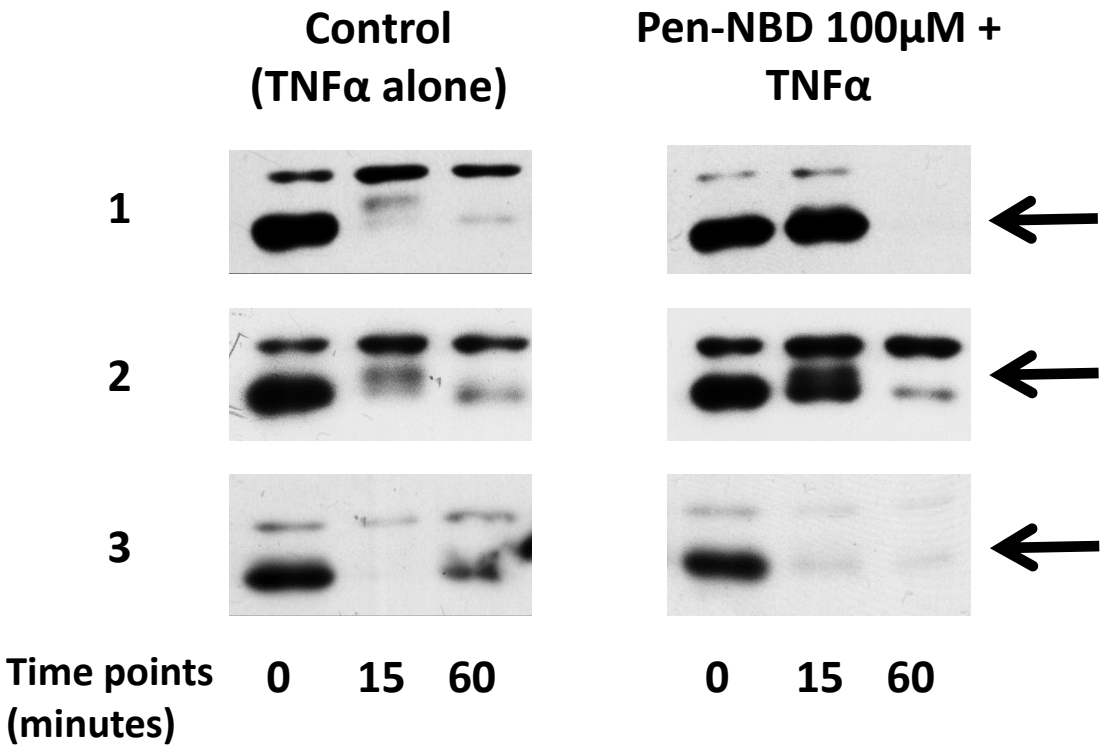

Figure 4.18 Variability of IκBα protein responses to TNFα.

Display of Western blots demonstrating IκBα protein expression (black arrows) over 60 minutes following TNFα exposure in the absence and presence of 100µM Pen-NBD inhibitor. Blots from all experiments performed (1-3) are shown to indicate the variability of protein degradation produced by this cytokine.

4.11 Effect of different CPP vector NBD conjugations on IL1β induced IκBα degradation

Figure 4.19A displays representative Western Blots comparing Pen-NBD, R8-NBD and TAT-NBD at 50μM against control (IL1β alone) samples over a 60 minute time course of cytokine stimulation. Figure 4.19B presents a summary bar graph of three such experiments. There were no differences between control groups or groups pre-incubated with any CPP-NBD conjugation at any of the time points, thus indicating that none of the CPP-NBD combinations inhibited the IL1β induced degradation of IκBα across the experimental time frame.

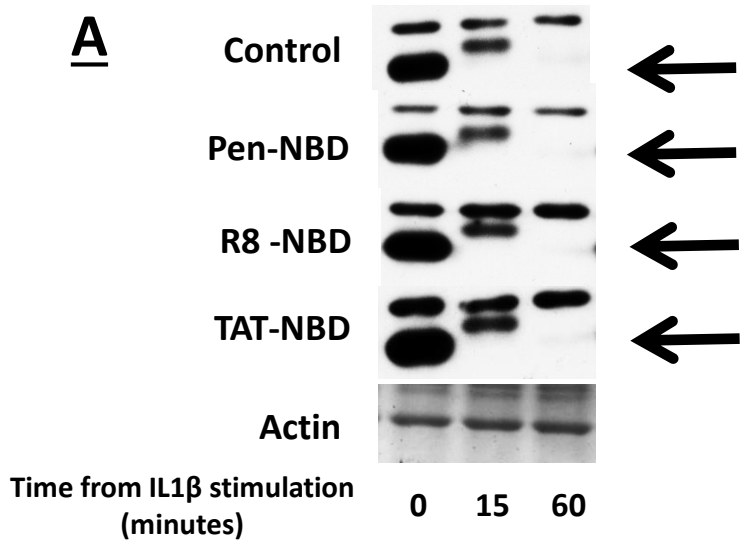

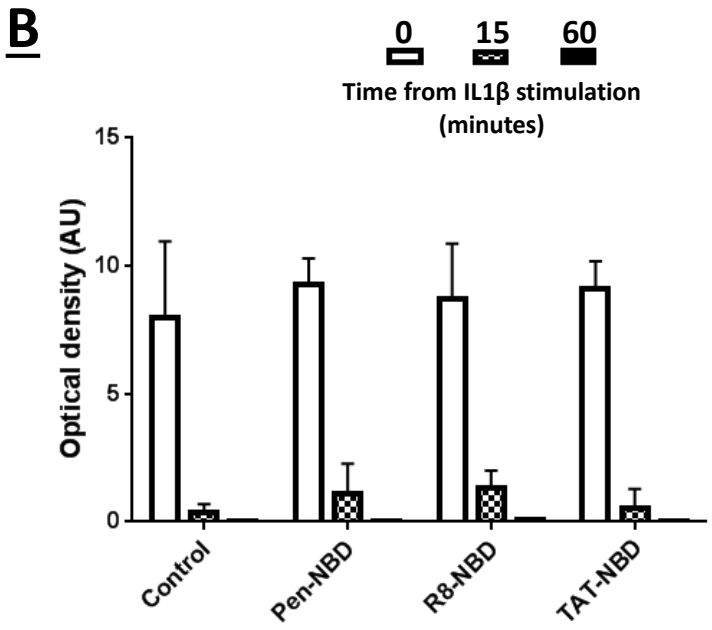

Figure 4.19 Effect of different CPP-NBD conjugations on IL1β stimulated IκBα protein responses

A Representative Western blots indicating IκBα protein expression (black arrow) in myometrial cells over a sixty minute time frame following IL1β exposure alone (Control) or with addition of 50μM of Pen-NBD, R8-NBD or TAT-NBD 1 hour prior to IL1β induction.

B Bar graph demonstrating mean (SD) optical density values (AU) of IκBα protein expression following IL1β exposure at all three time points indicated (n=3).

Statistical analysis compared optical densitometry data between the control group and CPP-NBD groups at 0, 15 and 60 minute time points using one-way ANOVA with Bonferroni's post-hoc testing. No significant differences were found.

4.12 IκBα cytokine degradation in response to peptide controls

IκBα protein expression following cytokine exposure was examined in the presence of a series of peptide and vehicle controls. These controls were identical to those tested for effects on COX2 protein expression and included Pen-NBD mutant peptide (1-100μM), unconjugated Pen and NBD peptide at 50μM and 0.25% / 0.5% DMSO. As can be observed from Figure 4.20; no alterations in cytokine induced IκBα degradation were seen at 15 or 60 minutes, this was observed across 3 experiments for both IL1βa and TNFα stimulated myometrial cells.

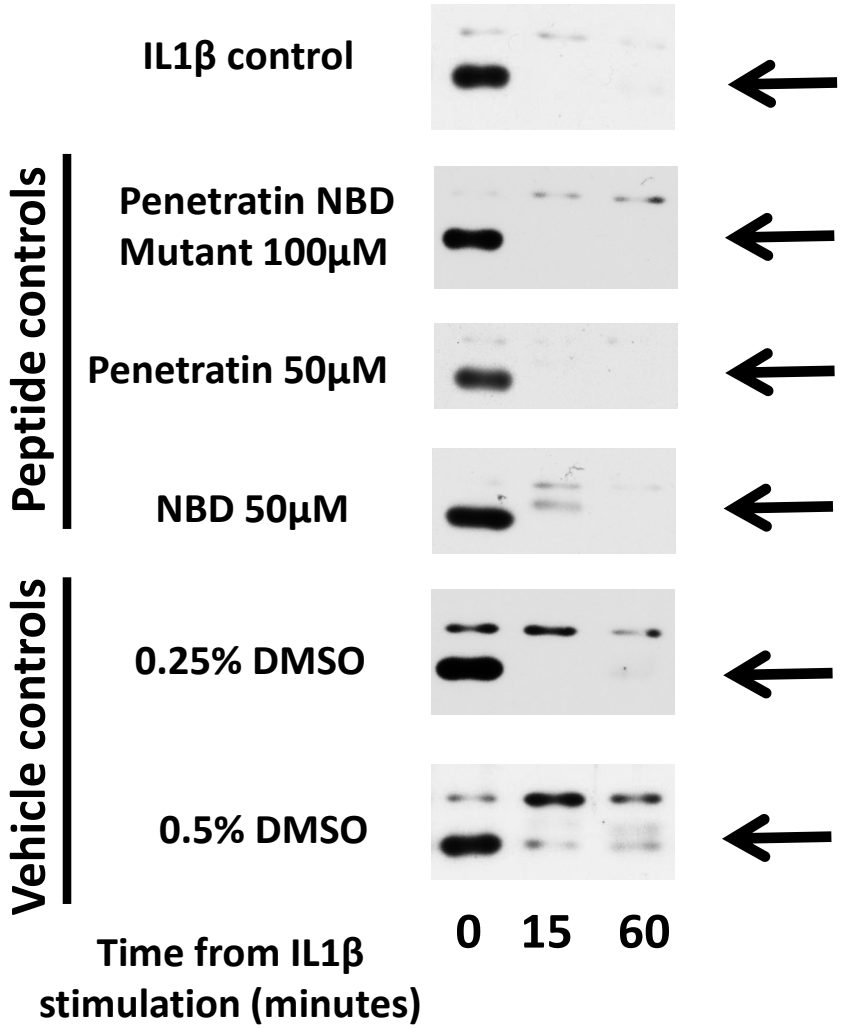

Figure 4.20 Effect of peptide and vehicle controls on IL1β stimulated IκBα protein responses

Representative Western blots showing IκBα protein expression (black arrows) at 0, 15 and 60 minutes following IL1β exposure alone (control) or following 1 hour pre-incubation with indicated control peptide or vehicle concentration (n=3). Similar results were observed using TNFα agonist (data not shown).

4.13 Comparison of the effects of Pen-NBD against a panel of non-peptidic putative NFκB inhibitors

The effectiveness of Pen-NBD to inhibit inflammatory responses in myometrial cells was matched against an array of non-peptide inhibitors known to inhibit inflammatory responses in utero-placental cells: N-acetyl cysteine (NAC), curcumin, Sc514 and Mg132. The inhibitors were each tested at two concentrations with previously proven efficacy in vitro as suggested from the existing literature.

The Pen-NBD data displayed in Figures 4.21 to 4.23 is replicated from figures presented in earlier sections of this chapter and is shown again here to allow for easy comparison between the CPP and non-peptide inhibitory approaches.

4.13.1 Comparison of non-peptide and Pen-NBD effect on cytokine stimulated COX2 induction

Figure 4.21 demonstrates representative Western blots illustrating COX2 responses to IL1β over a four hour time frame with pre-incubation of indicated doses of inhibitor. With the exception of NAC, all inhibitors at the higher concentration tested had an inhibitory effect on COX2 signal with varying efficacy.

In Figure 4.22 the mean optical densitometry values measured for COX2 protein signal 4 hours following IL1β addition are displayed for every inhibitor at two concentrations tested. One-way ANOVA with Bonferroni's post-hoc testing was used to analyse optical densitometry values. Except for NAC, inhibition of cytokine-induced COX2 responses were observed for all inhibitors when used at the higher concentration tested (Curcumin $p=0.002$, Sc514 $p=0.008$, Mg132 $p=0.002$, Pen-NBD $p=0.001$) (Figure 4.22A). However, inhibition was only observed using Mg132 ($p=0.02$) at the lower concentration tested (Figure 4.22 B).

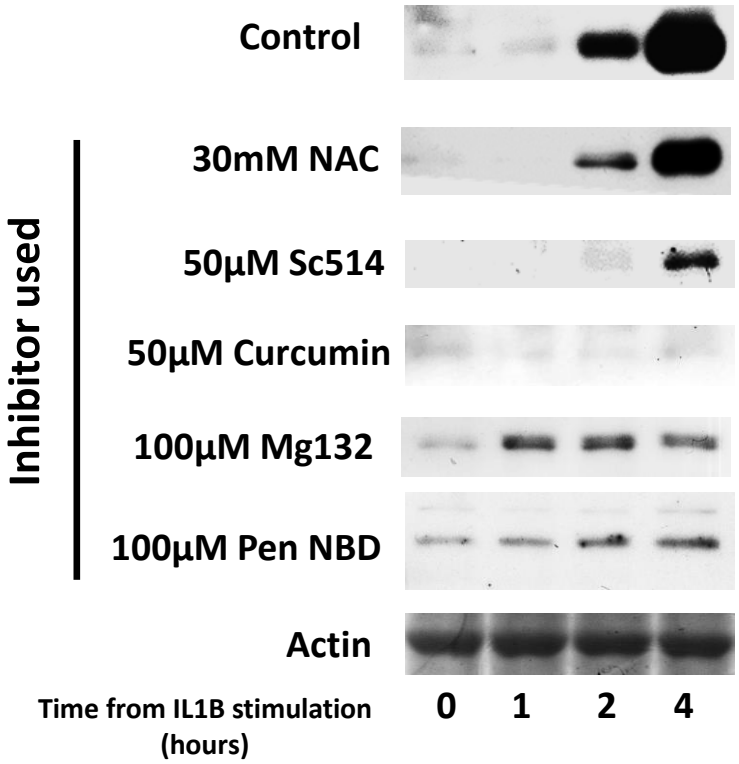

Figure 4.21 Effect of non-peptide inhibitors on IL1β stimulated COX2 protein expression.

Representative Western blots indicating COX2 protein following IL1β exposure over a 4 hour time frame in the presence or absence (Control) of indicated concentrations of non-peptide NFκB inhibitors compared to the effect of Pen-NBD peptide inhibitor.

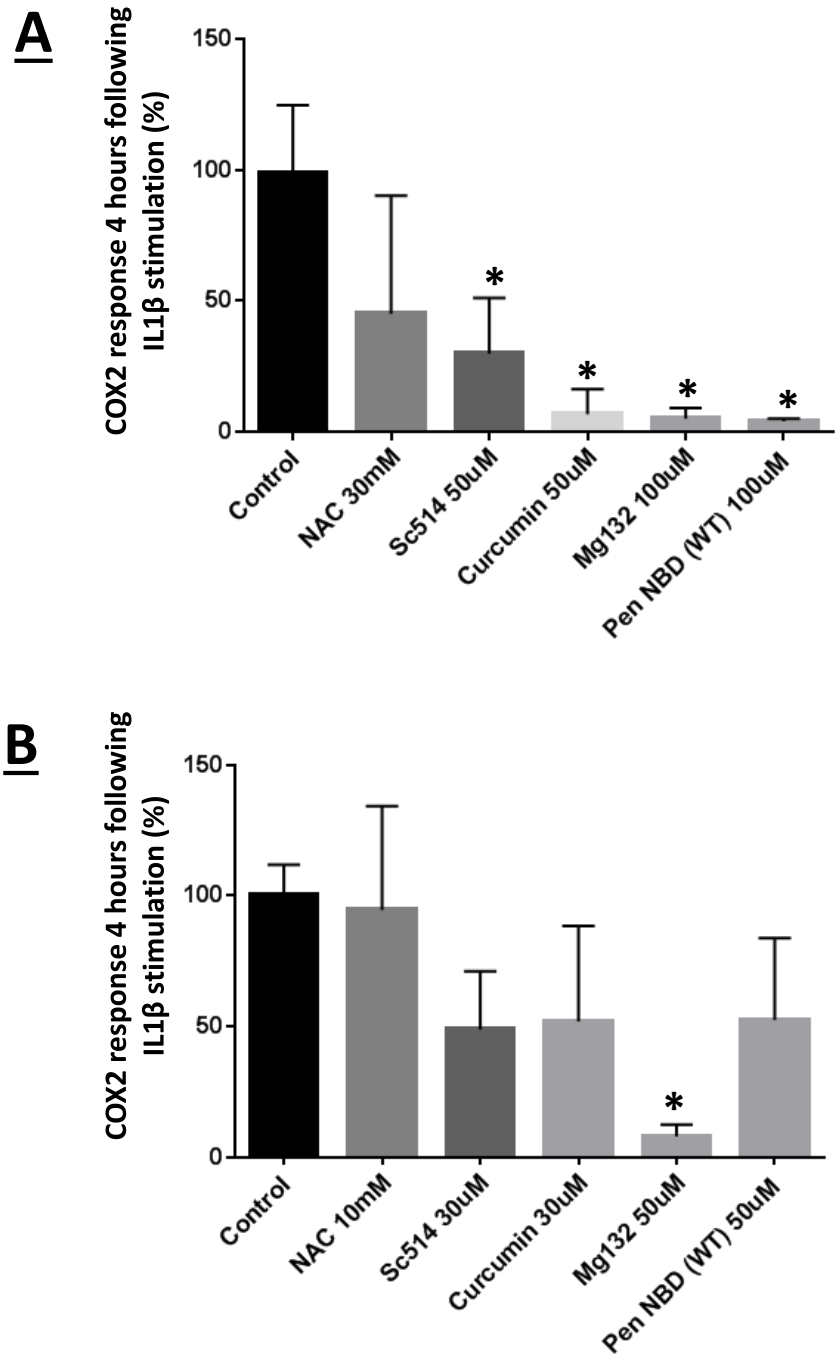

Figure 4.22: Comparison of effect of non-peptide inhibitors and Pen-NBD on IL1β stimulated COX2 protein signal.

Bar charts demonstrating summation of optical densitometry results of COX2 protein expression at 4 hours via Western blot. Cells pre-incubated with either Pen-NBD or small molecule inhibitor at higher concentration (**A**) or lower concentration (**B**) over 3-4 experiments. Each bar denotes mean (SD) average values as percentage of Control (IL1β alone) for each blot.

* Denotes statistical significance compared to Control values. One-way ANOVA with Bonferroni's post-hoc testing.

4.13.2 Comparison of non-peptide and Pen-NBD effect on IL1β stimulated IκBα degradation

IκBα responses secondary to IL1β stimulation were examined following pre-incubation with the panel of small molecule inhibitors. NAC and curcumin were not able to prevent the degradation of IκBα at any of the doses tested.

The representative Western blots presented in Figure 4.23A show that 50μM Sc514 was capable of preventing the IL1β induced degradation of IκBα at 15 minutes but not at 60 minutes, and 100μM Mg132 was able to prevent the degradation of this protein at both 15 and 60 minutes. As previously demonstrated, 100μM Pen-NBD did not exert an effect on IκBα degradation.

The bar chart in Figure 4.23B demonstrates the mean optical densitometry values of IκBα protein in the presence of IL1β alone (Control), 100μM Pen-NBD, 50μM Sc514 or 100μM Mg132, statistical analysis using one-way ANOVA with Bonferroni's post-hoc testing to compare differences in optical densitometry at the 15 minute and 60 minute time points demonstrated differences between Sc514 and Mg132 and control groups at the 15 minute time point; but no differences between Pen-NBD and control at 15 minutes and no differences between groups at 60 minutes. This suggests that both Sc514 and Mg132 were able to inhibit IκBα protein degradation 15 minutes following IL1β application.

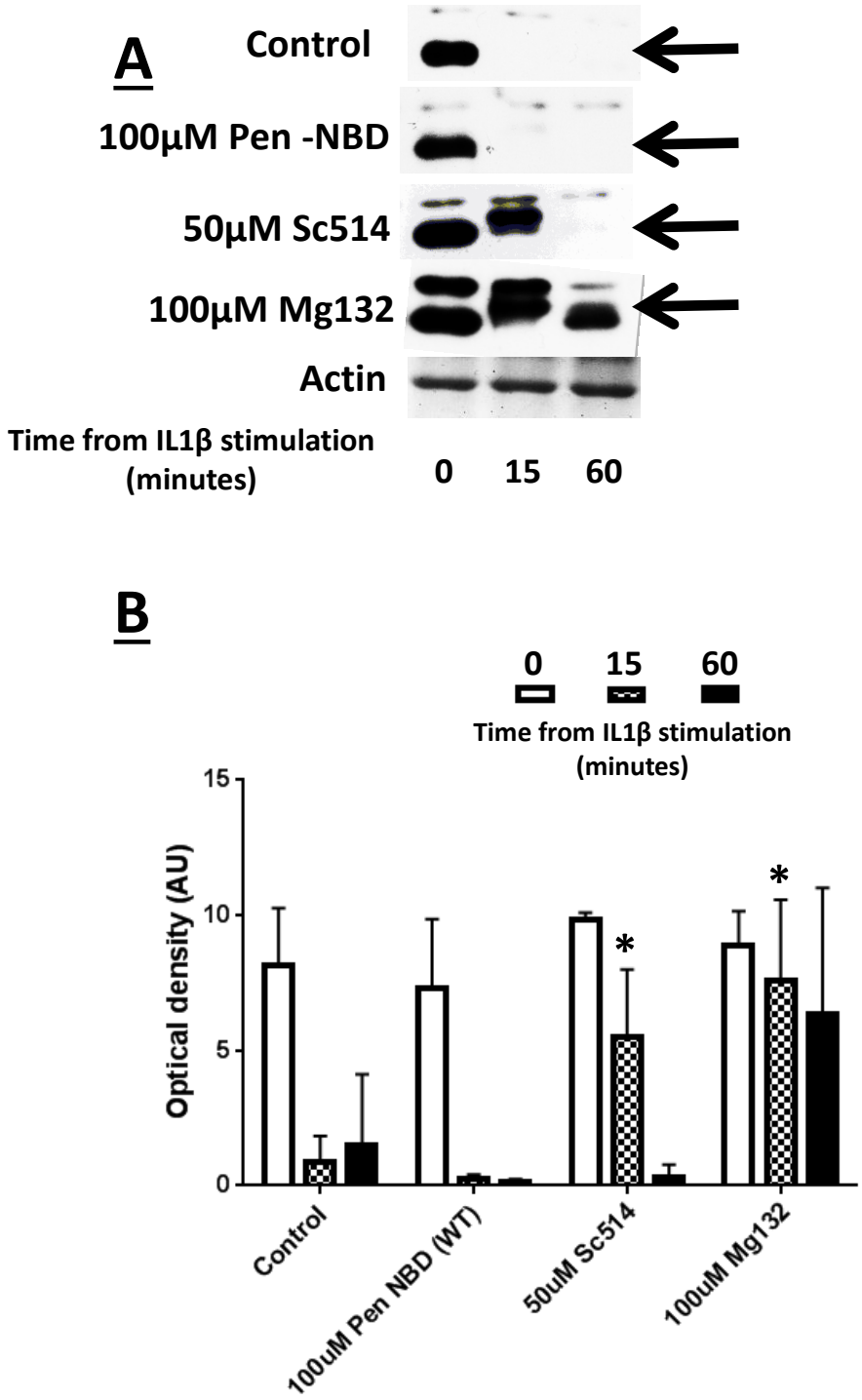

Figure 4.23 Effect of non-peptide inhibitors on IL1β stimulated IκBα protein degradation: comparison with Pen-NBD

A*:* Representative Western blots indicating IκBα protein expression (black arrows) in myometrial cells over 60 minutes following IL1β exposure alone (Control) or with addition of indicated inhibitor one hour prior to cytokine induction.

A*:* Bar graph demonstrating mean average (SD) optical density values (AU) of IκBα protein expression at T0, T15.T60 for IL1β alone (Control) or groups pre-treated with the indicated inhibitor (n=3).

*Statistically significant compared to control values. One-way ANOVA with Bonferroni's post-hoc testing.

4.14 Discussion

The results set out in this chapter tested the ability of the Pen-NBD peptide to dampen inflammatory responses to the cytokines IL1β and TNFα in myometrial cells. For IL1β simulated myometrial cells pre-treatment with 50μM Pen-NBD demonstrated a trend toward inhibition of COX2 protein responses, although this was not statistically significant. The higher concentration of 100μM inhibited expression of this protein.

Some inhibition of COX2 protein responses to TNFα were demonstrated via Western blot with the use of 100μM Pen-NBD, again these changes were not statistically significant. This may suggest that a higher dose of Pen-NBD is required to inhibit TNFα mediated inflammatory responses; however an alternative explanation is that the TNFα effect observed over 4 hours showed variability between experiments, with occasions where COX2 protein expression was comparatively low in control experiments. A substantial variability of human myometrial cell responses to TNFα stimulation has been reported previously in the literature (Lappas, 2013). Due to temporal constraints, small sample numbers were used in this part of the study. Such factors, alongside the variable TNFα effects observed in experimentation, may have lessened the likelihood of observing statistically significant results.

A form of 'naked' NBD peptide - without conjugation to CPP –used at 50μM concentration, failed to inhibit COX2 protein expression secondary to cytokine induction. As previously demonstrated in Chapter Three, the NBD peptide alone does not display cell penetrating properties when applied to myometrial cells, therefore the lack of effect seen with the use of NBD alone is likely due to the failure of unconjugated NBD to enter myometrial cells in sufficient concentrations and underlines the necessity of this cargo to be attached to CPP for biological use.

A mutant NBD peptide conjugated to Pen inhibited neither TNFα nor IL1β-induced COX2 protein expression when tested across an identical concentration range as wild type Pen-NBD. This failure to inhibit NFκB activation is consistent with previous studies examining the NBD mutant peptide as a control to NBD (Shibata et al., 2007). Data presented in Chapter Three (Figure 3.17A) indicates that the mutant CPP-peptide combination is capable of entering myometrial cells when applied at the same concentration as the non-mutant form.

Therefore the lack of biological effect seen with the use of the mutant NBD peptide is not due to the failure of this CPP-peptide conjugate to enter cells, a finding that has not previously been demonstrated in the existing literature. It is also notable that the CPP Pen applied without NBD cargo did not have inhibitory effects on COX2 protein. These data emphasise the requirement of the NBD peptide to have inhibitory effect on cytokine-induced COX2 expression in human myometrial cells.

The possibility that the inhibitory effects observed on COX2 with the use of Pen-NBD are vehicle mediated must be considered: high final concentrations of DMSO were required (up to 0.5%) and inhibitory effects on TNFα-induced COX2 protein expression at 4 hours were observed with the use 0.25% DMSO and on IL1β-induced COX2 expression with 0.5% DMSO. However, there were no significant differences between vehicle treated groups and control signal, nor were there any vehicle effects observed on cytokine induced IκBα protein degradation (Figure 4.20). It was also notable that both effector wild type peptide and mutant controls were dissolved in identical concentrations of DMSO vehicle. This makes the extent of vehicle effects uncertain and indicates that any wild type specific effects are less likely to be entirely vehicle-mediated.

Comparison of three CPP-NBD vectors at a selected concentration of 50μM demonstrated that neither R8-NBD nor TAT-NBD were able to inhibit IL1β induced COX2 signalling at that dose. Examination of the biological activity of all three CPP-NBD conjugations across a full concentration range was out-with the scope of this project, however research examining the ability of a range of CPPs conjugated to NBD to block IL1β induced NFκB activity in HeLa and HEK 293 cell lines found that cargo peptides conjugated to CPPs derived from antennopaedia or TAT proteins were the most effective in vitro (Khaja, 2010). Therefore further exploration of the effective concentration range of TAT-NBD in uterine cells could prove fruitful for future study.

The NBD peptide was matched against an array of small molecule inhibitors that have previously shown ability to block NFκB activation in uterine and placental cells (De Silva et al., 2010, Lappas et al., 2003, Belt et al., 1999, Lim et al., 2013). Pen-NBD demonstrated greater efficacy in inhibiting cytokine induced COX2 protein expression than N-Acetyl Cysteine and showed similar effectiveness to Sc514, Curcumin and Mg132, thus signifying

that the use of CPP-cargo conjugations to block inflammatory responses in gestational cells can be a successful approach when compared to non-peptide anti-inflammatory treatments.

Examination of the mechanism by which Pen-NBD may be targeting action in myometrial cells produced a surprising result: at all concentrations tested, the NBD peptide did not prevent the IL1β induced degradation of IκBα. As demonstrated in Figure 4.17, the TNFα induced degradation of this protein was inhibited by the peptide at 100μM in two out of three experiments demonstrating notable experiment to experiment variability for both control and inhibited groups. The possible conclusion remains that Pen-NBD at 100μM is capable of preventing TNFα but not IL1β induced IKK activation; however it is also possible that variability of TNFα inflammatory induction may have led to suboptimal IKK activation in two out of three cases.

These data indicate that NBD peptide is capable of exerting anti-inflammatory effect in myometrial cells when delivered by Pen CPP. The mechanism of action by which Pen-NBD blocks cytokine induced increases in COX2 protein is uncertain but may not be exclusive to inhibition of IKK complex activation. The following chapter explores broader inhibitory effects of Pen-NBD by examining cytokine induced gene expression changes in myometrial cells and aims to offer further clues as to the mechanism of anti-inflammatory action exerted by the NBD peptide, using the IKKβ inhibitor Sc514 as a comparative tool.

Chapter Five

Effects of CPP-peptide and non-peptide inhibitors on cytokine-induced gene expression changes in uterine cells

5.1 Introduction

Having determined that CPP-conjugated peptide inhibitors and small molecule non-peptide inhibitors could prevent the cytokine induced expression of COX2 protein in myometrial cells; it was important to investigate whether both inhibitory approaches could have broader anti-inflammatory effects and prevent changes in the expression of genes whose altered expression patterns have been associated with human labour.

A bespoke qPCR array of 42 genes, encompassing many genes with previously demonstrated expression changes associated with human labour (Khanjani et al., 2011, Chan et al., 2014, Kimura et al., 1992, Vadillo-Ortega and Estrada-Gutierrez, 2005, Lappas, 2013, Renthal et al., 2010, Mittal et al., 2010) were selected to quantitatively examine the effects of cytokine exposure on gene expression in myometrial cells and to subsequently test the ability of CPP-conjugated and non-peptide inhibitors to inhibit this gene expression. The rationale underpinning the selection of genes of interest (GOI) is explained in Chapter Two of this thesis (section 2.10.6).

As demonstrated in the previous chapter, Pen-NBD was capable of inhibiting cytokine stimulated inflammatory protein expression but did not prevent the IL1β induced degradation of IκBα, thus generating uncertainty regarding the mechanism of action of this inhibitory peptide in myometrial cells . To interrogate the mechanism of action further, the inhibitory effects of Pen-NBD on cytokine induced myometrial cell gene expression were compared to the IKKβ inhibitor Sc514.

The specific aims of this chapter were:

- To examine the changes in expression of selected myometrial genes subsequent to IL1β exposure.
- To identify the effects of CPP-linked peptide inhibitors and a non-peptide small molecule inhibitor on IL1β induced changes in myometrial cell gene expression.

5.2 Changes in myometrial cell gene expression following cytokine exposure

Figures 5.1 and 5.2 display the combined results of eight experiments demonstrating gene expression changes in myometrial cells 4 hours following the application of IL1β cytokine.

The clustergram in Figure 5.1 displays the hierarchical grouping of genes in terms of expression changes in response to IL1β application within each sample tested on the array. Of the 42 genes of interest (GOI) examined, 25 genes showed increased expression in the presence of IL1β, 2 genes showed decreased expression with IL1β and 15 genes demonstrated no change. The central portion of the clustergram displays a grouping of genes that exhibited a notably similar pattern of upregulated responses following IL1β addition to myometrial cells, broadly these genes encode for proteins involved in inflammatory responses.

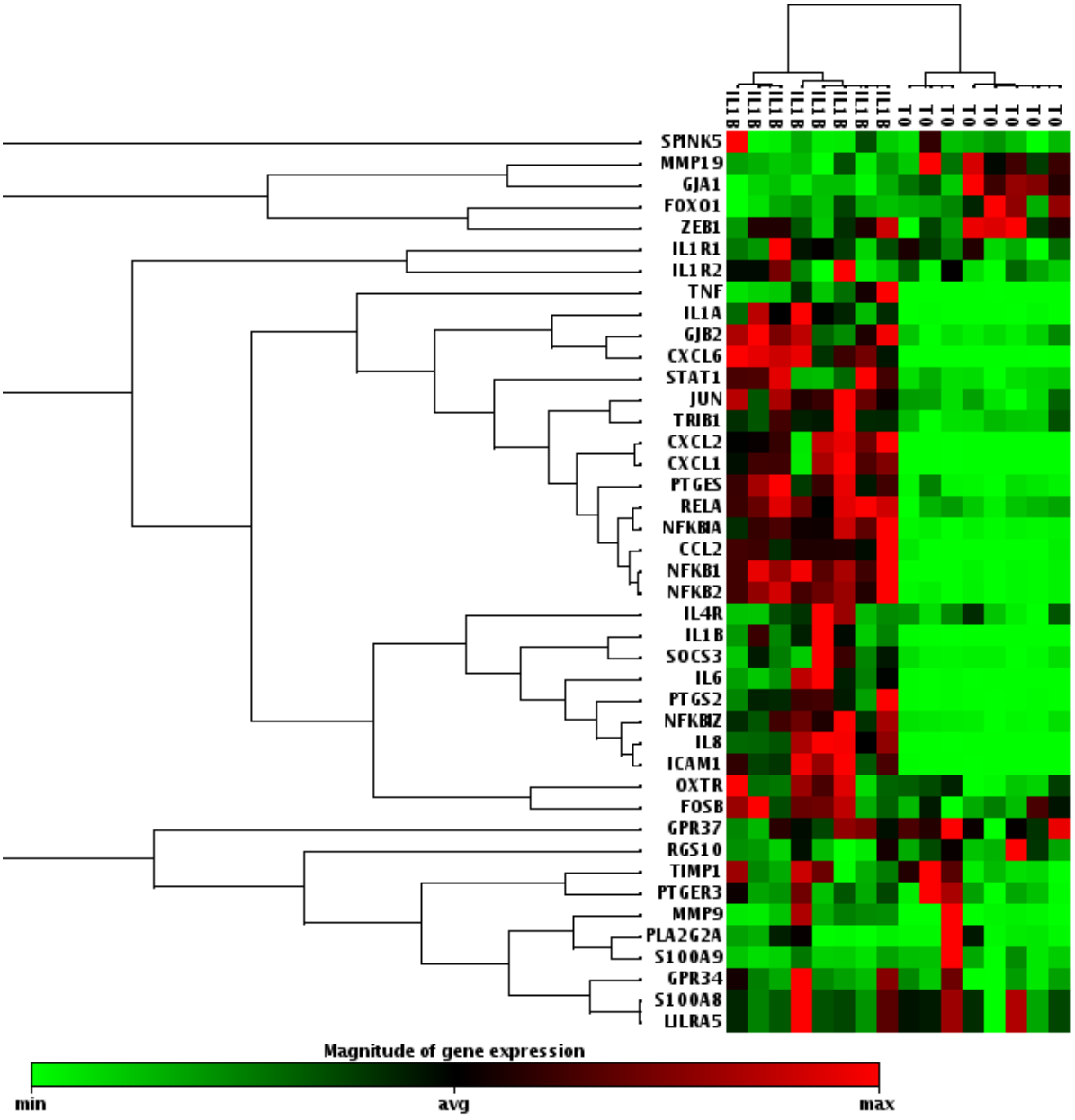

Figure 5.1 Clustergram demonstrating the hierarchical clustering of myometrial cell gene expression in response to IL1β cytokine stimulation.

The heat map in the right hand panel displays gene expression changes from an array of 42 genes of interest (GOI) for IL1β treated and untreated (labelled T0) samples from eight biological replicates. Highly expressed genes are displayed as shades of red and minimally expressed genes are shown as shades of green. Left hand panel shows a dendrogram to highlight groups of genes that demonstrate similar expression profiles across the two experimental situations.

Figure 5.2 presents a volcano plot; the x axis displays fold regulation changes between control (untreated) samples and IL1β treated samples, the y axis displays the inverse of p values for each gene of interest; both axis have been transformed logarithmically to allow a graphical representation of all genes within the array. Genes with a greater than two fold up-regulation (red circles) or two fold down-regulation (green circles) have been labelled in the diagram. The horizontal blue line represents the cut-off for significant changes in gene expression ($p<0.05$).

The results demonstrate that a series of genes exhibited altered expression in myometrial cells following IL1β exposure. Genes that underwent significant upregulation included those encoding for pro-inflammatory cytokines (IL8, IL6, IL1B, IL1A, TNF) and chemokines (CCL2, CXCL1, CXCL2, CXCL6), plus genes encoding for cytokine-responsive proteins (ICAM1, SOCS3). Genes encoding for components of the NFκB (NFKB1, NFKB2, RELA, NFKBIA, NFKBIZ) and AP1 (FOSB, JUN) pathways were also upregulated.

Several gene mediators of prostaglandin production (PTGES, PTGS2) and some of the genes encoding for contraction associated proteins (OXTR, GJB2, MMP9) were upregulated in the presence of IL1β. However, a number of genes within these two categories did not exhibit altered expression in response to cytokine addition (PTGER3, PLA2G2A, TIMP1).

IL1β stimulation did not significantly alter the expression of a number of genes within the array, most notably the genes associated with G-protein receptor pathways (GPR37, GPR34, RGS10) involved in promoting myometrial quiescence (Aguan et al., 2000, Mittal et al., 2010); additionally, genes encoding for cytokine receptor proteins demonstrated no alteration (IL1R1, IL1R2, IL4R).

Of the genes identified as potential novel target genes whose expression is altered in myometrial tissue in association with human labour (Chan et al., 2014), only STAT1 and TRIB1 demonstrated expression changes in myometrial cells following IL1β exposure, with the expression of both these genes significantly upregulated by cytokine induction.

GJA1 gene, which encodes for connexin 43 protein, and MMP19 gene were the only genes within the array to exhibit downregulation of expression in response to cytokine exposure.

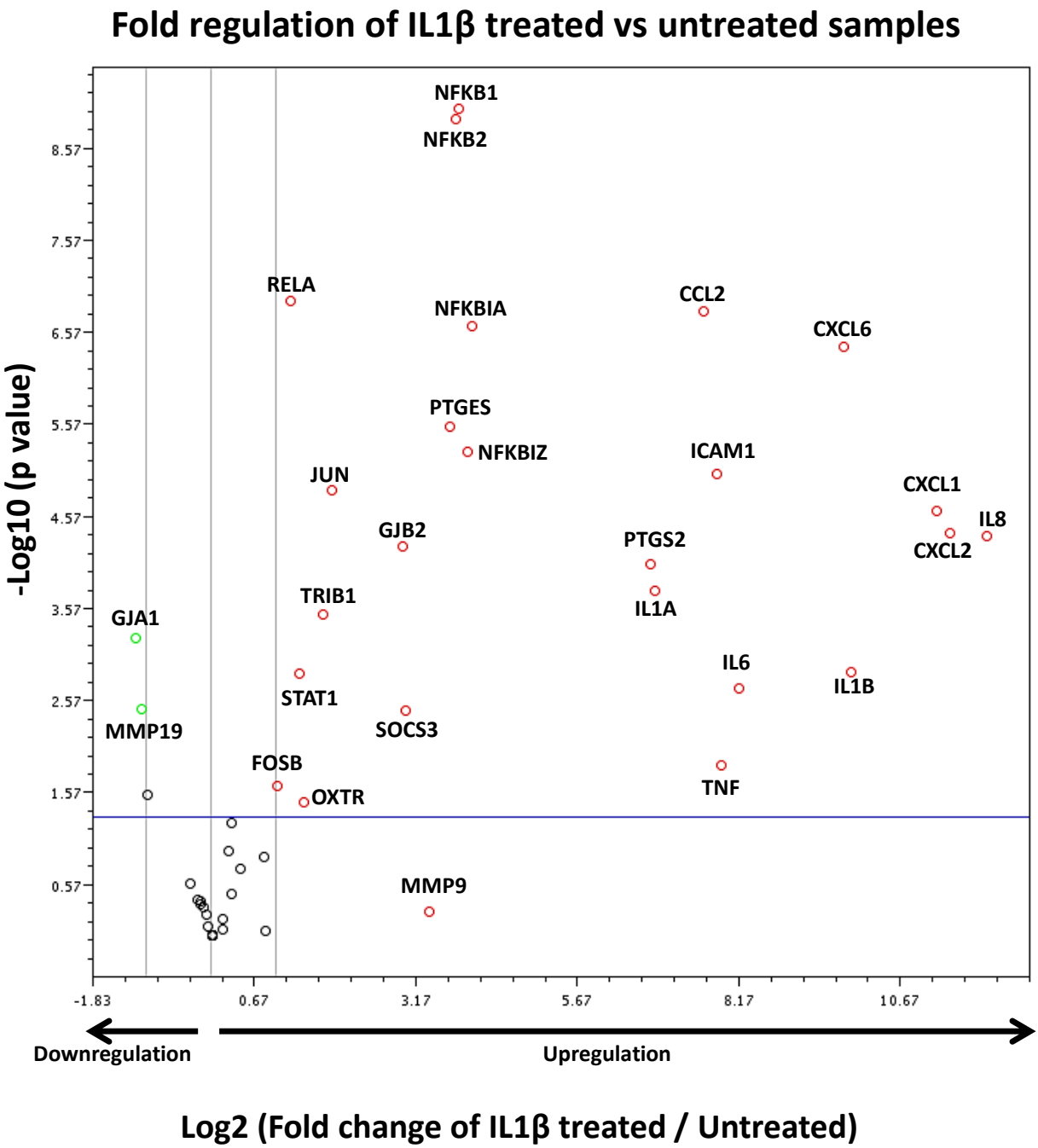

Figure 5.2 Volcano plot demonstrating gene expression changes in myometrial cells following IL1β exposure.

X axis shows fold regulation changes between IL1β treated and untreated samples four hours following cytokine addition. Y axis is the inverse of the p value generated for each gene of interest (GOI) via students T-test. All genes with >2 fold difference between IL1β treated and untreated samples are labelled on the figure. Upregulated genes are presented as red circles, downregulated genes are green circles and genes demonstrating no change are black circles. Genes above the blue horizontal line demonstrate significant change in the presence of IL1β. Data are summated from experiments from eight biological replicates.

5.3 Effects of CPP-linked and small molecule inhibitors on cytokine induced gene expression changes in human uterine cells

5.3.1 Anti- inflammatory effects of Pen-NBD, or Sc514

To assess the anti-inflammatory efficacy of CPP-linked (Pen-NBD) or non-peptide (Sc-514) therapeutic strategies, control samples (IL1β addition alone) were compared with inhibited samples (IL1β plus inhibitor). The concentration and pre-incubation time of inhibitors were selected on the basis of their ability to significantly inhibit IL1β induced COX2 protein expression at four hours, as established in Chapter Four.

Figure 5.3 displays the inhibitory effect of Pen-NBD (Figure 5.3A) and Sc514 (Figure 5.3B) on a panel of inflammatory pathway-related genes which were significantly upregulated in the presence of IL1β. It demonstrates that Pen-NBD inhibited cytokine-mediated increases in expression of many of these genes, including the chemokines IL8, CXCL1/2/6 and CCL2, and the cytokine IL1A but not IL1B, IL6 or ICAM1 gene expression. As displayed in Figure 5.3B, the non-peptide small molecule IKKβ inhibitor Sc514 attenuated the cytokine induced expression of all the pro-inflammatory genes demonstrated within the array. Neither inhibitory approach altered the increased expression profile of SOCS3 gene.

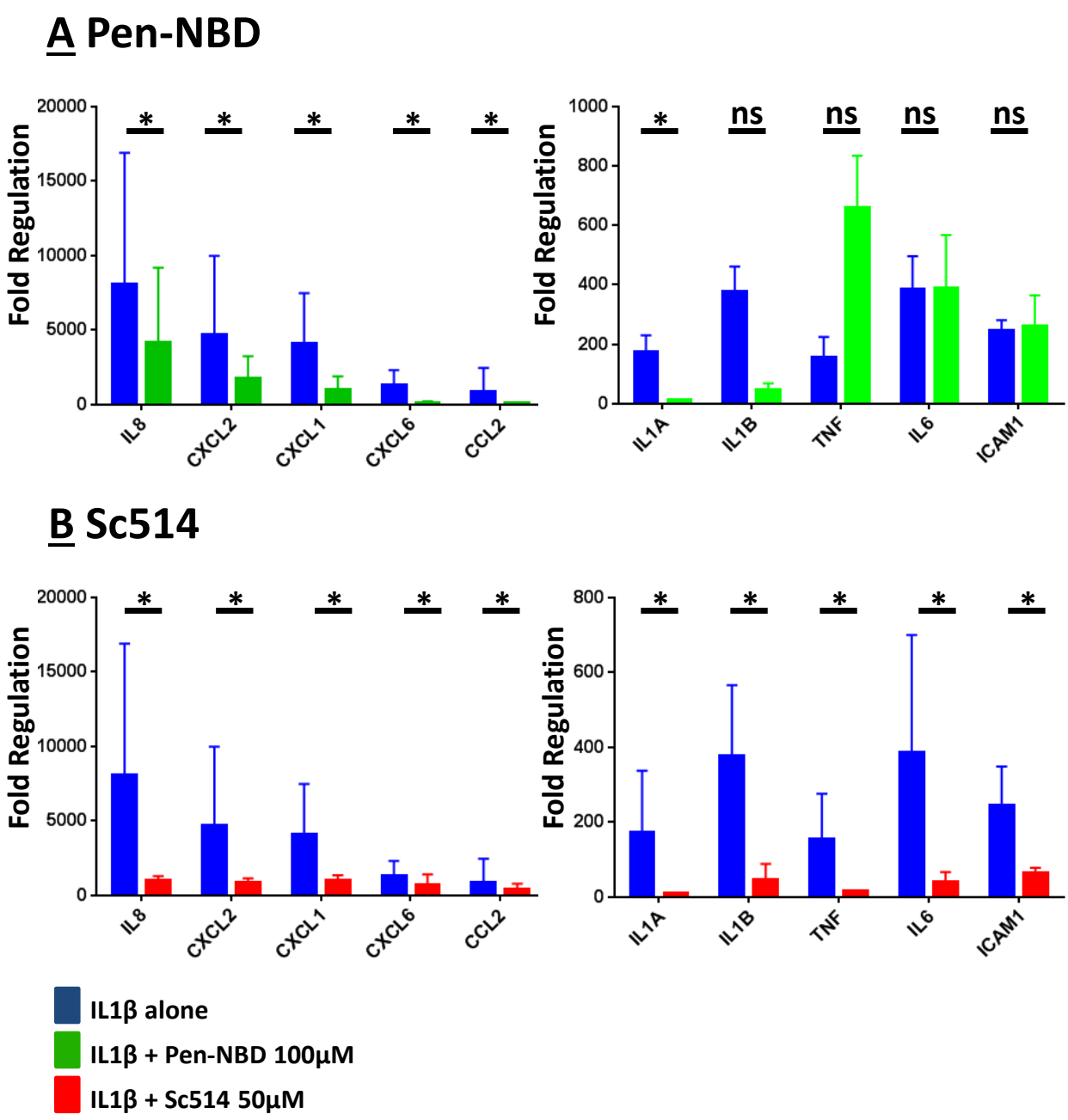

Figure 5.3 Anti-inflammatory effects of Pen-NBD or Sc514 on IL1β stimulated pro-inflammatory gene expression in uterine cells.

Bar charts representing mean average plus SD fold regulation changes of inflammatory genes compared to untreated samples either in the presence ofIL1β alone (blue bars) or pre-incubated with a CPP-linked (**A** Pen-NBD, green bars) or small molecule (**B** Sc514, red bars) inhibitor prior to IL1β addition.

*indicates significant difference in gene expression as derived from Student's t-test of replicate 2^ΔΔCt values (n=3).

5.3.2 Effects of Pen-NBD, or Sc514 on panel of labour associated genes

Figure 5.4 demonstrates a panel of genes taken from the array whose altered expression is associated with increased myometrial contractility and extracellular matrix remodelling that occurs in human labour (Kimura et al., 1992, Xu et al., 2002, Chan et al., 2014, Chow and Lye, 1994). Within the reproductive literature, the proteins produced from the activation of these genes including the oxytocin receptor (OXTR), connexin 43 (GJA1), COX2 (PTGS2) and matrix metalloproteinases are referred to collectively as the contraction associated proteins (CAPs) (Challis et al., 2000), as the increased expression of these proteins promotes the phenotypic switching of the uterus from quiescence to a pro-contractile state.

With the exception of TIMP1, all of these genes exhibited fold regulation changes in uterine cells in the presence of IL1β compared to untreated cells (Figure 5.1). Additional pre-incubation with Pen-NBD prior to IL1β induction did not significantly alter the gene expression profile in this panel.

Use of Sc514 led to inhibition of IL1β induced MMP9 increased gene expression, but did not alter the cytokine stimulated changes in fold change regulation for any of the other labour associated genes in this panel.

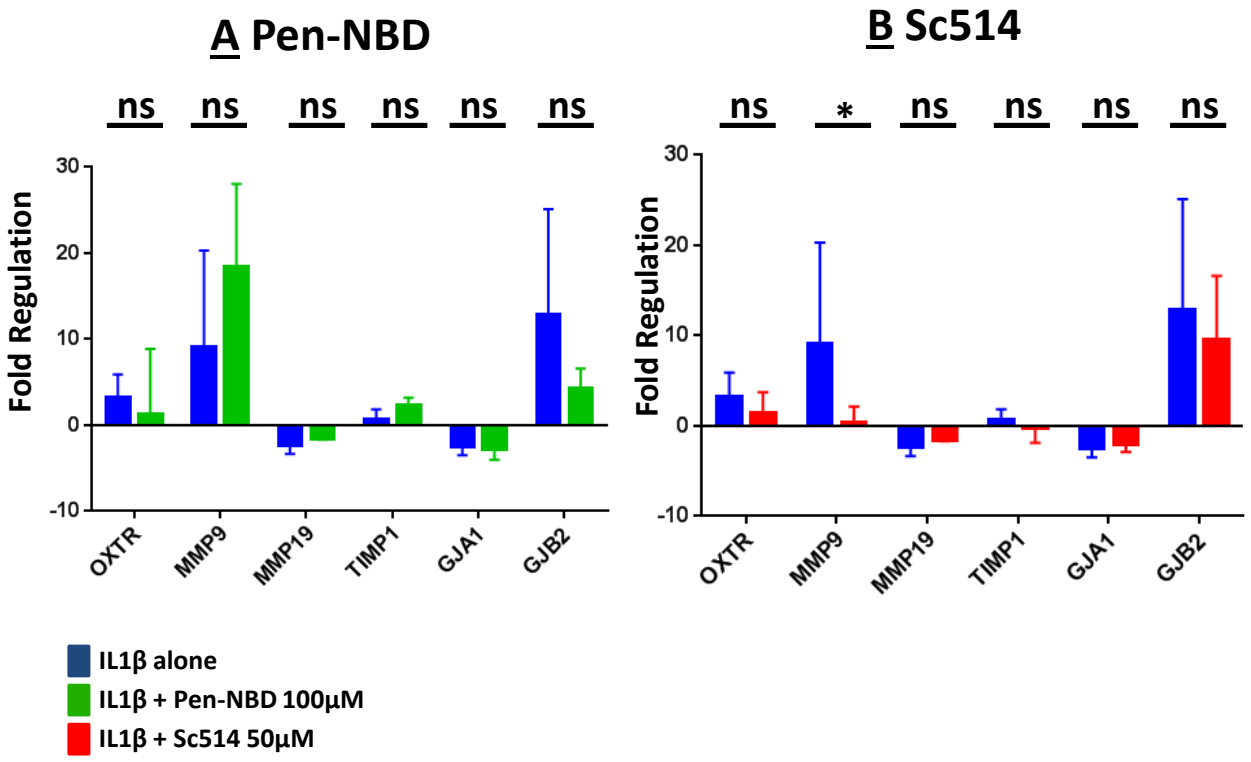

Figure 5.4 Effects of Pen-NBD and Sc514 on cytokine induced expression changes of labour associated genes

Bar charts represent a panel of genes whose expression has been previously reported to be differentially regulated in the presence labour in utero-placental cells. Bars represent mean (SD) fold regulation changes of inflammatory genes compared to untreated samples either in the presence ofIL1β alone (blue bars) or pre-incubated with a CPP-linked (**A** Pen-NBD, green bars) or small molecule (**B** Sc514, red bars) inhibitor prior to IL1β addition.

*indicates significant difference in gene expression as derived from Student's t-test of replicate 2^ΔΔCt values (n=3).

5.3.3 Effects of Pen-NBD, or Sc514 on NFκB pathway genes

The series of NFκB pathway genes included in the array are displayed in Figure 5.5. All the gene components of this pathway demonstrated significant upregulation in myometrial cells with the addition of IL1β (as seen in Figure 5.2).

As displayed in Figure 5.5A: pre-incubation of uterine cells with 100μM of Pen-NBD did not alter the cytokine induced expression profile of any of the genes looked at in this pathway. By contrast, use of 50μM Sc514 (Figure 5.5B) inhibited IL1β stimulated increases in fold change regulation of all the NFκB pathway genes included in the array.

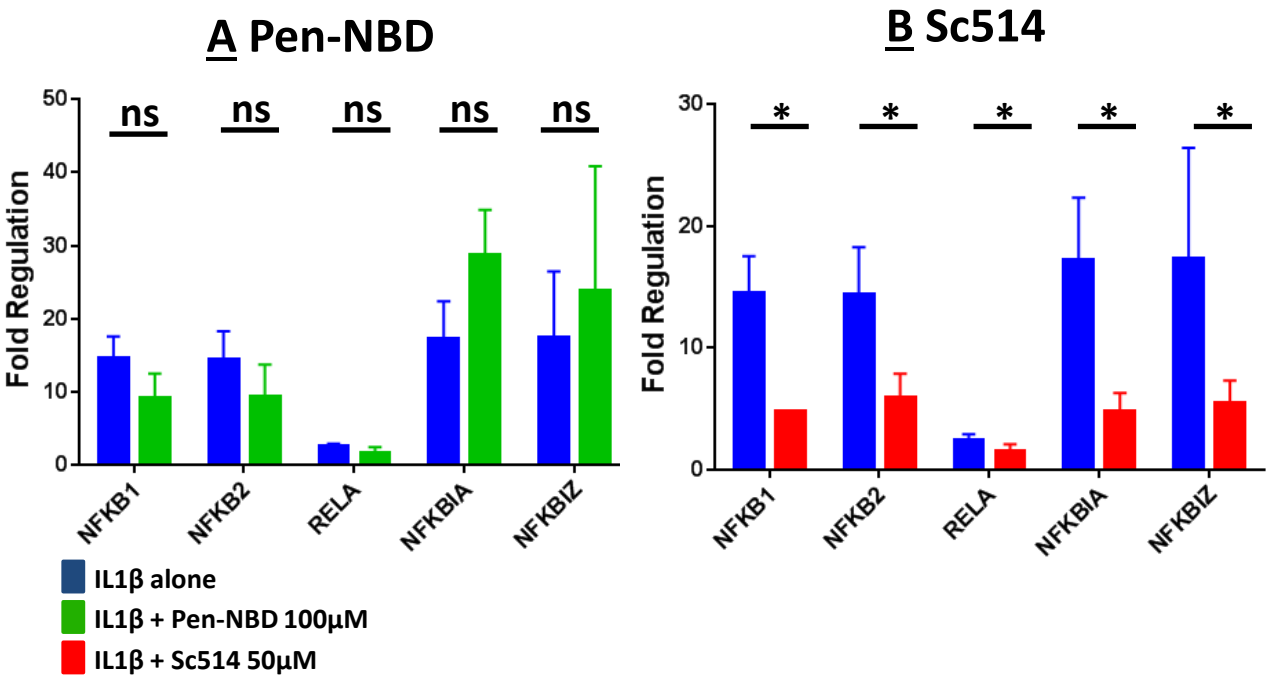

Figure 5.5 Effects of Pen-NBD or Sc514 on cytokine induced expression changes of NFκB pathway genes

Bar charts represent gene components of the NFκB pathway. Bars represent mean average plus SD fold regulation changes of inflammatory genes compared to untreated samples either in the presence ofIL1β alone (blue bars) or pre-incubated with a CPP-linked (**A** Pen-NBD, green bars) or small molecule (**B** Sc514, red bars) inhibitor prior to IL1β addition.

*indicates significant difference in gene expression as derived from Student's t-test of replicate 2^ΔΔCt values (n=3).

5.3.4 Effects of Pen-NBD, or Sc514 on genes involved in prostaglandin regulation

The effect of either inhibitor on two genes whose expression is required for the production of prostaglandins was examined. PTGS2 is the gene encoding for COX2 protein and PTGES encodes for prostaglandin E synthase, an enzyme that catalyses the production of prostaglandins E2 and F2α. The expression of both these genes was significantly increased in uterine cells following the application of IL1B (Figure 5.2).

The bar charts in Figure 5.6 demonstrate the fold change regulation of both these genes in the presence of IL1β alone; or with the pre-incubation of either Pen-NBD or Sc514 prior to IL1β addition. Pen-NBD did not alter the cytokine induced expression of either gene whereas the presence of Sc514 diminished both PTGS2 and PTGES gene expression.

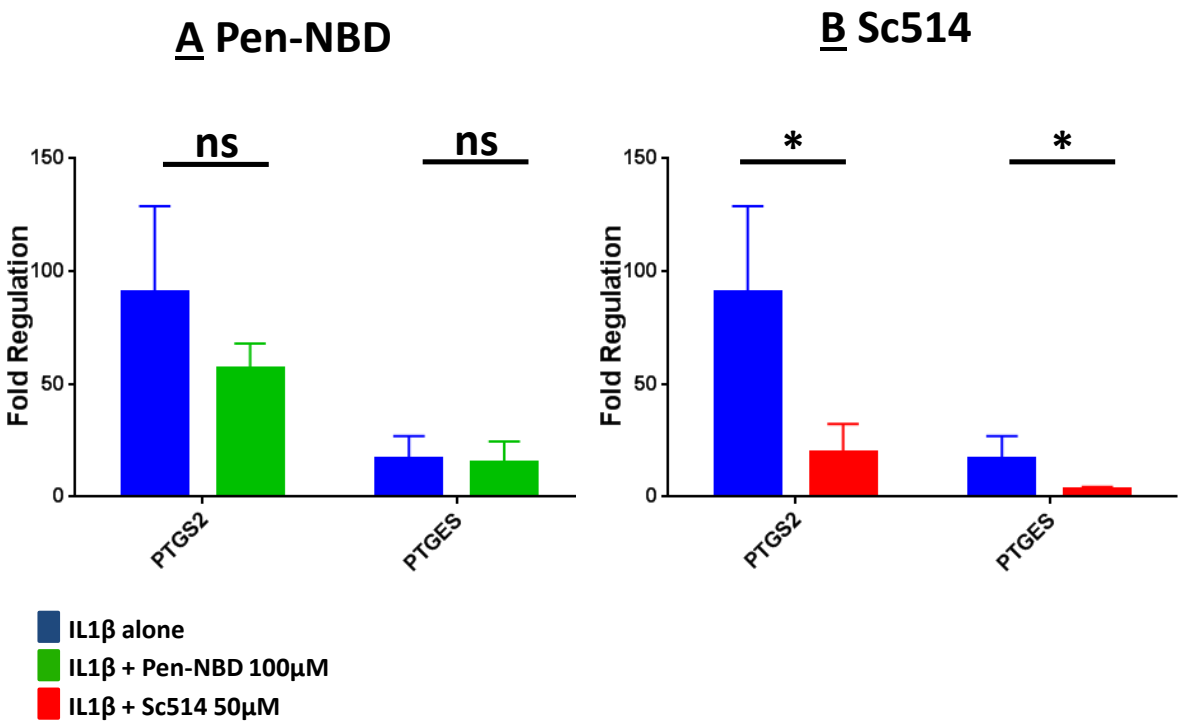

Figure 5.6 Effects of Pen-NBD or Sc514 on cytokine induced expression changes of genes involved in prostaglandin regulation

Bar charts demonstrating the fold change regulation of PTGS2 and PTGES genes. Bars represent mean average plus SD fold regulation changes of inflammatory genes compared to untreated samples either in the presence ofIL1β alone (blue bars) or pre-incubated with a CPP-linked (**A** Pen-NBD, green bars) or small molecule (**B** Sc514, red bars) inhibitor prior to IL1β addition.

*indicates significant difference in gene expression as derived from Student's t-test of replicate 2^ΔΔCt values (n=3).

5.3.5 Effects of Pen-NBD, or Sc514 on cytokine-stimulated changes in novel target genes

Amongst the genes selected for investigation within the array were a group of novel target genes that have previously displayed altered expression in association with human labour, but whose role within the regulation of term or preterm labour is not well characterised. The genes selected for this purpose and the rationale behind their selection is outlined in Chapter Two of this thesis. Of the group of novel target genes, only STAT1 and TRIB1 displayed altered expression in response to IL1β exposure, with both genes demonstrating increased expression (Figure 5.2).

The bar charts in Figure 5.7 demonstrate the fold change regulation of both these genes in the presence of IL1β alone; or with the pre-incubation of either Pen-NBD or Sc514 prior to IL1β addition. Pen-NBD diminished STAT1 and increased TRIB1 gene expression. Pre-incubation with Sc514 did not alter the cytokine induced expression of either of these genes.

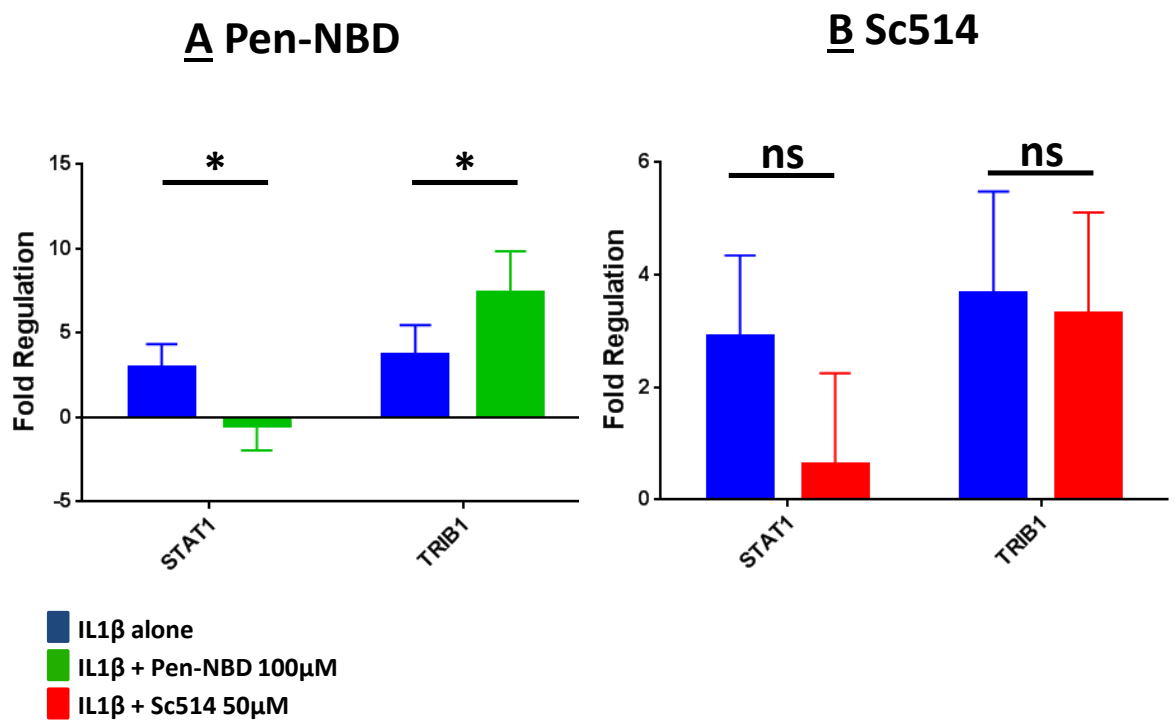

Figure 5.7 Effects of Pen-NBD or Sc514 on cytokine induced expression changes STAT1 and TRIB1 genes

Bar charts demonstrating the fold change regulation of STAT1 and TRIB1 genes. Bars represent mean average plus SD fold regulation changes of inflammatory genes compared to untreated samples either in the presence ofIL1β alone (blue bars) or pre-incubated with a CPP-linked (**A** Pen-NBD, green bars) or small molecule (**B** Sc514, red bars) inhibitor prior to IL1β addition.

*indicates significant difference in gene expression as derived from Student's t-test of replicate 2^ΔΔCt values (n=3).

5.4 Discussion

Using a bespoke array of genes selected to demonstrate expression changes in human gestational cells that have been associated in the literature with human labour (Khanjani et al., 2011, Chan et al., 2014, Kimura et al., 1992, Vadillo-Ortega and Estrada-Gutierrez, 2005, Lappas, 2013, Renthal et al., 2010, Mittal et al., 2010); this chapter demonstrates fold change regulation changes in human myometrial cells following addition of the cytokine IL1β.

Genes exhibiting upregulated expression included the pro-inflammatory cytokines IL16, IL8, TNFα and IL1β. Inflammatory preterm birth has been associated with increased production of these inflammatory mediators in the utero-placental environment (Cappelletti et al., 2015). IL8 displayed the greatest expression changes of the genes within this array in response to IL1β exposure. A study examining the transcriptional profile of human myometrial and cervical tissue in response to labour using microarray techniques also found IL8 to be the most highly expressed of the genes examined, and found a core inflammatory gene response in those tissues subject to labouring processes (Bollopragada et al., 2009).

Genes encoding for the chemokines CXCL1, CXCL2, CCL2 and CCL6 also showed substantial upregulation in the presence of cytokine within this study. This is similar to dramatic increases in expression of these genes previously seen in myometrial tissues of a mouse model systemically injected with LPS to induce preterm birth (Shynlova et al., 2014). These chemokine genes are also much more highly expressed in labouring human term myometrium when compared to non-labouring samples (Chan et al., 2014, Mittal et al., 2010). Upregulation in response to IL1β was seen with genes coding for components of the AP1 and NFκB pathways. This is consistent with an increased response of these molecular pathways within gestational cells following exposure to a pro-inflammatory environment, such as has been proposed to occur in inflammatory scenarios of preterm birth (MacIntyre et al., 2014, Lindstrom and Bennett, 2005).

Within the reproductive literature, the proteins produced from the activation of genes including the oxytocin receptor (OXTR), connexin 43 (GJA1), COX2 (PTGS2) and matrix metalloproteinases are referred to collectively as the contraction associated proteins (CAPs) (Challis et al., 2000). The increased expression of these proteins is proposed to promote the

phenotypic switching of the uterus from a quiescent to a pro-contractile state. A number of these genes within the array were upregulated in the presence of IL1β including genes encoding for the oxytocin receptor (OXTR), the gap junction protein connexin 25 (GJA2) and matrix metalloproteinase enzyme 9 (MMP9).

Taken together, the above data indicate that exposure to an inflammatory environment upregulates a pro-inflammatory transcription signature within myometrial cells which is similar to that seen in labouring uterine tissue at term (Bollopragada et al., 2009, Mittal et al., 2010) , and demonstrate that cytokine exposure may contribute to the upregulation of key proteins involved in the promotion of uterine contraction (Kimura et al., 1992, Xu et al., 2002, Chan et al., 2014, Chow and Lye, 1994). However, there are restrictions to the in vitro experimental model used in this study including the selection of a small number of genes, the timing of gene expression sampling and the use of only one agonist.

Examination of the effect of CPP-linked and small molecular inhibitors on cytokine-induced gene expression changes in myometrial cells found that both inhibitory approaches had important anti-inflammatory effects on myometrial gene expression. Sc514 demonstrated ability to inhibit cytokine induced increases in IL6, ICAM1, and TNF gene expression, changes which were not observed with the use of Pen-NBD. Neither inhibitor altered expression of AP1 pathway genes, nor exhibited broad ability to inhibit IL1β stimulated expression changes in genes within the panel of contraction associated genes. However, Sc-514 was able to inhibit MMP9 expression following application of cytokine. MMP9 is a matrix metalloproteinase enzyme involved in remodelling the extracellular matrix aiding processes such as cervical ripening and fetal membrane rupture (Athayde et al., 1998). It exhibits increased expression in fetal membrane tissue and maternal serum following term and preterm labour (Tency et al., 2012, Xu et al., 2002). Therefore, blocking the expression of this gene could be of therapeutic benefit in the context of preterm birth. Sc-514 inhibited cytokine-induced increases in expression of gene components of the NFκB and prostaglandin synthesis pathways. By contrast, the failure of Pen-NBD to effect similar changes suggests that the actions of Pen-NBD in dampening cytokine signalling in human uterine cells may not attributable to a single mechanism of action focussed on interaction with the IKK complex, a theme explored in detail in the General Discussion chapter.

Amongst the panel of novel target genes selected, only STAT1 and TRIB1 exhibited altered expression secondary to IL1β exposure. Sc514 pre-incubation did not inhibit the response of either gene to cytokine addition, Pen-NBD showed ability to inhibit expression of STAT1 but, increased TRIB1 gene expression above IL1β induced expression levels. STAT1 is a gene encoding for a member of the signal transducers and activators of transcription protein family which have a key involvement in interferon and inflammatory signalling (Ramana et al., 2000). A systematic review performing pathway analysis on human single nucleotide polymorphisms that have a previously described association with preterm birth and preterm premature rupture of membranes (PPROM) found that nearly all PPROM specific genes are linked upstream to the STAT1 gene (Capece et al., 2014). This suggests a regulatory function for STAT1 in the process of early membrane rupture and, therefore, inhibition of this gene may confer benefit in avoidance of this pathological process. TRIB1 encodes for a member of the Tribbles homolog family of putative protein kinases. Although the role of tribbles proteins in human labour is yet to be defined, TRIB1 protein is known to perform a regulatory role in the function of the MAPK pathway (Kiss-Toth et al., 2004). Given that activation of the MAPK pathway is associated with preterm birth (Bartlett et al., 1999b), it remains possible that increases of TRIB1 expression in the presence of Pen-NBD could have either pro-labour or tocolytic actions.

The data presented here and in Chapter Four of this thesis suggest that both Pen-NBD and Sc514 exhibit important anti-inflammatory effects on uterine cells and can block the cytokine induced expression of many genes whose upregulation is associated with both physiological human labour and inflammatory associated preterm birth (Khanjani et al., 2011, Chan et al., 2014). It was also interesting that both agents demonstrated ability to alter the expression of different genes, for example: Pen-NBD but not Sc514 significantly inhibited the cytokine-induced gene expression of STAT1, whereas only Sc514 inhibited changes in MMP9 gene expression. With increasing improvements in the characterisation of distinct preterm birth phenotypes which arise from differing causative mechanisms but result in a common outcome (Villar et al., 2012), the availability of a variety of agents that can treat both a broad insult (inflammation) but also aim to inhibit more discrete targets is a necessity. Therefore, both CPP-linked and small molecule inhibitory approaches can be due further consideration for development as tocolytic therapies.

Chapter Six

General Discussion

A shortage of candidate agents available for clinical testing has restricted attempts to develop new treatments targeted at the prevention of preterm birth. Aiming to address the problem, this study has taken an innovative approach to the development of such agents by testing the effectiveness of a class of peptide-based delivery vectors, Cell Penetrating Peptides which have the potential to deliver bioactive cargo to cells (Orange and May, 2008). Using the Nemo Binding Domain anti-inflammatory peptide cargo directed against the NFκB pathway the study aimed to ameliorate inflammatory signalling in uterine cells and compare this CPP-cargo effect against a group of small molecule inhibitors that have previously demonstrated anti-inflammatory effects in gestational cells (May et al., 2000, Lappas et al., 2003, Lim et al., 2013, Belt et al., 1999, De Silva et al., 2010).

The data presented in this thesis indicate that three CPPs (Pen, TAT, R8) can enter myometrial and placentally-derived cells and deliver cargo at low concentration within a short time period. Furthermore, Pen CPP was able to deliver the NBD peptide cargo internal to uterine cells whereby it inhibited increases in COX2 protein expression at four hours following cytokine exposure. The inhibitory effect observed was comparable to, or in some cases, greater than that seen with the use of non-peptide anti-inflammatory inhibitors.

The phenomenon of COX2 induction following uterine and placental cell surface exposure to cytokines or LPS has been demonstrated to precede increases in prostaglandin production (Belt et al., 1999, Yan et al., 2002b, Kniss et al., 2001). Prostaglandins are key mediators of labour and the inhibition of COX2 protein is an important target for putative agents developed with the aim of preventing preterm birth (Hirst et al., 2005, Olson, 2005). Thus, the use of CPPs may offer an attractive strategy for drug development within the preterm birth paradigm.

6.1 The choice of CPP and the potential for CPP-cargo interaction

The appropriate selection of CPP is a vital concern for the delivery of any designated cargo. This study used Pen CPP as the delivery vector for detailed examination of NBD peptide cargo cellular uptake and biological effectiveness. The rationale for this selection was multifactorial: due to the efficacy of uptake displayed by rhodamine-Pen and comparatively poor uptake of rhodamine-TAT when applied to myometrial cells; alongside the consideration that previous literature had indicated attenuation of poly-arginine uptake

once cargo is attached (Jones et al., 2005). Additionally, the original description of NBD peptide was as a peptide cargo attached to a CPP derived from antennopaedia protein (May et al., 2000), and many subsequent studies have used this CPP vector combination with NBD. Thus the use of Pen-NBD in this study allowed for comparison with previously published data (Strickland and Ghosh, 2006).

The literature also contains numerous in vitro and in vivo experimental examples of NBD attached to a variety of CPP vectors including those derived from antennopaedia, TAT and poly-arginine (Dai et al., 2004, Shibata et al., 2007, Choi et al., 2003, Habineza Ndikuyeze et al., 2014). Alongside this, two studies have aimed to assess the effect that attaching different CPP vectors may have on NBD cargo delivery and efficacy and found that cell toxicity and biological effectiveness can vary widely according to the vector used (Jones et al., 2005, Khaja, 2010). Such variation can be explained in part by differences in the delivery efficacy of any CPP with a selected cargo on any particular cell type. However, a further complicating factor is the possibility of interaction between the CPP and the cargo which may affect overall secondary structure and thus alter the properties of each component or the total CPP-cargo unit.

Although the effects of such interactions are not fully understood, there are notable examples in the literature where authors have altered the CPP-cargo combination or structure and investigated how these changes influence either intracellular delivery or biological effectiveness. A study using a peptide based MAP Kinase 2 (MK2) inhibitor designed for use with a CPP vector found that amino acid substitution or deletion within the CPP, or variation of the CPP vector itself could increase or decrease both the potency and specificity of inhibition. Furthermore, CPP vectors used alone were capable of producing significant inhibitory effects (Ward et al., 2009). The authors were unable to explain why these CPP changes led to such variation in biological activity; however, they proposed that the overall charge and hydrophobicity of CPP and cargo are likely to contribute to this phenomenon.

A recent paper examined a phenomenon of large complex formation between insulin protein cargo and CPPs derived from antennopaedia protein using dynamic light scattering and electron microscopy techniques (Kristensen et al., 2015). The authors reported that the

size and frequency of CPP-insulin complexes were dependent on environmental pH, with fewer and smaller complexes being formed at lower pH. They found that CPP-dependent delivery of insulin cargo through an epithelial monolayer was pH sensitive and required the presence of arginine residues within the CPP vector, and that alteration of the position of tryptophan residues within the CPP structure could also alter delivery efficacy. These findings highlight not only the effect that altering the CPP vector may have on an overall CPP-cargo unit; but also underlines that smaller differences in structure within the same CPP-cargo combination, for example, altering the position or frequency of key amino acid residues such as arginine and tryptophan, may influence the efficacy of both cellular delivery and biological effect.

Peptide Name	Peptide Structure	Isoelectric point	Net Charge at pH 7	No of Arginine Residues	No of Tryptophan Residues
Pen	**RQIKIWFQNRRMKW**	12.42	4	3	2
TAT	**YGRKKRRQRRR**	12.41	7	6	0
R8	**RRRRRRRR**	12.94	7	8	0
GS_4(GC)	**GSGSGSGSGC**	3.11	-0.1	0	0
Nemo Binding Domain	**TALDWSWLQTE**	0.71	-2	0	2
Pen Nemo Binding Domain (Wild type)	**Ac-RQIKIWFQNRRMKW-Aca- TALDWSWLQTE-NH2**	11.87	3	3	4
Pen Nemo Binding Domain (Mutant)	**Ac-RQIKIWFQNRRMKW-Aca-TALDASALQTE-NH2**	11.87	3	3	2
TAT Nemo Binding Domain	**Ac-YGRKKRRQRRR-Aca-TALDWSWLQTE-NH2**	12.12	6	5	2
R8 Nemo Binding Domain	**Ac-RRRRRRRR-Aca-TALDWSWLQTE-NH2**	12.58	6	8	2

Table 6.1 The structure and properties of peptides used in experimentation.

Table 6.1 indicates how changes in the CPP and cargo attachments used in this study altered the isoelectric point and net charge of the CPP-cargo complexes, thus varying the sensitivity of the overall unit to environmental pH changes. Each CPP-cargo combination also shows differences in the frequency of amino acid residues such as arginine and tryptophan, and it is possible that the three dimensional position of these residues differs within the secondary conformation of each CPP-cargo unit. The table highlights that low or negatively charged peptides with few to nil arginine residues, such as GS4(GC) or NBD alone, do not possess cell penetrating ability (as demonstrated experimentally in Chapter Three of this thesis). This is also consistent with literature suggesting that the guanidinium groups contained within arginine amino acids are essential for CPP cell entry (Wender et al., 2000).

The peptide structures listed in Table 6.1 suggest that the biological efficacy demonstrated by Pen-NBD in myometrial cells, but not observed with the use of NBD conjugated to TAT or R8, may be related to the slightly lower charge of this CPP-cargo combination or to the frequency or position of tryptophan and arginine residues within the overall unit. However, the exact significance of such changes is not yet known in the literature and this study was not designed to explain how such differences may affect cellular uptake or overall biological activity. There are a very large number of CPPs described in the literature, and even amongst well characterised CPPs such as AntP or TAT differences exist as to the precise amino acid structure used for experimentation (Gautam et al., 2012). Thus, there is a vital importance for any future study to clearly describe the CPP used, the exact amino acid structure and the method of conjugation with any given cargo to ensure consistency of data produced.

6.2 NBD peptide targeting in human myometrial cells

In this study the NBD peptide was selected as the CPP-linked cargo to examine due to well characterised anti-inflammatory properties both in vitro and in vivo, its putative selectivity towards NFκB dependent pathways and the association between NFκB upregulation and preterm birth (Strickland and Ghosh, 2006, May et al., 2000, Lindstrom and Bennett, 2005). A prime benefit of using this peptide cargo was also the reported specificity of targeting towards the IKK complex. It potentially offers inhibition of aberrant NFκB signalling without affecting physiological NFκB activation associated with normal cellular inflammatory

responses, thus minimising off-target effects (May et al., 2000). Consequently, the failure of Pen-NBD to prevent the IL1β induced degradation of IκBα in myometrial cells even at doses capable of COX2 protein inhibition was an unexpected result that required careful consideration.

The experiments involving the non-peptide inhibitor Sc514 were informative in this regard. Sc514 is a small molecule inhibitor suggested to exert a high degree of inhibitory selectivity for IKKβ above other IKK isoforms or serine-threonine or tyrosine kinases (Kishore et al., 2003), and, therefore, has an analogous mechanism of action to Pen-NBD via inhibition of IKK complex activation. Despite both Pen-NBD and Sc514 producing comparable inhibition of COX2 protein, Sc514 was additionally able to inhibit IL1β-induced degradation of IκBα protein, whereas Pen-NBD did not prevent such degradation (Chapter Four, section 4.13.2). Exposure to IL1β increased the expression of all NFκB pathway genes examined within a bespoke array of genes; Sc514 decreased expression changes in all of this gene family, whereas Pen-NBD exerted minimal effect (Chapter Five, section 5.3.3).

There are a number of possible explanations for such results. The specificity of Pen-NBD inhibitory effects directed towards the IKK complex may vary according to the type of inflammatory agonist used. IL1β has demonstrated the capability to activate the canonical NFκB pathway in cells deficient of the IKKβ subunit, suggesting that this agonist can trigger an IKKβ-independent mechanism of NFκB activation, a phenomenon not observed with TNFα (Solt et al., 2007). Indeed, agonist-specific variation of Pen-NBD effect was observed in this study with TNFα-induced IκBα protein degradation inhibited by Pen-NBD in two out of three experiments, but not in a third experiment (Chapter Four, section 4.10). This may be explained in part by the previously described variation of observed responses in myometrial cells to TNFα stimulation (Lappas, 2013), however it may reflect true Pen-NBD inhibition of TNFα, but not IL1β-induced IκBα protein degradation.

Further interrogation of the literature revealed only two studies which have directly examined the effect of NBD peptide on IL1β-dependent phosphorylation and degradation of IκBα protein with both studies demonstrating successful inhibition of IL1β stimulation. Baima et al. used concentrations of NBD ranging from 6.2 to 100μM to inhibit IκBα degradation in IL1β-stimulated rheumatoid arthritis synovial fluid (RASF) cells (Baima et al.,

2010) , and Tas et al. applied 50μM NBD to block IL1β-induced degradation in fibroblast-like synoviocyte (FLS) cells (Tas et al., 2006). Results from such studies indicate that Pen-NBD inhibitory responses may be cell type dependent; despite this, work completed by our collaborative group in Cardiff establishes that the observed inability of CPP-NBD conjugated peptides to inhibit cytokine mediated degradation of IκBα is not exclusive to primary myometrial cells. Figure 6.1 demonstrates that 100μM NBD conjugated to an antennopaedia CPP analogue did not inhibit TNFα-induced IκBα degradation in HeLa cells in any of three experiments.

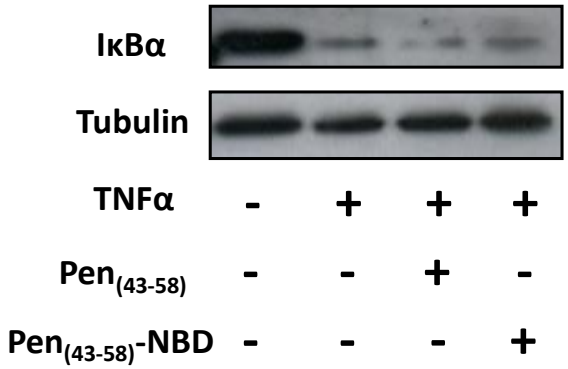

Figure 6.1 IκBα protein responses to TNFα in HeLa cells

Western blot displaying IκBα protein in the absence (-) or presence (+) of 20ng/ml TNFα. Last 2 lanes show effects of 1 hour pre-incubation of 100μM of Pen(43-58) or 100μM NBD conjugated to Pen(43-58) followed by application of TNFα for 30 minutes. Results are representative of 3 independent experiments. Tubulin used to demonstrate equal protein loading. Reproduced with kind permission from N. Eissa (School of Pharmacy and Pharmaceutical Sciences, University of Cardiff).

The papers described above used a lower concentration of agonist than the present study (1 - 2.5 ng/ml). The consideration arises, therefore, that the concentration of IL1β used in this study may have produced a hyper-stimulatory agonist effect which strongly activated the IKK complex, leading to robust IκBα protein degradation and de novo gene expression of NFκB pathway components (Baima et al., 2010). In such a scenario Pen-NBD would inhibit COX2 production but perhaps was unable to override the agonist activation effect on IKK.

This could be remedied experimentally by either reducing the agonist concentration or increasing the inhibitory concentration. Neither of these solutions is unproblematic: reducing the agonist dose may not reliably induce IκBα degradation (Chapter Four, section 4.7.2) thus diminishing the usefulness of using IκBα protein as a measure of IKK activation. Pen-NBD dose increases would lead to a further increase in vehicle concentration, may lead to toxic effects and would detract from one of the key advantages of the CPP approach: a reduced requirement for high concentrations due to ease of cellular entry of cargo.

Another potential explanation for the failure of Pen-NBD to inhibit IL1β-induced IκBα protein degradation and the expression of NFκB pathway genes may be that its inhibitory effect is exerted on pathways other than NFκB in myometrial cells. Potential candidate pathways would include those that are activated by the cytokines IL1β and TNFα including the AP1 and p38MAP kinase signalling pathways (Weber et al., 2010, Wajant et al., 2003). Although gene components of the MAPK pathway were not examined in this study and would warrant further investigation, the genes FOSB and JUN which encode proteins that dimerise to form the transcription factor AP1 (Davies and Tournier, 2012) demonstrated upregulated expression following myometrial cell stimulation with IL1β. Expression of these genes was not inhibited by Pen-NBD indicating that the NBD peptide cargo is not exerting anti-inflammatory action via suppression of these components of the AP1 pathway.

It is also possible that Pen-NBD may have mediated effect via molecular targets downstream of the IKK complex within the NFκB canonical pathway. Although outside of the temporal scope of this study, future work examining the effect of Pen-NBD on p65 NFκB subunit phosphorylation; p65 nuclear translocation expression and assessing p65 binding to NFκB specific transcription sites would aid clarification. Homodimers of the p50 subunit of NFκB can inhibit inflammation and are down-regulated in human myometrial tissue during pregnancy and labour (Lawrence, 2009, Chapman et al., 2004), thus examination of the effect of the NBD peptide on this subunit would also be a worthwhile endeavour.

However, this suggestion of IKK-independent cytokine activation of NFκB signalling seems not to be supported by data showing that Pen-NBD did not alter cytokine mediated increases in the expression of PTGS2, the gene coding for the transcription of COX2 protein in uterine cells, whereas Sc514 was capable of diminishing such increases (Chapter Five,

section 5.3.4). COX2 protein is known to undergo modification at a post transcriptional level and such changes may regulate the effectiveness of prostaglandin synthesis by this enzyme (Cok and Morrison, 2001). Although less well understood, post-translational modification in the form of nitration of tyrosine residues in the active site of the enzyme has been described (Parfenova et al., 1998), and a recent paper has identified two phosphorylation sites regulated by the FYN tyrosine kinase family (Alexanian et al., 2014). In these studies the post-translational modifications appeared to increase COX2 enzyme activity without changes in protein expression levels. Nonetheless, in uterine cells where COX2 expression is inducible by biologically-relevant stimuli, there could be the possibility that the NBD peptide may regulate a non-IKK kinase intermediary leading to a post-translational modification of COX2 that mediates its degradation. A summary of the potential mechanisms of Pen-NBD action in myometrial cells is displayed in Figure 6.2

Amongst the panoply of cargoes available for CPP linkage include other peptides, enzymes, proteins, antibodies, nucleic acid mimics (siRNA, morpholino), chemotherapeutics and nanoparticles (Reissmann, 2014). As highlighted in the Introductory chapter of this thesis, existing data supports an association between activation of the MAP Kinase and AP1 pathways and preterm birth (Bartlett et al., 1999b, MacIntyre et al., 2014). Cargo available for CPP-linkage includes peptide based MAP kinase inhibitors (Lopes et al., 2009) and inhibitors of the AP1 pathway (Meade et al., 2010), hence future work aimed at testing the effectiveness of such agents in preterm birth scenarios may prove fruitful.

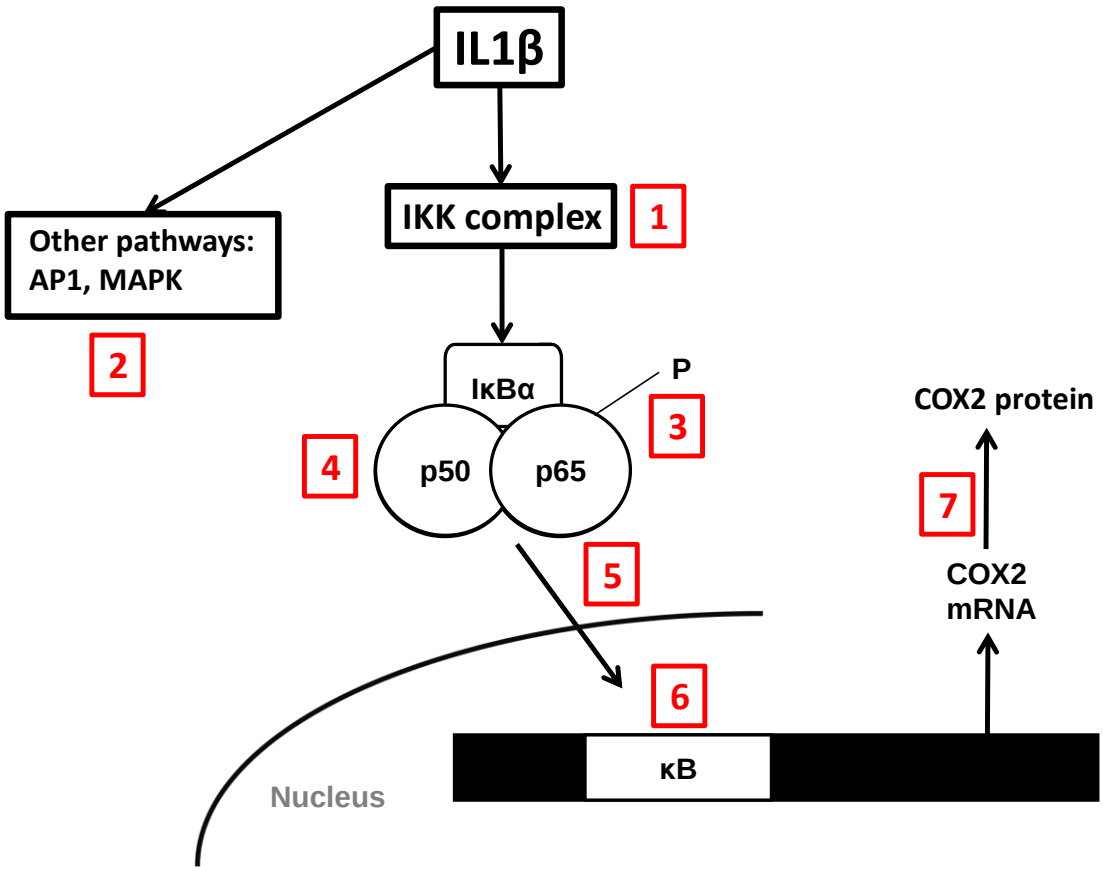

Figure 6.2 Schematic diagram displaying potential Pen-NBD sites of action in myometrial cells

1. Targeting IKK complex but with inhibitory effect bypassed by robust IL1β-stimulatory response
2. Inhibition of inflammatory pathways external to NFκB
3. Prevention of NFκB p65 subunit phosphorylation
4. Interaction with NFκB p50 subunit
5. Prevention of p50 / p65 heterodimer nuclear localisation
6. Interaction with NFκB binding sites
7. Post-translational modification of COX2 protein

6.3 Myometrial cell gene expression changes in response to inflammatory stimuli

The experiments presented in Chapter Five aimed to model a pro-inflammatory uterine environment in vitro by exposing myometrial cells to IL1β and examining subsequent changes in expression of a bespoke array of genes whose altered expression has been previously associated with human term labour (Khanjani et al., 2011, Chan et al., 2014, Kimura et al., 1992, Vadillo-Ortega and Estrada-Gutierrez, 2005, Lappas, 2013, Renthal et al., 2010, Mittal et al., 2010).

A recent systematic review and meta-analysis of transcriptome changes in all gestational tissues including myometrium, placenta, fetal membranes and cervix in human term and preterm pregnancies found that few studies had examined spontaneous preterm birth and as yet no study has looked at genome wide expression changes in human preterm myometrial tissue (Eidem et al., 2015). Therefore, until such a research gap is addressed, inferences regarding human myometrial gene expression changes during preterm birth must be drawn either from term labour studies or from in vitro studies that attempt to simulate changes in cellular environments associated with specific phenotypes of preterm birth. Indeed, the alterations of gene expression in cytokine-induced myometrial cells observed in this study are consistent with many of the changes seen in term labouring samples (Chan et al., 2014, Mittal et al., 2010, Wathes et al., 1999, Roh et al., 2000), thus adding further support to the theory that both preterm and term labour are associated with an inflammatory signature of molecular changes in gestational cells and tissues (Bollopragada et al., 2009).

The connexins are a family of proteins that oligomerise to form channels which link the cytoplasm of adjacent cells and thus can facilitate transmission of electrical signals through cells thus helping facilitate organ contraction (Hervé, 2012, Kidder and Winterhager, 2015). Connexin 43 protein has previously shown increased expression in association with labour, and is thought to comprise one of the key contraction associated proteins (CAPs) linked with phenotypic switching of the uterus from a quiescent to a contractile state (Lye et al., 1993, Cook et al., 2000, Chow and Lye, 1994). In this study, expression of GJA1 gene (encoding for connexin 43 protein) was significantly diminished in myometrial cells exposed to IL1β compared to untreated cells. This observation is worthy of further experimental observation

as it suggests that this protein may not play such a central role in mediating increased uterine contractility in inflammatory scenarios of labour as previously thought.

Both Pen-NBD and Sc514 exerted profound inhibitory effects on IL1β-stimulated myometrial cells, diminishing the expression of genes whose increased expression has been associated with inflammatory preterm birth including chemokines and the cytokines IL1A and IL8 (Cappelletti et al., 2015, Shynlova et al., 2014). Both agents also exhibited the ability to inhibit the expression of diverse genes, with Pen-NBD affecting STAT1 expression and Sc514 downregulating the expression of MMP9; however, neither agent was broadly successful in preventing cytokine-provoked alterations in expression for the contraction associated genes. This indicates that even if such agents are successful in blocking the upregulation of inflammatory pathways in utero-placental cells in an in vivo setting; there may be limitations in their ability to prevent or delay the onset of birth if used as monotherapy. It necessitates the consideration of such agents being used as adjuncts alongside other treatments including antibiotics or traditional tocolytics such as nifedipine or atosiban. A multiple therapy approach may prove successful (Olson et al., 2008, Adams Waldorf et al., 2011), but has yet to be tested in detail in clinical trial due to concerns regarding adverse drug reactions (de Heus et al., 2009).

A promising area of CPP usage is the potential intracellular delivery of small interfering RNA (siRNA). This is a naturally occurring endogenous regulatory process where short double-stranded RNA causes sequence-specific posttranscriptional gene silencing, potentially offering gene specific inhibition (Wang et al., 2010). Although the therapeutic use of siRNA has previously been limited by its inability to cross cellular membranes, CPPs have been shown to be very effective tools for delivering siRNA into cells (Meade and Dowdy, 2007). Therefore, further work could also combine the use of CPPs with siRNA with the aim of inhibiting selected gene targets identified within this study.

6.4 Translation of a CPP-cargo approach to clinical scenarios of preterm birth

The use of a CPP-cargo conjugate to downregulate inflammatory responses in uterine cells shows much promise. However, there are number of considerations that should be addressed further in preclinical work prior to translation of this method into tocolytic therapy.

Exposure to only one inflammatory agonist is unlikely to fully reflect the situation in vivo whereby a complex milieu of pro-inflammatory mediators are likely to interact within the utero-placental environment (Romero et al., 2007). Additionally, the measurement of gene expression five hours following exposure to cytokine will only give a snapshot into the dynamic chronology of changes that will be occurring at a transcript level in myometrial cells exposed to an inflammatory environment and it would be of interest to know if these changes are replicated over longer timeframes.

The use of only one cell type does not reflect the complex interactions that occur between gestational cells and tissue; however, this must be balanced against the previously noted difficulties of developing and propagating a primary placental cell type in this study. Therefore, myometrial cells were selected as the primary focus for examination as it is within these cells that many of the phenotypic changes of labour occur (Challis et al., 2000) and the myometrium is the target organ towards which the majority of previous tocolytic therapies have been directed, with prevention of myometrial contraction a primary aim (Olson et al., 2008).

The potential for toxicity must be fully explored, this is a particularly sensitive question in Obstetrics where one must consider the chances of toxic effects on both mother and fetus. A high specificity of any treatment towards its intended target would be likely to reduce toxicity caused by offsite effects. Therefore, the discovery that the NBD peptide may have a mechanism of action in myometrial cells that is distinct to the inhibition of IKK complex activation underline the requirement of further in vitro testing of this particular peptide cargo.

Experiments using a Cell Titre Blue assay demonstrate that CPPs were not toxic to myometrial cells over the experimental time frame (Chapter Four, section 4.3). Further testing across a full concentration range would also be required in pregnant animal models to underline the lack of toxicity observed in vitro. A special consideration in the pregnant patient is whether a therapy is likely to cross the placenta and, therefore, have effects on the fetus. Proteins do not tend to cross the placenta due to their large size and charge; however peptides and amino acids are readily transported across the placenta via active

transport. Although speculative, it is likely that CPPs and cargo would both cross the placenta and incorporate into placental and fetal cells.

In many cases of preterm birth the pregnancy may also be complicated by the presence of Fetal Inflammatory Response Syndrome (FIRS). This is a condition whereby an external inflammatory or infectious stimuli leads to a systemic fetal inflammatory response that can be deleterious or even fatal to the fetus (Gotsch et al., 2007). Thus, introducing a therapy that may cross the placenta, reach the fetus and exert an anti-inflammatory effect may not be harmful, and indeed could be an additional benefit of this therapeutic approach.

CPPs enter a very broad range of cell types. Although more traditional small molecule therapies are not cell type specific and many modern CPPs have demonstrated increased cell type selectivity (Reissmann, 2014), this is an issue which would need to be addressed in further development. There are two possible solutions to this problem: firstly, local drug delivery to the utero-placental environment could be attempted either using vaginal insertion as a drug pessary or via direct injection to the myometrium. This may still be an unsatisfactory approach as following introduction of a CPP based drug there would remain uncertainty as to the final concentration arriving at target tissues.

An alternative approach is via cell targeting peptides: short peptide sequences with the ability 'home in' to specific cell types (Vivès et al., 2008). Placental-specific homing peptides have recently been identified with the ability to deliver liposomes selectively to trophoblastic explants (Cureton et al., 2013). The future possibility of combining these homing peptides with CPP-cargo conjugates to target inflammatory processes in gestational cells is a very exciting one.

Preterm birth is a syndrome with multiple causative modalities, not all of which may involve inflammation, and the predominant intracellular molecular pathways driving the labouring process in any given case may differ (Romero et al., 2006b). In this context, the versatility of a CPP based treatment approach – whereby different cargo may be attached to influence selected intracellular molecular targets – is a great asset. The work presented in this study provides not only a 'proof of concept' of CPP based therapeutic delivery into myometrial cells, but also a foundation for future research that may explore a variety of CPP-cargo combinations aimed ultimately at the prevention of preterm birth.

Appendix

Funding awards

Wellbeing of Women Entry Level Grant Award 2011

Wellbeing of Women / PwC Research Training Fellowship 2013-2015

Oral presentations

June 2014 Physiological society conference
'Evaluation of small molecular inhibitors of nuclear factor kappa B (NFκB) in abrogating cytokine stimulated signalling in isolated human myometrial cells'

June 2015 British Maternal and Fetal Medicine Society Conference
'Cell penetrating peptides as tools to ameliorate inflammatory signalling in uterine cells'

Sept 2015 Liverpool Harris Wellbeing Preterm Birth Conference
'Use of cell penetrating peptides to treat inflammatory responses in uterine cells'

Poster presentations

January 2015 RCOG Annual Academic Meeting
'Cell penetrating peptide linked inhibitors: a novel approach to downregulating inflammatory responses in primary myometrial cells'
Awarded best poster presentation

June 2015 British Maternal and Fetal Medicine Society Conference
'Cell penetrating peptide and small molecule approaches to inhibiting inflammatory responses in myometrial cells'

July 2015 CPP Paris International symposium
'Application of CPP-Peptide vectors in human cells: is our cargo treasure or fools' gold?'

Other awards / prizes

Diploma Clinical Research awarded from Newcastle University November 2015

Famelab: a national competition in which competitors have three minutes to convey a scientific concept of their choice to a live audience.

Winner North East finals February 2015 with *'Ode to ergot'*
https://www.youtube.com/watch?v=2pI2MHQyOT4

Runner up national finals May 2015 with *'Role of progesterone in the timing of human birth'*
https://youtu.be/9ze4aRoLKzg?t=3023

References

ACKERMAN, W. E. T., SUMMERFIELD, T. L., VANDRE, D. D., ROBINSON, J. M. & KNISS, D. A. 2008. Nuclear factor-kappa B regulates inducible prostaglandin E synthase expression in human amnion mesenchymal cells. *Biology of Reproduction,* 78**,** 68-76.

ADAMS WALDORF, K. M., PERSING, D., NOVY, M. J., SADOWSKY, D. W. & GRAVETT, M. G. 2008. Pretreatment with toll-like receptor 4 antagonist inhibits lipopolysaccharide-induced preterm uterine contractility, cytokines, and prostaglandins in rhesus monkeys. *Reproductive Sciences,* 15**,** 121-7.

ADAMS WALDORF, K. M., RUBENS, C. E. & GRAVETT, M. G. 2011. Use of non-human primate models to investigate mechanisms of infection-associated preterm birth. *British Journal of Obstetrics and Gynaecology,* 118**,** 136-44.

AGGARWAL, B. B., SUNDARAM, C., MALANI, N. & ICHIKAWA, H. 2007. Curcumin: the Indian solid gold. *Advances in Experimental Medicine and Biology,* 595**,** 1-75.

AGUAN, K., CARVAJAL, J. A., THOMPSON, L. P. & WEINER, C. P. 2000. Application of a functional genomics approach to identify differentially expressed genes in human myometrium during pregnancy and labour. *Molecular Human Reproduction,* 6**,** 1141-5.

AL-TAEI, S., PENNING, N. A., SIMPSON, J. C., FUTAKI, S., TAKEUCHI, T., NAKASE, I. & JONES, A. T. 2006. Intracellular traffic and fate of protein transduction domains HIV-1 TAT peptide and octaarginine. Implications for their utilization as drug delivery vectors. *Bioconjugate Chemistry,* 17**,** 90-100.

ALEXANIAN, A., MILLER, B., CHESNIK, M., MIRZA, S. & SOROKIN, A. 2014. Post-translational regulation of COX2 activity by FYN in prostate cancer cells. *Oncotarget,* 5**,** 4232-4243.

ALLPORT, V. C., PIEBER, D., SLATER, D. M., NEWTON, R., WHITE, J. O. & BENNETT, P. R. 2001. Human labour is associated with nuclear factor-kappaB activity which mediates cyclo-oxygenase-2 expression and is involved with the 'functional progesterone withdrawal'. *Molecular Human Reproduction,* 7**,** 581-6.

ANKERMANN, T., REISNER, A., WIEMANN, T., KRAMS, M., KOHLER, H. & KRAUSE, M. F. 2005. Topical inhibition of nuclear factor-kappaB enhances reduction in lung edema by surfactant in a piglet model of airway lavage. *Critical Care Medicine,* 33**,** 1384-91.

APPLEBY, S. B., RISTIMAKI, A., NEILSON, K., NARKO, K. & HLA, T. 1994. Structure of the human cyclo-oxygenase-2 gene. *Biochemical Journal,* 302 (Pt 3)**,** 723-7.

ATHAYDE, N., EDWIN, S. S., ROMERO, R., GOMEZ, R., MAYMON, E., PACORA, P. & MENON, R. 1998. A role for matrix metalloproteinase-9 in spontaneous rupture of the fetal membranes. *American Journal of Obstetrics and Gynecology,* 179**,** 1248-53.

BAIMA, E. T., GUZOVA, J. A., MATHIALAGAN, S., NAGIEC, E. E., HARDY, M. M., SONG, L. R., BONAR, S. L., WEINBERG, R. A., SELNESS, S. R., WOODARD, S. S., CHRENCIK, J., HOOD, W. F., SCHINDLER, J. F., KISHORE, N. & MBALAVIELE, G. 2010. Novel Insights into the Cellular Mechanisms of the Anti-inflammatory Effects of NF-κB Essential Modulator Binding Domain Peptides. *The Journal of Biological Chemistry,* 285**,** 13498-13506.

BARTLETT, S. R., SAWDY, R. & MANN, G. E. 1999b. Induction of cyclooxygenase-2 expression in human myometrial smooth muscle cells by interleukin-1β: involvement of p38 mitogen-activated protein kinase. *The Journal of Physiology,* 520**,** 399-406.

BECHARA, C. & SAGAN, S. 2013. Cell-penetrating peptides: 20 years later, where do we stand? *The Federation of European Biochemical Society Letters,* 587**,** 1693-702.

BEHRMAN RE, B. A. 2007. *Preterm Birth: Causes, Consequences, and Prevention*, Washington (DC): National Academies Press (US).

BELOOSESKY, R., GAYLE, D. A., AMIDI, F., NUNEZ, S. E., BABU, J., DESAI, M. & ROSS, M. G. 2006. N-acetyl-cysteine suppresses amniotic fluid and placenta inflammatory cytokine responses to lipopolysaccharide in rats. *American Journal of Obstetrics and Gynecology,* 194**,** 268-73.

BELT, A. R., BALDASSARE, J. J., MOLNAR, M., ROMERO, R. & HERTELENDY, F. 1999. The nuclear transcription factor NF-kappaB mediates interleukin-1beta-induced expression of cyclooxygenase-2 in human myometrial cells. *American Journal of Obstetrics and Gynecology,* 181**,** 359-66.

BENNETT P, D. L. 2011. Tocolytic Drugs for Women in Preterm Labour. *Royal College of Obstetrics and Gynaecology,* Greentop Guidelines

BLENCOWE, H., COUSENS, S., CHOU, D., OESTERGAARD, M., SAY, L., MOLLER, A.-B., KINNEY, M. & LAWN, J. 2013. Born Too Soon: The global epidemiology of 15 million preterm births. *Reproductive Health,* 10**,** S2-S2.

BOLLOPRAGADA, S., YOUSSEF, R., JORDAN, F., GREER, I., NORMAN, J. & NELSON, S. 2009. Term labor is associated with a core inflammatory response in human fetal membranes, myometrium, and cervix. *American Journal of Obstetrics and Gynecology,* 200**,** 104.e1-104.e11.

BRANT, K. & CARUSO, R. L. 2005. Late-gestation rat myometrial cells express multiple isoforms of phospholipase A2 that mediate PCB 50-induced release of arachidonic acid with coincident prostaglandin production. *Toxicological Sciences,* 88**,** 222-30.

BURGESS, A., VIGNERON, S., BRIOUDES, E., LABBE, J. C., LORCA, T. & CASTRO, A. 2010. Loss of human Greatwall results in G2 arrest and multiple mitotic defects due to deregulation of the cyclin B-Cdc2/PP2A balance. *Proceedings of the National Academy of Sciences of the United States of America,* 107**,** 12564-9.

CAMPBELL, K. J. & PERKINS, N. D. 2004. Post-translational modification of RelA(p65) NF-kappaB. *Biochemical Society Transactions,* 32**,** 1087-9.

CAO, G., PEI, W., GE, H., LIANG, Q., LUO, Y., SHARP, F. R., LU, A., RAN, R., GRAHAM, S. H. & CHEN, J. 2002. In Vivo Delivery of a Bcl-xL Fusion Protein Containing the TAT Protein Transduction Domain Protects against Ischemic Brain Injury and Neuronal Apoptosis. *The Journal of Neurosciences,* 22**,** 5423-31.

CAPECE, A., VASIEVA, O., MEHER, S., ALFIREVIC, Z. & ALFIREVIC, A. 2014. Pathway Analysis of Genetic Factors Associated with Spontaneous Preterm Birth and Pre-Labor Preterm Rupture of Membranes. *Public Library of Sciences One,* 9**,** e108578.

CAPPELLETTI, M., DELLA BELLA, S., FERRAZZI, E., MAVILIO, D. & DIVANOVIC, S. 2015. Inflammation and preterm birth. *Journal of Leukocyte Biology*. 99(1):67-78

CARPENTER, A. E., JONES, T. R., LAMPRECHT, M. R., CLARKE, C., KANG, I. H., FRIMAN, O., GUERTIN, D. A., CHANG, J. H., LINDQUIST, R. A., MOFFAT, J., GOLLAND, P. & SABATINI, D. M. 2006. CellProfiler: image analysis software for identifying and quantifying cell phenotypes. *Genome Biology,* 7**,** R100.

CASEY, M. L. & MACDONALD, P. C. 1996. Interstitial collagen synthesis and processing in human amnion: a property of the mesenchymal cells. *Biology of Reproduction,* 55**,** 1253-60.

CASSELL G, H. J., ANDREWS W, CUTTER G, GOLDENBERG R 1993. Chorioamnion colonization: correlation with gestational age in women delivered following spontaneous labor versus indicated delivery. *American Journal of Obstetrics and Gynecology,* 168, 412-16.

CHALLIS, J. R. G., MATTHEWS, S. G., GIBB, W. & LYE, S. J. 2000. Endocrine and paracrine regulation of birth at term and preterm. *Endocrine Reviews,* 21**,** 514-50.

CHAN, Y. W., VAN DEN BERG, H. A., MOORE, J. D., QUENBY, S. & BLANKS, A. M. 2014. Assessment of myometrial transcriptome changes associated with spontaneous human labour by high-throughput RNA-seq. *Experimental Physiology,* 99**,** 510-24.

CHAPMAN, N. R., EUROPE-FINNER, G. N. & ROBSON, S. C. 2004. Expression and deoxyribonucleic acid-binding activity of the nuclear factor kappaB family in the human myometrium during pregnancy and labor. *Journal of Clinical Endocrinology Metabolism,* 89**,** 5683-93.

CHAPMAN, N. R., SMYRNIAS, I., ANUMBA, D. O., EUROPE-FINNER, G. N. & ROBSON, S. C. 2005. Expression of the GTP-binding protein (Galphas) is repressed by the nuclear factor kappaB RelA subunit in human myometrium. *Endocrinology,* 146**,** 4994-5002.

CHEN, L., FISCHLE, W., VERDIN, E. & GREENE, W. C. 2001. Duration of nuclear NF-kappaB action regulated by reversible acetylation. *Science,* 293**,** 1653-7.

CHEN, Z., HAGLER, J., PALOMBELLA, V. J., MELANDRI, F., SCHERER, D., BALLARD, D. & MANIATIS, T. 1995. Signal-induced site-specific phosphorylation targets I kappa B alpha to the ubiquitin-proteasome pathway. *Genes and Development,* 9**,** 1586-97.

CHOI, M., ROLLE, S., WELLNER, M., CARDOSO, M. C., SCHEIDEREIT, C., LUFT, F. C. & KETTRITZ, R. 2003. Inhibition of NF-κB by a TAT-NEMO–binding domain peptide accelerates constitutive apoptosis and abrogates LPS-delayed neutrophil apoptosis. *Blood,* 102**,** 2259-2267.

CHOI, S. J., OH, S., KIM, J. H. & ROH, C. R. 2007. Changes of nuclear factor kappa B (NF-kappaB), cyclooxygenase-2 (COX-2) and matrix metalloproteinase-9 (MMP-9) in human myometrium before and during term labor. *European Journal of Obstetrics and Gynecololgy Reproductive Biology,* 132**,** 182-8.

CHOW, L. & LYE, S. J. 1994. Expression of the gap junction protein connexin-43 is increased in the human myometrium toward term and with the onset of labor. *American Journal of Obstetrics and Gynecology,* 170**,** 788-95.

CHRISTIAENS, B., GROOTEN, J., REUSENS, M., JOLIOT, A., GOETHALS, M., VANDEKERCKHOVE, J., PROCHIANTZ, A. & ROSSENEU, M. 2004. Membrane interaction and cellular internalization of penetratin peptides. *European Journal of Biochemistry,* 271**,** 1187-1197.

CLEAL, K., HE, L., WATSON, P. D. & JONES, A. T. 2013. Endocytosis, intracellular traffic and fate of cell penetrating peptide based conjugates and nanoparticles. *Current Pharmaceutical Design,* 19**,** 2878-94.

COK, S. J. & MORRISON, A. R. 2001. The 3'-untranslated region of murine cyclooxygenase-2 contains multiple regulatory elements that alter message stability and translational efficiency. *The Journal of Biological Chemistry,* 276**,** 23179-85.

CONDON, J. C., JEYASURIA, P., FAUST, J. M. & MENDELSON, C. R. 2004. Surfactant protein secreted by the maturing mouse fetal lung acts as a hormone that signals the initiation of parturition. *Proceedings of the National Academy of Sciences of the United States of America,* 101**,** 4978-83.

CONSOLE, S., MARTY, C., GARCIA-ECHEVERRIA, C., SCHWENDENER, R. & BALLMER-HOFER, K. 2003. Antennapedia and HIV transactivator of transcription (TAT) "protein transduction domains" promote endocytosis of high molecular weight cargo upon binding to cell surface glycosaminoglycans. *The Journal of Biological Chemistry,* 278**,** 35109-14.

COOK, J. L., ZARAGOZA, D. B., SUNG, D. H. & OLSON, D. M. 2000. Expression of myometrial activation and stimulation genes in a mouse model of preterm labor: myometrial activation, stimulation, and preterm labor. *Endocrinology,* 141**,** 1718-28.

COOKSON, V. J. & CHAPMAN, N. R. 2010. NF-kappaB function in the human myometrium during pregnancy and parturition. *Histology Histopathology,* 25**,** 945-56.

COSTELOE, K. L., HENNESSY, E. M., HAIDER, S., STACEY, F., MARLOW, N. & DRAPER, E. S. 2012. Short term outcomes after extreme preterm birth in England: comparison of two birth cohorts in 1995 and 2006 (the EPICure studies). *British Medical Journal*, 345, e7976

CSAPO, A. I. & WIEST, W. G. 1969. An examination of the quantitative relationship between progesterone and the maintenance of pregnancy. *Endocrinology,* 85**,** 735-46.

CUNNINGHAM, F. G., MORRIS, G. B. & MICKAL, A. 1973. Acute Pyelonephritis of Pregnancy: A Clinical Review. *Obstetrics and Gynecology,* 42**,** 112-117.

CURETON, N., CELLESI, F., APLIN, J. & HARRIS, L. 2013. Homing peptide-mediated targeting of liposomes to term villous explants: novel nanocarriers for targeted drug delivery. *Placenta,* 34**,** A37.

DAI, S., HIRAYAMA, T., ABBAS, S. & ABU-AMER, Y. 2004. The IκB Kinase (IKK) Inhibitor, NEMO-binding Domain Peptide, Blocks Osteoclastogenesis and Bone Erosion in Inflammatory Arthritis. *Journal of Biological Chemistry,* 279**,** 37219-37222.

DAVIES, C. & TOURNIER, C. 2012. Exploring the function of the JNK (c-Jun N-terminal kinase) signalling pathway in physiological and pathological processes to design novel therapeutic strategies. *Biochemical Society Transactions,* 40**,** 85-9.

DE HEUS, R., MOL, B. W., ERWICH, J. J., VAN GEIJN, H. P., GYSELAERS, W. J., HANSSENS, M., HARMARK, L., VAN HOLSBEKE, C. D., DUVEKOT, J. J., SCHOBBEN, F. F., WOLF, H. & VISSER, G. H. 2009. Adverse drug reactions to tocolytic treatment for preterm labour: prospective cohort study. *British Medical Journal,* 338**,** b744.

DE SILVA, D., MITCHELL, M. D. & KEELAN, J. A. 2010. Inhibition of choriodecidual cytokine production and inflammatory gene expression by selective I-kappaB kinase (IKK) inhibitors. *British Journal of Pharmacology,* 160**,** 1808-22.

DEROSSI, D., CHASSAING, G. & PROCHIANTZ, A. 1998. Trojan peptides: the penetratin system for intracellular delivery. *Trends in Cell Biology,* 8**,** 84-7.

DEROSSI, D., JOLIOT, A. H., CHASSAING, G. & PROCHIANTZ, A. 1994. The third helix of the Antennapedia homeodomain translocates through biological membranes.*The Journal of Biological Chemistry,* 269**,** 10444-50.

DEVI, Y. S., DEVINE, M., DEKUIPER, J., FERGUSON, S. & FAZLEABAS, A. T. 2015. Inhibition of IL-6 Signaling Pathway by Curcumin in Uterine Decidual Cells. *Public Library of Science One,* 10**,** e0125627.

DI FERDINANDO, A., PATACCHIOLA, F., PERILLI, M. G., AMICOSANTE, G. & CARTA, G. 2010. Expression of matrix metalloproteinase-9 (MMP-9) in human midpregnancy amniotic fluid and risk of preterm labor. *Clinical and Experimental Obstetrics and Gynecology,* 37**,** 193-6.

DIGIULIO, D. B., CALLAHAN, B. J., MCMURDIE, P. J., COSTELLO, E. K., LYELL, D. J., ROBACZEWSKA, A., SUN, C. L., GOLTSMAN, D. S. A., WONG, R. J., SHAW, G., STEVENSON, D. K., HOLMES, S. P. & RELMAN, D. A. 2015. Temporal and spatial variation of the human microbiota during pregnancy. *Proceedings of the National Academy of Sciences of the United States of America,* 112**,** 11060-11065.

DORET, M., MELLIER, G., BENCHAIB, M., PIACENZA, J. M., GHARIB, C. & PASQUIER, J. C. 2002. In vitro study of tocolytic effect of rofecoxib, a specific cyclo-oxygenase 2 inhibitor. Comparison and

combination with other tocolytic agents. *British Journal of Obstetrics and Gynaecology,* 109**,** 983-8.

EIDEM, H. R., ACKERMAN, W. E., MCGARY, K. L., ABBOT, P. & ROKAS, A. 2015. Gestational tissue transcriptomics in term and preterm human pregnancies: a systematic review and meta-analysis. *BioMed Central Medical Genomics,* 8**,** 27.

ELLIOTT, C. L., ALLPORT, V. C., LOUDON, J. A., WU, G. D. & BENNETT, P. R. 2001. Nuclear factor-kappa B is essential for up-regulation of interleukin-8 expression in human amnion and cervical epithelial cells. *Molecular Human Reproduction,* 7**,** 787-90.

ELOVITZ, M. A., BARON, J. & PHILLIPPE, M. 2001. The role of thrombin in preterm parturition. *American Journal of Obstetrics and Gynecology,* 185**,** 1059-63.

ENDOH, T. & OHTSUKI, T. 2009. Cellular siRNA delivery using cell-penetrating peptides modified for endosomal escape. *Advanced Drug Delivery Reviews,* 61**,** 704-709.

EUROPE-FINNER, G. N., PHANEUF, S., TOLKOVSKY, A. M., WATSON, S. P. & LOPEZ BERNAL, A. 1994. Down-regulation of G alpha s in human myometrium in term and preterm labor: a mechanism for parturition. *Journal of Clinical Endocrinology and Metabolism,* 79**,** 1835-9.

EUROPE-FINNER, G. N., PHANEUF, S., WATSON, S. P. & LOPEZ BERNAL, A. 1993. Identification and expression of G-proteins in human myometrium: up-regulation of G alpha s in pregnancy. *Endocrinology,* 132**,** 2484-90.

FERNER, R. E., DEAR, J. W. & BATEMAN, D. N. 2011. Management of paracetamol poisoning. *British Medical Journal,* 342**,** d2218.

FISCHER, P. M., ZHELEV, N. Z., WANG, S., MELVILLE, J. E., FÅHRAEUS, R. & LANE, D. P. 2000. Structure–activity relationship of truncated and substituted analogues of the intracellular delivery vector Penetratin. *The Journal of Peptide Research,* 55**,** 163-172.

FISCHER, R., WAIZENEGGER, T., KÖHLER, K. & BROCK, R. 2002. A quantitative validation of fluorophore-labelled cell-permeable peptide conjugates: fluorophore and cargo dependence of import. *Biochemica et Biophysica Acta - Biomembranes,* 1564**,** 365-374.

FUCHS, A. R., FUCHS, F., HUSSLEIN, P., SOLOFF, M. S. & FERNSTROM, M. J. 1982. Oxytocin receptors and human parturition: a dual role for oxytocin in the initiation of labor. *Science,* 215**,** 1396-8.

FUCHS, A. R., ROMERO, R., KEEFE, D., PARRA, M., OYARZUN, E. & BEHNKE, E. 1991. Oxytocin secretion and human parturition: pulse frequency and duration increase during spontaneous labor in women. *American Journal of Obstetrics and Gynecology,* 165**,** 1515-23.

FUJIHARA, S., JAFFRAY, E., FARROW, S. N., ROSSI, A. G., HASLETT, C. & HAY, R. T. 2005. Inhibition of NF-kappa B by a cell permeable form of I kappa B alpha induces apoptosis in eosinophils. *Biochemica et Biophysica Acta Research Communications,* 326**,** 632-7.

FUTAKI, S. 2002. Arginine-rich peptides: potential for intracellular delivery of macromolecules and the mystery of the translocation mechanisms. *International Journal of Pharmacology,* 245**,** 1-7.

GARFIELD, R. E., SIMS, S. & DANIEL, E. E. 1977. Gap junctions: their presence and necessity in myometrium during parturition. *Science,* 198**,** 958-60.

GARGETT, C. E., BUCAK, K., ZAITSEVA, M., CHU, S., TAYLOR, N., FULLER, P. J. & ROGERS, P. A. W. 2002. Estrogen receptor-α and -β expression in microvascular endothelial cells and smooth muscle cells of myometrium and leiomyoma. *Molecular Human Reproduction,* 8**,** 770-775.

GAUTAM, A., SINGH, H., TYAGI, A., CHAUDHARY, K., KUMAR, R., KAPOOR, P. & RAGHAVA, G. P. 2012. CPPsite: a curated database of cell penetrating peptides. *Database (Oxford),* 2012**,** bas015.

GIBB, W. 1998. The role of prostaglandins in human parturition. *Annals of Medicine,* 30**,** 235-41.

GLOECKNER, H., JONULEIT, T. & LEMKE, H. D. 2001. Monitoring of cell viability and cell growth in a hollow-fiber bioreactor by use of the dye Alamar Blue. *Journal of Immunological Methods,* 252**,** 131-8.

GOLDENBERG, R. L., HAUTH, J. C. & ANDREWS, W. W. 2000. Intrauterine infection and preterm delivery. *New England Journal of Medicine,* 342**,** 1500-7.

GOMEZ-LOPEZ, N., ESTRADA-GUTIERREZ, G., JIMENEZ-ZAMUDIO, L., VEGA-SANCHEZ, R. & VADILLO-ORTEGA, F. 2009. Fetal membranes exhibit selective leukocyte chemotaxic activity during human labor. *Journal of Reproductive Immunology,* 80**,** 122-31.

GOMEZ-LOPEZ, N., STLOUIS, D., LEHR, M. A., SANCHEZ-RODRIGUEZ, E. N. & ARENAS-HERNANDEZ, M. 2014. Immune cells in term and preterm labor. *Cellular and Molecular Immunology,* 11**,** 571-81.

GOTSCH, F., ROMERO, R., KUSANOVIC, J. P., MAZAKI-TOVI, S., PINELES, B. L., EREZ, O., ESPINOZA, J. & HASSAN, S. S. 2007. The fetal inflammatory response syndrome. *Clinical Obstetrics and Gynecology,* 50**,** 652-83.

GRAMMATOPOULOS, D. K. 2007. The role of CRH receptors and their agonists in myometrial contractility and quiescence during pregnancy and labour. *Frontiers in Bioscience,* 12**,** 561-71.

GRAVETT, M. G., WITKIN, S. S., HALUSKA, G. J., EDWARDS, J. L., COOK, M. J. & NOVY, M. J. 1994. An experimental model for intraamniotic infection and preterm labor in rhesus monkeys. *American Journal of Obstetrics and Gynecology,* 171**,** 1660-7.

GROOM, K. M., SHENNAN, A. H., JONES, B. A., SEED, P. & BENNETT, P. R. 2005. TOCOX--a randomised, double-blind, placebo-controlled trial of rofecoxib (a COX-2-specific prostaglandin inhibitor) for the prevention of preterm delivery in women at high risk. *British Journal of Obstetrics and Gynaecology,* 112**,** 725-30.

GUPTA, S. C., SUNDARAM, C., REUTER, S. & AGGARWAL, B. B. 2010. Inhibiting NF-kappaB activation by small molecules as a therapeutic strategy. *Biochimica et Biophysica Acta,* 1799**,** 775-87.

GUZICK, D. S. & WINN, K. 1985. The association of chorioamnionitis with preterm delivery. *Obstetrics and Gynecology,* 65**,** 11-6.

GUZMAN, E. R., MELLON, C., VINTZILEOS, A. M., ANANTH, C. V., WALTERS, C. & GIPSON, K. 1998. Longitudinal assessment of endocervical canal length between 15 and 24 weeks' gestation in women at risk for pregnancy loss or preterm birth. *Obstetrics and Gynecology,* 92**,** 31-7.

HAAS, D. M., CALDWELL, D. M., KIRKPATRICK, P., MCINTOSH, J. J. & WELTON, N. J. 2012. Tocolytic therapy for preterm delivery: systematic review and network meta-analysis. *British Medical Journal,* 345**,** e6226.

HABINEZA NDIKUYEZE, G., GAURNIER-HAUSSER, A., PATEL, R., BALDWIN, A. S., MAY, M. J., FLOOD, P., KRICK, E., PROPERT, K. J. & MASON, N. J. 2014. A phase I clinical trial of systemically delivered NEMO binding domain peptide in dogs with spontaneous activated B-cell like diffuse large B-cell lymphoma. *Public Library of Science One,* 9**,** e95404.

HALLBRINK, M., OEHLKE, J., PAPSDORF, G. & BIENERT, M. 2004. Uptake of cell-penetrating peptides is dependent on peptide-to-cell ratio rather than on peptide concentration. *Biochimica et Biophysica Acta,* 1667**,** 222-8.

HAMILTON, S., OOMOMIAN, Y., STEPHEN, G., SHYNLOVA, O., TOWER, C. L., GARROD, A., LYE, S. J. & JONES, R. L. 2012. Macrophages Infiltrate the Human and Rat Decidua During Term and Preterm Labor: Evidence That Decidual Inflammation Precedes Labor. *Biology of Reproduction,* 86**,** 39, 1-9.

HAMILTON, S. A., TOWER, C. L. & JONES, R. L. 2013. Identification of Chemokines Associated with the Recruitment of Decidual Leukocytes in Human Labour: Potential Novel Targets for Preterm Labour. *Public Library of Science One,* 8**,** e56946.

HARDY, D. B., JANOWSKI, B. A., COREY, D. R. & MENDELSON, C. R. 2006. Progesterone receptor plays a major antiinflammatory role in human myometrial cells by antagonism of nuclear factor-kappaB activation of cyclooxygenase 2 expression. *Molecular Endocrinology,* 20**,** 2724-33.

HAYDEN, M. S. & GHOSH, S. 2004. Signaling to NF-kappaB. *Genes and Development,* 18**,** 2195-224.

HAYDEN, M. S. & GHOSH, S. 2012. NF-kappaB, the first quarter-century: remarkable progress and outstanding questions. *Genes and Development,* 26**,** 203-34.

HEITZ, F., MORRIS, M. C. & DIVITA, G. 2009. Twenty years of cell-penetrating peptides: from molecular mechanisms to therapeutics. *British Journal of Pharmacology,* 157**,** 195-206.

HERCE, H. D. & GARCIA, A. E. 2007. Cell Penetrating Peptides: How Do They Do It? *Journal of Biological Physics,* 33**,** 345-356.

HERVÉ, J.-C. 2012. The communicating junctions, composition, structure and characteristics. *Biochimica et Biophysica Acta (BBA) - Biomembranes,* 1818**,** 1803-1806.

HILLIER, S. L., NUGENT, R. P., ESCHENBACH, D. A., KROHN, M. A., GIBBS, R. S., MARTIN, D. H., COTCH, M. F., EDELMAN, R., PASTOREK, J. G., RAO, A. V., MCNELLIS, D., REGAN, J. A., CAREY, J. C. & KLEBANOFF, M. A. 1995. Association between Bacterial Vaginosis and Preterm Delivery of a Low-Birth-Weight Infant. *New England Journal of Medicine,* 333**,** 1737-1742.

HILLIER, S. L., WITKIN, S. S., KROHN, M. A., WATTS, D. H., KIVIAT, N. B. & ESCHENBACH, D. A. 1993. The relationship of amniotic fluid cytokines and preterm delivery, amniotic fluid infection, histologic chorioamnionitis, and chorioamnion infection. *Obstetrics and Gynecology,* 81**,** 941-8.

HIROSE, H., TAKEUCHI, T., OSAKADA, H., PUJALS, S., KATAYAMA, S., NAKASE, I., KOBAYASHI, S., HARAGUCHI, T. & FUTAKI, S. 2012. Transient focal membrane deformation induced by arginine-rich peptides leads to their direct penetration into cells. *Molecular Therapy,* 20**,** 984-993.

HIRST, J. J., PARKINGTON, H. C., YOUNG, I. R., PALLISER, H. K., PERI, K. G. & OLSON, D. M. 2005. Delay of preterm birth in sheep by THG113.31, a prostaglandin F2alpha receptor antagonist. *American Journal of Obstetrics and Gynecology,* 193**,** 256-66.

HITTI, J., RILEY, D. E., KROHN, M. A., HILLIER, S. L., AGNEW, K. J., KRIEGER, J. N. & ESCHENBACH, D. A. 1997. Broad-spectrum bacterial rDNA polymerase chain reaction assay for detecting amniotic fluid infection among women in premature labor. *Clinical Infectious Diseases,* 24**,** 1228-32.

HODEK, J.-M., VON DER SCHULENBURG, J. M. & MITTENDORF, T. 2011. Measuring economic consequences of preterm birth - Methodological recommendations for the evaluation of personal burden on children and their caregivers. *Health Economics Review,* 1**,** 6-6.

HOESEL, B. & SCHMID, J. A. 2013. The complexity of NF-kappaB signaling in inflammation and cancer. *Molecular Cancer,* 12**,** 86.

HOWEY CP, K. M., LAWN JE 2012. *Born Too Soon. The Global Action Report on Preterm Birth.,* Geneva, March of Dimes.

INAGAKI, K., HAHN, H. S., DORN, G. W., 2ND & MOCHLY-ROSEN, D. 2003. Additive protection of the ischemic heart ex vivo by combined treatment with delta-protein kinase C inhibitor and epsilon-protein kinase C activator. *Circulation,* 108**,** 869-75.

IRELAND, D. J., KEMP, M. W., MIURA, Y., SAITO, M., NEWNHAM, J. P. & KEELAN, J. A. 2015. Intra-amniotic pharmacological blockade of inflammatory signalling pathways in an ovine chorioamnionitis model. *Molecular Human Reproduction,* 21**,** 479-489.

JIAO, C.-Y., DELAROCHE, D., BURLINA, F., ALVES, I. D., CHASSAING, G. & SAGAN, S. 2009. Translocation and Endocytosis for Cell-penetrating Peptide Internalization. *The Journal of Biological Chemistry,* 284**,** 33957-33965.

JOHNSON, R. M., HARRISON, S. D. & MACLEAN, D. 2011. Therapeutic applications of cell-penetrating peptides. *Methods in Molecular Biology,* 683**,** 535-51.

JONES, A. T. & SAYERS, E. J. 2012. Cell entry of cell penetrating peptides: tales of tails wagging dogs. *Journal of Controlled Release,* 161**,** 582-91.

JONES, S. W., CHRISTISON, R., BUNDELL, K., VOYCE, C. J., BROCKBANK, S. M. V., NEWHAM, P. & LINDSAY, M. A. 2005. Characterisation of cell-penetrating peptide-mediated peptide delivery. *British Journal of Pharmacology,* 145**,** 1093-1102.

KAROLCZAK-BAYATTI, M., SWEENEY, M., CHENG, J., EDEY, L., ROBSON, S. C., ULRICH, S. M., TREUMANN, A., TAGGART, M. J. & EUROPE-FINNER, G. N. 2011. Acetylation of heat shock protein 20 (Hsp20) regulates human myometrial activity. *The Journal of Biological Chemistry,* 286**,** 34346-55.

KEELAN, J. A., BLUMENSTEIN, M., HELLIWELL, R. J., SATO, T. A., MARVIN, K. W. & MITCHELL, M. D. 2003. Cytokines, prostaglandins and parturition--a review. *Placenta,* 24 Suppl A**,** S33-46.

KEELAN, J. A., KHAN, S., YOSAATMADJA, F. & MITCHELL, M. D. 2009. Prevention of inflammatory activation of human gestational membranes in an ex vivo model using a pharmacological NF-kappaB inhibitor. *The Journal of Immunology,* 183**,** 5270-8.

KESKI-NISULA, L. T., AALTO, M.-L., KIRKINEN, P. P., KOSMA, V.-M. & HEINONEN, S. T. 2003. Myometrial Inflammation in Human Delivery and Its Association With Labor and Infection. *American Journal of Clinical Pathology,* 120**,** 217-224.

KHAJA, K. R., P 2010. Comparison of Functional Protein Transduction Domains Using the NEMO Binding Domain Peptide. *Pharmaceuticals,* 3**,** 110-124.

KHAMMANIT, R., CHANTAKRU, S., KITIYANANT, Y. & SAIKHUN, J. 2008. Effect of serum starvation and chemical inhibitors on cell cycle synchronization of canine dermal fibroblasts. *Theriogenology,* 70**,** 27-34.

KHANJANI, S., KANDOLA, M. K., LINDSTROM, T. M., SOORANNA, S. R., MELCHIONDA, M., LEE, Y. S., TERZIDOU, V., JOHNSON, M. R. & BENNETT, P. R. 2011. NF-kappaB regulates a cassette of immune/inflammatory genes in human pregnant myometrium at term. *Journal of Cellular and Molecular Medicine,* 15**,** 809-24.

KIMURA, T., TANIZAWA, O., MORI, K., BROWNSTEIN, M. J. & OKAYAMA, H. 1992. Structure and expression of a human oxytocin receptor. *Nature,* 356**,** 526-9.

KING, J., FLENADY, V., COLE, S. & THORNTON, S. 2005. Cyclo-oxygenase (COX) inhibitors for treating preterm labour. *Cochrane Database Systematic Reviews***,** CD001992.

KING, J. F., FLENADY, V. J., PAPATSONIS, D. N., DEKKER, G. A. & CARBONNE, B. 2003. Calcium channel blockers for inhibiting preterm labour. *Cochrane Database Systematic Reviews***,** CD002255.

KISHORE, N., SOMMERS, C., MATHIALAGAN, S., GUZOVA, J., YAO, M., HAUSER, S., HUYNH, K., BONAR, S., MIELKE, C., ALBEE, L., WEIER, R., GRANETO, M., HANAU, C., PERRY, T. & TRIPP, C. S. 2003. A selective IKK-2 inhibitor blocks NF-kappa B-dependent gene expression in interleukin-1 beta-stimulated synovial fibroblasts. *The Journal of Biological Chemistry,* 278**,** 32861-71.

KISS-TOTH, E., BAGSTAFF, S. M., SUNG, H. Y., JOZSA, V., DEMPSEY, C., CAUNT, J. C., OXLEY, K. M., WYLLIE, D. H., POLGAR, T., HARTE, M., O'NEILL L, A., QWARNSTROM, E. E. & DOWER, S. K. 2004. Human tribbles, a protein family controlling mitogen-activated protein kinase cascades. *The Journal of Biological Chemistry,* 279**,** 42703-8.

KNISS, D. A., ROVIN, B., FERTEL, R. H. & ZIMMERMAN, P. D. 2001. Blockade NF-kappaB activation prohibits TNF-alpha-induced cyclooxygenase-2 gene expression in ED27 trophoblast-like cells. *Placenta,* 22**,** 80-9.

KRISTENSEN, M., FRANZYK, H., KLAUSEN, M. T., IVERSEN, A., BAHNSEN, J. S., SKYGGEBJERG, R. B., FODERA, V. & NIELSEN, H. M. 2015. Penetratin-Mediated Transepithelial Insulin Permeation: Importance of Cationic Residues and pH for Complexation and Permeation. *American Association ofPhysiological Scientists Journal,* 17**,** 1200-9.

KUIPERS, R., IZHAR, Z., GERRITS, P. O., MINER, W. & HOLSTEGE, G. 2004. Location of bladder and urethral sphincter motoneurons in the male guinea pig (Cavia porcellus). *Neuroscience Letters,* 362**,** 57-60.

LAPPAS, M. 2013. Forkhead box O1 (FOXO1) in pregnant human myometrial cells: a role as a pro-inflammatory mediator in human parturition. *Journal of Reproductive Immunology,* 99**,** 24-32.

LAPPAS, M., PERMEZEL, M., GEORGIOU, H. M. & RICE, G. E. 2002. Nuclear factor kappa B regulation of proinflammatory cytokines in human gestational tissues in vitro. *Biology of Reproduction,* 67**,** 668-73.

LAPPAS, M., PERMEZEL, M. & RICE, G. E. 2003. N-Acetyl-cysteine inhibits phospholipid metabolism, proinflammatory cytokine release, protease activity, and nuclear factor-kappaB deoxyribonucleic acid-binding activity in human fetal membranes in vitro. *Journal of Clinical Endocrinology and Metabolism,* 88**,** 1723-9.

LAPPAS, M., PERMEZEL, M. & RICE, G. E. 2007. Mitogen-activated protein kinase proteins regulate LPS-stimulated release of pro-inflammatory cytokines and prostaglandins from human gestational tissues. *Placenta,* 28**,** 936-45.

LAWRENCE, T. 2009. The Nuclear Factor NF-κB Pathway in Inflammation. *Cold Spring Harbor Perspectives in Biology,* 1**,** a001651.

LIM, R., BARKER, G., WALL, C. A. & LAPPAS, M. 2013. Dietary phytophenols curcumin, naringenin and apigenin reduce infection-induced inflammatory and contractile pathways in human placenta, foetal membranes and myometrium. *Molecular Human Reproduction,* 19**,** 451-62.

LIN, R., BEAUPARLANT, P., MAKRIS, C., MELOCHE, S. & HISCOTT, J. 1996. Phosphorylation of IkappaBalpha in the C-terminal PEST domain by casein kinase II affects intrinsic protein stability. *Molecular and Cellular Biology,* 16**,** 1401-1409.

LIN, Y. Z., YAO, S. Y., VEACH, R. A., TORGERSON, T. R. & HAWIGER, J. 1995. Inhibition of nuclear translocation of transcription factor NF-kappa B by a synthetic peptide containing a cell membrane-permeable motif and nuclear localization sequence. *The Journal of Biological Chemistry,* 270**,** 14255-8.

LINDSTROM, T. M. & BENNETT, P. R. 2005. The role of nuclear factor kappa B in human labour. *Reproduction,* 130**,** 569-81.

LOPES, L. B., FLYNN, C., KOMALAVILAS, P., PANITCH, A., BROPHY, C. M. & SEAL, B. L. 2009. Inhibition of HSP27 phosphorylation by a cell-permeant MAPKAP Kinase 2 inhibitor. *Biochemica et Biophysica Acta Research Communications,* 382**,** 535-9.

LOUDON, J. A., GROOM, K. M. & BENNETT, P. R. 2003. Prostaglandin inhibitors in preterm labour. *Best Practice and Research in Clinical Obstetrics and Gynaecology,* 17**,** 731-44.

LYE, S. J., NICHOLSON, B. J., MASCARENHAS, M., MACKENZIE, L. & PETROCELLI, T. 1993. Increased expression of connexin-43 in the rat myometrium during labor is associated with an increase in the plasma estrogen:progesterone ratio. *Endocrinology,* 132**,** 2380-6.

M KIDDER, G. & WINTERHAGER, E. 2015. Physiological roles of connexins in labour and lactation. *Reproduction,* 150**,** R129-R136.

MACINTYRE, D. A., LEE, Y. S., MIGALE, R., HERBERT, B. R., WADDINGTON, S. N., PEEBLES, D., HAGBERG, H., JOHNSON, M. R. & BENNETT, P. R. 2014. Activator protein 1 is a key terminal mediator of inflammation-induced preterm labor in mice. *The Federation of American Scientists for Experimental Biology Journal,* 28**,** 2358-68.

MADANI, F., LINDBERG, S., LANGEL, U., FUTAKI, S. & GRASLUND, A. 2011. Mechanisms of cellular uptake of cell-penetrating peptides. *Biophysical Journal,* 2011**,** 414729.

MANCEUR, A. & AUDET, J. 2009. Measurement of Cell-Penetrating Peptide-Mediated Transduction of Adult Hematopoietic Stem Cells. *Methods of Molecular Biology,482,43-54.*

MANCEUR, A., WU, A. & AUDET, J. 2007. Flow cytometric screening of cell-penetrating peptides for their uptake into embryonic and adult stem cells. *Analytical Biochemistry,* 364**,** 51-9.

MANDERY, K., GLAESER, H. & FROMM, M. F. 2012. Interaction of innovative small molecule drugs used for cancer therapy with drug transporters. *British Journal of Pharmacology,* 165**,** 345-62.

MARKOVIC, D., VATISH, M., GU, M., SLATER, D., NEWTON, R., LEHNERT, H. & GRAMMATOPOULOS, D. K. 2007. The onset of labor alters corticotropin-releasing hormone type 1 receptor variant

expression in human myometrium: putative role of interleukin-1beta. *Endocrinology,* 148**,** 3205-13.

MATSUZAKI, K., YONEYAMA, S., MURASE, O. & MIYAJIMA, K. 1996. Transbilayer transport of ions and lipids coupled with mastoparan X translocation. *Biochemistry,* 35**,** 8450-6.

MAY, M. J., D'ACQUISTO, F., MADGE, L. A., GLOCKNER, J., POBER, J. S. & GHOSH, S. 2000. Selective inhibition of NF-kappaB activation by a peptide that blocks the interaction of NEMO with the IkappaB kinase complex. *Science,* 289**,** 1550-4.

MAY, M. J., MARIENFELD, R. B. & GHOSH, S. 2002. Characterization of the Ikappa B-kinase NEMO binding domain. *The Journal of Biological Chemistry,* 277**,** 45992-6000.

MCCORKELL, K. A. & MAY, M. J. 2015. NEMO-binding domain peptide inhibition of inflammatory signal-induced NF-kappaB activation in vivo. *Methods in Molecular Biology,* 1280**,** 505-25.

MCLEAN, M., BISITS, A., DAVIES, J., WOODS, R., LOWRY, P. & SMITH, R. 1995. A placental clock controlling the length of human pregnancy. *Nature Medicine,* 1**,** 460-3.

MEADE, A. J., MELONI, B. P., CROSS, J., BAKKER, A. J., FEAR, M. W., MASTAGLIA, F. L., WATT, P. M. & KNUCKEY, N. W. 2010. AP-1 inhibitory peptides are neuroprotective following acute glutamate excitotoxicity in primary cortical neuronal cultures. *Journal of Neurochemistry,* 112**,** 258-70.

MEADE, B. R. & DOWDY, S. F. 2007. Exogenous siRNA delivery using peptide transduction domains/cell penetrating peptides. *Advanced Drug Delivery Reviews,* 59**,** 134-40.

MENENDEZ, C., ORDI, J., ISMAIL, M. R., VENTURA, P. J., APONTE, J. J., KAHIGWA, E., FONT, F. & ALONSO, P. L. 2000. The Impact of Placental Malaria on Gestational Age and Birth Weight. *Journal of Infectious Diseases,* 181**,** 1740-1745.

MITCHELL, B. F. & WONG, S. 1993. Changes in 17 beta,20 alpha-hydroxysteroid dehydrogenase activity supporting an increase in the estrogen/progesterone ratio of human fetal membranes at parturition. *American Journal of Obstetrics and Gynecology,* 168**,** 1377-85.

MITCHELL, M. D., ROMERO, R. J., EDWIN, S. S. & TRAUTMAN, M. S. 1995. Prostaglandins and parturition. *Reproduction, Fertility and Development,* 7**,** 623-32.

MITTAL, P., ROMERO, R., TARCA, A. L., GONZALEZ, J., DRAGHICI, S., XU, Y., DONG, Z., NHAN-CHANG, C.-L., CHAIWORAPONGSA, T., LYE, S., KUSANOVIC, J. P., LIPOVICH, L., MAZAKI-TOVI, S., HASSAN, S. S., MESIANO, S. & KIM, C. J. 2010. Characterization of the myometrial transcriptome and biological pathways of spontaneous human labor at term. *Journal of Perinatal Medicine,* 38**,** 617-643.

MIZGERD, J. P., SCOTT, M. L., SPIEKER, M. R. & DOERSCHUK, C. M. 2002. Functions of IkappaB proteins in inflammatory responses to Escherichia coli LPS in mouse lungs. *American Journal of Respiratory Cell Molecular Biology,* 27**,** 575-82.

MOGAMI, H., KELLER, P. W., SHI, H. & WORD, R. A. 2014. Effect of thrombin on human amnion mesenchymal cells, mouse fetal membranes, and preterm birth. *The Journal of Biological Chemistry,* 289**,** 13295-307.

MOHAN, A. R., SOORANNA, S. R., LINDSTROM, T. M., JOHNSON, M. R. & BENNETT, P. R. 2007. The effect of mechanical stretch on cyclooxygenase type 2 expression and activator protein-1 and nuclear factor-kappaB activity in human amnion cells. *Endocrinology,* 148**,** 1850-7.

MORISAKI, N., TOGOOBAATAR, G., VOGEL, J. P., SOUZA, J. P., ROWLAND HOGUE, C. J., JAYARATNE, K., OTA, E., MORI, R., ON BEHALF OF THE, W. H. O. M. S. O. M. & NEWBORN HEALTH RESEARCH, N. 2014. Risk factors for spontaneous and provider-initiated preterm delivery in high and low Human Development Index countries: a secondary analysis of the World Health Organization Multicountry Survey on Maternal and Newborn Health. *British Journal of Obstetrics and Gynaecology,* 121**,** 101-109.

MYATT, L. & SUN, K. 2010. Role of fetal membranes in signaling of fetal maturation and parturition. *International Journal of Developmental Biology,* 54**,** 545-53.

NAKASE, I., NIWA, M., TAKEUCHI, T., SONOMURA, K., KAWABATA, N., KOIKE, Y., TAKEHASHI, M., TANAKA, S., UEDA, K., SIMPSON, J. C., JONES, A. T., SUGIURA, Y. & FUTAKI, S. 2004. Cellular Uptake of Arginine-Rich Peptides: Roles for Macropinocytosis and Actin Rearrangement. *Molecular Therapy,* 10**,** 1011-1022.

NEILSON, J. P., WEST, H. M. & DOWSWELL, T. 2014. Betamimetics for inhibiting preterm labour. *Cochrane Database Systematic Reviews,* 2**,** CD004352.

NG, P. Y., IRELAND, D. J. & KEELAN, J. A. 2015. Drugs to block cytokine signaling for the prevention and treatment of inflammation induced preterm birth. *Frontiers in Immunology,* 6.

NORMAN, J. E. & CAMERON, I. T. 1996. Nitric oxide in the human uterus. *Reviews of Reproduction,* 1**,** 61-8.

OFFICE OF NATIONAL STATISTICS, U. (2014). *Gestation Specific Infant Mortality,2012* [Online]. Available: http://www.ons.gov.uk/ons/rel/child-health/gestation-specific-infant-mortality-in-england-and-wales/2012/index.html

OKA, S., KAMATA, H., KAMATA, K., YAGISAWA, H. & HIRATA, H. 2000. N-acetylcysteine suppresses TNF-induced NF-kappaB activation through inhibition of IkappaB kinases. *Federation of European Biochemical Societies Letters,* 472**,** 196-202.

OLSON, D. M. 2005. The promise of prostaglandins: have they fulfilled their potential as therapeutic targets for the delay of preterm birth? *Journal of the Society for Gynecologic Investigation,* 12**,** 466-78.

OLSON, D. M., CHRISTIAENS, I., GRACIE, S., YAMAMOTO, Y. & MITCHELL, B. F. 2008. Emerging tocolytics: challenges in designing and testing drugs to delay preterm delivery and prolong pregnancy. *Expert Opinion on Emerging Drugs,* 13**,** 695-707.

ORANGE, J. S. & MAY, M. J. 2008. Cell penetrating peptide inhibitors of nuclear factor-kappa B. *Cellular and Molecular Life Sciences,* 65**,** 3564-91.

OSMAN, I., YOUNG, A., LEDINGHAM, M., THOMSON, A., JORDAN, F., GREER, I. & NORMAN, J. 2003. Leukocyte density and pro-inflammatory cytokine expression in human fetal membranes, decidua, cervix and myometrium before and during labour at term. *Molecular Human Reproduction,* 9**,** 41 - 45.

OSMERS, R. G., ADELMANN-GRILL, B. C., RATH, W., STUHLSATZ, H. W., TSCHESCHE, H. & KUHN, W. 1995. Biochemical events in cervical ripening dilatation during pregnancy and parturition. *Journal of Obstetrics and Gynaecology,* 21**,** 185-94.

PAL, R., MAMIDI, M. K., DAS, A. K. & BHONDE, R. 2012. Diverse effects of dimethyl sulfoxide (DMSO) on the differentiation potential of human embryonic stem cells. *Archives of Toxicology,* 86**,** 651-61.

PAPATSONIS, D., FLENADY, V., COLE, S. & LILEY, H. 2005. Oxytocin receptor antagonists for inhibiting preterm labour. *Cochrane Database Systematic Reviews***,** CD004452.

PARFENOVA, H., BALABANOVA, L. & LEFFLER, C. W. 1998. Posttranslational regulation of cyclooxygenase by tyrosine phosphorylation in cerebral endothelial cells. *American Journal of Physiology,* 274**,** C72-81.

PERKINS, N. D. 2007. Integrating cell-signalling pathways with NF-kappaB and IKK function. *Nature Reviews Molecular Cell Biology,* 8**,** 49-62.

PIRIANOV, G., WADDINGTON, S. N., LINDSTROM, T. M., TERZIDOU, V., MEHMET, H. & BENNETT, P. R. 2009. The cyclopentenone 15-deoxy-delta 12,14-prostaglandin J(2) delays lipopolysaccharide-induced preterm delivery and reduces mortality in the newborn mouse. *Endocrinology,* 150**,** 699-706.

RAMANA, C. V., CHATTERJEE-KISHORE, M., NGUYEN, H. & STARK, G. R. 2000. Complex roles of Stat1 in regulating gene expression. *Oncogene,* 19**,** 2619-27.

REAY, D. P., YANG, M., WATCHKO, J. F., DAOOD, M., O'DAY, T. L., REHMAN, K. K., GUTTRIDGE, D. C., ROBBINS, P. D. & CLEMENS, P. R. 2011. Systemic delivery of NEMO binding domain/IKKgamma inhibitory peptide to young mdx mice improves dystrophic skeletal muscle histopathology. *Neurobiology of Disease,* 43**,** 598-608.

REISSMANN, S. 2014. Cell penetration: scope and limitations by the application of cell-penetrating peptides. *Journal of Peptide Science,* 20**,** 760-784.

RENTHAL, N. E., CHEN, C. C., WILLIAMS, K. C., GERARD, R. D., PRANGE-KIEL, J. & MENDELSON, C. R. 2010. miR-200 family and targets, ZEB1 and ZEB2, modulate uterine quiescence and contractility during pregnancy and labor. *Proceedings of the National Academy of Sciences of the United States of America,* 107**,** 20828-33.

RICHARD, J. P., MELIKOV, K., BROOKS, H., PREVOT, P., LEBLEU, B. & CHERNOMORDIK, L. V. 2005. Cellular uptake of unconjugated TAT peptide involves clathrin-dependent endocytosis and heparan sulfate receptors. *The Journal of Biological Chemistry,* 280**,** 15300-6.

RICHARD, J. P., MELIKOV, K., VIVES, E., RAMOS, C., VERBEURE, B., GAIT, M. J., CHERNOMORDIK, L. V. & LEBLEU, B. 2003. Cell-penetrating peptides. A reevaluation of the mechanism of cellular uptake. *The Journal of Biological Chemistry,* 278**,** 585-90.

RINALDI, S. F., CATALANO, R. D., WADE, J., ROSSI, A. G. & NORMAN, J. E. 2014. Decidual Neutrophil Infiltration Is Not Required for Preterm Birth in a Mouse Model of Infection-Induced Preterm Labor. *The Journal of Immunology,* 192**,** 2315-2325.

RINALDI, S. F., ROSSI, A. G., SAUNDERS, P. T. & NORMAN, J. E. 2015. Immune cells and preterm labour: do invariant NKT cells hold the key? *Molecular Human Reproduction,* 21**,** 309-12.

ROGERS, L. K. & VELTEN, M. 2011. Maternal inflammation, growth retardation, and preterm birth: insights into adult cardiovascular disease. *Life Sciences,* 89**,** 417-21.

ROH, C., OH, W., YOON, B. & LEE, J. 2000. Up-regulation of matrix metalloproteinase-9 in human myometrium during labour: a cytokine-mediated process in uterine smooth muscle cells. *Molecular Human Reproduction,* 6**,** 96 - 102.

ROMERO, R., ESPINOZA, J., GONCALVES, L. F., KUSANOVIC, J. P., FRIEL, L. & HASSAN, S. 2007. The role of inflammation and infection in preterm birth. *Seminars in Reproductive Medicine,* 25**,** 21-39.

ROMERO, R., ESPINOZA, J., GONCALVES, L. F., KUSANOVIC, J. P., FRIEL, L. A. & NIEN, J. K. 2006a. Inflammation in preterm and term labour and delivery. *Seminars in Fetal and Neonatal Medicine,* 11**,** 317-26.

ROMERO, R., ESPINOZA, J., KUSANOVIC, J. P., GOTSCH, F., HASSAN, S., EREZ, O., CHAIWORAPONGSA, T. & MAZOR, M. 2006b. The preterm parturition syndrome. *British Journal of Obstetrics and Gynaecology,* 113 Suppl 3**,** 17-42.

ROMERO, R., MAZOR, M., BRANDT, F., SEPULVEDA, W., AVILA, C., COTTON, D. B. & DINARELLO, C. A. 1992. Interleukin-1 alpha and interleukin-1 beta in preterm and term human parturition. *American Journal of Reproductive Immunology,* 27**,** 117-23.

ROMERO, R., QUINTERO, R., OYARZUN, E., WU, Y. K., SABO, V., MAZOR, M. & HOBBINS, J. C. 1988. Intraamniotic infection and the onset of labor in preterm premature rupture of the membranes. *American Journal of Obstetrics and Gynecology,* 159**,** 661-6.

ROMERO, R., SIRTORI, M., OYARZUN, E., AVILA, C., MAZOR, M., CALLAHAN, R., SABO, V., ATHANASSIADIS, A. P. & HOBBINS, J. C. 1989. Infection and labor. V. Prevalence, microbiology, and clinical significance of intraamniotic infection in women with preterm labor and intact membranes. *American Journal of Obstetrics and Gynecology,* 161**,** 817-24.

ROSA, M. I., PIRES, P. D., MEDEIROS, L. R., EDELWEISS, M. I. & MARTINEZ-MESA, J. 2012. Periodontal disease treatment and risk of preterm birth: a systematic review and meta-analysis. *Cadernos de Saude Publica,* 28**,** 1823-33.

ROY, A., MONDAL, S., KORDOWER, J. H. & PAHAN, K. 2015. Attenuation of microglial RANTES by NEMO-binding domain peptide inhibits the infiltration of CD8 T cells in the nigra of hemiparkinsonian monkey. *Neuroscience*, 302:36-46

SADOWSKY, D. W., ADAMS, K. M., GRAVETT, M. G., WITKIN, S. S. & NOVY, M. J. 2006. Preterm labor is induced by intraamniotic infusions of interleukin-1beta and tumor necrosis factor-alpha but not by interleukin-6 or interleukin-8 in a nonhuman primate model. *American Journal of Obstetrics and Gynecology,* 195**,** 1578-89.

SALIM, R., GARMI, G., NACHUM, Z., ZAFRAN, N., BARAM, S. & SHALEV, E. 2012. Nifedipine compared with atosiban for treating preterm labor: a randomized controlled trial. *Obstetrics and Gynecology,* 120**,** 1323-31.

SAYERS, E. J., CLEAL, K., EISSA, N. G., WATSON, P. & JONES, A. T. 2014. Distal phenylalanine modification for enhancing cellular delivery of fluorophores, proteins and quantum dots by cell penetrating peptides. *Journal of Controlled Release,* 195**,** 55-62.

SCHLAFER, D. H., YUH, B., FOLEY, G. L., ELSSASER, T. H., SADOWSKY, D. & NATHANIELSZ, P. W. 1994. Effect of Salmonella endotoxin administered to the pregnant sheep at 133-142 days gestation on fetal oxygenation, maternal and fetal adrenocorticotropic hormone and cortisol, and maternal plasma tumor necrosis factor alpha concentrations. *Biology of Reproduction,* 50**,** 1297-302.

SCHONTHALER, H. B., GUINEA-VINIEGRA, J. & WAGNER, E. F. 2011. Targeting inflammation by modulating the Jun/AP-1 pathway. *Annals of Rheumatic Disease,* 70 Suppl 1**,** i109-12.

SCHWARZE, S. R., HO, A., VOCERO-AKBANI, A. & DOWDY, S. F. 1999. In vivo protein transduction: delivery of a biologically active protein into the mouse. *Science,* 285**,** 1569-72.

SCOTT, M. L., FUJITA, T., LIOU, H. C., NOLAN, G. P. & BALTIMORE, D. 1993. The p65 subunit of NF-kappa B regulates I kappa B by two distinct mechanisms. *Genes and Development,* 7**,** 1266-76.

SENNSTROM, M. B., EKMAN, G., WESTERGREN-THORSSON, G., MALMSTROM, A., BYSTROM, B., ENDRESEN, U., MLAMBO, N., NORMAN, M., STABI, B. & BRAUNER, A. 2000. Human cervical ripening, an inflammatory process mediated by cytokines. *Molecular Human Reproduction,* 6**,** 375-81.

SHAHIN, A. Y., HASSANIN, I. M., ISMAIL, A. M., KRUESSEL, J. S. & HIRCHENHAIN, J. 2009. Effect of oral N-acetyl cysteine on recurrent preterm labor following treatment for bacterial vaginosis. *International Journal of Gynaecololgy and Obstetrics,* 104**,** 44-8.

SHIBATA, W., MAEDA, S., HIKIBA, Y., YANAI, A., OHMAE, T., SAKAMOTO, K., NAKAGAWA, H., OGURA, K. & OMATA, M. 2007. Cutting Edge: The IκB Kinase (IKK) Inhibitor, NEMO-Binding Domain

Peptide, Blocks Inflammatory Injury in Murine Colitis. *The Journal of Immunology,* 179**,** 2681-2685.

SHOJI, T., YOSHIDA, S., MITSUNARI, M., MIYAKE, N., TSUKIHARA, S., IWABE, T., HARADA, T. & TERAKAWA, N. 2007. Involvement of p38 MAP kinase in lipopolysaccharide-induced production of pro- and anti-inflammatory cytokines and prostaglandin E(2) in human choriodecidua. *Journal of Reproductive Immunology,* 75**,** 82-90.

SHYNLOVA, O., DOROGIN, A., LI, Y. & LYE, S. 2014. Inhibition of infection-mediated preterm birth by administration of broad spectrum chemokine inhibitor in mice. *Journal of Cellular and Molecular Medicine,* 18**,** 1816-1829.

SLATER, D. M., DENNES, W. J., CAMPA, J. S., POSTON, L. & BENNETT, P. R. 1999. Expression of cyclo-oxygenase types-1 and -2 in human myometrium throughout pregnancy. *Molecular Human Reproduction,* 5**,** 880-4.

SMITH, R. 2007. Parturition. *New England Journal of Medicine,* 356**,** 271-83.

SMITH, R., SMITH, J. I., SHEN, X., ENGEL, P. J., BOWMAN, M. E., MCGRATH, S. A., BISITS, A. M., MCELDUFF, P., GILES, W. B. & SMITH, D. W. 2009. Patterns of plasma corticotropin-releasing hormone, progesterone, estradiol, and estriol change and the onset of human labor. *Journal of Clinical Endocrinology and Metabolism,* 94**,** 2066-74.

SNYDER, E. L., MEADE, B. R., SAENZ, C. C. & DOWDY, S. F. 2004. Treatment of terminal peritoneal carcinomatosis by a transducible p53-activating peptide. *Public Library of Science Biology,* 2**,** E36.

SOLOFF, M. S., COOK, D. L., JR., JENG, Y. J. & ANDERSON, G. D. 2004. In situ analysis of interleukin-1-induced transcription of cox-2 and il-8 in cultured human myometrial cells. *Endocrinology,* 145**,** 1248-54.

SOLT, L. A., MADGE, L. A., ORANGE, J. S. & MAY, M. J. 2007. Interleukin-1-induced NF-kappaB activation is NEMO-dependent but does not require IKKbeta. *The Journal of Biological Chemistry,* 282**,** 8724-33.

SONCINI, M., VERTUA, E., GIBELLI, L., ZORZI, F., DENEGRI, M., ALBERTINI, A., WENGLER, G. S. & PAROLINI, O. 2007. Isolation and characterization of mesenchymal cells from human fetal membranes. *Journal of Tissue Engineering and Regenerative Medicine,* 1**,** 296-305.

SOORANNA, S. R., LEE, Y., KIM, L. U., MOHAN, A. R., BENNETT, P. R. & JOHNSON, M. R. 2004. Mechanical stretch activates type 2 cyclooxygenase via activator protein-1 transcription factor in human myometrial cells. *Molecular Human Reproduction,* 10**,** 109-13.

STINSON, L. F., IRELAND, D. J., KEMP, M. W., PAYNE, M. S., STOCK, S. J., NEWNHAM, J. P. & KEELAN, J. A. 2014. Effects of cytokine-suppressive anti-inflammatory drugs on inflammatory activation in ex vivo human and ovine fetal membranes. *Reproduction,* 147**,** 313-20.

STRICKLAND, I. & GHOSH, S. 2006. Use of cell permeable NBD peptides for suppression of inflammation. *Annals of Rheumatic Disease,* 65 Suppl 3**,** iii75-82.

TAICHMAN, R. S. & HAUSCHKA, P. V. 1992. Effects of interleukin-1 beta and tumor necrosis factor-alpha on osteoblastic expression of osteocalcin and mineralized extracellular matrix in vitro. *Inflammation,* 16**,** 587-601.

TAKADA, Y., SINGH, S. & AGGARWAL, B. B. 2004. Identification of a p65 peptide that selectively inhibits NF-kappa B activation induced by various inflammatory stimuli and its role in down-regulation of NF-kappaB-mediated gene expression and up-regulation of apoptosis. *The Journal of Biological Chemistry,* 279**,** 15096-104.

TAS, S. W., VERVOORDELDONK, M. J., HAJJI, N., MAY, M. J., GHOSH, S. & TAK, P. P. 2006. Local treatment with the selective IκB kinase β inhibitor NEMO-binding domain peptide ameliorates synovial inflammation. *Arthritis Research and Therapy,* 8**,** R86-R86.

TENCY, I., VERSTRAELEN, H., KROES, I., HOLTAPPELS, G., VERHASSELT, B., VANEECHOUTTE, M., VERHELST, R. & TEMMERMAN, M. 2012. Imbalances between matrix metalloproteinases (MMPs) and tissue inhibitor of metalloproteinases (TIMPs) in maternal serum during preterm labor. *Public Library of Science One,* 7**,** e49042.

TERZIDOU, V., LEE, Y., LINDSTROM, T., JOHNSON, M., THORNTON, S. & BENNETT, P. R. 2006. Regulation of the human oxytocin receptor by nuclear factor-kappaB and CCAAT/enhancer-binding protein-beta. *Journal of Clinical Endocrinology and Metabolism,* 91**,** 2317-26.

TERZIDOU, V., SOORANNA, S. R., KIM, L. U., THORNTON, S., BENNETT, P. R. & JOHNSON, M. R. 2005. Mechanical stretch up-regulates the human oxytocin receptor in primary human uterine myocytes. *Journal of Clinical Endocrinology and Metabolism,* 90**,** 237-46.

THOMAKOS, N., DASKALAKIS, G., PAPAPANAGIOTOU, A., PAPANTONIOU, N., MESOGITIS, S. & ANTSAKLIS, A. 2010. Amniotic fluid interleukin-6 and tumor necrosis factor-alpha at mid-trimester genetic amniocentesis: relationship to intra-amniotic microbial invasion and preterm delivery. *European Journal of Obstetrics and Gynecology Reproductive Biology,* 148**,** 147-51.

THOMSON, A., TELFER, J., YOUNG, A., CAMPBELL, S., STEWART, C., CAMERON, I., GREER, I. & NORMAN, J. 1999. Leukocytes infiltrate the myometrium during human parturtion: further evidence that labour is an inflammatory process. *Human Reproduction,* 14**,** 229 - 236.

THORÉN, P. E. G., PERSSON, D., ISAKSON, P., GOKSÖR, M., ÖNFELT, A. & NORDÉN, B. 2003. Uptake of analogs of penetratin, Tat(48–60) and oligoarginine in live cells. *Biochemical and Biophysical Research Communications,* 307**,** 100-107.

VADILLO-ORTEGA, F. & ESTRADA-GUTIERREZ, G. 2005. Role of matrix metalloproteinases in preterm labour. *British Journal of Obstetrics and Gynaecology,* 112 Suppl 1**,** 19-22.

VAN VEEN, A. J., PELINCK, M. J., VAN PAMPUS, M. G. & ERWICH, J. J. 2005. Severe hypotension and fetal death due to tocolysis with nifedipine. *British Journal of Obstetrics and Gynaecology,* 112**,** 509-10.

VAN VLIET, E. O., SCHUIT, E., HEIDA, K. Y., OPMEER, B. C., KOK, M., GYSELAERS, W., PORATH, M. M., WOISKI, M., BAX, C. J., BLOEMENKAMP, K. W., SCHEEPERS, H. C., JAQUEMYN, Y., VAN BEEK, E., DUVEKOT, H. J., FRANSSEN, M. T., BIJVANK, B. N., KOK, J. H., FRANX, A., MOL, B. W. & OUDIJK, M. A. 2014. Nifedipine versus atosiban in the treatment of threatened preterm labour (Assessment of Perinatal Outcome after Specific Tocolysis in Early Labour: APOSTEL III-Trial). *BioMed Central Pregnancy and Childbirth,* 14**,** 93.

VARNER, M. W. & ESPLIN, M. S. 2005. Current understanding of genetic factors in preterm birth. *British Journal of Obstetrics and Gynaecology,* 112 Suppl 1**,** 28-31.

VILLAR, J., PAPAGEORGHIOU, A. T., KNIGHT, H. E., GRAVETT, M. G., IAMS, J., WALLER, S. A., KRAMER, M., CULHANE, J. F., BARROS, F. C., CONDE-AGUDELO, A., BHUTTA, Z. A. & GOLDENBERG, R. L. 2012. The preterm birth syndrome: a prototype phenotypic classification. *American Journal of Obstetrics and Gynecology,* 206**,** 119-23.

VIVES, E., BRODIN, P. & LEBLEU, B. 1997. A truncated HIV-1 Tat protein basic domain rapidly translocates through the plasma membrane and accumulates in the cell nucleus. *The Journal of Biological Chemistry,* 272**,** 16010-7.

VIVÈS, E., SCHMIDT, J. & PÈLEGRIN, A. 2008. Cell-penetrating and cell-targeting peptides in drug delivery. *Biochimica et Biophysica Acta - Reviews on Cancer,* 1786**,** 126-138.

WADIA, J. S. & DOWDY, S. F. 2005. Transmembrane delivery of protein and peptide drugs by TAT-mediated transduction in the treatment of cancer. *Advanced Drug Delivery Reviews,* 57**,** 579-596.

WAJANT, H., PFIZENMAIER, K. & SCHEURICH, P. 2003. Tumor necrosis factor signaling. *Cell Death Differentiation,* 10**,** 45-65.

WANG, H. & HIRSCH, E. 2003. Bacterially-induced preterm labor and regulation of prostaglandin-metabolizing enzyme expression in mice: the role of toll-like receptor 4. *Biology of Reproduction,* 69**,** 1957-63.

WANG, J., LU, Z., WIENTJES, M. G. & AU, J. L. S. 2010. Delivery of siRNA Therapeutics: Barriers and Carriers. *The American Association of Pharmaceutical Scientists Journal,* 12**,** 492-503.

WARD, B., SEAL, B. L., BROPHY, C. M. & PANITCH, A. 2009. Design of a bioactive cell-penetrating, peptide: when a transduction domain does more than transduce. *Journal of Peptide Science,* 15**,** 668-674.

WATHES, D. C., BORWICK, S. C., TIMMONS, P. M., LEUNG, S. T. & THORNTON, S. 1999. Oxytocin receptor expression in human term and preterm gestational tissues prior to and following the onset of labour. *The Journal of Endocrinology,* 161**,** 143-51.

WEBB, R. C. 2003. Smooth muscle contraction and relaxation. *Advances in Physiology Education,* 27**,** 201-6.

WEBER, A., WASILIEW, P. & KRACHT, M. 2010. Interleukin-1 (IL-1) pathway. *Science Signalling,* 3**,** cm1.

WEBSTER, S. J., WAITE, S. L., COOKSON, V. J., WARREN, A., KHAN, R., GANDHI, S. V., EUROPE-FINNER, G. N. & CHAPMAN, N. R. 2013. Regulation of GTP-binding protein (Galphas) expression in human myometrial cells: a role for tumor necrosis factor in modulating Galphas promoter acetylation by transcriptional complexes. *The Journal of Biological Chemistry,* 288**,** 6704-16.

WENDER, P. A., MITCHELL, D. J., PATTABIRAMAN, K., PELKEY, E. T., STEINMAN, L. & ROTHBARD, J. B. 2000. The design, synthesis, and evaluation of molecules that enable or enhance cellular uptake: Peptoid molecular transporters. *Proceedings of the National Academy of Sciences of the United States of America,* 97**,** 13003-13008.

WENSTROM, K. D., ANDREWS, W. W., HAUTH, J. C., GOLDENBERG, R. L., DUBARD, M. B. & CLIVER, S. P. 1998. Elevated second-trimester amniotic fluid interleukin-6 levels predict preterm delivery. *American Journal of Obstetrics and Gynecology,* 178**,** 546-50.

WHITESIDE, S. T. & ISRAEL, A. 1997. I kappa B proteins: structure, function and regulation. *Seminars in Cancer Biology,* 8**,** 75-82.

XU, P., ALFAIDY, N. & CHALLIS, J. R. 2002. Expression of matrix metalloproteinase (MMP)-2 and MMP-9 in human placenta and fetal membranes in relation to preterm and term labor. *Journal of Clinical Endocrinology Metabolism,* 87**,** 1353-61.

YAN, X., WU XIAO, C., SUN, M., TSANG, B. K. & GIBB, W. 2002a. Nuclear factor kappa B activation and regulation of cyclooxygenase type-2 expression in human amnion mesenchymal cells by interleukin-1beta. *Biology of Reproduction,* 66**,** 1667-71.

YAN, X., WU XIAO, C., SUN, M., TSANG, B. K. & GIBB, W. 2002b. Nuclear Factor Kappa B Activation and Regulation of Cyclooxygenase Type-2 Expression in Human Amnion Mesenchymal Cells by Interleukin-1β. *Biology of Reproduction,* 66**,** 1667-1671.

ZARAGOZA, D. B., WILSON, R. R., MITCHELL, B. F. & OLSON, D. M. 2006. The interleukin 1beta-induced expression of human prostaglandin F2alpha receptor messenger RNA in human myometrial-derived ULTR cells requires the transcription factor, NFkappaB. *Biology of Reproduction,* 75**,** 697-704.

ZARUBIN, T. & HAN, J. 2005. Activation and signaling of the p38 MAP kinase pathway. *Cell Research,* 15**,** 11-8.